



INSTITUTO
SUPERIOR
TÉCNICO

UNIVERSIDADE TÉCNICA DE LISBOA
INSTITUTO SUPERIOR TÉCNICO

Stars as cosmological tools: giving light to Dark Matter

Jordi Casanellas Rius

Supervisor: Doctor Ilídio Pereira Lopes

Thesis approved in public session to obtain the PhD Degree in **Physics**
Jury final classification: **Pass with Distinction**

Jury

Chairperson: Chairman of the IST Scientific Board

Members of the Committee:

Doctor Jordi Isern Vilaboy
Doctor Jorge Venceslau Comprido Dias de Deus
Doctor Alfredo Barbosa Henriques
Doctor José Pizarro de Sande e Lemos
Doctor Ilídio Pereira Lopes
Doctor Patrick Colin Scott

2012





INSTITUTO
SUPERIOR
TÉCNICO

UNIVERSIDADE TÉCNICA DE LISBOA
INSTITUTO SUPERIOR TÉCNICO

Stars as cosmological tools: giving light to Dark Matter

Jordi Casanellas Rius

Supervisor: Doctor Ilídio Pereira Lopes

Thesis approved in public session to obtain the PhD Degree in **Physics**

Jury final classification: **Pass with Distinction**

Jury

Chairperson: Chairman of the IST Scientific Board

Members of the Committee:

Doctor Jordi Isern Vilaboy, Full Professor at Institut de Ciències de l'Espai, Bellaterra, Spain

Doctor Jorge Venceslau Comprido Dias de Deus, Full Professor at the Instituto Superior Técnico, Universidade Técnica de Lisboa

Doctor Alfredo Barbosa Henriques, Full Professor at Instituto Superior Técnico, Universidade Técnica de Lisboa

Doctor José Pizarro de Sande e Lemos, Full Professor at Instituto Superior Técnico, Universidade Técnica de Lisboa

Doctor Ilídio Pereira Lopes, Invited Assistant Professor (with habilitation) at Instituto Superior Técnico, Universidade Técnica de Lisboa

Doctor Patrick Colin Scott, Research Scientist at McGill University, Montreal, Canada

FUNDING INSTITUTIONS:

Fundação para a Ciência e Tecnologia, REF: SFRH/BD/44321/2008



2012

Usando as estrelas como laboratórios cósmicos: dar luz à matéria escura

Jordi Casanellas Rius

Doutoramento em Física

Orientador: Professor Doutor Ilídio Pereira Lopes

Resumo

Um dos mistérios mais interessantes da ciência moderna é a evidência de 83% de toda a matéria do Universo existir sob uma forma ainda não descoberta, chamada Matéria Escura (ME), diferente de todos os tipos de matéria conhecidos. Apesar dos notáveis esforços na investigação do problema da ME, ainda não foi possível identificar a sua natureza. Nesta Tese propomos uma abordagem complementar às actuais pesquisas de ME: o uso das propriedades das estrelas para investigar a natureza da ME.

Estudámos a captura e aniquilação de partículas de ME no interior de estrelas de pequena massa e o seu impacto na evolução estelar. Encontrámos assinaturas muito peculiares nas características das estrelas quando estas evoluem em meios com densidades de ME muito altas. Propusémos então uma estratégia para identificar estes tipos de estrelas usando as oscilações estelares. Estudámos também a captura estelar de partículas de ME considerando diferentes tipos de ME e de estrelas. Além disso, estudámos os impactos da ME nas propriedades globais dum enxame estelar.

Destacamos que, no caso de partículas de ME que não se auto-aniquilam, conseguimos estabelecer limites às características da ME usando observações astrosismológicas de estrelas próximas. Esta descoberta pode encetar um novo e prometededor campo para a pesquisa da ME, com centenas de estrelas na sequência principal e gigantes vermelhas a serem actualmente observadas pelas sondas *Kepler* e *CoRoT*.

Além destes resultados, nesta Tese aplicámos também uma abordagem similar à área das teorias da gravitação. Estabelecemos limites a uma teoria de gravidade modificada baseada em Eddington comparando as medições da heliosismologia e dos fluxos dos neutrinos solares com os nossos modelos solares modificados.

Palavras-chave: matéria escura, estrelas, astrosismologia, gravidade, Sol, Centro Galáctico, diagrama de Hertzsprung-Russell, heliosismologia, neutrinos solares, alfa centauri

Stars as cosmological tools: giving light to Dark Matter

Abstract

One of the more tantalizing mysteries in modern science is the evidence that 83% of all the matter in the Universe exists in an undiscovered form, known as Dark Matter (DM), different from any other type of matter. Despite the extensive efforts dedicated to investigate the DM problem, the identification of its nature remains elusive. In this Thesis we propose a complementary approach to present DM searches: the use of the properties of stars to investigate the nature of DM.

We studied the capture and self-annihilation of DM particles on the cores of low-mass stars and their impact on stellar evolution. Very characteristic signatures in the stellar properties were found when stars evolve within very high environmental DM densities. A strategy to identify a DM burning star using the stellar oscillations was proposed. The stellar capture of DM particles was thoroughly studied considering different assumptions regarding the characteristics of the DM particles and the stars. Furthermore, the DM impacts on the global properties of stellar clusters were evaluated.

Remarkably, in the case of non-annihilating DM particles we found that present asteroseismic observations of nearby stars provide constraints to the DM parameter space mass versus DM-proton scattering cross section. This discovery may open a new and promising field of DM research, with hundreds of main-sequence stars and red giants being presently observed by the *Kepler* and *CoRoT* asteroseismic missions.

In addition to the results mentioned above, in this Thesis we also applied a similar approach to the field of gravity theories. We constrained an Eddington-inspired modified theory of gravity comparing the measurements of the solar neutrino fluxes and helioseismic data with our modified solar models.

Key-words: dark matter, stars, asteroseismology, gravity, Sun, galactic center, Hertzsprung-Russell diagram, helioseismology, solar neutrinos, alpha centauri

Acknowledgements

Em primeiro lugar, quero agradecer sinceramente ao orientador desta Tese, o Professor Ilídio Lopes, não só o seu apoio, dedicação e orientação durante o doutoramento, mas também a sua filosofia e empenho em procurar ter um aluno feliz como condição necessária para a obtenção de resultados científicos. Agradeço-lhe ainda o entusiasmo que sempre teve com este projecto e com a investigação em geral, e que me conseguiu transmitir, motivando-me ao longo deste percurso.

Quero agradecer também o apoio que recebi das pessoas do CENTRA, além de quaisquer expectativas tanto a nível profissional como a nível humano: os Professores Jorge Dias de Deus, José Sande Lemos e Alfredo Barbosa, e ainda as seguintes pessoas, também imprescindíveis ao bom funcionamento do CENTRA: a Dulce, o Sérgio e o Manuel. Muito obrigado também aos Professores Vitor Cardoso, Ana Mourão, Amaro J. Rica da Silva e Mário Pimenta pela confiança que depositaram em mim ao darem-me a oportunidade de leccionar e pelo apoio recebido. O meu agradecimento especial ao Dário, que me guiou nos primeiros passos na investigação e continua ainda a fazê-lo, e à Marta, pela paciência e boa disposição que teve ao partilhar comigo o mesmo gabinete nestes 4 anos.

Thanks to all the colleagues with whom I shared good moments, chats, mutual help, work, lunch, football and more: Enzo, Caio, Isabella, Helvi, Andrea, Jorge, Paolo, Mariam, Jan, Vitor, Mário, Vallery, Antonino, Gonçalo, Sayan, TERENCE, Marc, Lluís, António, Steve, Hiro, Seb, Vladan and Raphael.

Estou grato também à FCT e à Fundação Calouste Gulbenkian pelo apoio recebido.

I finalment, gràcies de tot cor à Vanda, als meus pares, germana, Dani, Arnau, Gerard, Mar, àvia Lolita i àvia Maria, à Celeste e ao Zé Carlos, i a tota la meva família, i a tots els meus amics, i a totes les persones, éssers vius i altres éssers i coses, including stars, dark matter and all the beauty of the Universe. Gràcies!

Preface

This Thesis is dedicated to the investigation of the impact that different dark matter candidates produce on the properties of low-mass stars, as well as to the research and proposal of different strategies to observe such effects and their use to constrain the nature of dark matter. This topic constitutes the core of this Thesis. In addition, we successfully applied the skills and methods developed during this PhD to the field of gravity theories, which led us to provide constraints to a particular alternative to general relativity.

It is also important to comment on the format of this Thesis. The central part of the Thesis is formed by the articles published during the PhD, organized according to the regulations of the IST PhD program as follows. In Chapter 1 the publications are put into a broader context: Section 1.1 introduces the reader to the dark matter topic, Section 1.2 outlines the basics of stellar modelling and seismology, and Section 1.3 reviews how stars can be used to investigate dark matter. Chapter 2 contains summaries of the published articles, while Chapter 3 outlines the most important conclusions and future prospects arising from this Thesis. Finally, the publications are presented in their original format in Appendix A

List of Publications

Publications included in this Thesis:

The formation and evolution of young low-mass stars within halos with high concentration of dark matter particles (Paper I)

Casanellas J. & Lopes I.

The Astrophysical Journal, 705, 135-14 (2009)

arXiv:0909.1971

Towards the use of asteroseismology to investigate the nature of dark matter (Paper II)

Casanellas J. & Lopes I.

Mon. Not. R. Astron. Soc. 410, 535-540 (2011)

arXiv:1008.0646

The capture of dark matter particles through the evolution of low-mass stars (Paper III)

Lopes I., Casanellas J. & Eugénio D.

Physical Review D 83, 063521 (2011)

arXiv:1102.2907

Signatures of dark matter burning in nuclear star clusters (Paper IV)

Casanellas J. & Lopes I.

The Astrophysical Journal Letters, 733:L51, 5pp (2011)

arXiv:1104.5465

First asteroseismic limits on the nature of dark matter (Paper V)

Casanellas J. & Lopes I.

submitted for publication

arXiv:1212.2985

Testing alternative theories of gravity using the Sun (Paper VI)

Casanellas J., Pani P., Lopes I. & Cardoso V.

The Astrophysical Journal, 745:15, 6pp, (2012)

[arXiv:1109.0249](#)

Other works related with this Thesis:

Casanellas J. & Lopes I.

Low-mass stars within dense dark matter halos.

Proceedings of the Invisible Universe International Conference, Paris, France (2009)

[arXiv:1002.2326](#)

Cardoso V., **Casanellas J.**, Pani P., Lopes I. & Delsate T.

Stars in alternative theories of gravity.

Proceedings of The Multidisciplinary Universe Conference, Lisbon, Portugal, (2011)

Lopes I. & **Casanellas J.**

The Sun and stars: giving light to dark matter.

Proceedings of The Multidisciplinary Universe Conference, Lisbon, Portugal, (2011)

Contents

Abstract	i
Acknowledgments	v
Preface	vii
List of Publications	ix
Contents	xi
1 Introduction	1
1.1 Introduction to the Dark Matter problem	2
1.1.1 Evidence for the existence of Dark Matter	2
1.1.2 Dark Matter particle candidates	10
1.1.3 Searches for Dark Matter	13
1.2 Stellar evolution and seismology	16
1.3 Using stars to investigate Dark Matter	19
2 Summaries of the publications	27
2.1 The formation and evolution of young low-mass stars within halos with high concentration of dark matter particles (Paper I)	28
2.2 Towards the use of asteroseismology to investigate the nature of dark matter (Paper II)	30
2.3 The capture of dark matter particles through the evolution of low-mass stars (Paper III)	32
2.4 Signatures of dark matter burning in nuclear star clusters (Paper IV)	34
2.5 First asteroseismic limits on the nature of dark matter (Paper V)	36
2.6 Testing alternative theories of gravity using the Sun (Paper VI)	39
3 Conclusions	41

A Appendix: Publications	45
A.1 Paper I	47
A.2 Paper II	57
A.3 Paper III	65
A.4 Paper IV	77
A.5 Paper V	83
A.6 Paper VI	89
Bibliography	97

1

Introduction

The hypothesis of the existence of dark matter is substantiated by a range of observational evidences spanning from cosmological to galactic scales. A selection of some of these evidences is presented in Section 1.1.1.

This unknown component of the Universe is expected to constitute 23% of its energy density and to be formed by new particles which do not belong to the present Standard Model of particle physics. Fortunately, well-motivated extensions of the Standard Model, such as supersymmetry, provide a range of new particles which naturally fulfill the characteristics required to constitute the dark matter of the Universe. A short review of the dark matter candidates which are relevant to the scope of this Thesis is presented in Section 1.1.2.

Several experimental efforts are being carried out with the aim of unveiling the true nature of dark matter. While colliders may probe the theoretical framework that explains the existence of particles with the dark matter properties, other experiments were conceived with the aim of detecting the dark matter that populates our galaxy. The present status of these experiments is exciting: several possible detections were claimed by different experiments, but at the same time these results have been challenged by incompatible results from other experiments, so no conclusive judgment is possible until further evidence is accumulated. Section 1.1.3 summarizes the present status of dark matter searches.

In the above context of elusivity of detection and controversy, the approach proposed in this Thesis provides a complementary strategy to probe the nature of dark matter. Dark

matter particles have been shown to change the evolution and properties of stars after accumulating in their interior in a sufficient number, the importance of these effects depending on characteristics such as the mass of the dark matter particle and its scattering cross section off baryons. Both the discovery of the impact of dark matter on stars or the confirmation of its absence can be used to constrain the properties of the proposed dark matter candidates. While Section 1.2 reviews the basics of stellar evolution and stellar seismology, Section 1.3 introduces the reader on how stars can be used to investigate the nature of dark matter.

1.1 Introduction to the Dark Matter problem

1.1.1 Evidence for the existence of Dark Matter

Evidence at galactic scales

Back in the decade of the 1920's astronomers such as J. Kaptein [1], J. Jeans [2] and B. Lindblad [3] tried to infer the mean density of mass in the local galactic neighborhood from the dynamics of the stars, and compared this value with the estimated mass from the number of observed stars in order to calculate the amount of *dark matter*, that is, the non-visible mass. These works constitute the first hints of the omnipresent dark matter component of the Universe.

In 1932 Jan Oort extended these works by measuring the vertical motions of the stars in the disk in order to deduce the gravitational potential that was keeping these stars in the galactic plane. In his detailed study [4] he found that:

"the total density of matter near the Sun is equal to $6.3 \cdot 10^{-24}$ g/cm³ or 0.092 solar masses per cubic parsec. The observed total mass of the stars down to + 13.5 visual absolute magnitude is found to be 0.038 solar masses per pc³".

However, later in the same article, in a chapter entitled "*The amount of dark matter*" he concludes:

"It is not necessary to conclude from this ... that there is a greater percentage of nebulous or dark matter in this region: we might reverse the argument and conclude that some 85% of the light of the galactic system is obscured before it reaches us".

The first doubtlessly claim of the existence of very important quantities of invisible mass in the Universe was stated by Fritz Zwicky back in 1933 [5]. He observed that **the velocities of individual galaxies** in the Coma Cluster were too high, that is, he showed that there was not enough mass in the cluster to keep the galaxies gravitationally bound together. Comparing the luminous mass of the cluster and the gravitational mass inferred using the

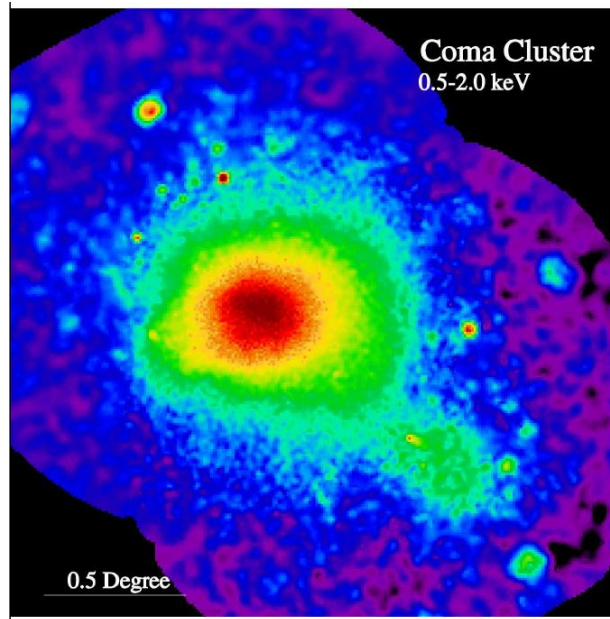


Figure 1.1: The Coma cluster observed by the X-ray telescope ROSAT [6]. The temperature of the intracluster gas is used to infer the total mass of the cluster, revealing the existence of large amounts of invisible mass.

virial theorem (relating the kinetic and potential energy of the system), he estimated that hidden dark matter was about 400 times more abundant than the luminous mass of the cluster. However, the relevance of his discovery, hidden among his outstanding seminal works on supernovae, neutron stars and gravitational lenses, was not acknowledged at that time.

Nowadays, the realization that invisible, hot gas accounts for most of the mass in the clusters of galaxies allows a more precise determination of the luminous to dark matter ratio in clusters. The gas of the intracluster medium is virialized, thus its temperature, measured with **the X-rays emitted by the hot gas**, can be used to infer the total potential energy of the system and therefore the total cluster mass. Observations of the Coma cluster performed by the ROSAT X-ray telescope ([6], see Figure 1.1) have shown that the total gravitational mass of this cluster is indeed much larger than its luminous mass [7], although well below the initial estimations of F.Zwicky.

The true importance of the dark matter component of the Universe was fully understood only in the late 70's, thanks to the systematic measurements of the **rotational velocities around spiral galaxies** performed by Vera Rubin and Kent Ford [8] from the Doppler effect in $H\alpha$ lines (see Figure 1.2.a). They showed that the problem of the missing mass was evident also at galactic scales. The velocities of HII regions outside the disk of the M31 galaxy were found to be higher than expected, being approximately constant at large radius

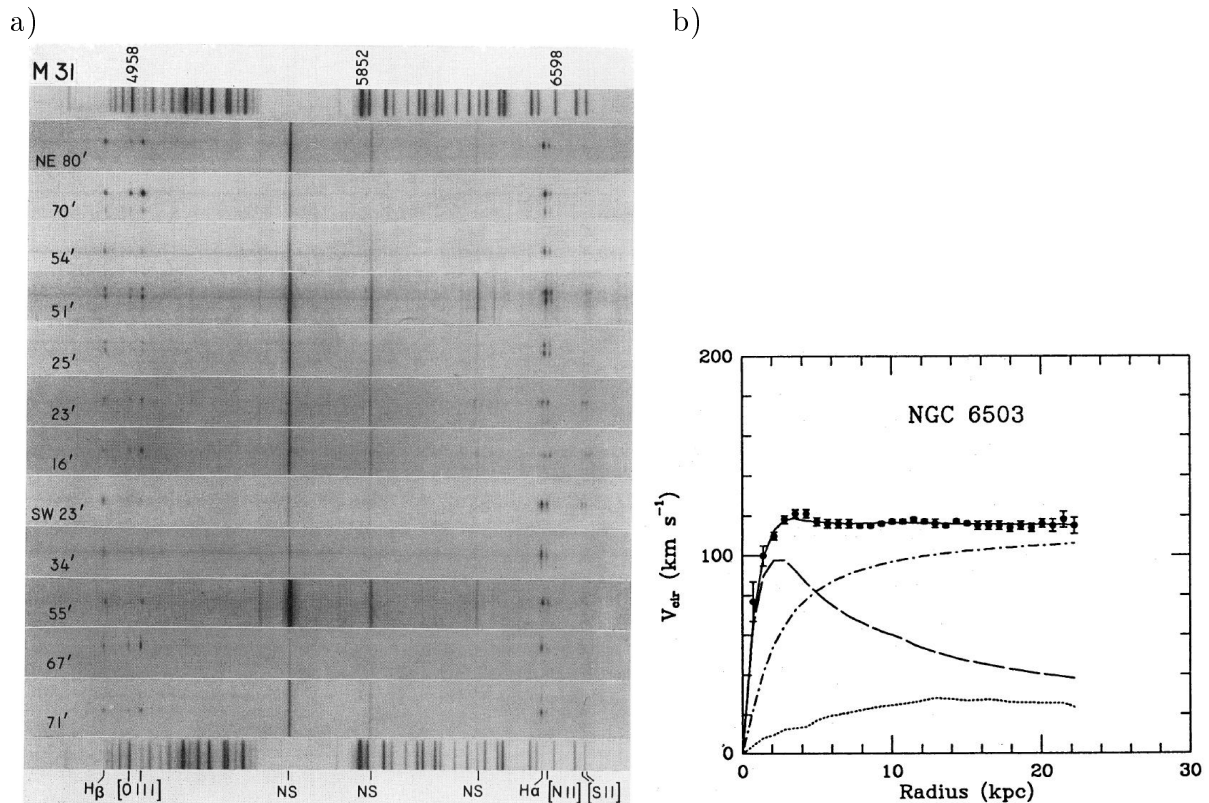


Figure 1.2: (a) Spectrum of emission regions in galaxy M31, as obtained by V. Rubin and K. Ford in 1970 to measure the rotation velocities. From [8]. (b) Observed rotation curve of galaxy NGC 6503 (dots with error bars) decomposed into its stellar (dashed), gaseous (dotted), and dark (dashed-dot) components. The solid line is the best-fit to the rotation curve, using a particular density profile for the dark matter halo. From [9].

(*i.e.*, a flat rotation curve) instead of decreasing when the distance from the central mass increased as is expected from a Keplerian orbit ahead of the central mass. The existence of a spherical halo of dark matter embedding the galaxies, with the edges far beyond the radius of the galaxy and with a mass several times greater than the galactic mass, has been found to easily explain the galactic rotation curves (see Figure 1.2.b).

Moreover, presently there is an additional method to measure the total mass of a system, independently of its nature: **gravitational lensing**. The trajectories of light from distant galaxies are bent by the gravitational attraction of the mass between them and the observer, so the mass acts as a lens. Thus, the amount of mass that is causing the gravitational lensing can be calculated without relying on astrophysical assumptions by measuring the distortion of the images. Measurements of the gravitational lensing effect have confirmed that the total mass of the clusters of galaxies exceeds by a large factor the mass inferred from their luminosity. Furthermore, gravitational lensing has been used to create impressive 3D maps of the large-scale distribution of dark matter. Filamentary structures were found, intersecting in massive halos at the locations of clusters of galaxies (see Figure 1.3), as was

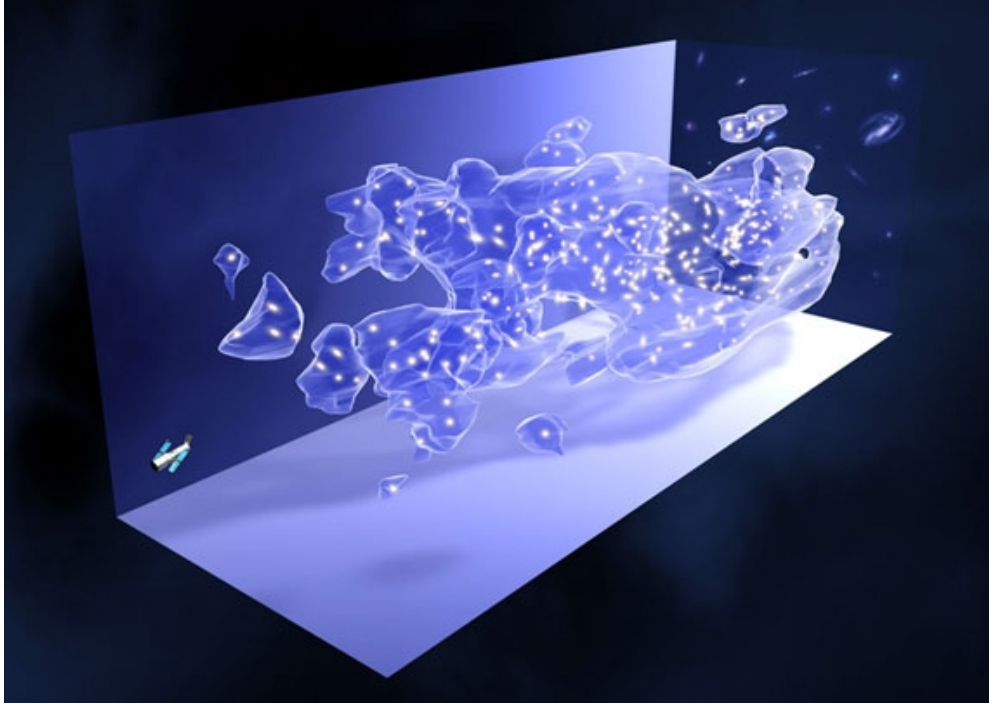


Figure 1.3: A three-dimensional map of the large-scale distribution of dark matter, reconstructed from weak-lensing data. The blue surface is an isodensity contour, chosen arbitrarily to highlight the filamentary structure, while the white points were added to represent the observed galaxies, formed in the denser points of the dark matter distribution. From [10].

predicted by numerical N-body simulations.

The combination of gravitational lensing and X-ray observations of the so-called "**Bullet cluster**" provide altogether one of the more convincing probes for the existence of dark matter ahead of alternative explanations such as modified theories of gravity. The picture of the Bullet cluster shown in Figure 1.4 is thought to depict two clusters of galaxies after their collision. The location of the hot gas in the intracluster medium, traced by the X-ray observations shown in red in Figure 1.4, is clearly separated from the position of the galaxies themselves. This is an indication of a past violent collision between the gas of the two clusters: the gas experienced friction while the galaxies passed through each other. Another signature of the collision is the bullet-shape of the gas in the smaller of the two clusters, on the right-hand side of the Figure, which gives name to the cluster. Having the gas and the galactic components of the cluster separated, this cluster offers an excellent opportunity to test the dark matter explanation against theories with modified newtonian dynamics (MOND [11, 12]), which state that only the known matter exists but it produces a different gravitational acceleration at large radius. If a dark matter halo of weakly interacting particles existed, it would have followed the trajectories of the galaxies during the collision, therefore

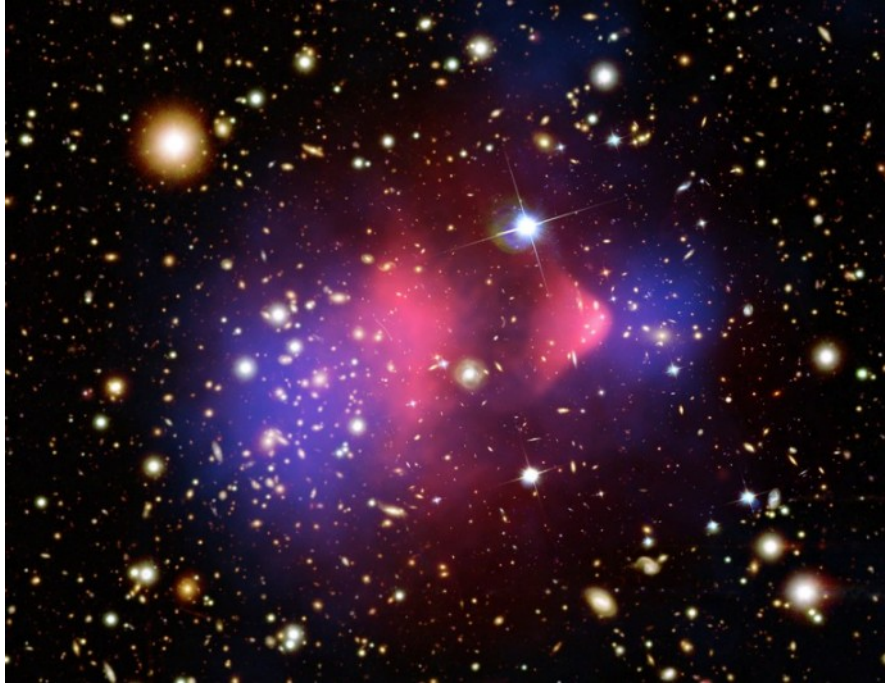


Figure 1.4: Composite image of the galaxy cluster 1E 0657-56, also known as the "Bullet cluster", joining Chandra X-rays observations of the intracluster hot gas ([13], in red), optical observations from the Magellan telescopes and the Hubble Space Telescope [14], and the location of the mass inferred by gravitational lensing ([14], in blue). From [15].

we would expect most of the gravitational mass to be in the location of the galaxies. On the other hand, if no dark matter existed, we would expect most of the mass of the system to be in the form of hot intracluster gas. The true location of the mass, measured independently by gravitational lensing as shown in blue in Figure 1.4, confirms the existence of a dark matter halo, excluding the MOND explanation unless additional new physics is invoked.

Another evidence of the existence of dark matter was found in the **velocity dispersions of stars in the dwarf spheroidal galaxies**, dispersions which were found to be larger than what was expected from the low central surface brightnesses and large core radii of the dwarf galaxies. These galaxies have a very large mass-to-light ratio, so they are thought to contain significant amounts of dark matter (see for instance [16]).

Evidence at a cosmological scale

The existence of dark matter is necessary for **the formation of structure** at cosmological scales. The dark matter particles, due to their weak interactions, decoupled from the primordial soup before the baryonic matter, collapsing around the primordial fluctuations and

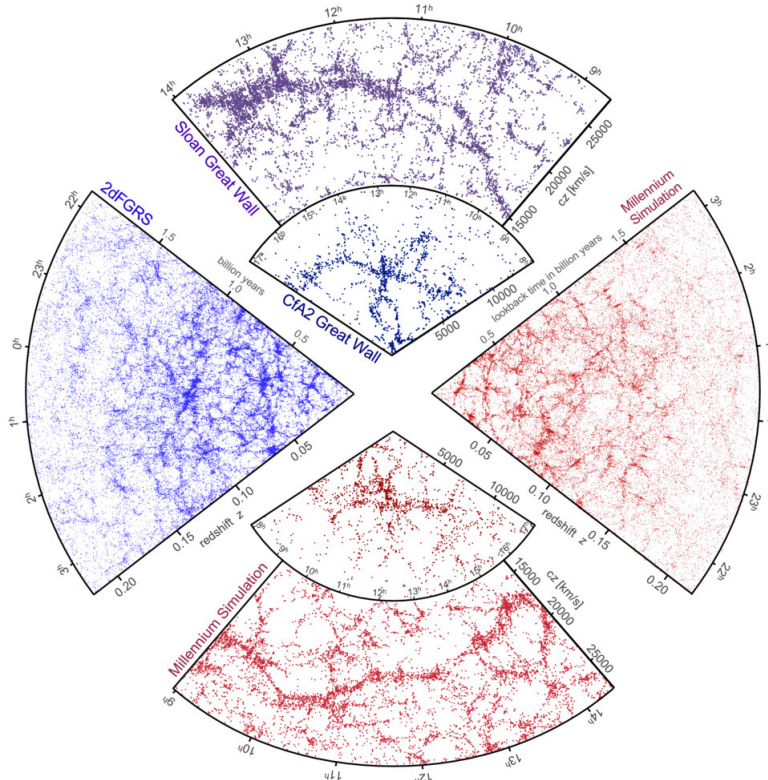


Figure 1.5: Large-scale distribution of galaxies obtained from spectroscopic redshift surveys (blue) compared with mock catalogs constructed from the Millennium simulations (red). The comparison of the images shows that Λ CDM cosmological simulations reproduce the same features in the large scale structure (voids, filaments) as observed in the real Universe (from Ref. [17]).

creating the first overdense regions where baryonic matter collapsed *a posteriori*. The formation of structure was hierarchical, that is, first the smaller structures were formed, and then they came together by gravitational collapse and tidal disruption when falling into greater halos. Large-scale **N-body simulations** have revealed this scenario and demonstrated that substantial amounts of dark matter are needed in order to correctly reproduce the large-scale structure of the Universe as it is observed ([17], see Figure 1.5). In addition, these simulations reveal that most of the dark matter has to be cold, *i.e.*, very non-relativistic, to allow the formation of small structures, and non-dissipative, *i.e.*, with no strong interactions, to avoid the losses of energy and the subsequent collapse with the baryonic matter in disks. Moreover, large-scale structure provides a measurement of the total (dark + baryonic) mass density of the Universe. The scale of the baryonic density perturbations that survived and formed galaxies points to a total matter density of $\Omega_m \approx 0.20$.

An independent measure of the baryonic budget of the Universe comes from the primordial abundances of light elements: deuterium, He^3 , He^4 and Li^7 . The production of these isotopes in the **Big Bang nucleosynthesis** depended critically on the baryon-to-photon

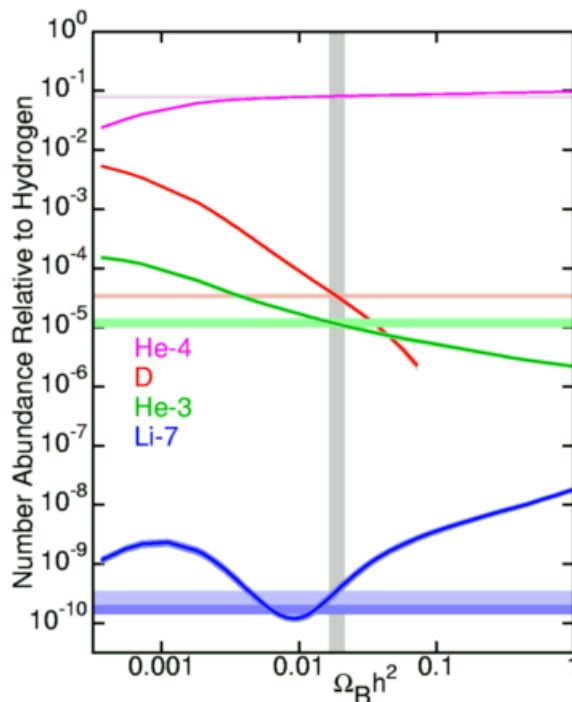


Figure 1.6: The relative primordial abundances of light elements (horizontal bars) and their dependence on the baryon density (lines) leads to a measurement of the baryon density of $\Omega_b h^2 \approx 0.021$, that is $\Omega_b \approx 0.04$ with $h = 0.72$ [18]. From [19].

ratio at that time. The value of the baryon density that fits the observed primordial abundances of these isotopes is $\Omega_b \approx 0.04$ (see Figure 1.6). Together with large-scale structure measurement of Ω_m we can see that approximately 80% of the matter of the Universe is non-baryonic. Further evidence of the non-baryonic nature of dark matter comes from the fact that we do not observe its electromagnetic interaction with photons: we can transparently see through dark matter clouds, and the evidence points to spherical halos of dark matter instead of the collapsed disks that would be formed if the dark matter particles were able to radiate away angular momentum.

Perhaps the most impressive evidence of the existence of dark matter comes from its signature in the **cosmic microwave background** (CMB). If only baryonic matter existed, we would expect the temperature fluctuations in the CMB to be of the order of 10^{-3} to explain the observed large-scale structure. However, if dark matter structures formed first, they would have left no imprint on the temperature due to their null electromagnetic interactions, so the temperature inhomogeneities would be smaller. In fact, the CMB is measured to be a perfect black body spectrum of temperature 2.725 K with anisotropies of the order of 10^{-5} (see Figure 1.7). The structure of the angular power spectrum of the CMB (*i.e.*, the position and height of the acoustic peaks) is sensitive, among other parameters, to the total energy density of the Universe and its baryon fraction. The high precision of the 7-year WMAP data

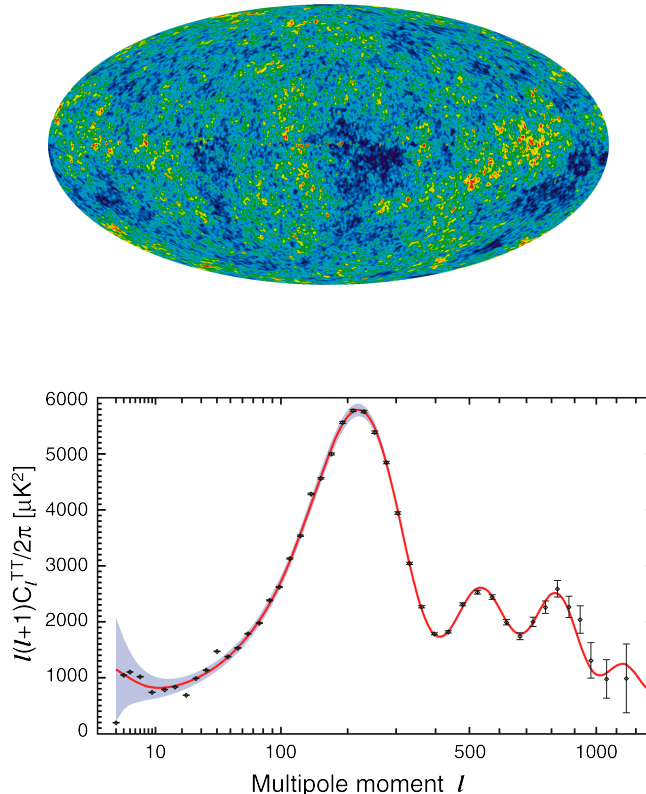


Figure 1.7: Top: all-sky map of the temperature fluctuations (the colors show a temperature range of $\pm 200 \mu\text{K}$) of the Universe as it was 13.7 billion years ago (from WMAP [21]). Bottom: temperature power spectrum from 7-year WMAP data [22]. The red line is the ΛCDM model best fit to the 7-year WMAP data: $\Omega_b h^2 = 0.02270$, $\Omega_c h^2 = 0.1107$, $\Omega_\Lambda = 0.738$.

of the CMB allows tight constraints on the baryon and dark matter fraction, respectively $\Omega_b = 0.0449 \pm 0.0028$, $\Omega_{DM} = 0.222 \pm 0.026$ [20], in excellent agreement with the independent measures mentioned above in this Section. In conclusion, CMB anisotropies show that dark matter must be non-baryonic and interact only weakly with atoms and radiation, and show that dark matter is roughly 5 times more abundant than baryonic matter at cosmological scales, in agreement with what is measured at galactic scales.

The CMB data shows that the Universe is spatially flat, rather than curved. The remaining of the energy density of the Universe, $\Omega_\Lambda = 0.739 \pm 0.029$, is thought to be in an unknown form of dark energy. The combination of the CMB, the measurements of the expansion rate of the Universe by the receding velocities of distant supernovae, and the baryon acoustic oscillation data, demonstrate that the Universe is essentially flat and formed by approximately 5% of baryonic matter, 23% of dark matter, and 72% of dark energy, the so-called

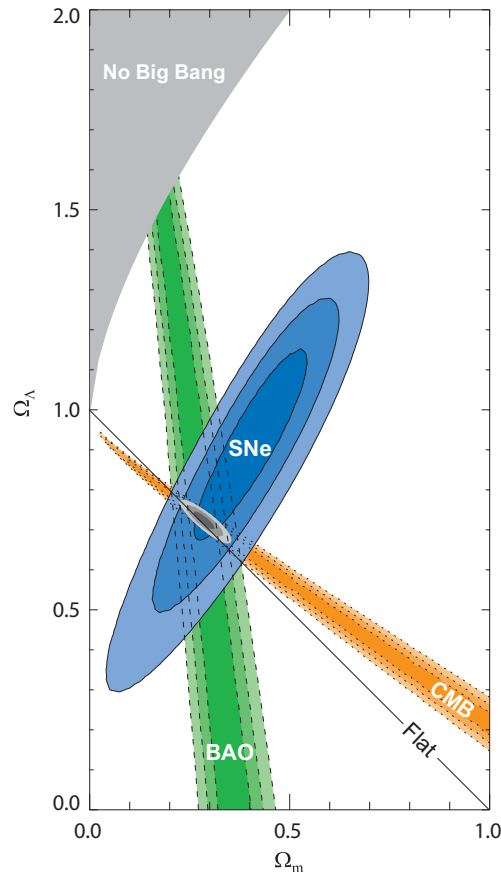


Figure 1.8: Different cosmological observations, namely supernovae (SNe), baryon acoustic oscillations (BAO) and the cosmic microwave background (CMB), point to the fact of our Universe being flat, with most of its energy density in the form of an unknown dark energy ($\sim 72\%$). The abundance of the light isotopes produced in Big Bang nucleosynthesis, the CMB, and the large-scale structure of the Universe tell us that most of the remaining $\sim 28\%$ is in the form of cold, non-baryonic dark matter. From [23]

concordance model of cosmology, Λ CDM (see Figure 1.8).

1.1.2 Dark Matter particle candidates

The collection of evidence reviewed in the previous Section points to the existence of a new type of particles with the following properties: massive, neutral, non-baryonic, with non-strong interactions with other dark matter particles, neither with normal matter nor with photons, with non-relativistic velocities, and produced in sufficient number in the early Universe so that it can account for the right abundance observed in the present Universe, meaning that it also has to be stable at cosmological scales.

None of the particles of the Standard Model can account for a significant fraction of the dark matter of the Universe. Thus, we will now briefly review the dark matter particle candidates arising from extensions of the Standard Model. These theories, while initially

proposed to solve longstanding problems of particle physics, have also been shown to satisfactorily predict the existence of good dark matter candidates that fulfill all the properties mentioned above.

WIMPs

The family of the Weakly Interacting Massive Particles (WIMPs) is one of most widely studied and preferred dark matter candidates [24]. Their existence is predicted by strongly motivated theories, such as supersymmetry [25] or models with extra dimensions [26]. To guarantee the stability of the dark matter, these particles are the lightest among those proposed by the new theory. In addition, the decay into standard model particles is prevented by new symmetries, by the conservation of an additional quantum number which takes the value +1 for standard model particles and -1 for the new particles.

In many supersymmetric models, such as those arising from the Minimal Supersymmetric Standard Model (MSSM) [27], the stability of the lightest particle may be guaranteed by the conservation of the quantum number $R = (-1)^{3(B-L)+2s}$ (B the baryon number, L the lepton number and s the spin of the particle), which is also necessary to forbid problematic couplings. In these theories, the best dark matter candidate is the lightest **neutralino**:

$$\chi_1^0 = a_1 \tilde{B}^0 + a_2 \tilde{W}^0 + a_3 \tilde{H}_1^0 + a_4 \tilde{H}_2^0, \quad (1.1)$$

a combination of superpartners of the Higgs boson (the Higgsinos \tilde{H}^0) and of the bosons W (the wino \tilde{W}^0) and B (the bino \tilde{B}^0).

If standard model particles propagate in extra spacetime dimensions, the new partner states can be good dark matter candidates. In the case of universal extra dimensions, the fiducial dark matter candidate would be the **lightest Kaluza-Klein particle** [26, 28], which can have the desired relic density, and which stability is guaranteed by the KK-parity.

The weak scale of the mass and couplings of the WIMP dark matter candidates (thermally produced before Big Bang nucleosynthesis) made them decouple from the primordial soup at a temperature ($T \sim m_\chi/20$) such that they qualify as cold for purposes of structure formation. In this scenario, their relic density approximately depends only on their thermally averaged self-annihilation cross section $\langle\sigma v\rangle$ [24]:

$$\Omega_\chi h^2 \sim \frac{3 \cdot 10^{-27} \text{cm}^3 \text{s}^{-1}}{\langle\sigma v\rangle}. \quad (1.2)$$

The natural value of $\langle\sigma v\rangle$ for a weakly interacting particle, $\langle\sigma v\rangle \approx \frac{\alpha^2}{E_{weak}^2}$ [29], surprisingly leads to a relic density of the same order than that implied by cosmological observations, $\Omega_\chi h^2 \sim 0.11$. This coincidence, the so-called "WIMP miracle", makes the WIMPs a natural

dark matter candidate: if a neutral stable particle exists around the electroweak scale, it must have been produced in the early Universe with the right abundance to account for the observed dark matter.

The existence of WIMPs is not only motivated as a solution to the dark matter problem. Another amazing *coincidence* is that the resolution of the hierarchy problem appears to require new physics at the right scale for the associated particles to be WIMPs.

In this Thesis we have concentrated on the study of the effects of classical WIMP dark matter candidates in stellar evolution. Moreover, we have also studied the case of a particular class of WIMPs, the so-called **asymmetric dark matter** [30]. In this case, the relic density of dark matter is determined by a dark matter asymmetry that is inherited from the baryonic asymmetry, thus explaining the fact that both densities are of the same order. In particular, $\Omega_{DM} \sim (m_{DM}/m_b)\Omega_b$, so this theory predicts dark matter candidates with a mass around 5 GeV. Interestingly, asymmetric dark matter candidates have the right properties to explain the positive signals in various direct detection experiments [31]. These type of candidates can potentially be severely constrained with stellar dark matter searches. Asymmetric dark matter particles are not their own anti-particle, so they do not self-annihilate inside stars and can accumulate in large numbers.

Other dark matter candidates

Several dark matter candidates have been proposed in the literature. Most of the non-WIMP candidates require non-standard mechanisms in the early Universe to achieve the dark matter relic density, while others are *ad-hoc* models proposed to explain particular experimental results.

Axions arise from attempts to explain the strong CP problem [32]. In particular models, axions would be very light particles (< 1 eV) and could have been created by a non-thermal process in the right amount and with the slow velocity required to account for the dark matter of the Universe.

The gravitino (the superpartner of the graviton in some supersymmetric scenarios [33]) can also be the lightest supersymmetric particle and be stable thanks to a conserved R-parity. It could therefore also be a good dark matter candidate. However, it would be practically undetectable as it only interacts gravitationally with the rest of the particles.

Sterile neutrinos [34] arise from attempts to explain the neutrino masses, are more massive than ordinary neutrinos, and can make a good warm dark matter candidate, although their production rate in the early Universe has to be generally fine-tuned. It is worth noticing that warm dark matter candidates are severely constrained by cosmological data [35].

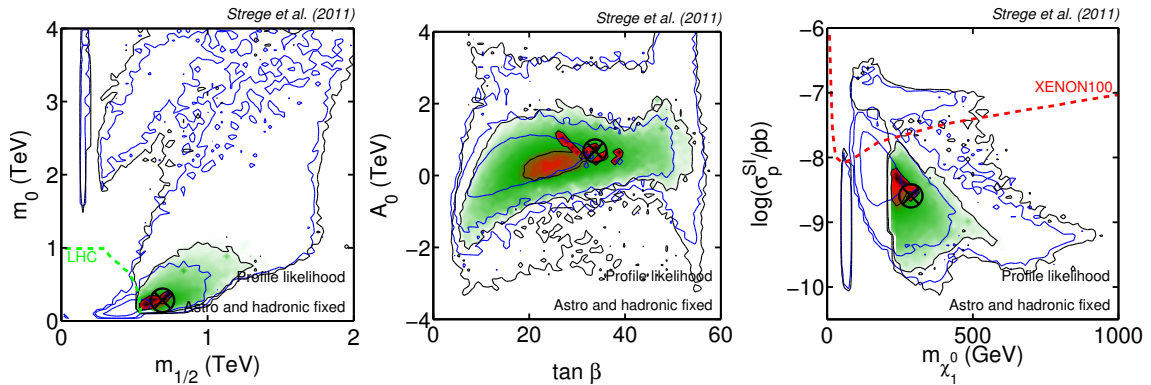


Figure 1.9: Profile likelihoods for the cMSSM parameters from the constraints of WMAP and LHC data. The dashed green and red lines represent the current exclusion limits from LHC and XENON100, respectively. From [36].

1.1.3 Searches for Dark Matter

Several strategies are presently being pursued with the aim to shed some light on the nature of dark matter. These strategies can be classified in three main groups: collider dark matter searches, direct detection, and indirect detection experiments.

Collider dark matter searches

Dark matter particles may be produced in the collisions undergoing at the Large Hadron Collider (LHC). If new supersymmetric particles appear to exist at an energy reachable by the LHC, then the quarks and gluons constituents of the accelerated protons may annihilate into new particles such as gluinos or squarks, which in turn may decay into the lightest supersymmetric particle, the neutralino. In any case, the hypothetical dark matter particles created at the LHC will not be directly detected: their signature would be missing transversal energy in the events. What is more, even if weakly interacting particles are indirectly detected in such a way, it will be difficult to know if they are the long-lived particles that constitute the dark matter of the Universe.

On the other hand, collider searches may be able to discover the fundamental parameters of the theories that predict dark matter candidates. For instance, in the case of constrained MSSM, multiple measurements of supersymmetric observables may allow the determination of the parameters m_0 , $m_{1/2}$, $\tan\beta$, etc. (see Figure 1.9), which in turn may be used to calculate the relic density of the dark matter particle produced in the LHC. If this relic density happens to be equal to that implied by cosmological observations, $\Omega_\chi h^2 = \Omega_{DM} h^2$, it will be a major breakthrough in the understanding of the nature of dark matter.

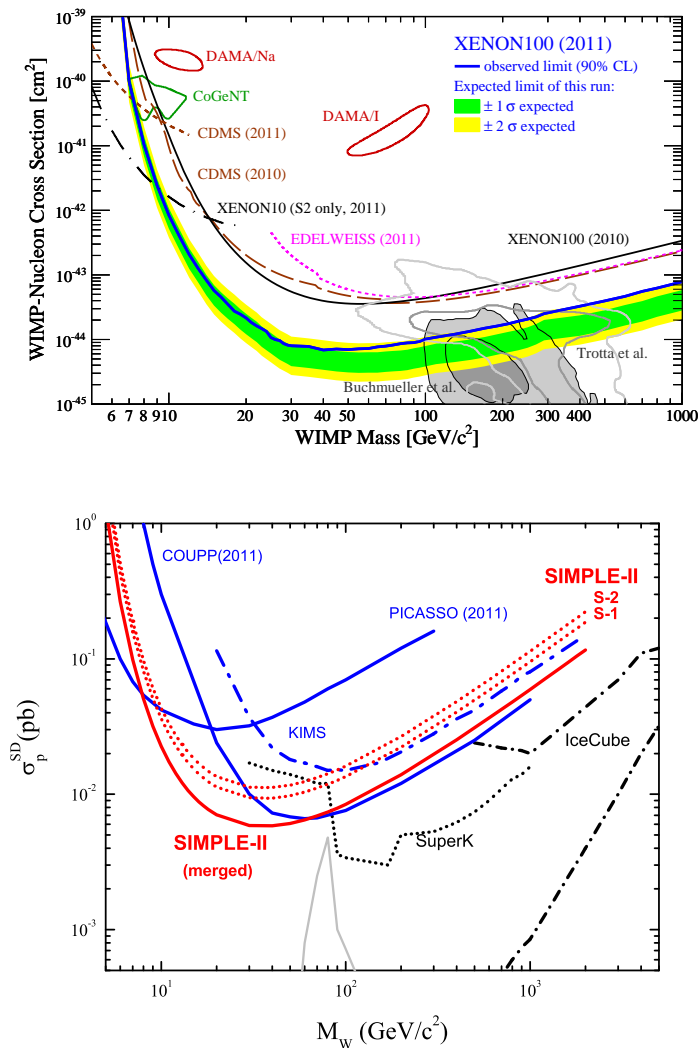


Figure 1.10: Exclusion contours on the spin-independent elastic WIMP-nucleon cross-section, from [37] (top), and on the spin-dependent WIMP-proton cross section, from [38] (bottom), as a function of WIMP mass.

Direct detection

Direct detection experiments are those trying to detect the collisions of the dark matter particles of the galactic halo, which are crossing the Earth at a high rate at any time, with nuclei in the detectors. Despite the fact that these events are expected to be very rare (of the order of 10 events/100kg/year), and that the energy deposited by the dark matter particles is very small (of the order of 10 keV), these experiments have reached the sensitivity to probe regions of the dark matter parameter space with the properties expected for supersymmetric dark matter candidates. The null results above background from XENON100 [37], CDMS-II [39], PICASSO [40], COUPP [41] and SIMPLE [38] experiments, among others, can be used to set constraints to the strength of the interactions between dark matter particles

and baryons. In Figure 1.10 the present exclusion limits on the spin-dependent and spin-independent WIMP-nucleon scattering cross sections are shown.

On the other hand, there are several experiments that have detected a signal that can be interpreted in terms of collisions of dark matter particles. The DAMA/LIBRA and DAMA/NaI experiments have accumulated evidence since 1998 [42] of an annual modulation in the signal due to seasonal changes in the relative velocity of the Earth and the dark matter particles in the galactic halo. These results have been recently confirmed by the CoGeNT experiment [43]. Remarkably, the CRESST-II experiment has recently detected sixty-seven events in the acceptance region where a WIMP signal is expected [44]. The dark matter interpretation of all these results seems to be in conflict with the null results of other experiments [37, 39, 40, 41, 38]. However, there is still room for models of low-mass WIMPs that can account simultaneously for the results of all the experiments [45, 31].

A convincing detection of dark matter will only be achieved through the combined results of different experiments. In this sense, the future experiment DM-ICE [46] will check the dark matter interpretation of the DAMA modulation signal by using the same technology (NaI scintillation detectors) deeply deployed in the South Pole ice. A dark matter signal would have the same seasonal phase as in DAMA, while many environmental effects and backgrounds would be absent or opposite in phase in respect to DAMA.

Indirect detection

Indirect detection experiments are looking for the products of the annihilation of dark matter particles, focusing mainly in gamma-rays and neutrinos. Other annihilation products such as charged particles introduce further complications due to the complexity of the understanding of the standard astrophysical sources of these particles as well as the diffusion processes.

Since the annihilation rate goes as the square of the dark matter density, the best locations to look for a dark matter signal are very dense dark matter objects, such as galaxy clusters, the center of our galaxy or the dwarf spheroidal galaxies around the Milky Way. Gamma-ray searches from these locations have been used to put constraints on the self-annihilation cross section of the dark matter particles. In the case of the dwarf galaxies, the constraints from FERMI [47] exclude a significant region of low-mass thermal WIMPs in some models (see Figure 1.11).

High dark matter densities are also reached inside compact astrophysical objects such as the Sun. Searches for neutrinos from dark matter annihilations in the Sun are performed in various experiments, led by Super-Kamiokande [48] and IceCube [49]. The constraints set by these experiments on the spin-dependent WIMP-proton cross section are shown in the bottom of Figure 1.10.

Indirect searches have also detected possible dark matter signals. Among others, the

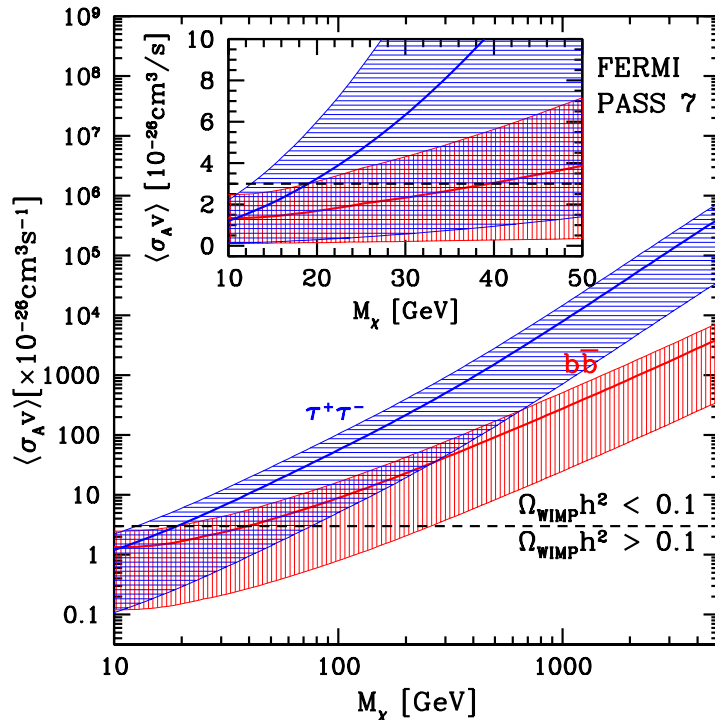


Figure 1.11: Upper limit on the WIMP self-annihilation cross section as a function of the WIMP mass for annihilation into $b\bar{b}$ and $\tau^+\tau^-$ from a joint analysis of Milky Way dwarfs with FERMI data. From [47].

cosmic positrons and electrons observed by PAMELA [50] and Fermi-LAT [51], or the recent gamma-ray excess at 130 GeV in Fermi-LAT data [52, 53].

1.2 Stellar evolution and seismology

The use of stars as laboratories of fundamental physics [54] is possible thanks to the precise understanding of the processes governing the stellar structure and evolution, which has exceptionally evolved since the seminal works of Chandrasekhar [55] and M. Schwarzschild [56], among others. Nowadays, techniques as the observation of the solar neutrinos and helio- and astroseismology have revealed the interior of stars to an unprecedented level [57, 58].

The theory of stellar structure and evolution is based on a spherically symmetric model which correctly reproduces the quasi-static phases of stellar evolution [59, 60, 61]. The model is governed by four ordinary differential equations: the continuity equation for the conservation of mass, the hydrostatic equilibrium equation, the equation for thermal equilibrium, and the equation for the energy transport, which takes place mainly by radiation or convection. The present standard solar model also includes a thorough understanding of the stellar matter: the tabulated equation of state and opacities of the stellar plasma under

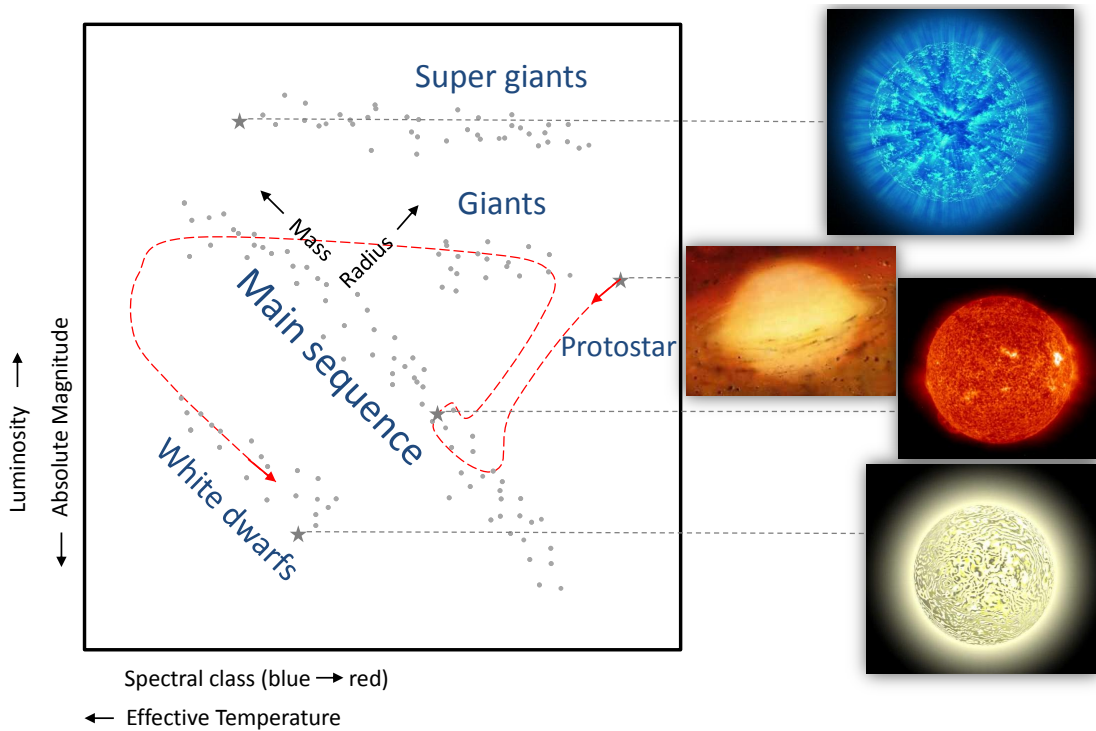


Figure 1.12: Schematic Hertzsprung-Russell diagram with the location and illustrative pictures of the main phases of stellar evolution. The red line shows the approximate evolutionary track of a star similar to the Sun.

the extreme conditions of pressure and temperature inside the stars, the precise rates and cross-sections of the several steps in the thermonuclear fusion reactions that take place inside the stars (mainly the pp chain, the CNO cycle, and the triple alpha process), and detailed measurements of the solar composition [62], which have a strong influence in the radiative opacity of the stellar plasma [63].

The photometric and spectroscopic observation of thousands of stars has permitted the understanding of the different phases of stellar evolution. This evolutionary scenario, summarized in the Hertzsprung-Russell diagram in Figure 1.12, is largely consistent with the standard stellar model outlined above. Stars are formed by the gravitational collapse of a gas cloud formed mainly by hydrogen and helium. The ignition of the thermonuclear reactions in the core of the protostar, fusing hydrogen atoms into helium, halts the collapse and leads to a stable phase, the so-called main sequence. This phase, where most of the stars are found, only ends when the star runs out of hydrogen in its center. At that stage, the combustion of hydrogen takes place only in a shell out of the inert helium core. It follows a rapid contraction of the stellar nucleus and an expansion of the envelope, forming a much brighter star called red giant. Then, the star may evolve through subsequent phases of combustion of heavier elements depending on its mass. Most of the stars, having a relatively low-mass ($\leq 8 M_{\odot}$), end up forming a white dwarf, a dim star constituted mainly by carbon

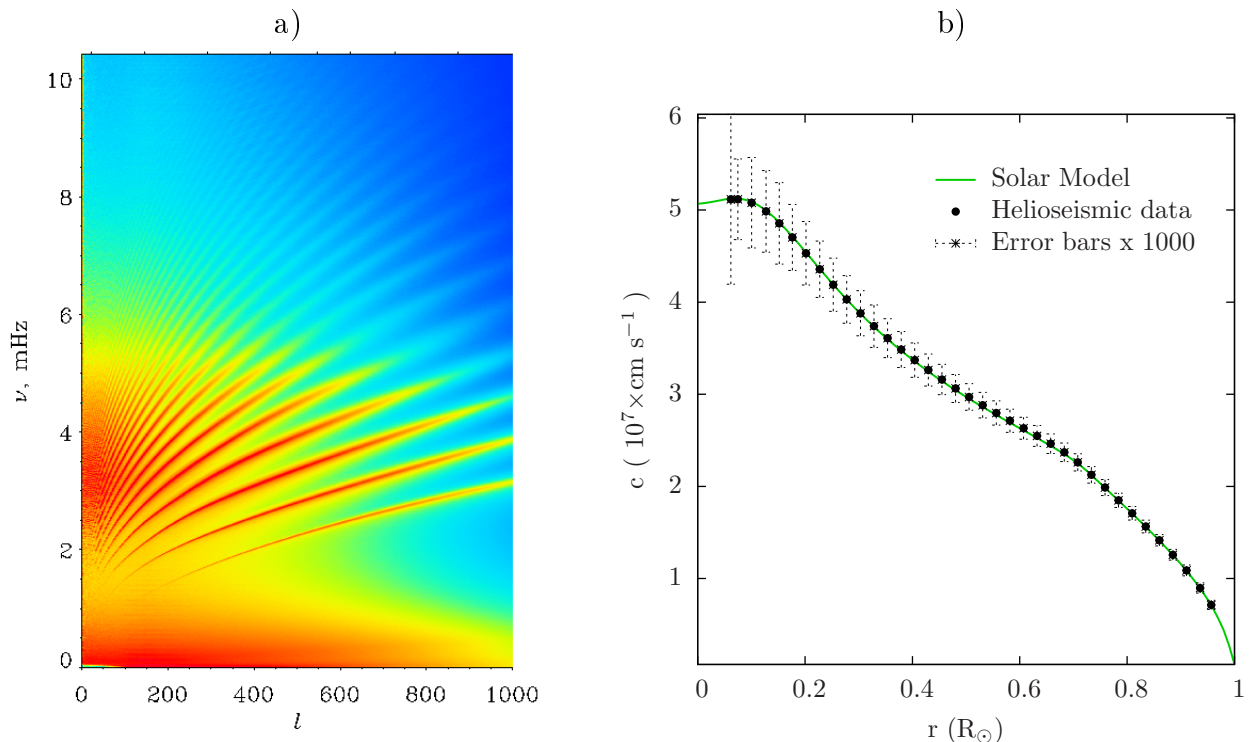


Figure 1.13: a) Power spectrum of the solar acoustic modes as measured by SOHO/MDI [68]. The ridges correspond to the normal modes with different radial order n . b) Comparison of the sound speed profile predicted by our standard solar model with that derived from the measurements of the helioseismic mission BiSON [69].

and oxygen which slowly releases its stored thermal energy and which further gravitational collapse is prevented by electron degeneracy pressure.

The success of the stellar modeling is not limited to the understanding of the different evolutionary phases of the observed stars. Remarkably, it is also able to correctly reproduce the observations of the stellar interiors. For instance, the measurement of the neutrinos originated in the solar thermonuclear reactions provides a unique window into the solar core. In particular, the ${}^8\text{B}$ flux, produced in the inner 10% (in radius) through the pp chain, is very sensitive to the central temperature of the Sun: $\phi_{8\text{B}} \propto T_c^{18}$ [64]. The standard solar model correctly predicts the ${}^8\text{B}$ and ${}^7\text{Be}$ neutrino fluxes measured by the SNO [65, 66] and Borexino [67] telescopes.

On the other hand, helioseismology has been able to probe the solar internal structure and dynamics by measuring the acoustic waves that propagate throughout the Sun. These waves, which are thought to have originated in the solar convective zone, are reflected by the solar surface and propagate into different depths depending on their frequency. The frequencies of thousands of normal modes of the solar oscillations have already been determined with high accuracy (see Figure 1.13.a). Given that the period of the oscillations (~ 5 min) is much smaller than the solar evolutionary timescale, the oscillations can be considered as

small perturbations around a static equilibrium state, and the frequencies of the modes can be used to determine the properties of the solar interior. The first helioseismic inversions date from the early 80's [70]. Nowadays, the sound speed profile of the Sun is measured with high precision and is accurately reproduced by standard solar models (see Figure 1.13.b). It is worth noticing that two helioseismically measured quantities, the location of the base of the solar convective envelope and the surface helium mass fraction, are in disagreement with the results of present solar models, leading to the so-called solar abundance problem [63]. This discrepancy may be solved with a revision of the Ne/O abundance [71] or with further improvements of the solar modeling, which may include the accretion of material from the protoplanetary disk [72] and the incorporation of dynamical processes such as rotation or magnetism.

Asteroseismology extends the principles of helioseismology to the study of different types of pulsating stars. In particular, solar-like oscillations have already been detected in hundreds of stars [73]. The identification of the frequency of maximum power (ν_{max}) and the large frequency separation ($\Delta\nu_{n,l} = \nu_{n,l} - \nu_{n-1,l}$, where n is number of nodes in the radial direction and l the spherical harmonic degree) has been used to determine the radii of main-sequence stars with an accuracy better than $\sim 4\%$ [74]. In addition, other seismic parameters such as the small separation ($\delta\nu_{n,l} = \nu_{n,l} - \nu_{n-1,l+2}$) are sensitive to the temperature and chemical gradient in the deep interior and can be used to detect the presence of a convective core inside a star [75, 76]. The prospects of asteroseismology to test theories of stellar evolution and to probe the stellar interiors are promising, with hundreds of giants and main-sequence stars being presently observed by the *CoRoT* and *Kepler* missions.

The accuracy of stellar modeling, tested with the high precision observations of the Sun and other stars, allows the use of stars to investigate dark matter.

1.3 Using stars to investigate Dark Matter

Historical perspective

The first studies on the effects that hypothetical dark matter particles may produce on stars were performed in the 80's in the context of a possible solution to the old solar neutrino problem. It was shown that the existence of weakly interacting massive particles would simultaneously solve the problem of the missing mass in the Universe and reconcile the predictions of the solar models with the unexplained low measurements of the ^8B solar neutrinos [77, 78, 79, 80, 81, 82, 83]. Soon after these seminal works it was pointed out that helioseismology, in particular the analysis of the frequency separations of the solar low-degree p-modes, provided an independent test of the presence of WIMPs inside the Sun because of its sensitivity to the solar core [84, 85]. These works constitute the first attempts to use the

properties of stars to investigate the nature of dark matter.

Following the pioneer works mentioned above, and still on the decade of the 80's, these studies were generalized to other stars such as horizontal-branch stars [86, 87], main sequence stars [88] and red giants [89]. These works demonstrated that, in some cases, dark matter particles may strongly influence stellar evolution. Despite the fact that some potential observable signatures were found, such as the thermal pulses induced on horizontal-branch stars [90], the lack of availability of numerical codes and precise stellar observations at that time prevented these studies to progress any further. After the confirmation of the neutrino oscillations [91, 92], the interest in this topic decreased temporarily.

The formalism used nowadays to compute the influence of dark matter particles on stars was already developed in these early works. It accounts for the processes of stellar capture of dark matter particles, their accumulation and distribution inside the star, and their influence on the star by providing a new cooling mechanism and by self-annihilating.

Stellar capture and distribution of DM particles

Firstly, it is necessary to calculate the number of DM particles that accumulate in the stellar core. Stars are assumed to be embedded in a halo of DM particles which can be gravitationally captured by the star. The fraction of captured DM particles can be significant, provided that these particles have a non-negligible scattering cross section with baryons. In this case, some of the DM particles collide with the stellar plasma, lose some energy, and are therefore more easily captured. The capture rate is usually computed according to the expressions of Gould [93]:

$$C_{\chi}(t) = \sum_i \int_0^{R_{\star}} 4\pi r^2 \int_0^{\infty} \frac{f_{v_{\star}}(u)}{u} w \Omega_{v,i}^{-}(w) du dr , \quad (1.3)$$

$$\Omega_{v,i}^{-}(w) = \frac{\sigma_{\chi,i} n_i(r)}{w} \left(v_e^2 - \frac{\mu_{-,i}^2}{\mu_i} u^2 \right) \theta \left(v_e^2 - \frac{\mu_{-,i}^2}{\mu_i} u^2 \right), \quad (1.4)$$

$$\mu_i \equiv \frac{m_{\chi}}{m_{n,i}}, \quad \mu_{\pm,i} \equiv \frac{\mu_i \pm 1}{2}, \quad (1.5)$$

where:

$\Omega_{v,i}^{-}(w)$ is the rate of scattering of a DM particle with the nucleus of an element i , from an initial velocity w at the radius of the collision to a velocity lower than the escape velocity of the star $v_e(r)$ at that radius,

$f_{v_{\star}}(u)$ is the velocity distribution of the DM particles seen by the star, which depends on the velocity of the star v_{\star} and on the velocity distribution of the DM particles in the

halo $f_0(u)$, which is usually assumed to be a Maxwell-Boltzmann distribution with a dispersion \bar{v}_χ ,

m_χ is the mass of the DM particle,

$\sigma_{\chi,i}$ is its scattering cross section with an element i , which is: $\sigma_{\chi,i} = \sigma_{\chi,SI} A_i^2 \left(\frac{m_\chi m_{n,i}}{m_\chi + m_{n,i}} \right)^2 \left(\frac{m_\chi + m_p}{m_\chi m_p} \right)^2$ for all stellar elements except for hydrogen, which also has the contribution from the spin dependent (SD) interactions: $\sigma_{\chi,H} = \sigma_{\chi,SI} + \sigma_{\chi,SD}$.

$m_{n,i}$, A_i are the nuclear mass and the atomic number of the element i ,

$n_i(r)$ is the density of the element i at a radius r , and

R_\star is the total radius of the star.

For stellar elements other than hydrogen a suppression form factor is considered to account for the influence of the size of the nucleus on the interactions. Thus, the scattering rate is:

$$\Omega_{v,i}^-(w) = \frac{\sigma_{\chi,i} n_i(r)}{w} \frac{2E_0}{m_\chi} \frac{\mu_{+,i}^2}{\mu_i} \left\{ \exp\left(-\frac{m_\chi u^2}{2E_0}\right) - \exp\left(-\frac{m_\chi u^2}{2E_0} \frac{\mu_i}{\mu_{+,i}^2}\right) \exp\left(-\frac{m_\chi v_e^2}{2E_0} \frac{\mu_i}{\mu_{-,i}^2} \left(1 - \frac{\mu_i}{\mu_{+,i}^2}\right)\right) \right\}, \quad (1.6)$$

where $E_0 \simeq 3\hbar/(2m_{n,i}(0.91m_{n,i}^{1/3} + 0.3)^2)$ is the characteristic coherence energy.

Once the dark matter particles are captured they accumulate in a very small region in the core of the star. Their distribution can be approximated by a thermal distribution in which the WIMPs have all the same temperature, T_χ , equal to the central temperature of the regular baryonic matter inside the star T_c . Thus, the normalized density number distribution n_χ is given by $n_\chi(r) = \pi^{-3/2} r_\chi^{-3} e^{-r^2/r_\chi^2}$ [94, 95, 96], where $r_\chi = \sqrt{3\kappa_B T_c / 2\pi G \rho_c m_\chi}$ is the characteristic radius of this isothermal distribution. In the limit when the ratio between the WIMPs mean free path $l_\chi = (\sum \sigma_{\chi,i} n_i(r))^{-1}$, where the sum goes over all the stellar elements, and r_χ , $K_\chi = l_\chi / r_\chi$ (the so-called Knudsen number), is very small, the WIMPs collide so often that they are in local thermal equilibrium with the stellar plasma, so $T_\chi(r) = T_\star(r)$. In this case the normalized WIMPs number distribution is [97]:

$$n_\chi(r) = \left(\frac{T(r)}{T_c} \right)^{3/2} \exp\left(-\int \frac{k_B \alpha(r) \frac{dT}{dr} + m_\chi \frac{d\phi}{dr}}{k_B T(r)} dr\right). \quad (1.7)$$

To calculate the total number of DM particles that are accumulated inside the star at a given time, $N_\chi(t)$, two additional processes have to be also taken into account: the

evaporation rate E_χ and the annihilation rate A_χ :

$$\frac{dN_\chi}{dt} = C_\chi - 2A_\chi N_\chi^2 - E_\chi N_\chi, \quad (1.8)$$

where A_χ depends on the velocity-averaged annihilation cross section $\langle\sigma_a v\rangle$,

$$A_\chi = 4\pi \int_0^{R_\star} r^2 \frac{\langle\sigma_a v\rangle n_\chi^2}{2} dr, \quad (1.9)$$

and E_χ is negligible for the cases studied in this Thesis [98], thus:

$$N_\chi(t) = C_\chi \tau_{\chi,eq} \tanh\left(\frac{t}{\tau_{\chi,eq}}\right). \quad (1.10)$$

The annihilation and capture processes rapidly balance each other (when A_χ reaches the value of $C_\chi/2$), in a timescale $\tau_{\chi,eq} \approx \sqrt{\pi^{3/2} r_\chi^3 / (C_\chi \langle\sigma_a v\rangle)}$ much shorter than the stellar evolutionary timescale, leading to an equilibrium with a constant number of WIMPs inside the star: $N_{\chi,eq} = C_\chi \tau_{\chi,eq}$. For DM candidates such as asymmetric DM the number of WIMPs inside the star grows indefinitely: $N_\chi(t) = C_\chi t$.

Dark matter energy production

The self-annihilation of DM particles acts as a new source of energy for the star, as most of the products of the DM annihilations interact with the stellar plasma, transferring their energy to the star. Only a fraction, which we conservatively assume to be a third, escapes the star in the form of neutrinos. When the capture and annihilation processes are in equilibrium, the total luminosity injected by the DM annihilations is:

$$L_{\chi,prod} = \frac{2}{3} C_\chi m_\chi. \quad (1.11)$$

As it will be shown in this Thesis, the energy from the DM annihilations may be important for stars embedded within a very dense DM halo. However, for environmental DM densities such as those expected in the solar neighborhood, the dominant factor by which the DM particles may influence a star is by providing a new energy transport mechanism.

Dark matter energy transport

The accumulated dark matter particles provide a new cooling mechanism, which efficiency depends mainly on the Knudsen number of the system [78]. We have implemented the energy

transport following the prescription of Ref. [97]:

$$L_{\chi,trans}(r) = 4\pi r^2 n_{\chi}(r) l_{\chi} \kappa(r) \left(\frac{k_B T(r)}{m_{\chi}} \right)^{1/2} k_B \frac{dT}{dr} f(K) h(r), \quad (1.12)$$

where the suppression factors $f(K) = 1 - (1 + (0.4/K)^{1/\tau})^{-1}$ and $h(r) \approx ((r - r_{\chi})/r_{\chi})^3 + 1$ were introduced to extend the expression for the energy transport in local thermal equilibrium to regimes with a larger mean free path l_{χ} and a larger K_{χ} . The factors $\alpha(r) = \sum_i [(\sigma_{\chi,i} n_i(r) \alpha_i(\mu_i)) / \sum_j \sigma_{\chi,j} n_j(r)]$ and $\kappa(r) = [l_{\chi} \sum_i (\sigma_{\chi,i} n_i(r) / \kappa_i(\mu_i))]^{-1}$ approximate the thermal diffusivity and conductivity, respectively, by averaging over the individual α_i and κ_i obtained by Ref. [97] numerically solving the Boltzmann collision equation for a gas of WIMPs and nucleus i . The tabulated values of α_i and κ_i , as well as the asymptotic behavior for $m_{\chi} \gg m_{nuc,i}$, can be found in Ref. [97].

The DMP-CESAM code

It was not until a decade ago that the formalism described above was introduced in modern stellar evolution codes. Lopes *et al.* [99] implemented the capture, energy transport, and self-annihilation of Dark Matter Particles (DMP) in **CESAM** [100], a self-consistent numerical code for stellar structure and evolution developed during 10 years by P. Morel and his team at Nice Observatory, France. The main physical inputs of the stellar models of the **CESAM** code are the following: the nuclear reaction rates are taken from Adelberger *et al.* [101], with the Mitler [102] intermediate screening; the opacities are taken from the OPAL95 tables [103] for temperatures above 5600 K and from Alexander & Ferguson [104] for lower temperatures; the tabulated OPAL EOS [105] are used; microscopic diffusion is included following the prescription of Michaud & Proffitt [106]; and the stellar composition is taken from the solar abundances in Asplund *et al.* (2005) [107].

The first version of the **DMP-CESAM** code was designed for the study of the effects of dark matter on the Sun. More recently (see [108]), the code was upgraded with the full formalism for the calculation of the capture rate, thanks to the implementation of modified subroutines of the **DarkSUSY** code [109], allowing the computation of the dark matter capture by other stars. The **DMP** code has also been upgraded to interact with the new version of **CESAM**, the **CESAM2k** code, which includes more up-to-date calculations of the standard stellar physical processes (see [110]) and the more recent determination of the solar composition [62]. Moreover, the present version of **DMP-CESAM** allows the calibration of models of stars different than the Sun. The code also interacts with the **ADIPLS** package [111] to compute the frequencies of the stellar oscillation modes.

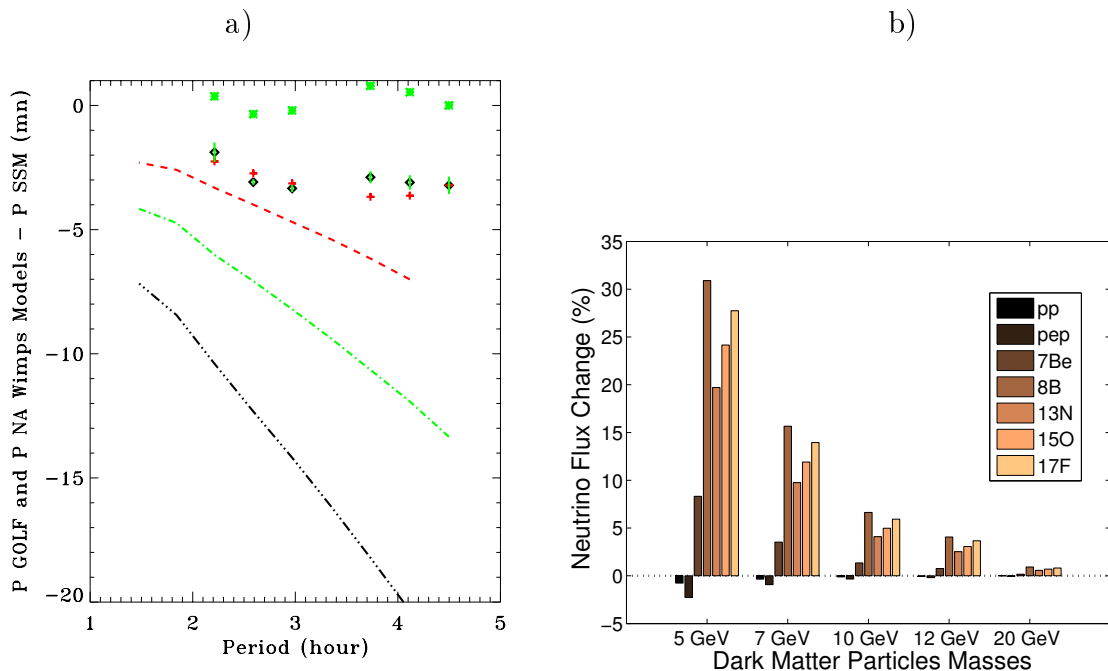


Figure 1.14: (a) Solar gravity mode period differences between GOLF measurements (circles with error bars) or the standard solar model [120] (crosses) and a DM-modified solar model [118] or between GOLF and the standard solar model (stars). Superimposed are non-annihilating DM models with spin-dependent cross sections of $5 \cdot 10^{-36} \text{ cm}^2$ for respectively 5, 7 and 10 GeV (black, green and red lines). From Ref [119]. (b) Percentage decrease changes in the solar neutrino fluxes when the accumulation of non-annihilating dark matter particles in the center of the Sun is taken into account. The dark matter particles scatter with nucleons with $\sigma_{SD} = 10^{-40} \text{ cm}^2$ and $\sigma_{SI} = 10^{-37} \text{ cm}^2$. From Ref. [121].

The Sun and other Stars as Dark Matter probes

The Sun, being observed and modeled with a high precision, can be used as a laboratory to test the existence and the nature of dark matter particles. In Refs. [99, 112, 113, 114] it was shown that, for a certain range of WIMP-proton spin-dependent scattering cross sections and masses, the accumulation of WIMPs in the Sun leads to a small reduction of the solar central temperature with potentially detectable modifications in the solar neutrino flux and in the low-degree acoustic modes of solar oscillations. Presently, this topic has drawn the attention of several groups. The impact of several DM candidates on the Sun has been studied, and constraints have been derived for types of DM particles with particular properties such as those of asymmetric DM and self-interacting DM [115, 116, 117]. The analysis of the solar gravity modes ([118, 119], see Figure 1.14. a) and the solar neutrinos from various thermonuclear reactions ([122], see Figure 1.14.b) seem the most promising strategies, as they have been shown to probe a region of the DM parameter space which, for cases such as the isospin-violating DM, is compatible with present bounds from direct

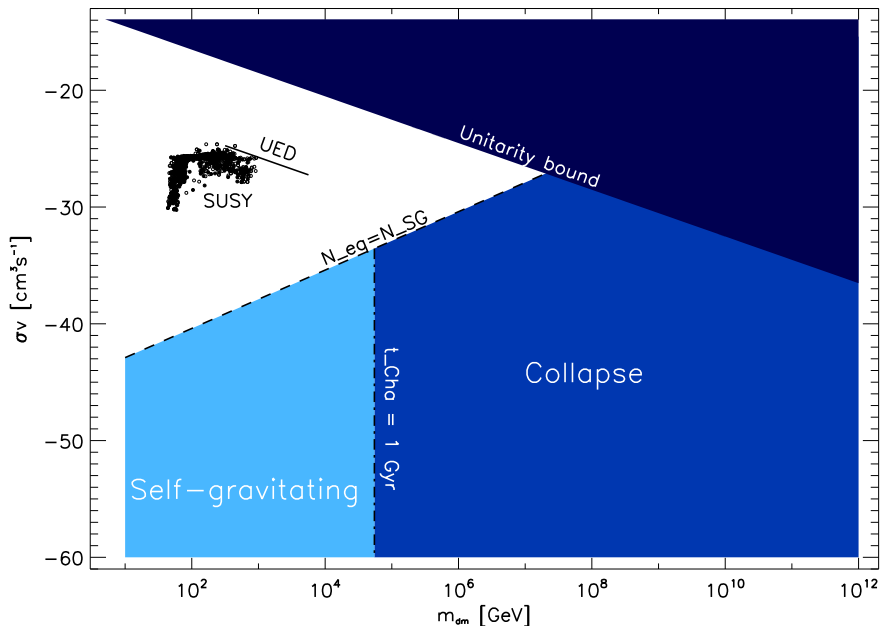


Figure 1.15: For DM particles with masses (x-axis) and annihilation cross sections (y-axis) as those in the region labeled "collapse", neutron stars are thought to be rapidly destroyed due to the gravitational collapse of the DM into a Black Hole. This approach was used to put constraints on the DM parameters in Ref. [129].

detection experiments [121].

The impact of DM has also been extensively studied in the case of other stars. Very compact objects such as neutron stars and white dwarfs have been shown to capture DM particles very efficiently. In environments with very high DM densities, this scenario may lead to unusually hot stars, powered by the annihilation of DM particles instead of by thermonuclear reactions [123, 124, 125]. On the other hand, the extra cooling in white dwarfs has been used to constrain the mass of axion DM [126, 127, 128]. For asymmetric DM candidates, the accumulation of huge quantities of DM may lead to the destruction of the neutron star after the formation of a black hole in the stellar core [129, 130, 131, 132, 133, 134, 135]. Therefore, the simple observation of the existence of neutron stars has been used to derive some constraints on the properties of the DM particles (see Figure 1.15).

Of particular interest is the case of the first stars formed in the early Universe. These stars are thought to have formed in the center of primordial DM halos. The adiabatic contraction of the DM halo due to the collapse of the protostar leads to extremely high DM densities and therefore to the annihilation of huge amounts of DM, which can act as the only source of energy of the star [136, 137, 138, 139, 140, 141, 142, 143, 144], although this is still a controversial possibility (see also [145]). When the star runs out of its original DM, which takes about a million years [146], this stalling phase ends and the collapse continues

until capture replenishes the fuel for DM annihilation [147]. The implications for the cosmic reionization, the pair production supernova rate and the cosmic microwave background were also studied [148, 149, 150], as well as the prospects for observation of such unusual first stars (the so-called Dark Stars) by next-generation telescopes [151, 152, 153].

As it will be shown in the next Chapter, the accumulation of self-annihilating dark matter particles may also have a strong impact on main-sequence stars in our own Galaxy. This topic has also been addressed in the literature, in a series of works (see Refs. [154, 155, 156]) which have been computed with the publicly available `DarkStars` code [157].

2

Summaries of the publications

In this Chapter, the main conclusions of each of the publications included in this Thesis are briefly summarized. The original publications are presented in the Appendix.

The core of this Thesis is constituted by the publications [Paper I](#), [Paper II](#), [Paper III](#), [Paper IV](#) and [Paper V](#). In these publications we presented a contribution to the investigation of the dark matter problem from a complementary perspective to ongoing direct and indirect searches: we proposed the use of stars as tools to test and constrain the dark matter particle candidates that are being put forward by particle physicists.

In addition, in [Paper VI](#) a similar approach was applied to show that the precise knowledge of the solar interior, thanks to solar neutrinos and helioseismic data, can be used to efficiently constrain alternative theories of gravity.

Following the regulations of the IST PhD program, we specify here the contribution of the candidate to the publications. In [Paper I](#), [Paper II](#), [Paper III](#), [Paper IV](#) and [Paper V](#) the candidate performed necessary modifications in the codes, ran the computations, analyzed and interpreted the results (together with the other authors), created all the figures and tables and wrote most of the article. In [Paper VI](#) the modifications on the code were done together with another author. The candidate ran the computations, analyzed and interpreted the results, created all the figures and tables and wrote sections 3.2 and 4.

2.1 The formation and evolution of young low-mass stars within halos with high concentration of dark matter particles (Paper I)

Casanellas J. & Lopes I.

The Astrophysical Journal, 705, 135-14 (2009)

arXiv:0909.1971

In [Paper I](#) we studied the new scenarios of stellar evolution that arise when low-mass stars are embedded within very dense halos of dark matter particles. For the first time, the evolution from the collapse of the protostar to the end of the main sequence was analyzed. Stars with different masses (from 0.7 to 3 M_{\odot}) and metallicities (from 0.0004 to 0.04) were investigated using a modified version of a sophisticated stellar evolution code (CESAM [100]).

The annihilation of captured dark matter particles in the core of the star was found to produce the following signatures on the stellar properties:

- reduction of the central temperature and, consequently, slower evolutionary speed throughout the main sequence. For instance, a star as the Sun would double its main sequence lifetime if it evolved within an extremely dense DM halo,
- creation of a convective core, due to the very concentrated production of energy by DM annihilations, in stars where we would normally expect a radiative interior,
- different evolutionary tracks in the Hertzsprung-Russell diagram, and,
- in the more extreme cases, when the annihilation of dark matter is the only source of energy of the stars, new equilibrium states in the Hayashi track where the stars may remain indefinitely (see [Figure 2.1.a](#)).

The changes in the stellar properties were found to depend critically on the characteristics of the DM particles, so the formers may potentially be used to constrain the DM parameters. In [Figure 2.1.b](#)) we showed the variations in the effective temperature of stars for different WIMP-proton spin-dependent scattering cross sections and dark matter halo densities.

While these signatures are very distinctive, their hypothetical observation is challenging: the very high DM densities required to produce these strong effects restrict the locations where these stars may be found to very specific places such as the inner parsec of our Galaxy or the dwarf spheroidal galaxies. The remoteness of these places and particularly the presence of dust in the case of the Galactic center hinder the observations of low-mass stars in these spots. We hope that further improvement on the observational techniques will allow the use of the DM diagnostic method developed in this work.

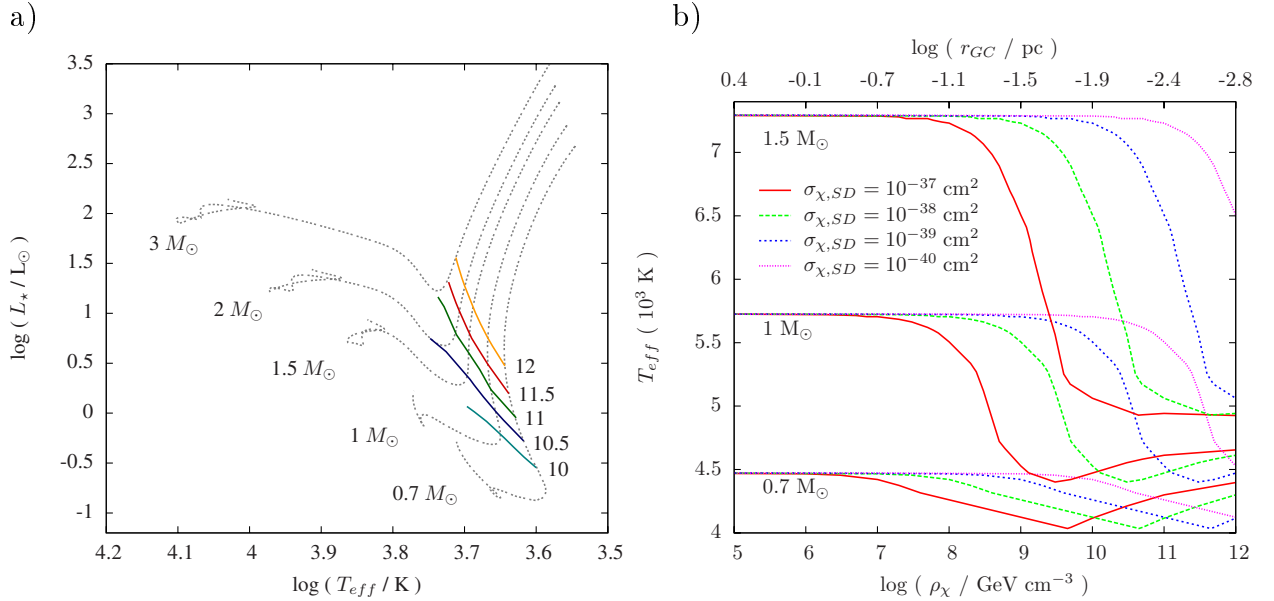


Figure 2.1: a) Stationary states reached by stars with masses from 0.7 to $3 M_\odot$ when the energy from DM annihilation compensates the gravitational energy during the collapse. These equilibrium positions, where stars will remain for an indefinite time, are plotted for different dark matter halo densities, indicated in units of $\log(\rho_\chi / \text{GeV cm}^{-3})$ at the side of each line. The grey lines are the classical evolutionary paths. b) Effective temperature of the stars as a function of the dark matter halo density, considering different WIMP-proton spin-dependent scattering cross sections. At the top horizontal axis are shown the distances to the galactic center at which these DM densities are expected to be found, following the profile of [158]. From Paper I.

Present observations of stars in the inner parsec of our Galaxy have indeed puzzling characteristics, leading to two unsolved problems: the so-called "paradox of youth" (apparently young stars observed in a region where recent star formation seems impossible, see Refs. [159, 160]) and the "conundrum of old age" (the dearth of late-type stars in the central few arcseconds, meaning that our Galactic center could have a stellar core instead of a stellar cusp, as believed for some decades, see Refs. [161, 162, 163]). Taking into account the very high DM densities expected in the Galactic center and the results of Paper I, it seems that the role of DM is crucial to understand the properties of these stars.

2.2 Towards the use of asteroseismology to investigate the nature of dark matter (Paper II)

Casanellas J. & Lopes I.

Mon. Not. R. Astron. Soc. 410, 535-540 (2011)

[arXiv:1008.0646](https://arxiv.org/abs/1008.0646)

In [Paper II](#) we explored a very characteristic signature of the annihilation of DM inside low-mass stars that had been found in our previous work: the creation of a convective core in stars which are expected to have a radiative interior. In fact, a new convective region is a major structural variation that introduces strong discontinuities in the sound-speed and density profiles of the star (see [Figure 2.2.a](#)). These discontinuities can be detected by the analysis of the stellar oscillations, in particular using asteroseismic parameters such as combinations of small separations or ratios between small and large separations of low-degree acoustic modes.

The creation of an unexpected, DM-induced convective core was found for stars that would appear as perfectly standard stars following the usual evolutionary paths through the Hertzsprung-Russell diagram. Interestingly, we demonstrated that an asteroseismic analysis of these stars would reveal the presence of self-annihilating dark matter in the stellar core. For example, a star identical to the Sun, with the same mass, metallicity, luminosity and effective temperature, but evolving within a very dense DM halo was found to show asteroseismic signatures that depend on the characteristics of the DM particles (see [Figure 2.2.b](#)).

The present observational difficulties to perform this DM diagnostic technique are the same as those reported above for the findings of [Paper I](#). However, our novel approach opened a new promising method to investigate the nature of dark matter. It set the foundations for further works (see [Paper V](#)) in which a similar strategy, for other models of DM particles, was applied to stars in the solar neighborhood which are already observed with the required precision.

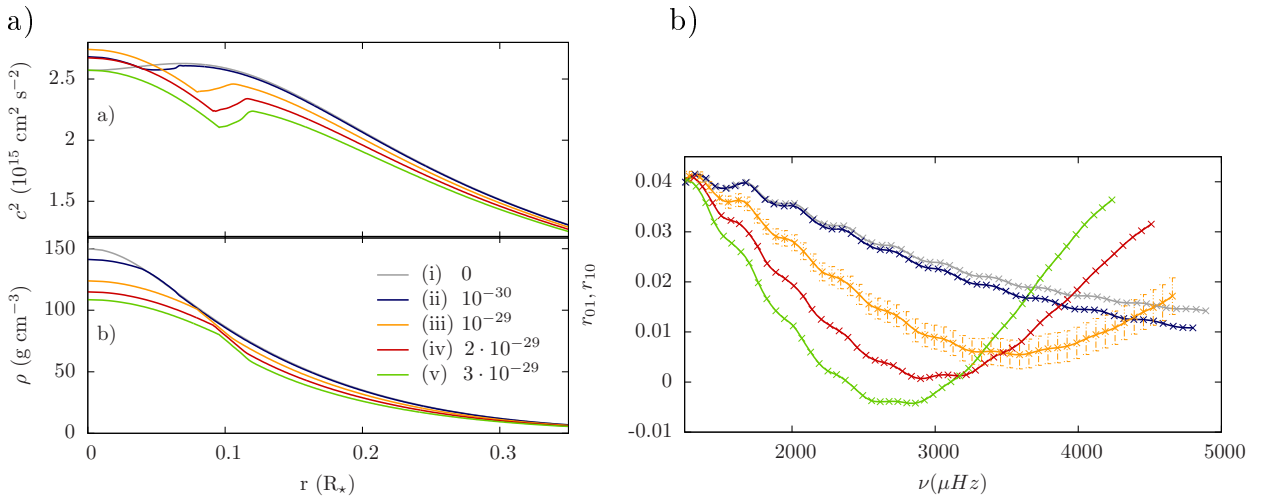


Figure 2.2: a) Sound-speed (a.a), density profiles (a.b), and b) the seismological ratios r_{01} and r_{10} of $1 M_\odot$ stars that evolved in DM halos with different densities ρ_χ and SD WIMP-nucleon cross-sections $\sigma_{\chi,SD}$ when they reached a luminosity $L = 1 L_\odot$ (for each star, the product $\rho_\chi \sigma_\chi$ is indicated in the legend in GeV cm^{-1}). Error bars are shown for star (iii) assuming a relative error in the identification of the frequencies of 10^{-4} . From [Paper II](#).

2.3 The capture of dark matter particles through the evolution of low-mass stars. (Paper III)

Lopes I., **Casanellas J.** & Eugénio D.
[Physical Review D 83, 063521 \(2011\)](#)
[arXiv:1102.2907](#)

In [Paper III](#) we addressed the question of how variations in the stellar and dark matter parameters change the rate at which stars capture dark matter particles. We realized that, in the literature, the solar values (for the stellar velocity and metallicity) and fiducial dark matter characteristics (for the mass, velocity distribution and scattering cross section off nucleons) were always assumed. Therefore, we computed the capture rate modifying the parameters mentioned above, exploring with special attention the scenario in which the spin-independent nucleon-dark matter interactions dominate the capture rate. We found that, in contrast with the general assumption of spin-dependent hydrogen collisions dominating the capture, other stellar isotopes such as oxygen, helium and iron also play an important role in capturing dark matter particles (see [Figure 2.3.a](#))

Moreover, in order to evaluate the reliability of the hypothetical use of stars other than the Sun to investigate dark matter, in [Paper III](#) we also quantified the uncertainties in the computed capture rate (C_χ) and in the ratio between the luminosities from DM annihilations and thermonuclear (L_χ/L_{nuc}) reactions derived from an imprecise knowledge of the stellar structure and DM parameters. The results are shown in the table in [Figure 2.3.b](#)). For example, we found that an uncertainty of 10% in the typical DM velocity leads to similar errors on the computed C_χ and L_χ/L_{nuc} , while the same uncertainty in the stellar mass is much more relevant and introduces errors twice as large.

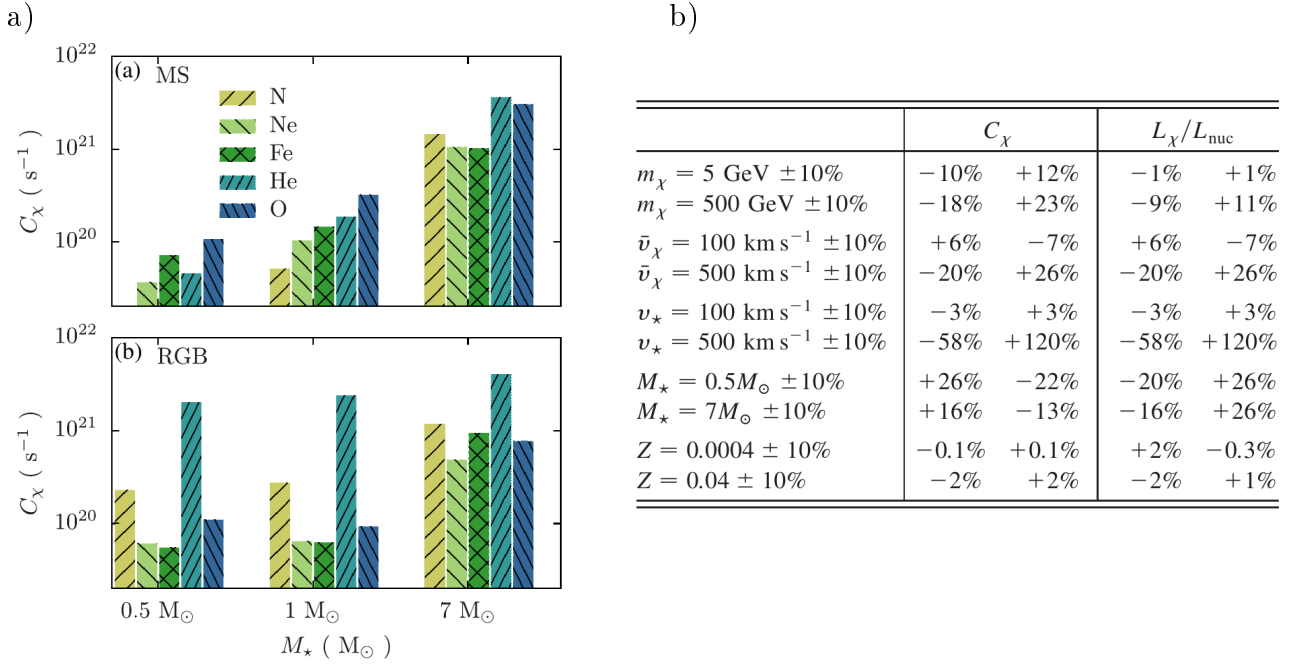


Figure 2.3: a) Rate at which DM particles are captured discriminated by the elements responsible for the collisions that lead to the capture, in the Main Sequence (a.a), and in the Red Giant Branch (a.b) for stars with different masses. b) Variations in the total capture rate, C_χ , and in the ratio between the luminosities from DM annihilations and thermonuclear reactions, L_χ/L_{nuc} , when there is an uncertainty of 10% in the knowledge of one parameter of the DM characteristics or of the stellar structure. If not stated otherwise, we assumed a halo of DM particles with masses $m_\chi = 100 \text{ GeV}$, a density $\rho_\chi = 0.3 \text{ GeV cm}^{-3}$, a velocity dispersion $\bar{v}_\chi = 270 \text{ km s}^{-1}$, a DM-nucleon scattering dominated by the spin-independent (SI) component: $\sigma_{\chi,SI} = \sigma_{\chi,SD} = 10^{-44} \text{ cm}^2$, and a star of $1 M_\odot$ in the middle of the MS, with a metallicity $Z=0.019$ and a velocity $v_\star = 220 \text{ km s}^{-1}$. From [Paper III](#).

2.4 Signatures of dark matter burning in nuclear star clusters (Paper IV)

Casanellas J. & Lopes I.

[The Astrophysical Journal Letters, 733:L51, 5pp \(2011\)](#)

[arXiv:1104.5465](#)

In our previous works we found that, for the DM candidates studied, environmental DM densities above 10^8 GeV cm^{-3} are needed to produce measurable impacts on the stellar properties. This fact reduces the observability of individual stars with the precision needed to detect the acoustic modes of the stellar oscillations. On the other hand, present observations of the Galactic center do allow the identification of the magnitude and effective temperature of the stars and their membership in stellar clusters.

Therefore, in [Paper IV](#) we studied the impacts of the stellar annihilation of dark matter particles on the global appearance of a cluster of stars. Two characteristic signatures were found (see [Figure 2.4.a](#)):

- The turnoff point of the isochrones moves to brighter and hotter positions in the Hertzsprung-Russell diagram due to the fact that low-mass stars within dense DM halos evolve at a speed slower than classical stars. Consequently, stellar clusters may be classified as younger than their true age if this effect is not properly taken into account.
- The bottom of the isochrones, corresponding to the low-mass main sequence stars, rises to higher luminosities because these stars, being only powered by DM annihilation, inflate and go back through the Hayashi track. This is a very peculiar signature so, if it is found in a stellar cluster it will be a strong indication of the presence of self-annihilating dark matter in the cluster.

It is worth noticing that the global signatures on a stellar cluster are relevant for environmental DM densities lower than those required for individual stars. For instance, if DM is formed by the 8 GeV WIMPs recently invoked to reconcile the results from different direct detection experiments, then the brighter and hotter turnoff point is predicted for halos of DM with a density *as low as* $\rho_\chi = 3 \cdot 10^5 \text{ GeV cm}^{-3}$ (see [Figure 2.4.b](#)). In addition, the identification of the shape of a cluster of stars in the Hertzsprung-Russell diagram does not require a high observational precision. These two facts encourage us to pursue, in future works, a study of the stellar clusters already observed both in the dwarf spheroidal galaxies and in the Galactic center, where stellar populations with atypical properties were already found.

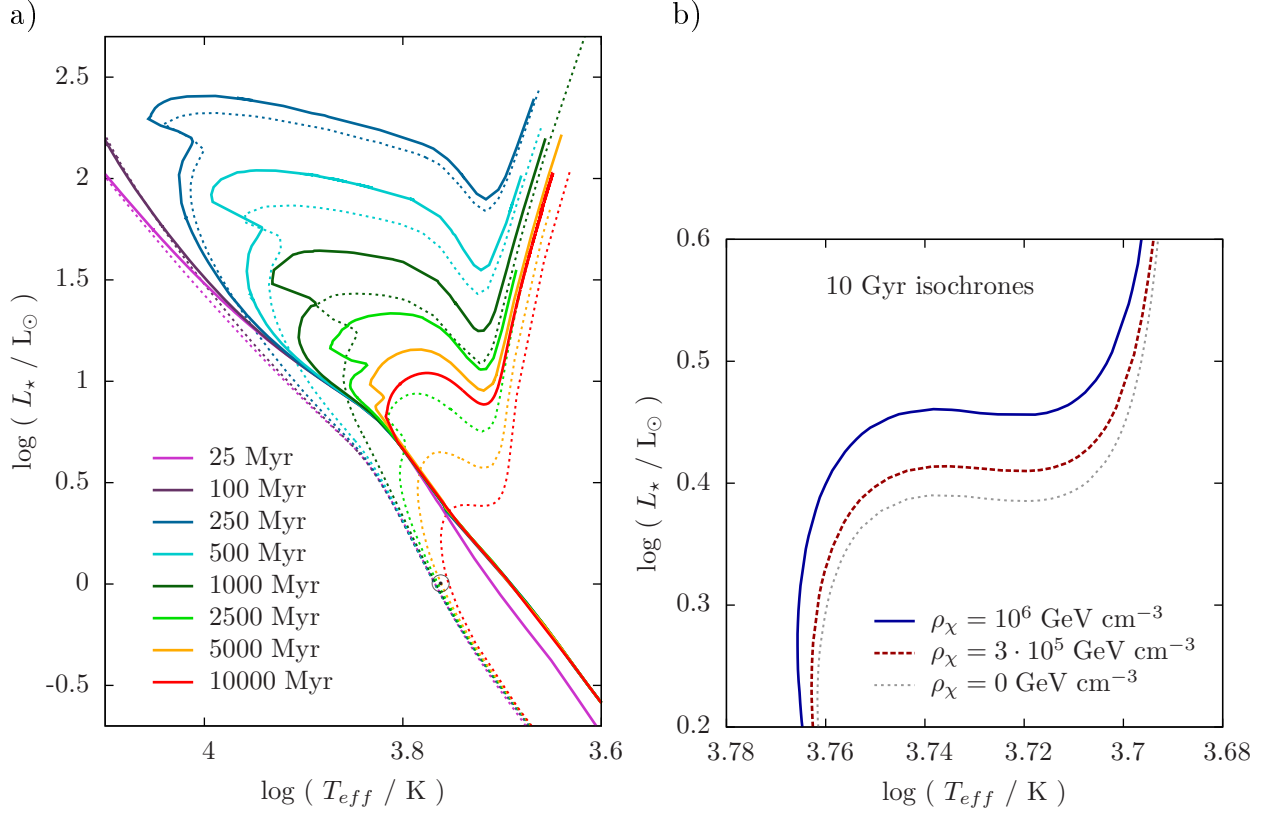


Figure 2.4: a) Isochrones for a cluster of stars with masses between $0.7 M_\odot$ - $3.5 M_\odot$ that evolved in a halo of DM with a density $\rho_\chi = 10^{10} \text{ GeV cm}^{-3}$ (continuous lines) and for the same cluster in the classical scenario without DM (dashed lines). We considered DM particles with a mass $m_\chi = 100 \text{ GeV}$ and a spin-dependent scattering cross section with protons $\sigma_{\chi,SD} = 10^{-38} \text{ cm}^2$. b) Isochrones of 10 Gyr for clusters of stars that evolved in halos of DM with different densities. We considered DM particles with the particular characteristics that fit DAMA observations and constraints from direct detection experiments: a mass $m_\chi = 8 \text{ GeV}$ and a spin-dependent scattering cross section with protons $\sigma_{\chi,SD} = 10^{-36} \text{ cm}^2$. From [Paper IV](#).

2.5 First asteroseismic limits on the nature of dark matter (Paper V)

Casanellas J. & Lopes I.
 submitted for publication
[arXiv:1212.2985](https://arxiv.org/abs/1212.2985)

Compared to the previous approaches to stellar DM searches (Paper I, Paper II, Paper III and Paper IV), in Paper V we gave a leap forward: from the purely theoretical exploration we proceeded to the modeling of real stars and the comparison with observational data. We were able to provide the first constraints to the characteristics of DM using asteroseismology and to demonstrate the potential of this technique as a complementary strategy for DM searches.

In this work we focused on the study of asymmetric DM (ADM) candidates. In this model, DM has a relic asymmetry, so it does not annihilate as thermal relic WIMPs do, leading to the accumulation of huge quantities of ADM inside stars and strong impacts on their structure.

We modeled the *Kepler* star KIC 8006161, the *CoRoT* star HD 52265, and α Cen B. The additional cooling mechanism due to accumulated asymmetric DM particles was found to reduce the central temperature and increase the central density of these stars. In addition, we found that, even for an environmental DM density as low as the expected in the solar neighborhood, the convective core expected in star HD 52265 is suppressed due to the new DM energy transport mechanism. More generally, we found that stars with masses between 1.1-1.3 M_{\odot} may lose the convective core that is predicted in the standard picture of stellar evolution. The suppression of the convective core depends on the characteristics of the DM particles (see Figure 2.5.a). Unfortunately, there is not yet a definitive asteroseismic diagnostic of the presence or the absence of a convective core in these stars.

We calibrated these stars to the observed characteristics and found that only the models not strongly influenced by the accumulated ADM were able to reproduce simultaneously all stellar parameters and the large and small frequency separations. The small separations of the acoustic modes of low degree $\langle \delta\nu_{02} \rangle$, being sensitive to the characteristics of the stellar core, were found to be systematically lower than the observed value for the models with strong impact of the DM particles. This fact is shown in Figure 2.5, where the $\langle \delta\nu_{02} \rangle$ of the calibrated stellar models of α Cen B is shown for different DM masses m_{χ} and spin-dependent proton scattering cross sections $\sigma_{\chi,SD}$. Models with low m_{χ} and large $\sigma_{\chi,SD}$ predict values of $\langle \delta\nu_{02} \rangle$ which are more than 5 observational errors away from the true value. Being α Cen B a star with its fundamental characteristics determined with high precision thanks to its

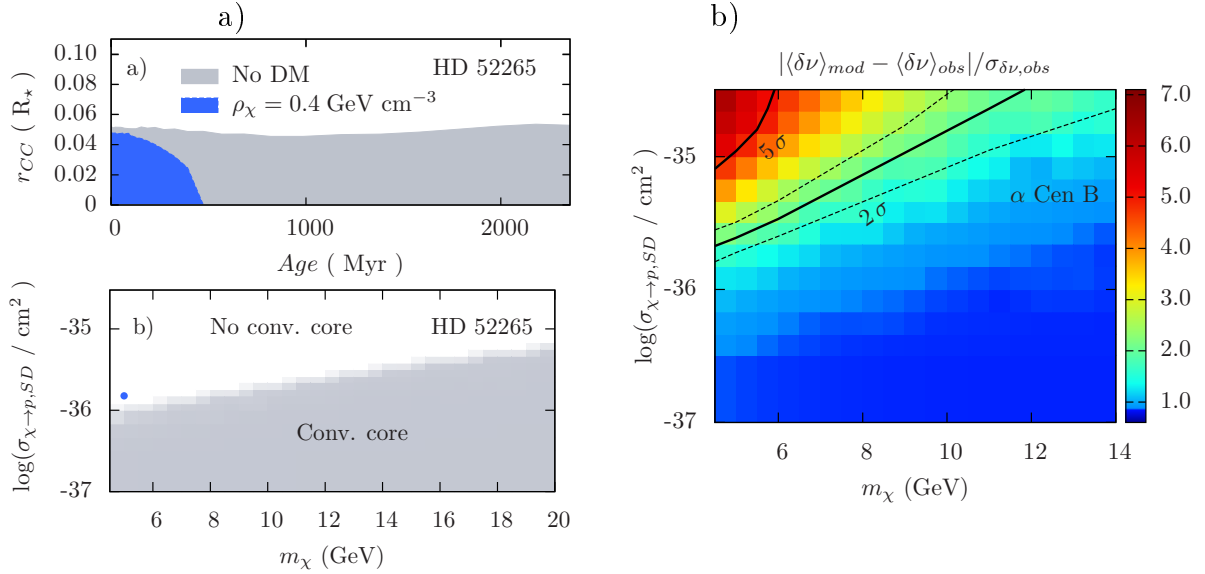


Figure 2.5: (a.a) Size and duration of the convective core in the modeling of the star HD 52265 in the classical picture (grey) and taking into account the energy transport due to the conduction of ADM particles with $m_{\chi} = 5$ GeV and $\sigma_{\chi,SD} = 1.5 \cdot 10^{-36}$ cm² (blue). (a.b) The presence of a convective core in HD 52265 depends on the mass and SD scattering cross section of the DM particles. (b) Deviation of the $\langle \delta \nu_{02} \rangle$ of the DM-modified stellar models from the true value measured in α Cen B. All the stellar models are calibrated to fit the M , L , T_{eff} , Z and $\langle \Delta \nu_{n,l} \rangle$ of α Cen B within the observational error. The dashed black lines around the 2σ line show the theoretical uncertainty in the modeling arising from the uncertainties in the stellar characteristics. The density of DM around the stars is assumed to be 0.4 GeV cm⁻³. From [Paper V](#).

belonging to a binary system, the theoretical error in the modeling is small (see dashed lines around the 2σ lines). Thus, the existence of DM particles with properties above the 2σ line can be excluded with 95% confidence level by the asteroseismic analysis of α Cen B. The constraints set using this approach are comparable with the limits from direct detection experiments, particularly for $m_{\chi} = 5$ GeV, when the sensitivity of the detectors drops.

Compared to helioseismic DM searches, asteroseismology allows the study of stars with masses lower than that of the Sun, which are more strongly influenced by the captured DM, and therefore with the potential to provide stronger constraints to the DM characteristics. In addition, it allows the analysis of stars with 1.1 - $1.3 M_{\odot}$. An asteroseismic determination of the presence or the absence of a convective core in these type of low-mass stars may provide further constraints to the DM characteristics.

Even more promising seems the future prospects for asteroseismic DM searches. If the small frequency spacings are identified in the oscillations of stars located in environments with high expected DM densities, such as globular clusters, then the sensitivity of the approach we proposed will reach much smaller WIMP-baryon scattering cross sections and larger WIMP masses. Moreover, in the event of a successful identification of the properties of DM through a

combined analysis of hypothetical positive results in different experiments, asteroseismology may allow the determination of the density of DM at any specific location where a star is observed.

2.6 Testing alternative theories of gravity using the Sun (Paper VI)

Casanellas J., Pani P., Lopes I. & Cardoso V.
The Astrophysical Journal, 745:15, 6pp, (2012)
 arXiv:1109.0249

In **Paper VI** we extended the approach developed during the previous works, that is using the stellar properties to probe fundamental physics, to the field of gravitational theories. General relativity is a successful theory that has been tested at very different scales. However, much less is known about the validity of Einstein's equations inside matter. In this work we demonstrated that the precision of solar modeling and of solar observations provide the first constraints to the gravity-matter coupling.

We focused on a particular alternative theory, an Eddington-inspired gravitational theory recently proposed by Bañados and Ferreira [164], which is equivalent to general relativity in vacuum, but its gravity-matter coupling results in non-singular cosmology and collapse. Inside matter, this theory leads to a modified Poisson equation for the gravitational field and, consequently, to a modified hydrostatic equilibrium equation in the solar modeling. This equation can be re-written as the classical hydrostatic equilibrium equation, but with an effective gravitational constant: $G_{\text{eff}}(r) \equiv G + \frac{\kappa_g r^2 \rho'(r)}{4 m(r)}$, where κ_g is the only parameter of the theory, which we aimed to constrain. Since $\rho'(r) < 0$ inside the Sun, $G_{\text{eff}} \leq G$ when $\kappa_g \geq 0$. When $\kappa_g < 0$, we expect a stronger effective gravitational force which, for main sequence stars in hydrostatic equilibrium, leads to an increase in the central temperature and, consequently, in the rate of thermonuclear reactions.

We explored the signatures of this modified gravity in the solar neutrino fluxes and in several helioseismic parameters. The strongest constraints arose from the comparison of modified calibrated solar models and helioseismic data, in particular from the differences in the sound-speed profiles and in the small frequency separations of low degree (see Figure 2.5.a). In addition, modified solar models with a large negative value of the parameter κ_g led to predictions of the ^8B neutrino flux more than 40% greater than the predictions of our standard solar model (see Figure 2.5.b). In summary, we were able to establish the first constraints in the strength of the gravity-matter coupling, excluding values of $|\kappa_g| \gtrsim 3 \times 10^5 \text{m}^5 \text{s}^{-2} \text{kg}^{-1}$ (see Figure 2.5.c).

In addition, we also studied the implications of the Eddington-inspired gravity theory in the context of the solar abundance problem [63]. Models with $\kappa_g < 0$ predict the base of the convective envelope at a smaller radius than the standard solar model, reconciling the prediction with the helioseismically inferred value. However, the predicted helium surface abundance for the same models with $\kappa_g < 0$ is then even more underestimated than for

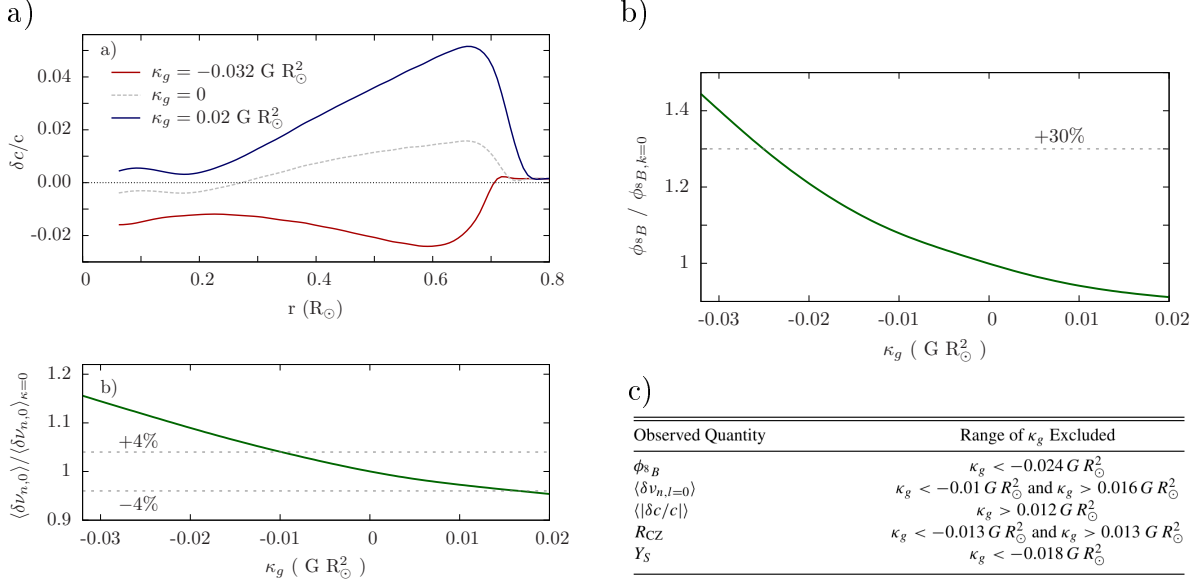


Figure 2.6: (a.a) Relative differences between the sound speed profiles of our modified solar models and the solar sound speed from helioseismic data [165]. (a.b) Mean small separation for $l=0$ and $\nu > 2000 \mu\text{Hz}$ for our modified solar models, normalized to the prediction for $\kappa_g = 0$. (b) ^8B neutrino flux predicted by our modified solar models normalized to the flux predicted by our standard solar model. (c) Summary of the range of the parameter κ_g ruled out using different solar characteristics. From Paper VI.

standard solar models. Although this particular theory only offers a partial solution to this problem, other gravitational corrections could affect the solar interior in a different way and may be relevant as an alternative approach to the solar abundance problem.

3

Conclusions

In this Thesis we have developed a new approach to investigate the nature of dark matter. The dark matter particles of the galactic halo are efficiently captured by low-mass stars and accumulate in their cores. In some cases, this fact leads to a strong impact on the stellar properties. We have demonstrated that the observation of the existence/absence of the influence of dark matter on stars can be used to learn about the dark matter characteristics.

We first studied the new stellar evolutionary scenarios that arise when the self-annihilation of gravitationally captured dark matter particles is taken into account. For environments with very high dark matter densities, such as those expected in the Galactic center, we predicted very characteristic signatures in the properties of low-mass stars ([Paper I](#)).

Then, using one of those signatures, we proposed a method to identify a dark matter burning core inside a star similar to the Sun. The self-annihilation of huge quantities of dark matter creates a convective core, unexpected in $\sim 1 M_{\odot}$ stars, that leaves a distinctive imprint in the stellar oscillations. Asteroseismology can thus be used to indirectly detect dark matter, being able to distinguish the impact of dark matter in stars that would appear as normal stars in the Hertzsprung-Russell diagram ([Paper II](#)).

Since the rate at which a star captures dark matter particles is the critical quantity in the problem studied in this Thesis, we then addressed in a thorough way the dependencies of this quantity on the characteristics of the stars and the dark matter particles. We evaluated the error on the capture rate, as well as on the weight of the dark matter annihilations over

the classical stellar energy sources, arising from uncertainties in the knowledge of the stellar mass, metallicity, velocity, and the dark matter mass and velocity distribution. We also studied the scenario where the spin-independent dark matter-nucleon interactions dominate, characterizing the stellar isotopes that are responsible for most of the collisions leading to dark matter captures (Paper III).

We also characterized the impacts of the stellar capture and annihilation of dark matter particles on the global properties of a cluster of stars. We found that the age of a nuclear star cluster may be underestimated if the influence of dark matter is not taken into account. In addition, in the more extreme case of very high environmental dark matter densities, we predicted a very peculiar dark matter signature in the shape of the clusters in the Hertzsprung-Russell diagram (Paper IV).

The influence of dark matter annihilations on stars is very likely occurring at this moment in locations with very high environmental dark matter densities such as the center of our Galaxy. However, the present observation of these signatures is particularly difficult due to two reasons: (i) the distance and the presence of dust towards the Galactic center; (ii) the fact that only the stars with low masses, and therefore with the lower intrinsic luminosities, are influenced enough by the dark matter annihilation. These difficulties may be overcome with eventual experimental improvements in the observations or with the study of the dark matter effects on giant (and thus more luminous) stars, the latter a strategy we aim to pursue in the near future. Further promising locations to observe these effects are globular clusters and dwarf spheroidal galaxies, where very high dark matter densities are also predicted. Moreover, other dark matter particle candidates may have specific properties that can lead to observable effects in nearby stars.

This is the case of non-annihilating dark matter particles (i.e. asymmetric dark matter). In this scenario, the dark matter accumulated in the stellar cores provides a new cooling mechanism, modifying the central properties of the stars and eventually suppressing the convective core expected in 1.1-1.3 M_{\odot} stars, even for an environmental dark matter density as low as the expected in the solar neighborhood. We proposed the use of asteroseismology to search for these modifications, since the stellar oscillations, namely the acoustic modes of low degree, are sensitive to the properties of the core of the stars. Remarkably, we were able to provide the first asteroseismic constraints to the dark matter characteristics, namely to the mass of the dark matter particle and to the strength of its spin-dependent interactions with protons, by analyzing the oscillations of the star α Cen B (Paper V).

This new approach to investigate the nature of dark matter has promising prospects. Asteroseismology has reached the necessary maturity and is presently providing the first insights in the structure of stars at different evolutionary stages. The *Kepler* and *CoRoT* missions are observing hundreds of main-sequence stars and red giants, which oscillation

frequencies have the potential to provide further constraints to the dark matter characteristics. Stars with masses lower than that of the Sun and stars that theoretically lose their convective core due to the dark matter are particularly promising targets. Red giants may also have interesting prospects, a possibility we intend to explore in future studies.

In the hypothetical event of a successful identification of the dark matter properties, which may happen only after the combination of positive results in different experiments, the signatures and strategies described in this Thesis may provide a method to indirectly measure the density of dark matter at any specific location where a star is observed, helping to understand the shape of galactic dark matter halos. Moreover, in this scenario, the impact of the $\sim 83\%$ of the matter of the Universe on the $\sim 1\%$ that constitutes the stars will have to be understood. We hope this Thesis may help to provide a first approach toward this objective.

On the other hand, if dark matter continues to evade the attempts to its identification, an innovative approach such as the proposed in this Thesis will be particularly valuable as a complementary strategy to ongoing dark matter searches. In this Thesis we have demonstrated that stellar dark matter searches provide constraints to the dark matter properties comparable to present direct detection experiments.

In addition to our contribution to the investigation of the dark matter problem, in this Thesis we have also proved that the high precision of solar modeling and observations can be used to test alternative theories of gravity. We have studied the case of an Eddington-inspired modified theory of gravity, equivalent to standard gravity in vacuum but significantly different from it within matter, resulting in modifications in the hydrostatic equilibrium equation for compact objects. If this theory is valid we would expect variations in the solar temperature and density profiles and, in turn, changes in the predicted solar neutrino fluxes and solar oscillations, which strength depends on the only parameter of the theory. Comparing our sophisticated modified solar model with the observations, we were able to establish the first constraints to the gravity-matter coupling ([Paper VI](#)).



Appendix: Publications

A.1 Paper I

THE FORMATION AND EVOLUTION OF YOUNG LOW-MASS STARS WITHIN HALOS WITH HIGH CONCENTRATION OF DARK MATTER PARTICLES

Casanellas J. & Lopes I.

The Astrophysical Journal, 705, 135-14 (2009)

arXiv:0909.1971

THE FORMATION AND EVOLUTION OF YOUNG LOW-MASS STARS WITHIN HALOS WITH HIGH CONCENTRATION OF DARK MATTER PARTICLES

JORDI CASANELLAS¹ AND ILÍDIO LOPES^{1,2}

¹ Centro Multidisciplinar de Astrofísica, Instituto Superior Técnico, Av. Rovisco Pais, 1049-001 Lisboa, Portugal; jordicasanelas@ist.utl.pt

² Departamento de Física, Universidade de Évora, Colégio António Luis Verney, 7002-554 Évora, Portugal; ilidio.lopes@ist.utl.pt

Received 2008 October 24; accepted 2009 September 2; published 2009 October 8

ABSTRACT

The formation and evolution of low-mass stars within dense halos of dark matter (DM) leads to evolution scenarios quite different from the classical stellar evolution. As a result of our detailed numerical work, we describe these new scenarios for a range of DM densities on the host halo, for a range of scattering cross sections of the DM particles considered, and for stellar masses from 0.7 to 3 M_{\odot} . For the first time, we also computed the evolution of young low-mass stars in their Hayashi track in the pre-main-sequence phase and found that, for high DM densities, these stars stop their gravitational collapse before reaching the main sequence, in agreement with similar studies on first stars. Such stars remain indefinitely in an equilibrium state with lower effective temperatures ($|\Delta T_{\text{eff}}| > 10^3$ K for a star of one solar mass), the annihilation of captured DM particles in their core being the only source of energy. In the case of lower DM densities, these protostars continue their collapse and progress through the main-sequence burning hydrogen at a lower rate. A star of 1 M_{\odot} will spend a time period greater than the current age of the universe consuming all the hydrogen in its core if it evolves in a halo with DM density $\rho_{\chi} = 10^9$ GeV cm⁻³. We also show the strong dependence of the effective temperature and luminosity of these stars on the characteristics of the DM particles and how this can be used as an alternative method for DM research.

Key words: dark matter – Galaxy: center – Hertzsprung–Russell (HR) diagram – stars: evolution – stars: formation – stars: interiors

Online-only material: color figures

1. INTRODUCTION

Modern observational cosmology has revealed a more complex and unknown universe than previously expected. The current cosmological observations of the baryon acoustic oscillations, distance measurements by means of Type Ia supernovae, cosmic microwave background, and primordial light elements abundances, are all observations that confirm that the standard cosmological model is a good description of our universe undergoing an accelerated expansion (Spergel et al. 2007; Komatsu et al. 2009). We now know that only about 5% of all matter in the universe is regular visible matter, usually known as baryons. The rest is very likely to be in the form of unknown particles that have not yet been detected, even though we are able to observe its effect on the formation of cosmological structures, usually known to us as dark matter (DM) and dark energy. The universe is composed of 20% of DM, particles that do not interact with the electromagnetic field, but whose presence can be inferred from gravitational effects on visible matter. The remaining 75% is known as dark energy. This component is very homogeneous and not very dense, and is known to have interacted through any of the fundamental forces other than gravity. In this paper, we investigate the impact of the DM component on the evolution of stars.

There is an abundant number of particle physics models providing candidates for DM particles. Among others, the Supersymmetric Standard Model (SUSY) is one of the best-studied candidates for physics beyond the Standard Model (Bertone et al. 2005). DM particles must be massive particles, electrically neutral and, very likely, non-colored. The lightest supersymmetric particle (LSP), such as the neutralino, is the favorite SUSY particle among the particle physics community. The LSP belongs to a generic family of neutral massive particles, usually

known as weakly interacting, massive particles (WIMPs) that are by definition the best DM particle candidates. WIMPs interact through gravity and possibly through the weak nuclear force, and very likely through no other interactions stronger than the weak force.

Despite their weak interactions, WIMPs can lead to significant changes in the formation and evolution of stars, provided they have a sizeable scattering cross section with baryons. Concerning WIMPs' interaction with baryons, the consequence is two-fold: WIMPs can affect a star by annihilating among themselves into standard model particles in its core, providing a source of energy additional to standard nuclear energy (Salati & Silk 1989). A second way by which WIMPs can influence a stellar structure is by providing an additional mechanism of heat transport inside the star (Bouquet & Salati 1989a). This can reduce the local temperature gradient, potentially inhibiting convection and enhancing the pulsation of horizontal branch stars (Dearborn et al. 1990). In the case of the Sun, the current values favored by WIMP self-annihilation cross section, WIMP–nucleus scattering cross sections, and local DM density indicate that this effect is not significant for the evolution of our star.

The study of the effects of DM particles accretion on stars is an alternative approach to investigate the properties of such particles. These effects were first studied in the Sun by Spergel & Press (1985) and later on by Lopes et al. (2002a) and Bottino et al. (2002). Recently, Moskalenko & Wai (2007) for white dwarfs, Scott et al. (2007) for low-mass stars, and Spolyar et al. (2008) for the first generation of stars, showed that, if embedded in halos with high-DM densities, stars can be fuelled only by the energy from DM annihilation. Many authors confirmed and developed these results. DM capture and annihilation were studied for white dwarfs and neutron stars by

Bertone & Fairbairn (2008) and Kouvaris (2008). The same was done for first stars by Iocco (2008), Taoso et al. (2008), Freese et al. (2008c), and Yoon et al. (2008), and their implications for cosmic reionization and the pair production supernova rate were studied by Schleicher et al. (2009) and Iocco (2009), respectively. In the case of first stars formed at the center of DM minihalos, DM annihilation may become the primary source of energy during the adiabatic contraction regime of the DM halo, counteracting the gravitational collapse even before DM capture becomes efficient (Spolyar et al. 2008; Freese et al. 2008a, 2008b; Natarajan et al. 2009; Ripamonti et al. 2009). When the star runs out of its original DM, which takes about a million years (Freese 2009), this stalling phase ends and the collapse continues until capture replenishes the fuel for DM annihilation (Iocco et al. 2008).

Regarding low-mass stars, Scott et al. (2009) carried out an extensive study on how the stars located at the galactic center may be affected by the dense DM densities which are expected to exist there. They assumed that these stars were already formed in a scenario without DM. Therefore, their evolution on a DM halo was considered from the zero-age main sequence (ZAMS). In addition to that, we also took into account the capture of DM particles from the collapse of the protostar, as Iocco et al. (2008) did for first stars. The influence of DM in that early stage may have dramatic consequences in the forming star, as will be shown.

The paper is organized as follows: in Section 2, there is a short description of the stellar evolution code used here. The process of accretion of annihilating DM particles in stars is briefly reviewed in Section 3. The different evolution paths found for low-mass stars evolving within DM halos are discussed in Section 4. In Section 5, we discuss the implication of our results to observational stellar astrophysics. Finally, in Section 6, we present a brief summary of the results and discuss the implication of such results for DM research.

2. THE STELLAR EVOLUTION CODE

The models computed in this work were made using the stellar evolution code CESAM (Morel 1997). The CESAM code is a consistent set of programs and routines which performs calculations of one-dimensional quasi-static stellar evolution including diffusion, rotation, and mass loss. CESAM computes structure equilibrium models by the collocation method based on piecewise polynomials approximations projected on their B-spline basis, the evolution of the chemical composition is solved by stiffly stable schemes of orders up to 4, the solution of the diffusion equation employs the Petrov–Galerkin scheme (Morel 1997). The code determines the evolution of a star by the integration of the set of conservation structure equations, coupled with a set of nuclear reactions describing the nucleosynthesis of chemical elements and the production of energy, using an adaptive space time mesh, i.e., the code chooses an optimal step in time and space by computing the rate of variation of the equilibrium quantities. CESAM allows calculations of stellar models with various physical assumptions, physical data, external boundary conditions, numerical methods, and numerical accuracy; in this work, the accuracy is set to 10^{-5} . This code has the ability to compute the evolution of stars from the pre-main-sequence up until the beginning of the ^4He burning cycle for various stellar masses, and for a range of metallicities ($0.0004 < Z < 0.04$, in the present configuration). The initial chemical abundances are the solar ones (Asplund et al. 2005),

and the initial metallicity, unless stated otherwise, is assumed to be $Z = 0.014$, similar to that of the Sun.

The microscopic physics, including the equation of state, opacities, nucleosynthesis, microscopic diffusion, and chemical abundances, is very refined in this stellar evolution code, since this part of the code was tested in the case of the Sun against helioseismic data. The CESAM evolution code is well established in the solar and stellar physics community, being used either to compute solar models (Couvidat et al. 2003; Berthomieu et al. 1993) or models of other stars (among others: PMS δ Scuti star V346 Ori (Bernabei et al. 2009), β Chepe star ν Eridani (Suárez et al. 2009), 0.8–8 M_{\odot} PMS and MS stars (Marques et al. 2008), Vega-like stars α PsA, β Leo, β Pic, ε Eri, and τ Cet (Di Folco et al. 2004), α CMi star Procyon A (Kervella et al. 2004), solar-like 0.8–1.4 M_{\odot} stars and PMS stars (Piau & Turck-Chièze 2002), α Cen A&B stars (Thévenin et al. 2002), and MS stars with convective overshooting (Audard et al. 1995)).

We modified this code to take into account the impact of DM particles in the evolution of low-mass stars. In particular, we have already used this code to study the evolution of the Sun within a halo of DM (Lopes et al. 2002a, 2002b; Lopes & Silk 2002); we predicted the results of two groups of observables: solar neutrinos and helioseismology data (including the sound speed profile).

3. ACCUMULATION OF DARK MATTER PARTICLES INSIDE STARS

WIMPs travel through stars, where they experience scattering off the nuclei that they encounter in the stellar cores. Although most WIMPs travel right through the star without suffering any type of interaction, some of them will scatter off nuclei losing energy. If they lose enough energy, they would no longer be able to escape the gravitational field of the star. The number of WIMPs trapped inside the star is measured by the capture rate C_{χ} . The capture rate is proportional to the WIMP scattering cross section off nuclei σ_{χ} and the DM density of the halo ρ_{χ} . It is inversely proportional to the WIMP mass m_{χ} and to the WIMP dispersion velocity \bar{v}_{χ} . Capture rates of WIMPs were first calculated by Press & Spergel (1985) in the case of the Sun, by Gould (1987) for generic massive bodies and for the Earth in particular, and by Bouquet & Salati (1989a) for main-sequence stars. We computed the capture rate using Equation (2.31) of Gould (1987):

$$C_{\chi} = \sum_i \left(\frac{8}{3\pi} \right)^{1/2} \sigma_i \frac{\rho_{\chi}}{m_{\chi}} \bar{v}_{\chi} \frac{x_i M_{\star}}{A_i m_p} \frac{3v_{\text{esc}}^2}{2\bar{v}_{\chi}^2} \zeta, \quad (1)$$

where $v_{\text{esc}} = \sqrt{2GM_{\star}/R_{\star}}$ is the escape velocity, M_{\star} and R_{\star} are the mass and radius of the star, m_p is the proton mass, and x_i and A_i are, respectively, the mass fraction and the number of nucleons of element i . We included the contributions from 13 nuclei: H, ^4He , ^{12}C , ^{14}N , ^{16}O , ^2H , ^3He , ^7Li , ^7Be , ^{13}C , ^{15}N , ^{17}O , and ^9Be , the abundances of which are followed by our code. For all of them, we computed their spin-independent (SI) interaction with WIMPs (coherent scattering), which scales as the fourth power of the nucleus mass number, leading to a scattering cross section $\sigma_i = A_i^4 \sigma_{\chi, \text{SI}}$. For hydrogen, we also took into account the contribution of the spin-dependent (SD) interaction (incoherent scattering), which lead to $\sigma_{\text{H}} = A_{\text{H}}^4 \sigma_{\chi, \text{SI}} + \sigma_{\chi, \text{SD}}$. The last term in Equation (1), ζ , is the product of the suppression factors due to the motion of the star through the halo $\xi_{\eta}(\infty)$,

Table 1Comparison of Different Capture Rates in the Literature, Considering Different Stellar Masses and DM Halo Densities ρ_χ

Mass (M_\odot)	$\log \rho_\chi$ (GeV cm^{-3})	C_χ (s^{-1})	Reference
0.8	9	0.6×10^{34}	Scott et al. (2009) ^a
		0.9×10^{34}	Fairbairn et al. (2008)
		1.7×10^{34}	Freese et al. (2008c) ^b
		1.6×10^{34}	Casannellas & Lopes (this paper) ^a
1	10	0.8×10^{35}	Scott et al. (2009) ^a
		0.9×10^{35}	Fairbairn et al. (2008)
		1.1×10^{35}	Bertone et al. (2005) ^c
		1.7×10^{35}	Freese et al. (2008c) ^b
		2.9×10^{35}	Moskalenko & Wai (2006) ^b
		1.6×10^{35}	Casannellas & Lopes (this paper) ^a
	9	1.0×10^{34}	Scott et al. (2009) ^a
		1.1×10^{34}	Fairbairn et al. (2008)
		1.1×10^{34}	Bertone et al. (2005) ^c
		2.0×10^{34}	Freese et al. (2008c) ^b
	8	1.9×10^{34}	Casannellas & Lopes (this paper) ^a
		0.8×10^{33}	Scott et al. (2009) ^a
1.1×10^{33}		Fairbairn et al. (2008)	
1.1×10^{33}		Bertone et al. (2005) ^c	
2	10	2.1×10^{33}	Freese et al. (2008c) ^b
		1.9×10^{33}	Casannellas & Lopes (this paper) ^a
		2.3×10^{35}	Fairbairn et al. (2008)
		4.4×10^{35}	Freese et al. (2008c) ^b
3	10	4.5×10^{35}	Scott et al. (2009) ^a
		4.1×10^{35}	Casannellas & Lopes (this paper) ^a
		4.5×10^{35}	Fairbairn et al. (2008)
		8.1×10^{35}	Freese et al. (2008c) ^b
		8.1×10^{35}	Casannellas & Lopes (this paper) ^a

Notes. In all cases: $m_\chi = 100 \text{ GeV}$, $\sigma_{\chi,SD} = 10^{-38} \text{ cm}^2$. The metallicity of the stars goes as follows: ^a: $Z = 0.01$, ^b: $Z = 0$ and ^c: $Z = 0.018$.

the mismatch between WIMP and nuclei masses, and the dimensionless gravitational potential averaged over the star $\langle \phi \rangle$, all present in the original expression of Gould (1987). We evaluated these factors for a WIMP mass $m_\chi = 100 \text{ GeV}$, a velocity of the star $v_* = 220 \text{ km s}^{-1}$, and a WIMP dispersion velocity $\bar{v}_\chi = 270 \text{ km s}^{-1}$, and found that, for these values and for all stars studied here, we can approximate ζ to the order of unity, similar to other authors (Moskalenko & Wai 2007; Bertone & Fairbairn 2008; Freese et al. 2008c). This approximation retains the main aspects of WIMPs' capture, while it simplifies the calculations and reduces the time of computation. Furthermore, the difference in values between this capture rate and others (see Table 1) is relatively small. We confirmed that the overall conclusions of this paper will not be affected by the accuracy of this capture expression.

The values of the scattering cross sections used in our simulations, $\sigma_{\chi,SD}$ from 10^{-40} cm^2 to 10^{-37} cm^2 and $\sigma_{\chi,SI} = 10^{-44} \text{ cm}^2$, are consistent with the experimental bounds given by direct detection experiments (CDMS, Akerib et al. 2006; XENON10, Angle et al. 2008b; NAIAD, Alner et al. 2005; PICASSO, Barnabe-Heider et al. 2005; COUPP, Behnke et al. 2008; for $\sigma_{\chi,SD}$, and CDMS-II, Ahmed et al. 2009; XENON10, Angle et al. 2008a; CRESST-II, Angloher et al. 2005; and EDELWEISS, Sanglard et al. 2005 for $\sigma_{\chi,SI}$). Only one indirect detection experiment (Super-Kamiokande, Desai et al. 2004) predicted an upper limit for $\sigma_{\chi,SD}$ below 10^{-37} cm^2 . The bounds on the WIMP–nucleon scattering cross sections are much less

constraining for SD interactions than for SI, due to the presence of the A^4 factor in the latter type of interactions. For this reason, the WIMP capture rate was always dominated by SD scattering in all our computations.

After being captured, WIMPs will then sink to the core of the star, where they can annihilate with one another at an annihilation rate Γ_χ . The total number of WIMPs N_χ inside the star is then determined by the balance between the capture rate and the annihilation rate. Therefore, the evolution of the number of WIMPs inside the star over time is

$$\frac{dN_\chi}{dt} = C_\chi - 2\Gamma_\chi. \quad (2)$$

The capture and annihilation of WIMPs in the core of a star are very efficient processes; capture and annihilation processes balance each other out in around 100 years (Salati & Silk 1989) and the system rapidly comes to equilibrium, $\dot{N}_\chi = 0$ or $C_\chi = 2\Gamma_\chi$. The timescale for the steady state to be reached will be much inferior than the typical evolutionary timescale of a main-sequence star. WIMPs will get distributed in the core of the star very rapidly following an approximately thermal internal distribution with a characteristic radius $r_\chi = \sqrt{3\kappa T_c / 2\pi G \rho_c m_\chi}$, where T_c and ρ_c are the central temperature and density of regular baryonic matter inside the star, and G and κ are the Newton and Boltzman constants. The density number distribution n_χ is given by $n_\chi(r) = N_\chi \pi^{-3/2} r_\chi^{-3} e^{-r^2/r_\chi^2}$ (Dearborn et al. 1990, 1991; Kaplan et al. 1991).

DM particles can transport energy by scattering off nuclei inside the star, thus constituting an alternative mechanism of energy transport (Bouquet & Salati 1989b). This energy transport mechanism by WIMPs is implemented in our stellar evolution code (for a detailed description, see Lopes et al. 2002b), although the contribution of such process to the evolution of the star is negligible compared with other effects. More significantly, DM particles in the stellar core provide an extra source of energy (Salati & Silk 1989). The energy generation rate ε_χ due to pair annihilation of DM particles is given by

$$\varepsilon_\chi(r) = f_\chi m_\chi n_\chi^2(r) \rho(r)^{-1} \langle \sigma_a v \rangle \quad (3)$$

in units of energy per mass per time (in cgs: $\text{erg g}^{-1} \text{ s}^{-1}$). It follows that every pair of DM particles captured into the star is instantly converted into additional luminosity. We assume that all products of DM annihilation, except neutrinos, interact either by electromagnetic or nuclear strong forces with the core nuclei, so they have short mean free paths inside the star and these particles rapidly reach the thermal equilibrium. We chose the coefficient $f_\chi = \frac{2}{3} \times 2$ to take into account that $\frac{1}{3}$ of the energy is lost in the form of neutrinos that escape from the star, and that each annihilation involves two DM particles, due to the assumption that the neutralino is a Majorana particle, i.e., it is its own anti-particle. The coefficient f_χ has different values in the literature. Its former factor, which quantifies the energy that remains inside the star, could be underestimated in our work: following the recent simulations of Scott et al. (2009), the energy loss could be as low as 10% of the total energy from DM annihilations. Our choice, more conservative, is in agreement with other authors (Freese et al. 2008a; Iocco et al. 2008; Yoon et al. 2008). In our simulations, we assumed the annihilation cross section to be $\langle \sigma_a v \rangle = 3 \times 10^{-26} \text{ cm}^3 \text{ s}^{-1}$, a value that is fixed by the relic density through the following approximation: $\Omega_\chi h^2 \approx 3 \times 10^{-27} \text{ cm}^3 \text{ s}^{-1} / \langle \sigma_a v \rangle$ (e.g., Scherrer & Turner 1986; Srednicki et al. 1988; Bertone et al. 2005).

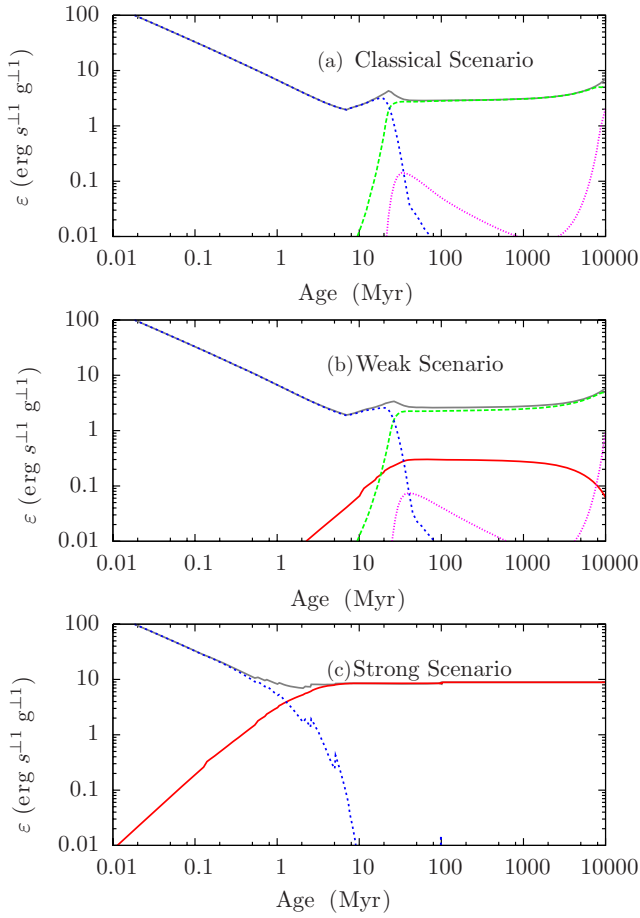


Figure 1. Energy rates during the evolution of a $1 M_{\odot}$ star on the Classical, Weak, and Strong cases. The densities of DM in the halo are, respectively, 0 , 3×10^8 , and $3 \times 10^{11} \text{ GeV cm}^{-3}$. Curves are as follows: ε_T (light gray dashed line), ε_{χ} (red continuous line), $\varepsilon_{\text{grav}}$ (blue dashed line), ε_{pp} (green long dashed line), ε_{CNO} (pink dotted line). The DM halo is assumed to be composed by WIMPs with mass $m_{\chi} = 100 \text{ GeV}$, spin-dependent scattering cross section, $\sigma_{\chi,\text{SD}} = 10^{-38} \text{ cm}^2$, and annihilation cross section $\langle \sigma_a v \rangle = 3 \times 10^{-26} \text{ cm}^3 \text{ s}^{-1}$. (A color version of this figure is available in the online journal.)

4. EVOLUTION OF LOW-MASS STARS WITHIN A DARK MATTER HALO

We have implemented the effects of the annihilation of DM particles in our stellar evolution code and followed the evolution of low-mass stars since their protostar phase and throughout the main-sequence phase. These stars may experience dramatic changes on their evolution depending upon the amount of DM the star accumulates in its interior. The accretion of DM depends mainly on the particle halo density ρ_{χ} , and also on the WIMP–nucleus spin-dependent scattering cross section $\sigma_{\chi,\text{SD}}$. The more accretion of DM particles happens inside the core of the star, the more energy is produced by WIMP pair annihilation. The existence of this new source of energy leads to significantly different scenarios of stellar evolution. Figure 1 shows the contribution of the different energy sources to the total energy generation rate, ε_T , of a star of $1 M_{\odot}$. The evolution of the star depends on the balance between DM energy rate, ε_{χ} , the thermonuclear energy rate produced by the pp chain, ε_{pp} , the thermonuclear energy rate produced by the CNO cycle, ε_{CNO} , and the gravitational energy rate, $\varepsilon_{\text{grav}}$, produced by the gravitational contraction of the star. Depending upon the

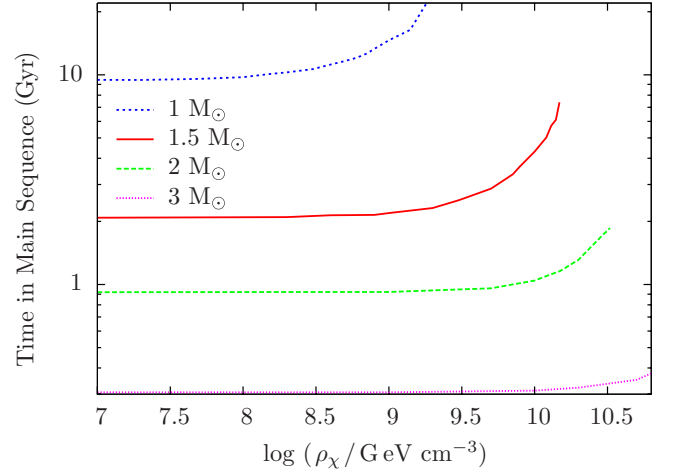


Figure 2. Time spent in main sequence (from $\varepsilon_{\text{grav}} < 1\% \varepsilon_T$ to $X_c < 0.001$) by stars of masses 1 , 1.5 , 2 , and $3 M_{\odot}$ embedded in DM halos of different densities. The DM particles are as described in Figure 1.

(A color version of this figure is available in the online journal.)

amount of DM present in the host halo, we found that stars can experiment quite different evolution paths, which we classified in three distinct cases: weak, intermediate and strong case scenarios.

4.1. Scenarios of Stellar Evolution within DM

4.1.1. Weak Case Scenario: Slowly Evolving Stars

Normal stars are self-gravitating systems that most of the time are experimenting a gravitational contraction, leading to an increase in the temperature inside their cores. The gravitational collapse is stopped by an additional source of energy, such as thermonuclear energy produced by the pp chain or CNO cycle in stars on the main-sequence phase. Nevertheless, stars evolving in DM halos can experiment a quite different scenario of evolution. For stars evolving within halos with low-DM density ρ_{χ} , the energy from WIMPs' annihilation is a complementary source to the thermonuclear energy (see Figure 1(b)) that slightly delays the gravitational collapse, slowing down the arrival of the hydrogen-burning phase. The equilibrium is reached at a lower central temperature than that of the classical evolution case, leading to a smaller rate of energy produced by thermonuclear reactions $\varepsilon_{pp} + \varepsilon_{\text{CNO}}$ (stars will evolve in the weak scenario if their thermonuclear energy accounts for more than 10% of the total energy in the beginning of the MS). Therefore, the time that a star spends in the main-sequence phase is enlarged with respect to the classical evolution scenario (see Figure 2). The more massive the star, the more DM will be necessary to produce the same effects. A star of $1 M_{\odot}$ will stay in the MS for a time greater than the current age of the universe if it evolves in a DM halo of $\rho_{\chi} = 10^9 \text{ GeV cm}^{-3}$ and $\sigma_{\chi,\text{SD}} = 10^{-38} \text{ cm}^2$, while a star of $2 M_{\odot}$ evolving in the same halo will not be affected. In the case of one solar mass stars, Scott et al. (2009) obtained the same extension in the main-sequence lifetime for almost identical DM densities on the host halo. On the other hand, for greater masses our results are more conservative due to the lower WIMP capture rates obtained for $M_{\star} > 1 M_{\odot}$. This evolution scenario is qualitatively similar to that predicted for Pop III stars by Taoso et al. (2008).

To grasp the role of the metallicity, we computed models with metallicities from $Z = 0.0004$ to $Z = 0.04$ and found that the main differences in the stellar evolution are those

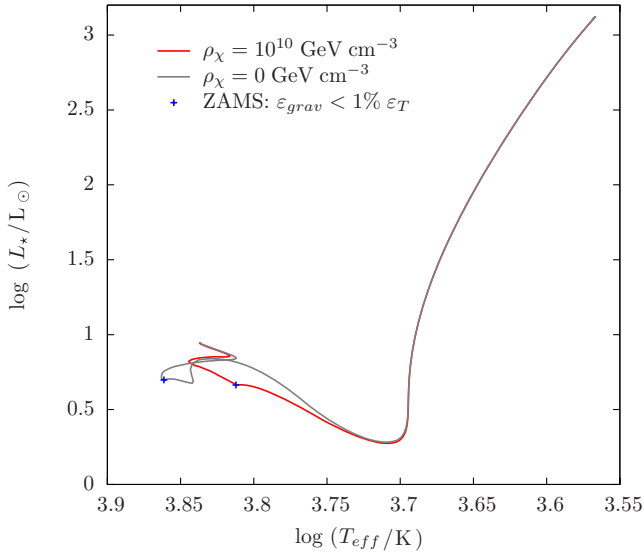


Figure 3. HR diagram of the formation and evolution through the main sequence of a star of $1.5 M_{\odot}$ embedded in halos without DM (gray line) and with a DM halo density $\rho_{\chi} = 10^{10} \text{ GeV cm}^{-3}$ (red line). The DM particles are as described in Figure 1.

(A color version of this figure is available in the online journal.)

Table 2

Energy Rates (and Its Percentage Over the Total Energy) for Stars of $1 M_{\odot}$ with Different Initial Metallicities, Evolving in a Halo with a DM Density $\rho_{\chi} = 10^9 \text{ GeV cm}^{-3}$, At an Age Such that Their Central Hydrogen Mass Fraction is $X_c = 0.60$

Z	X_{in}	Y_{in}	ε_{χ} ($\text{erg g}^{-1} \text{ s}^{-1}$)	ε_{pp} ($\text{erg g}^{-1} \text{ s}^{-1}$)
0.0004	0.7584	0.2412	0.8 (12%)	5.8 (88%)
0.001	0.756	0.243	0.7 (12%)	5.4 (88%)
0.02	0.680	0.300	0.6 (23%)	2.1 (77%)
0.04	0.620	0.340	0.6 (25%)	1.7 (74%)

already expected in the classical picture; stars with higher metallicities have lower thermonuclear energy production rates and, therefore, extended main-sequence lifetimes (Schaller et al. 1992; Schaerer et al. 1993; Lejeune & Schaerer 2001). Table 2 shows the energy rates ε_{pp} and ε_{χ} for stars with metallicities $Z = 0.0004, 0.001, 0.02,$ and 0.04 that evolve in a halo with a DM density $\rho_{\chi} = 10^9 \text{ GeV cm}^{-3}$. Even though ε_{χ} is lower in high-metallicity stars (due to a lower capture because of the smaller hydrogen mass fraction), its percentage over the total energy is higher given the strong reduction in ε_{pp} . Consequently, stars with higher initial metallicities will be affected by the energy from DM annihilation at slightly lower DM densities.

The competition between the nuclear burning and the energy from WIMP annihilation leads to another important change with respect to the classical scenario. The path that these stars follow on the Hertzsprung–Russell (HR) diagram may be significantly altered if there is enough DM in their interior. This can be seen in Figure 3, where we plotted the tracks of a star of $1.5 M_{\odot}$ evolving in halos without DM and with a DM density $\rho_{\chi} = 10^{10} \text{ GeV cm}^{-3}$. In the latter case, the rates of energy production were, in the beginning of the MS: $\varepsilon_{\chi} \simeq 42\%$, $\varepsilon_{pp} \simeq 55\%$, and $\varepsilon_{\text{CNO}} \simeq 3\%$. In this case, the contribution of ε_{χ} rapidly starts to compensate the collapse of the protostar, stopping it when the star has a larger radius than that of the classical scenario. Consequently, the ZAMS position of these stars shifts to lower effective temperatures.

The internal structure of the star also experiences some important changes. In the classical scenario, a Sun-like star of one solar mass will develop a small convective core within the radiative interior, which will disappear when the star reaches the main-sequence phase. Then, this star will develop a radiative core and a convective envelope on the outer layers. Alternatively, in this new scenario, the central convective zone remains for a longer period during the evolution of the star, because the extra luminosity amount produced by the WIMPs annihilation requires a more efficient mechanism to evacuate this energy from the stellar core. Typically, in a halo of DM particles with $\rho_{\chi} = 10^9 \text{ GeV cm}^{-3}$ and $\sigma_{\chi, \text{SD}} = 10^{-38} \text{ cm}^2$, a star of $1 M_{\odot}$ develops a convective core with a radius of approximately $0.05 R_{\star}$. This radius decreases with time, until it disappears completely at an age of 6 Gyr. Similarly to the Sun, this star conserves its convective external region throughout its evolution. In the case of the present Sun, the external convective region is located above $0.7 R_{\star}$. The thickness of this external convective layer grows with ρ_{χ} , and it is also conserved in more dense DM halos, as in the case discussed in the next section, the intermediate case scenario.

4.1.2. Intermediate Case Scenario: Convective–Radiative “Frozen” Stars

As the ambient density of DM particles ρ_{χ} increases, the capture rate inside the star increases too. As a consequence, the energy source resulting from the annihilating DM particles eventually starts to compensate the gravitational energy source, thus keeping the temperature of different core regions below the threshold needed to start the thermonuclear reactions. In this scenario, WIMP pair annihilation becomes the only source of the star’s luminosity and ε_{χ} is high enough to stop the gravitational collapse at an early stage. Stars in this scenario can live forever without the production of thermonuclear energy.

Since WIMP annihilation occurs in a more centralized region than the nuclear one, at least for very massive DM particles, the temperature gradient is much steeper in the core of the star than it would be otherwise, and the star has the conditions to maintain a convective core for the rest of its life. Outside the convective core, less energy is generated per unit volume than if the nuclear burning was proceeding normally, so the temperature gradient is smaller. The actual temperature is lower than in a normal star, however, it remains high enough to prevent any major increase in opacity, ensuring that energy transport in the region above the core remains radiative. The energy from the core is easily transmitted through this radiative region to the surface of the star. The external envelope of this star is very much similar to a typical young Sun. In the outer layers, the star develops a convective region; due to the rapid temperature drop, some chemical elements such as oxygen, carbon and nitrogen, fully ionized in the interior, are partially ionized in the most external layers. This increases significantly the radiative opacity, and makes convection the only efficient mechanism of energy transport toward the surface.

4.1.3. Strong Case Scenario: Fully Convective “Frozen” Stars

At high enough WIMP capture rates, the energy produced by the annihilation of DM is sufficient to fully compensate the gravitational energy (see Figure 1(c)). The star’s gravitational collapse stops before reaching enough central temperature to begin nuclear fusion, as in the intermediate case. This equilibrium is reached quite early in the formation of these stars, depending upon the value of ρ_{χ} , as illustrated in Figure 4.

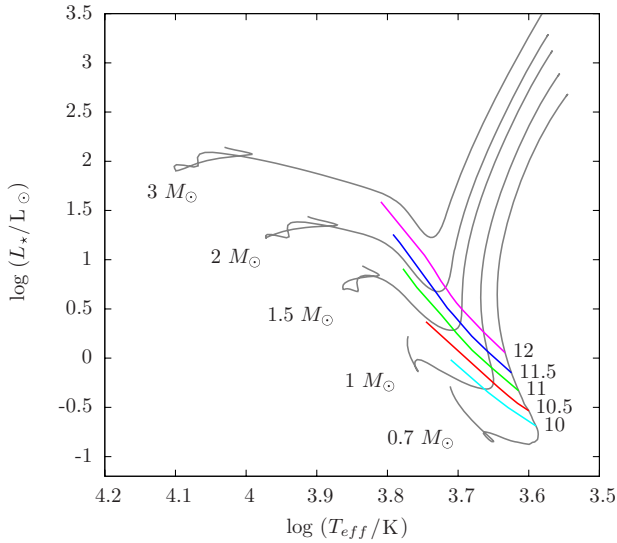


Figure 4. Stationary states reached by stars with masses from 0.7 to $3 M_{\odot}$ when the energy from DM annihilation compensates the gravitational energy during the collapse. These equilibrium positions, where stars will remain for an indefinite time, are plotted for different DM halo densities, indicated in units of $\log(\rho_{\chi}/\text{GeV cm}^{-3})$ at the side of each line. The gray lines are the classical evolutionary paths, which these stars follow before stopping. The DM particles are as described in Figure 1.

(A color version of this figure is available in the online journal.)

This figure shows solid gray lines corresponding to the classical evolution tracks of stars from 0.7 to $3 M_{\odot}$, along with the position on the HR diagram of the early equilibrium states reached by these stars, considering formation scenarios with different WIMP densities ρ_{χ} . These cases are strongly reminiscent of the Hayashi track which young stars follow when traveling along the protostar phase onto the final stages of their formation toward the main-sequence phase. If no extra source of DM energy existed, these stars would shrink in size within the Kelvin–Helmholtz timescale as they radiate away gravitational energy. Alternatively, a constant energy generation in the core by WIMP pair annihilation creates stars that can in principle remain in the same position in the HR diagram for an arbitrarily long time. A star of one solar mass evolving within a halo of DM particles with a scattering cross section $\sigma_{\chi,\text{SD}} = 10^{-38} \text{ cm}^2$ and $\rho_{\chi} = 3 \times 10^{11} \text{ GeV cm}^{-3}$ completely stops its collapse at the age of 50 Myr and remains forever with a stellar radius $R_{\star} = 1.75 R_{\odot}$, effective temperature $T_{\text{eff}} = 4555 \text{ K}$, and luminosity $L_{\star} = 1.2 L_{\odot}$ (cf. Figure 4).

The addition of more WIMPs dramatically increases the central luminosity of these stars, requiring the convective core to grow in order to transport the additional energy to the surface layers. In this scenario, the surface convection zone merges with the inner core and the star becomes fully convective.

Our approach on the evolution of low-mass stars within DM halos consists in considering the influence of DM capture since the collapse of the star. Iocco et al. (2008) did the same to study the evolution of first stars; they also found that the collapse of these stars, the so-called *dark stars*, may be stopped at an early stage if there is enough DM on their interior. On the other hand, another approach considered in the literature is to evolve, from the ZAMS, stars that were already formed without DM. This scenario was first analytically estimated by Salati & Silk (1989) for main-sequence stars and recently numerically simulated by Scott et al. (2009) for low-mass stars.

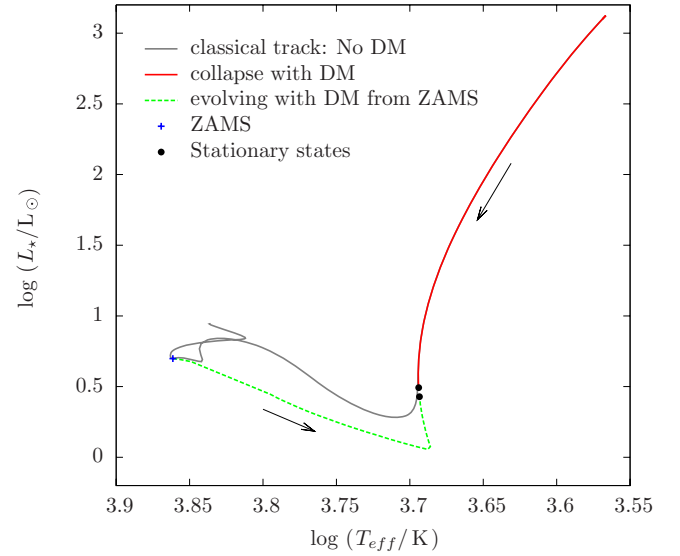


Figure 5. HR diagram of a star of $1.5 M_{\odot}$ evolving in a halo of DM with $\rho_{\chi} = 10^{12} \text{ GeV cm}^{-3}$. The stationary states are new equilibrium states where the star is powered only by energy from DM annihilation. These states are approximately equivalent either if they are reached from the collapse of the protostar (red line), or considering that the star evolves in a halo of DM from the ZAMS (green line). The gray line shows the normal HR track of a $1.5 M_{\odot}$ star without DM. The DM particles are as described in Figure 1.

(A color version of this figure is available in the online journal.)

To compare the two different scenarios, we evolved stars using both approaches and found that they lead to equivalent final equilibrium states, even though the tracks followed by these stars are completely different. When evolved from the ZAMS, stars go back through the pre-main-sequence phase, where they reach the same equilibrium states (fuelled only by the energy from DM annihilation) than those obtained when the collapse is *frozen* (see Figure 5).

4.2. Isochrones for Low-mass Stars Evolving in DM Halos

As a synthesis of the new stellar evolution scenarios presented here, we show in Figures 6 and 7 the paths on the HR diagram followed by stars from 0.7 to $3 M_{\odot}$ that form and evolve in halos of different DM densities ρ_{χ} , as well as the isochrones of different stages during their evolution. In Figure 6, we plotted the collapse until the ZAMS of stars that form in halos with densities $\rho_{\chi} = 0$ and $\rho_{\chi} = 3 \times 10^{10} \text{ GeV cm}^{-3}$. Note that, in the latter case, stars with masses $< 1.8 M_{\odot}$ completely stop their collapse before reaching the ZAMS (as can be seen from the 10 Gyr isochrone). More massive stars are less affected by DM; their classical evolutionary path is only slightly delayed in a halo with the same DM density. This can also be seen by looking at the 1000 Myr isochrone in Figure 7. In this figure, we plotted the paths of these stars through the MS, that is, from $\varepsilon_{\text{grav}} < 1\% \varepsilon_T$ to $X_c < 10^{-3}$.

5. STELLAR DIAGNOSTIC ON THE NATURE OF DARK MATTER PARTICLES

We have computed luminosity and effective temperature of stars in all scenarios for different values of spin-dependent cross section $\sigma_{\chi,\text{SD}}$ and DM density ρ_{χ} , which we varied from 10^5 GeV cm^{-3} up to $10^{12} \text{ GeV cm}^{-3}$. The results are displayed in Figure 8, which also shows the possible location of these stars toward the center of our Galaxy, where the highest densities are

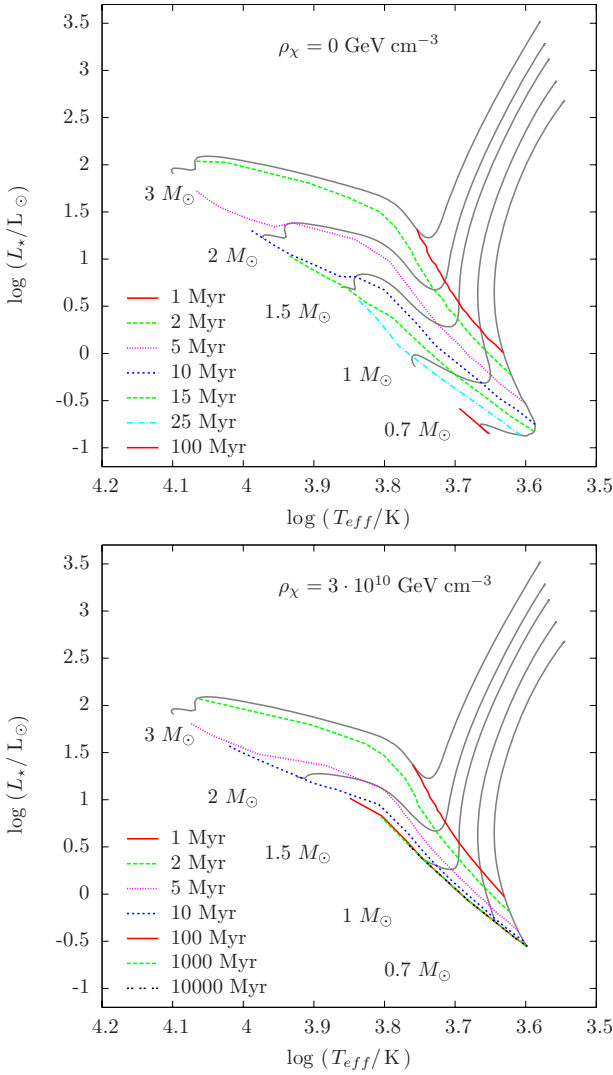


Figure 6. Tracks on the HR diagram of the collapse of stars of different masses until the ZAMS (gray lines), together with the isochrones of different ages, for DM halo densities $\rho_\chi = 0$ and $\rho_\chi = 3 \times 10^{10} \text{ GeV cm}^{-3}$. The DM particles are as described in Figure 1.

(A color version of this figure is available in the online journal.)

expected (Navarro et al. 1996; Salvador-Solé et al. 2007). In that region, the DM density ρ_χ may be enhanced due to the presence of a supermassive black hole (Gondolo & Silk 1999). We computed the DM distribution around the center of the Milky Way using the adiabatic contracted profile of Bertone & Merritt (2005). The predicted T_{eff} and L_\star in Figure 8 may be used as an alternative method to constrain the WIMP–proton SD scattering cross section $\sigma_{\chi, \text{SD}}$, to help in the validation or rejection of DM particles’ models, as well as to infer indirectly the DM density ρ_χ in the place where the star is observed. It is worth noting that, at the present moment, these results offer a qualitative picture more than an exact approach, due to the uncertainties in our knowledge of the inner region of our galaxy. In addition to the density profile $\rho_\chi(r_{GC})$, both the velocities of the star and of the DM particles also play an important role when studying the stars at the galactic center. Scott et al. (2009) did precise simulations of possible orbits of low-mass stars in that region, and found that only those stars with elliptical orbits are efficient at capturing DM particles.

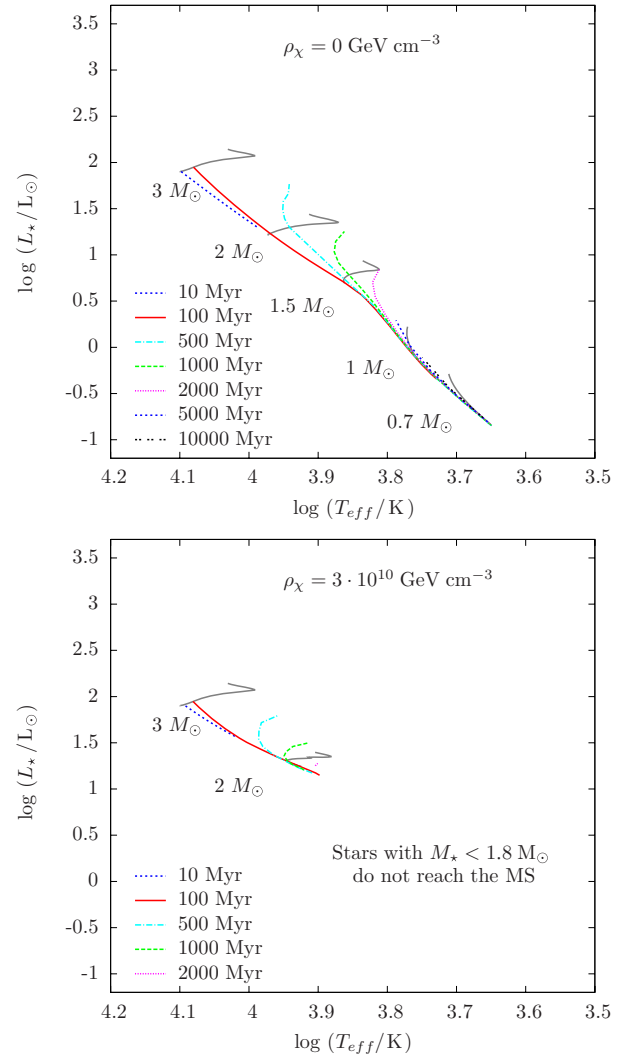


Figure 7. Tracks on the HR diagram of the evolution through the MS (from $\varepsilon_{\text{grav}} < 1\% \varepsilon_T$ to $X_c < 0.001$) of stars of different masses (gray lines), together with the isochrones of different ages, for DM halo densities $\rho_\chi = 0$ and $\rho_\chi = 3 \times 10^{10} \text{ GeV cm}^{-3}$. The DM particles are as described in Figure 1.

(A color version of this figure is available in the online journal.)

In Figure 8, are plotted the T_{eff} and L_\star at such an age that all the stars are already in energy equilibrium. Stars that evolve on DM halos of low densities (Weak scenario) are in equilibrium in the beginning of the MS. As ρ_χ increases, the curves mimic a slower evolution through a classical evolution track on the HR diagram (see Figures 6 and 7). For high ρ_χ (Intermediate and Strong scenarios), stars are in equilibrium, powered only by the energy from DM annihilation. The higher the value of ρ_χ , the sooner the star will freeze its position on the HR diagram at a lower effective temperature T_{eff} and a higher luminosity L_\star (see Figure 4). In the case of $1 M_\odot$ star, the T_{eff} decreases more than 10^3 K and the L_\star raises up to three times higher than in the MS. The rapid drop in temperature is related to the fact that the star becomes fully convective. Our results are more conservative than the similar ones found by Fairbairn et al. (2008), although they predicted the same behavior of T_{eff} at lower DM densities. Probably, our underestimation could be overcome by increasing the resolution of our code in the very center of the star, where the energy from DM annihilation is produced.

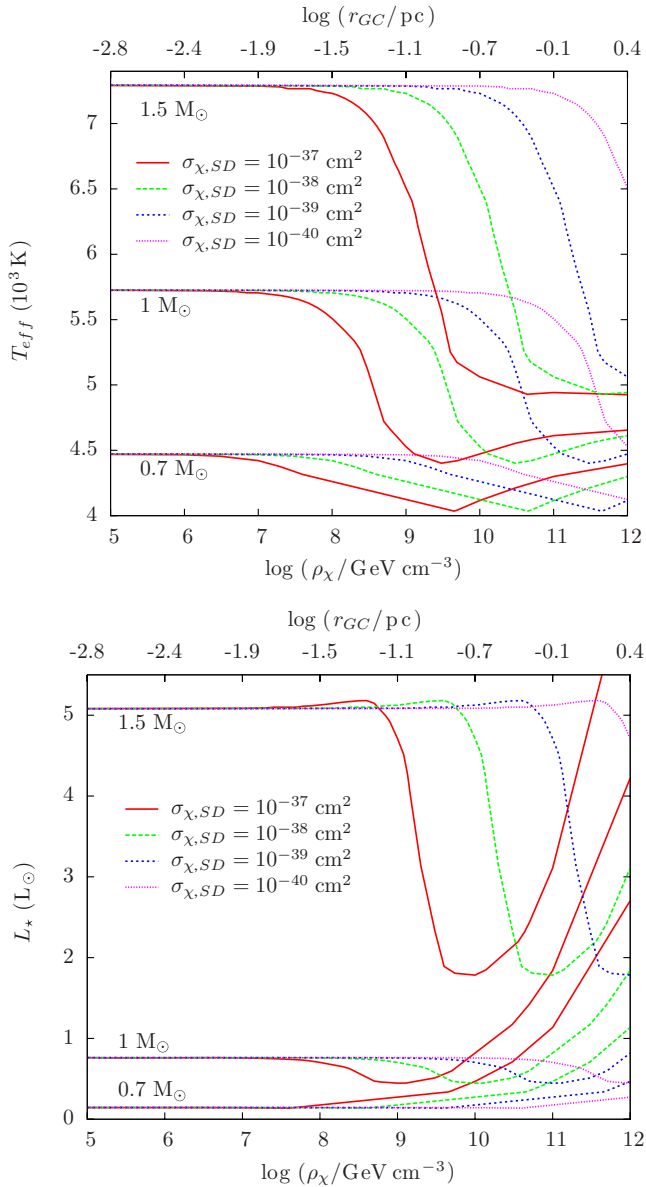


Figure 8. Effective temperature (a) and luminosity (b) of stars of 0.7, 1, and $1.5 M_{\odot}$ as a function of the DM halo density, considering different WIMP–proton spin-dependent scattering cross sections. At the top horizontal axis of each figure we show at which distance to the galactic center are these DM densities expected to be found, following the profile of Bertone & Merritt (2005). The DM particles are as described in Figure 1.

(A color version of this figure is available in the online journal.)

6. CONCLUSIONS

One of the consequences of the formation of structures in the universe is the creation of localized regions with high concentrations of DM. The formation of stars in such peculiar neighborhoods should be quite different from the usual picture of the formation of young stars by gravitational collapse. A striking observational case of such high density DM regions is the young stellar formation regions near the supermassive black holes, located in the center of galaxies, such as our own Milky Way (Genzel et al. 2003; Krabbe et al. 1995). In the attempt to grasp the formation of young stars in such unexpected neighborhoods, in this work we have shown some numerical simulations of stars with masses from 0.7 to $3 M_{\odot}$

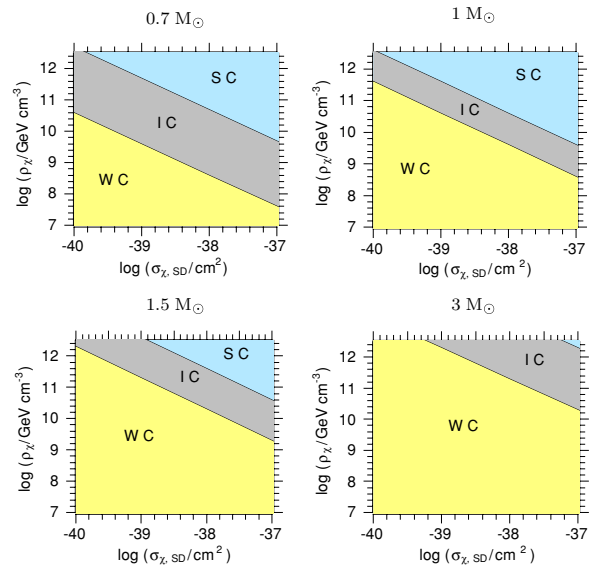


Figure 9. Classification of the different cases of stellar evolution within DM halos for stars of 0.7, 1, 1.5, and $3 M_{\odot}$. Labels “WC”, “IC”, and “SC” indicate, respectively, that these stars are expected to evolve in the Weak, Intermediate, or Strong scenarios, considering halos with different DM densities and WIMP–proton spin-dependent scattering cross sections. The DM particles are as described in Figure 1.

(A color version of this figure is available in the online journal.)

evolving within halos with high density of annihilating DM particles.

We have found that the evolution of a young star can be affected slightly, moderately or strongly depending on the DM density of the host halo. Conveniently, we chose to classify the formation and evolution of low-mass stars in three major possible evolution scenarios: Weak, Intermediate, and Strong, which are directly related to the amount of DM density. The evolution of the star also depends on the scattering cross section of the DM particles. Figure 9 shows in which of these three stellar evolution scenarios should stars of 0.7, 1, 1.5, and $3 M_{\odot}$ evolve, for different values of the SD scattering cross section and the DM density in the halo.

We have shown that low-mass stars in the Strong and Intermediate cases evolve quite differently from the classical path of stars on the HR diagram. During their pre-main-sequence phase, these stars will stop their collapse before reaching enough central temperature to start thermonuclear reactions, and will remain indefinitely in the same position on the HR, fuelled only by the energy from WIMP annihilation. In particular, stars immersed in high density DM halos have their effective temperature and luminosity strongly affected due to the change in the energy transport in their interior (cf. Figure 8).

The new data obtained by means of the near-IR instrumentation allowed the observation of stars in the inner parsec of our own galaxy (Lu et al. 2009; Ghez et al. 2005; Eisenhauer et al. 2005). The observations have revealed a population of apparently young stars in this region, whose current conditions seem to be unsuitable for star formation. This stellar population is usually considered to be a population of old stars that have followed quite an atypical evolution path. If some of these stars were found to be low-mass stars, they would become candidates for this new population of stars evolving in DM halos, as initially suggested by Moskalenko & Wai (2006).

If found, such stars would be interesting probes of DM particles near super-massive black holes. Their luminosity, or

rather their excess of luminosity, attributed to WIMPs' burning, can be used to derive the WIMPs' matter density at their location. On the other hand, the lack of such unusual stars may provide constraints on WIMPs' density, WIMP-nuclei scattering and pair annihilation cross section.

Finally, it is worth mentioning that more detailed studies should be done aimed at testing the validity of our model against new stellar observations. This paper should set the foundations for further works.

We acknowledge the anonymous referee for his useful comments. This work was supported by a grant from "Fundação para a Ciência e Tecnologia" (reference numbers POCTI/FNU/50210/2003 and SFRH/BD/44321/2008).

REFERENCES

- Ahmed, Z., et al. 2009, *Phys. Rev. Lett.*, **102**, 011301
- Akerib, D. S., et al. 2006, *Phys. Rev. D*, **73**, 011102
- Alner, G. J., et al. 2005, *Phys. Lett. B*, **616**, 17
- Angle, J., et al. 2008a, *Phys. Rev. Lett.*, **100**, 021303
- Angle, J., et al. 2008b, *Phys. Rev. Lett.*, **101**, 091301
- Angloher, G., et al. 2005, *Astropart. Phys.*, **23**, 325
- Asplund, M., Grevesse, N., & Sauval, A. J. 2005, in ASP Conf. Ser. 336, Cosmic Abundances as Records of Stellar Evolution and Nucleosynthesis, ed. T. G. Barnes, III & F. N. Bash (San Francisco, CA: ASP), **25**
- Audard, N., Provost, J., & Christensen-Dalsgaard, J. 1995, *A&A*, **297**, 427
- Barnabe-Heider, M., et al. 2005, *Phys. Lett. B*, **624**, 186
- Behnke, E., et al. 2008, *Science*, **319**, 933
- Bernabei, S., et al. 2009, *A&A*, **501**, 279
- Berthomieu, G., Provost, J., Morel, P., & Lebreton, Y. 1993, *A&A*, **268**, 775
- Bertone, G., & Fairbairn, M. 2008, *Phys. Rev. D*, **77**, 043515
- Bertone, G., Hooper, D., & Silk, J. 2005, *Phys. Rep.*, **405**, 279
- Bertone, G., & Merritt, D. 2005, *Mod. Phys. Lett. A*, **20**, 1021
- Bottino, A., Fiorentini, G., Fomengo, N., Ricci, B., Scopel, S., & Villante, F. L. 2002, *Phys. Rev. D*, **66**, 053005
- Bouquet, A., & Salati, P. 1989a, *ApJ*, **346**, 284
- Bouquet, A., & Salati, P. 1989b, *A&A*, **217**, 270
- Couvidat, S., Turck-Chièze, S., & Kosovichev, A. G. 2003, *ApJ*, **599**, 1434
- Dearborn, D., Griest, K., & Raffelt, G. 1991, *ApJ*, **368**, 626
- Dearborn, D., Raffelt, G., Salati, P., Silk, J., & Bouquet, A. 1990, *ApJ*, **354**, 568
- Desai, S., et al. 2004, *Phys. Rev. D*, **70**, 083523
- Di Folco, E., Thévenin, F., Kervella, P., Domiciano de Souza, A., Coudé du Foresto, V., Ségransan, D., & Morel, P. 2004, *A&A*, **426**, 601
- Eisenhauer, F., et al. 2005, *ApJ*, **628**, 246
- Fairbairn, M., Scott, P., & Edsjö, J. 2008, *Phys. Rev. D*, **77**, 047301
- Freese, K. 2009, *EAS Publications Series*, **36**, 113
- Freese, K., Bodenheimer, P., Spolyar, D., & Gondolo, P. 2008a, *ApJ*, **685**, L101
- Freese, K., Gondolo, P., & Spolyar, D. 2008b, in AIP Conf. Proc. 990, First Stars III, ed. B. W. O'Shea, A. Heger, & T. Abel (Melville, NY: AIP), **42**
- Freese, K., Spolyar, D., & Aguirre, A. 2008c, *J. Cosmol. Part. Phys.*, JCAP11(2008)011
- Genzel, R., et al. 2003, *ApJ*, **594**, 812
- Ghez, A. M., Salim, S., Hornstein, S. D., Tanner, A., Lu, J. R., Morris, M., Becklin, E. E., & Duchêne, G. 2005, *ApJ*, **620**, 744
- Gondolo, P., & Silk, J. 1999, *Phys. Rev. Lett.*, **83**, 1719
- Gould, A. 1987, *ApJ*, **321**, 571
- Iocco, F. 2008, *ApJ*, **677**, L1
- Iocco, F. 2009, arXiv:0906.4106
- Iocco, F., Bressan, A., Ripamonti, E., Schneider, R., Ferrara, A., & Marigo, P. 2008, *MNRAS*, **390**, 1655
- Kaplan, J., Martin de Volnay, F., Tao, C., & Turck-Chièze, S. 1991, *ApJ*, **378**, 315
- Kervella, P., Thévenin, F., Morel, P., Berthomieu, G., Bordé, P., & Provost, J. 2004, *A&A*, **413**, 251
- Komatsu, E., et al. 2009, *ApJS*, **180**, 330
- Kouvaris, C. 2008, *Phys. Rev. D*, **77**, 023006
- Krabbe, A., et al. 1995, *ApJ*, **447**, L95
- Lejeune, T., & Schaerer, D. 2001, *A&A*, **366**, 538
- Lopes, I. P., Bertone, G., & Silk, J. 2002a, *MNRAS*, **337**, 1179
- Lopes, I. P., & Silk, J. 2002, *Phys. Rev. Lett.*, **88**, 151303
- Lopes, I. P., Silk, J., & Hansen, S. H. 2002b, *MNRAS*, **331**, 361
- Lu, J. R., Ghez, A. M., Hornstein, S. D., Morris, M. R., Becklin, E. E., & Matthews, K. 2009, *ApJ*, **690**, 1463
- Marques, J. P., Monteiro, M. J. P. F. G., & Fernandes, J. M. 2008, *Ap&SS*, **316**, 173
- Morel, P. 1997, *A&AS*, **124**, 597
- Moskalenko, I. V., & Wai, L. L. 2006, arXiv:astro-ph/0608535
- Moskalenko, I. V., & Wai, L. L. 2007, *ApJ*, **659**, L29
- Natarajan, A., Tan, J. C., & O'Shea, B. W. 2009, *ApJ*, **692**, 574
- Navarro, J. F., Frenk, C. S., & White, S. D. M. 1996, *ApJ*, **462**, 563
- Piau, L., & Turck-Chièze, S. 2002, *ApJ*, **566**, 419
- Press, W. H., & Spergel, D. N. 1985, *ApJ*, **296**, 679
- Ripamonti, E., Iocco, F., Bressan, A., Schneider, R., Ferrara, A., & Marigo, P. 2009, arXiv:0903.0346
- Salati, P., & Silk, J. 1989, *ApJ*, **338**, 24
- Salvador-Solé, E., Manrique, A., González-Casado, G., & Hansen, S. H. 2007, *ApJ*, **666**, 181
- Sanglard, V., et al. 2005, *Phys. Rev. D*, **71**, 122002
- Schaerer, D., Charbonnel, C., Meynet, G., Maeder, A., & Schaller, G. 1993, *A&AS*, **102**, 339
- Schaller, G., Schaerer, D., Meynet, G., & Maeder, A. 1992, *A&AS*, **96**, 269
- Scherrer, R. J., & Turner, M. S. 1986, *Phys. Rev. D*, **33**, 1585
- Schleicher, D. R. G., Banerjee, R., & Klessen, R. S. 2009, *Phys. Rev. D*, **79**, 043510
- Scott, P., Edsjö, J., & Fairbairn, M. 2007, arXiv:0711.0991
- Scott, P., Fairbairn, M., & Edsjö, J. 2009, *MNRAS*, **394**, 82
- Spergel, D. N., et al. 2007, *ApJS*, **170**, 377
- Spergel, D. N., & Press, W. H. 1985, *ApJ*, **294**, 663
- Spolyar, D., Freese, K., & Gondolo, P. 2008, *Phys. Rev. Lett.*, **100**, 051101
- Srednicki, M., Watkins, R., & Olive, K. A. 1988, *Nucl. Phys. B*, **310**, 693
- Suárez, J. C., Moya, A., Amado, P. J., Martín-Ruiz, S., Rodríguez-López, C., & Garrido, R. 2009, *ApJ*, **690**, 1401
- Taoso, M., Bertone, G., Meynet, G., & Ekström, S. 2008, *Phys. Rev. D*, **78**, 123510
- Thévenin, F., Provost, J., Morel, P., Berthomieu, G., Bouchy, F., & Carrier, F. 2002, *A&A*, **392**, L9
- Yoon, S.-C., Iocco, F., & Akiyama, S. 2008, *ApJ*, **688**, L1

A.2 Paper II

TOWARDS THE USE OF ASTEROSEISMOLOGY TO INVESTIGATE THE NATURE OF DARK MATTER

Casanellas J. & Lopes I.

Mon. Not. R. Astron. Soc. 410, 535-540 (2011)

[arXiv:1008.0646](https://arxiv.org/abs/1008.0646)

Towards the use of asteroseismology to investigate the nature of dark matter

Jordi Casanellas^{1★} and Ilídio Lopes^{1,2★}

¹*Centro Multidisciplinar de Astrofísica, Instituto Superior Técnico, Av. Rovisco Pais, 1049-001 Lisboa, Portugal*

²*Departamento de Física, Universidade de Évora, Colégio Luis António Verney, 7002-554 Évora, Portugal*

Accepted 2010 July 30. Received 2010 July 21; in original form 2010 June 1

ABSTRACT

The annihilation of huge quantities of captured dark matter (DM) particles inside low-mass stars has been shown to change some of the stellar properties, such as the star's effective temperature or the way the energy is transported throughout the star. While in the classical picture, without DM, a star of $1 M_{\odot}$ is expected to have a radiative interior during the main sequence, the same star evolving in a halo of DM with a density $\rho_{\chi} > 10^8 \text{ GeV cm}^{-3}$ will develop a convective core in order to evacuate the energy from DM annihilation in a more efficient way. This convective core leaves a discontinuity in the density and sound-speed profiles that can be detected by the analysis of the stellar oscillations. In this paper we present an approach towards the use of asteroseismology to detect the signature produced by the presence of DM inside a star, and we propose a new methodology to infer the properties of a DM halo from the stellar oscillations (such as the product of the DM density and the DM particle-nucleon scattering cross-section).

Key words: asteroseismology – stars: fundamental parameters – stars: interiors – stars: low-mass – Galaxy: centre – dark matter.

1 INTRODUCTION

Different observations in a wide range of scales, from galactic to cosmological, suggest the existence of a new kind of matter, called dark matter (DM), formed by unknown particles. Among the possible constituents of DM, the WIMPs, massive particles with non-negligible scattering cross-section with baryons, are considered one of the best candidates (Bertone, Hooper & Silk 2005).

Soon was realised that, if WIMPs exist, they will accumulate inside stars (Press & Spergel 1985) and their annihilation may lead to significant changes in the classical picture of stellar evolution if the halo where the stars evolve has a very high density of DM particles (Bouquet & Salati 1989; Salati & Silk 1989; Dearborn et al. 1990). In this context, the effects of the capture of WIMPs by the Sun were studied, addressing the prospects of helioseismology to test models that solved the old solar neutrino problem (Dappen, Gilliland & Christensen-Dalsgaard 1986; Faulkner, Gough & Vahia 1986), and to give constraints to the nature of DM particles (Bottino et al. 2002; Lopes & Silk 2002; Lopes, Bertone & Silk 2002b; Lopes, Silk & Hansen 2002a; Cumberbatch et al. 2010; Frandsen & Sarkar 2010; Taoso et al. 2010).

Recently, particular attention has been given to the first stars formed in the early Universe due to the high DM content in that

epoch (Freese, Spolyar & Aguirre 2008b; Iocco 2008; Spolyar, Freese & Gondolo 2008; Taoso et al. 2008; Natarajan, Tan & O'Shea 2009; Schleicher, Banerjee & Klessen 2009; Ripamonti et al. 2010; Sivertsson & Gondolo 2010), including the prospects for their detection with the *James Webb Space Telescope (JWST)* (Freese et al. 2010; Zackrisson et al. 2010). Similarly, other authors focused on the DM effects on stars in the local Universe, either on compact stars (Moskalenko & Wai 2007; Bertone & Fairbairn 2008; de Lavallaz & Fairbairn 2010; Isern et al. 2008, 2010; Kouvaris & Tinyakov 2010; Perez-Garcia, Silk & Stone 2010) or on low-mass stars (Fairbairn, Scott & Edsjö 2008; Casanellas & Lopes 2009; Scott, Fairbairn & Edsjö 2009).

The purpose of this paper is to pave the way for the use of asteroseismology to provide an evidence of the footprint left by DM annihilation on the stellar oscillations. To do this, we will concentrate on solar-mass stars that evolve in haloes with very high DM densities, and we will show how asteroseismology may tell us about the properties of such DM haloes.

2 STELLAR EVOLUTION WITHIN DENSE DARK MATTER HALOES

The evolution of a star within a halo of DM depends strongly on the ability of the gravitational field of the star to capture the DM particles that populate the halo. The rate at which the DM particles

*E-mail: jordicasanellas@ist.utl.pt (JC); ilidio.lopes@ist.utl.pt (IL)

are captured is given by (Gould 1987)

$$C_\chi(t) = \sum_i \int_0^{R_*} 4\pi r^2 \int_0^\infty \frac{f_{v_*}(u)}{u} w \Omega_{v_i}^-(w) du dr, \quad (1)$$

where $f_{v_*}(u)$ is the velocity distribution of the DM particles seen by the star (which is proportional to the density of DM on the host halo ρ_χ and inversely proportional to the mass of the DM particles m_χ) and $\Omega_{v_i}^-$ is the probability of a DM particle to be captured after the collision with an element i (which is proportional to the scattering cross-section of the DM particle with the nucleus i , $\sigma_{\chi,i}$). The numerical subroutines to calculate the capture rate (equation 1) were adapted from the publicly available DARKSUSY code (Gondolo et al. 2004). Our assumptions regarding this calculation are described in Casanellas & Lopes (2010).

Once DM particles are captured, they accumulate in a small region in the core of the star ($r_\chi \simeq 0.01 R_*$ for $m_\chi = 100$ GeV). There, assuming that they are Majorana particles, they annihilate providing a new source of energy for the star. Capture and annihilation processes balance each other in a short time-scale, and consequently almost all captured particles will be converted to energy, contributing to the total luminosity with $L_\chi = f_\chi C_\chi m_\chi$. The factor f_χ , which in this paper we assumed to be 2/3 (Freese et al. 2008a; Iocco et al. 2008; Yoon, Iocco & Akiyama 2008), accounts for the energy that escapes out of the star in the form of neutrinos. Recent Monte Carlo simulations suggest that the fraction of the energy lost in neutrinos may be even smaller (Scott et al. 2009).

Due to this new source of energy, stars will evolve differently from the classical picture if surrounded by a dense halo of DM. For very high DM densities ($\rho_\chi > 3 \times 10^9$ GeV cm $^{-3}$ for a $1 M_\odot$ star), the energy from DM annihilation prevents the gravitational collapse of the star, stopping its evolution in the pre-main-sequence phase, before the star could reach enough central temperature to trigger hydrogen burning (Casanellas & Lopes 2009).

For lower DM densities ($10^8 < \rho_\chi < 3 \times 10^9$ GeV cm $^{-3}$ for a $1 M_\odot$ star), DM burning is a complementary source of energy for the star. As it is produced in a region much more concentrated than the nuclear burning, which normally extends up to 0.1 – $0.2 R_*$, the radiative temperature gradient ($\nabla_{\text{rad}} = d \ln T / d \ln P_g$) is much steeper in the core of the star. Consequently, as the radiative transport is not efficient enough to evacuate all the energy in the central region, the star develops a convective core which was not present in the classical scenario without DM. The radius and duration of the convective core increase when more energy from DM annihilation is produced (Scott et al. 2009); therefore, they depend on the density of DM in the place where the star evolves and on the properties of the DM particles. The balance between DM annihilation, nuclear burning and the gravitational energy leads to a new hydrostatic equilibrium with a lower central temperature. The star consumes its hydrogen at a lower rate, extending the time that it spends in the main sequence. These new properties allow us, as it will be shown, to provide a tool to infer the DM characteristics from the stellar oscillations using the seismological analysis.

3 BASICS OF ASTEROSEISMOLOGY

With the improvement on the quality of the data, asteroseismology is now becoming a precise tool to infer the properties of stars showing solar-like oscillations (Michel et al. 2008; García et al. 2009; Bedding et al. 2010), which are driven by turbulence in the superficial layers of the star. The eigenfrequencies of solar-like oscillations can be approximated, for $l/n \rightarrow 0$ (where l and n are the degree and

the radial order of the modes), by the asymptotic expression

$$v_{n,l} \simeq \left(n + \frac{l}{2} + \epsilon_v \right) v_0 + O(v^{-2}), \quad (2)$$

where $v_0 = [2 \int_0^R dr/c]^{-1}$ is the inverse of twice the time spent by the sound to travel between the centre and the acoustic surface of the star and ϵ_v is determined by the properties of the surface layers. For a more in-depth explanation of the basics of the seismological analysis, the reader is referred to Tassoul (1980), Gough (1985) and Lopes & Turck-Chieze (1994). The value of v_0 can be estimated through the *large separation* $\Delta v_{n,l}$:

$$\Delta v_{n,l} = v_{n,l} - v_{n-1,l} \simeq v_0. \quad (3)$$

This parameter is sensitive to the mean density of the star: $\Delta v_{n,l} \propto (M/R^3)^{1/2}$ (Cox 1980), while the *small separation* $\delta v_{n,l}$, given by

$$\delta v_{n,l} = v_{n,l} - v_{n-1,l+2}, \quad (4)$$

is sensitive to the temperature and chemical gradient in the deep interior.

In the last years, other relations between the frequencies of the oscillation modes were proposed (for a recent review, see Christensen-Dalsgaard & Houdek 2009; Aerts, Christensen-Dalsgaard & Kurtz 2010), broadening the diagnostic potential of seismology. Among the possible diagnostic methods of convective cores and envelopes (Monteiro, Christensen-Dalsgaard & Thompson 1994; Lopes et al. 1997; Lopes & Gough 2001), we highlight the ratios between the small separations and the large separations developed by Roxburgh & Vorontsov (2003) in order to suppress the effects of the modelling of the near-surface layers:

$$r_{01} = \frac{d_{01}}{\Delta v_{n,1}}, \quad r_{10} = \frac{d_{10}}{\Delta v_{n+1,0}}, \quad (5)$$

where

$$d_{01} = \frac{1}{8}(v_{n-1,0} - 4v_{n-1,1} + 6v_{n,0} - 4v_{n,1} + v_{n+1,0}), \quad (6)$$

$$d_{10} = -\frac{1}{8}(v_{n-1,1} - 4v_{n,0} + 6v_{n,1} - 4v_{n+1,0} + v_{n+1,1}). \quad (7)$$

The mixing of elements produced in the convective regions introduces a sharp structural variation in the border with the radiative regions that can be seen in the density and sound-speed profiles. This sharp structural variation produces an oscillatory signal in the frequency spectrum (Gough 1990) whose period is related with the acoustic depth of the discontinuity inside the star. Recently, Silva Aguirre et al. (2010) proposed the use of the ratios r_{01} and r_{10} to determine the size of a convective core by fitting a sine wave to their oscillation pattern. Similarly, another combination of the small and large separations,

$$dr_{0213} \equiv \frac{D_{02}}{\Delta v_{n-1,1}} - \frac{D_{13}}{\Delta v_{n,0}}, \quad (8)$$

where $D_{l,l+2} \equiv \delta v_{n,l}/(4l+6)$, was suggested by Cunha & Metcalfe (2007) to measure the amplitude of the sound-speed discontinuity at the edge of a convective core. These seismic parameters (equations 5 and 8) are sensitive to the presence of DM inside a star, given that they are uniquely dependent on the star's core structure and almost independent of the physical processes occurring in the surface layers.

4 ASTEROSEISMIC SIGNATURE OF DARK MATTER PARTICLES

To grasp the signature that the annihilation of captured DM particles leaves on low-mass stars we evolved a set of $1 M_\odot$ stars, with the

Table 1. Characteristics of stars of mass $1 M_{\odot}$ when they reached a luminosity $L = 1 L_{\odot}$ after evolving in haloes of DM with different densities ρ_{χ} and different SD WIMP-nucleon cross-sections $\sigma_{\chi,SD}$. The last two columns are the radius and the acoustic radius ($\tau = \int_0^r dr/c$) of the convective core (CC). All the stars had the same initial conditions ($Z = 0.018$).

	$\rho_{\chi} \sigma_{\chi}$ (GeV cm^{-1})	X_c	R_{\star} (R_{\odot})	T_{eff} (K)	T_c (MK)	ρ_c (g cm^{-3})	r_{CC} (R_{\star})	τ_{CC} (s)
(i)	0	0.35	1.000	5777.5	15.52	148.7	No CC	–
(ii)	10^{-30}	0.38	1.003	5768.1	15.66	137.0	0.04	53.6
(iii)	10^{-29}	0.40	1.024	5708.5	15.25	123.8	0.08	110.8
(iv)	2×10^{-29}	0.38	1.047	5646.0	15.78	114.9	0.09	132.7
(v)	3×10^{-29}	0.35	1.071	5582.4	15.65	108.5	0.10	145.6

same initial conditions ($Z = 0.018$), in haloes of DM with different densities ρ_{χ} and different spin-dependent (SD) WIMP-nucleon cross-sections $\sigma_{\chi,SD}$. Throughout our work, we considered fiducial values for the mass of the DM particles, $m_{\chi} = 100 \text{ GeV}$, and for their self-annihilation cross-section, $\langle \sigma_a v \rangle = 3 \times 10^{-26} \text{ cm}^3 \text{ s}^{-1}$. The evolution of the stars was computed using a well-established stellar evolution code (CESAM; Morel 1997) used to compute sophisticated solar models for helioseismology (Couvidat, Turck-Chièze & Kosovichev 2003; Turck-Chièze et al. 2010) and more recently used in the context of asteroseismic studies (Kervella et al. 2004; De Ridder et al. 2006; Suárez et al. 2010). When the stars reached a luminosity equal to that of the Sun, a very precise mesh (with 1000 layers) was generated. Then, we calculated the frequencies of the oscillation modes of the stars using the ADIPLS code (Christensen-Dalsgaard 2008). The characteristics of some of these stars are shown in Table 1, and their sound-speed and density profiles, in Fig. 1.

The accretion and the annihilation of DM particles in the core of the stars may change significantly their properties. As expected, we found that the effective temperature of the stars that evolved in haloes with high DM densities is shifted to lower values (see Table 1), due to the presence of a convective core (see Fig. 2a), in agreement with previous works (Fairbairn et al. 2008; Casanellas & Lopes 2009). The lower effective temperature and the larger radius lead to a decrease in the large separation $\Delta \nu_{n,l}$ (see Fig. 2b). For a star with a known mass, the drop in $\Delta \nu_{n,l}$, predicted by the relation $\Delta \nu_{n,l} \propto M^{1/2} R^{-3/2}$, is unmistakably related with the radius of the

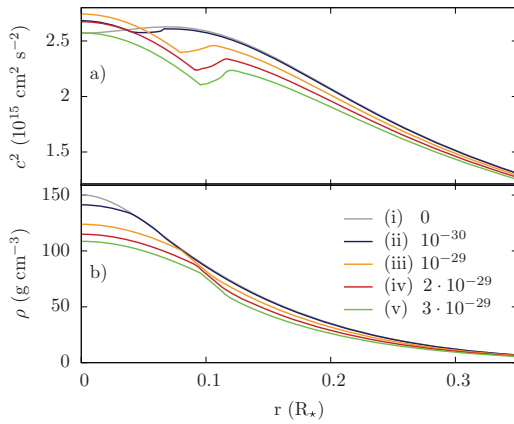


Figure 1. Sound-speed (a) and density (b) profiles of $1 M_{\odot}$ stars that evolved in DM haloes with different densities ρ_{χ} and SD WIMP-nucleon cross-sections $\sigma_{\chi,SD}$ when they reached a luminosity $L = 1 L_{\odot}$ (for each star, the product $\rho_{\chi} \sigma_{\chi}$ is indicated in the legend in GeV cm^{-1}).

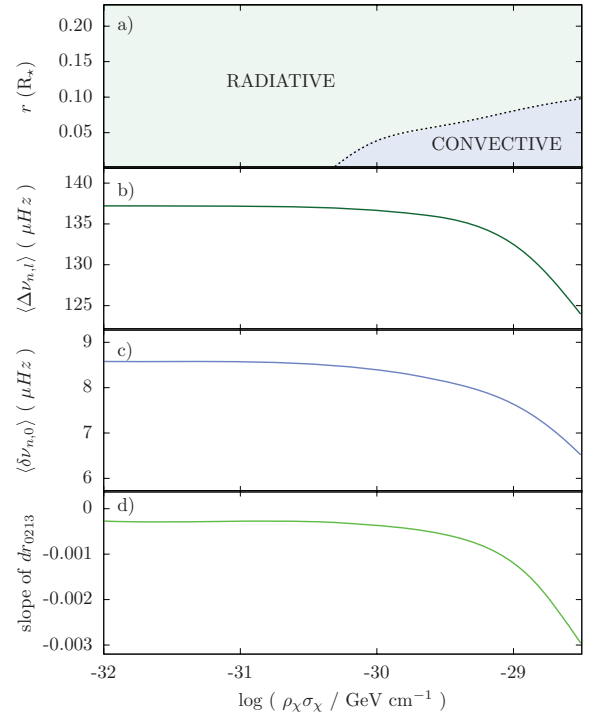


Figure 2. (a) Size of the convective core and the calculated seismological parameters, (b) mean large separation (for $l = 0, 1, 2, 3$), (c) mean small separation (for $l = 0$) and (d) slope of dr_{0213} , for $1 M_{\odot}$ stars that evolved in DM haloes with different densities ρ_{χ} and SD WIMP-nucleon cross-sections $\sigma_{\chi,SD}$, when the stars reached a luminosity $L = 1 L_{\odot}$.

star. Furthermore, we also observed a drop on the small separation $\delta \nu_{n,0}$ (see Fig. 2c), caused by a decrease in the central density. The strong dependence of the global modes on the density profile of the star is responsible for that drop.

In order to test the validity of our method, we checked if classical stars with similar characteristics may mimic the properties we described for stars evolving in DM haloes. In particular, we found that a star with a mass $M_{\star} = 0.955 M_{\odot}$ and a metallicity $Z = 0.04$ reaches, near the end of the main sequence, the same luminosity and effective temperature as the star (iv) in our set (see Table 1). At that moment, the radius of both stars is identical, leading to very similar great separations [$\langle \Delta \nu_{n,l} \rangle = 128 \mu\text{Hz}$ for star (iv) and $126 \mu\text{Hz}$ for the other]. However, as the star that evolved without DM is in a later stage of evolution ($X_c = 0.03$, while $X_c = 0.38$ for star iv), the small separation, being very sensitive to the chemical gradient in the deep interior, allows us to differentiate both stars. In our case, star

(iv), which evolved in a dense halo of DM, has a $\langle \delta v_{n,0} \rangle = 7 \mu\text{Hz}$. This is almost double than that of the star with different M_* and Z ($\langle \delta v_{n,0} \rangle = 4 \mu\text{Hz}$ in that case).

In addition, one of the most promising signatures of annihilating DM in stars is the fact that it can originate the formation of a convective core (unexpected in the classical picture for stars with masses $< 1.2 M_\odot$) whose radius grows with the DM density ρ_χ . The convective core leaves a peculiar footprint in the profiles of the sound speed and density (see Fig. 1) characterized by a discontinuity in the edge of the core. The presence of the convective core can be detected by the seismological analysis using a relation between the small separation of modes with different degrees (and therefore with different depths of penetration inside the star). For that purpose low-degree modes ($l = 0, 1, 2, 3$) are chosen, because these modes are the ones that penetrate deep into the stellar core.

In particular, we found that the seismological parameter dr_{0213} (see equation 8) is sensitive to the sound-speed discontinuity at the edge of the convective core and, consequently, to the characteristics of the DM halo. In Fig. 3(a) we show the behaviour of the parameter dr_{0213} for stars that evolve in DM haloes with different characteristics. We found that the absolute value of the slope of dr_{0213} at high frequencies increases with the amplitude of the sound-speed discontinuity caused by the convective core, as predicted by Cunha & Metcalfe. Therefore, the slope of dr_{0213} is directly related with the amount of DM in the halo where the star evolves (see also Fig. 2d).

We also tested the method recently proposed by Silva Aguirre et al. (2010) designed to estimate the size of a convective core in $1.5 M_\odot$ stars. We found that the period of the sinusoidal fit to the ratios r_{01} and r_{10} (see Fig. 3b) does not match exactly the acoustic radius of the convective cores (see Table 1), most probably because we are applying this method to stars of mass $1 M_\odot$. However, the ratios r_{01} and r_{10} have a great sensitivity to the amplitude of the

sharp variation of the sound speed caused by the annihilation of DM particles inside the star. We conclude that these ratios may be used in the future as a stellar probe to confirm the presence of DM in the neighbourhood of low-mass stars.

If enough radial modes are identified with the precision presently achieved by space-based telescopes as *CoRoT* [a relative error on the individual frequencies of $\sim 10^{-4}$ (Deheuvels et al. 2010)], then our method will allow the discrimination between haloes of DM with different characteristics. To illustrate this point, we plotted in Fig. 3 the error bars on dr_{0213} , r_{01} and r_{10} for star (iii) derived from the mentioned uncertainty ($10^{-4}\nu$) on the determination of the frequencies, as done by Cunha & Metcalfe (2007).

5 DISCUSSION AND CONCLUSIONS

In this paper, we have presented a new methodology towards the use of asteroseismology to prove the presence of DM in the location where a star evolves. For a main-sequence star of mass $1 M_\odot$ evolving in a DM halo with a density $\rho_\chi > 10^8 \text{ GeV cm}^{-3}$ (assuming $\sigma_{\chi,\text{SD}} = 10^{-38} \text{ cm}^2$), the annihilation of captured DM particles on its interior leads to decreases in the large and small separations, when compared with the same star in the classical scenario without DM, which are related to changes in the global properties of the star. Furthermore, the highly concentrated production of energy by DM annihilation creates a convective core which is not present in the classical picture. This convective core leaves a discontinuity signature in the sound-speed and density profiles which can be detected by the analysis of the stellar oscillations.

We have shown that seismological parameters such as dr_{0213} and the ratios r_{01} and r_{10} are very sensitive to the size of the convective core, which is determined by the density of DM, ρ_χ , where the star evolved and by the scattering cross-section of the DM particles off nuclei, σ_χ . Consequently, this relationship may be used in the future to help in the determination of these parameters (or at least to their product, $\rho_\chi \sigma_\chi$) and to provide a stellar probe that identifies the presence of self-annihilating DM.

The method presented in this paper is valid for haloes with very high DM densities. In Fig. 4 we show the DM densities at which a $1 M_\odot$ star with a luminosity $1 L_\odot$ is expected to have a small separation 25 per cent smaller than that in the classical picture, because of the annihilation of DM particles with different characteristics (m_χ , $\sigma_{\chi \rightarrow p,\text{SD}}$) in its interior. If found, this kind of star will also have strong signatures on the seismic parameters $\Delta\nu$, dr_{0213} , r_{01} and r_{10} when compared with a star with the same luminosity that evolved without DM. In the same figure are also shown the current limits on $\sigma_{\chi \rightarrow p,\text{SD}}$ from the direct detection experiments XENON10 (Angle et al. 2008), PICASSO (Archambault et al. 2009), COUPP (Behnke et al. 2008) and the allowed region from the DAMA/LIBRA experiment (Savage et al. 2009).

The extreme DM densities shown in Fig. 4 may be present within the inner parsec of our Galaxy, according to models that account for the effect of the baryons on the DM halo via adiabatic contraction (Blumenthal et al. 1986; Gnedin et al. 2004). For instance, following the adiabatically contracted profile of Bertone & Merritt (2005), DM densities as high as $\rho_\chi = 10^8 \text{ GeV cm}^{-3}$ are expected at 0.1 pc from the Galactic Centre (GC). Even higher DM densities may be present at the GC if a hypothetical spike is formed due to the influence of the central black hole (Gondolo & Silk 1999). However, as other models predict lower central DM densities [the so-called *core models* (Burkert 1995)], the open questions about the DM halo profile at the inner parsec of our Galaxy are still far from being solved [for a recent review on this topic, see Merritt (2010) and de

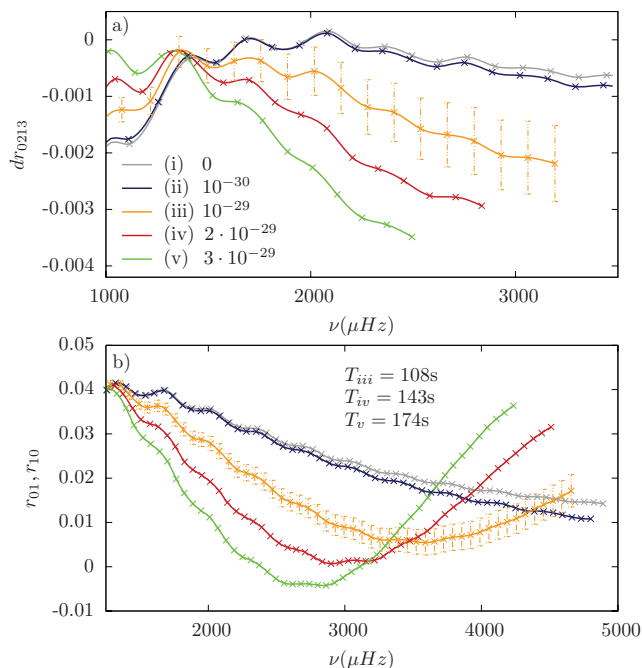


Figure 3. (a) The seismological parameter dr_{0213} and (b) the ratios r_{01} and r_{10} for stars that evolved in DM haloes with different densities ρ_χ and different SD WIMP-nucleon cross-sections $\sigma_{\chi,\text{SD}}$ when they reached a luminosity $L = 1 L_\odot$ (for each star, the product $\rho_\chi \sigma_\chi$ is indicated in the legend in GeV cm^{-1}). Error bars are shown for star (iii) assuming a relative error on the identification of the frequencies of 10^{-4} .

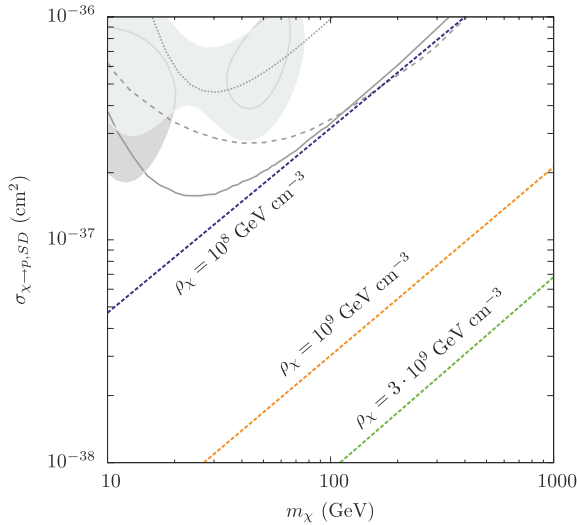


Figure 4. DM densities at which $1M_{\odot}$ stars with a luminosity $1L_{\odot}$ are expected to show strong signatures on the seismological parameters $\Delta\nu$, $\delta\nu$, dr_{0213} , r_{01} and r_{10} (see text) due to the annihilation of DM particles with different characteristics (m_{χ} , $\sigma_{\chi \rightarrow p, SD}$) in their interior. In the particular case of the Galactic Centre (GC), the DM densities in the figure (from top to bottom) are expected at a distance from the GC of 0.1, 0.04 and 0.02 pc, following the adiabatically contracted profile of Bertone & Merritt. The grey lines are the present limits from direct detection experiments: XENON10 (dotted), PICASSO (dashed) and COUPP (solid), and the grey region is the DAMA/LIBRA allowed region.

Blok (2010)]. In this sense, the method proposed here may provide a complementary tool to help in the discrimination of different models. Other possible locations of environments with such high DM densities are the dwarf spheroidal galaxies around the Milky Way (Dekel & Silk 1986; Kormendy & Freeman 2004; Diemand, Kuhlen & Madau 2007).

The precision required for our analysis is similar to the one achieved by present asteroseismic missions in observations of one hundred days. Nevertheless, the most likely place to find the kind of stars described here is near the centre of our Galaxy, where the distance and the presence of dust makes the observations difficult. These difficulties encourage us to extend our study to more massive and luminous stars in a future work. Future technical improvements in the observations of the GC and of the Milky Way dwarf galaxies may open the possibility of using the method proposed here to investigate the nature of DM.

ACKNOWLEDGMENTS

We acknowledge the anonymous referee for his useful comments, as well as the authors of CESAM, ADIPLS and DARKSUSY, and the Brown University's Particle Astrophysics Group, which maintains the DM tools web site, used for the $\sigma_{\chi \rightarrow p, SD}$ limits in Fig. 4. This work was supported by grants from 'Fundação para a Ciência e Tecnologia' (SFRH/BD/44321/2008) and 'Fundação Calouste Gulbenkian'.

REFERENCES

Aerts C., Christensen-Dalsgaard J., Kurtz D. W., 2010, *Asteroseismology*. Springer, Dordrecht
 Angle J. et al., 2008, *Phys. Rev. Lett.*, 101, 91301
 Archambault S. et al., 2009, *Phys. Lett. B*, 682, 185
 Bedding T. R. et al., 2010, *ApJ*, 713, L176

Behnke E. et al., 2008, *Sci*, 319, 933
 Bertone G., Fairbairn M., 2008, *Phys. Rev. D*, 77, 43515
 Bertone G., Merritt D., 2005, *Modern Phys. Lett. A*, 20, 1021
 Bertone G., Hooper D., Silk J., 2005, *Phys. Rep.*, 405, 279
 Blumenthal G. R., Faber S. M., Flores R., Primack J. R., 1986, *ApJ*, 301, 27
 Bottino A., Fiorentini G., Fornengo N., Ricci B., Scopel S., Villante F. L., 2002, *Phys. Rev. D*, 66, 53005
 Bouquet A., Salati P., 1989, *ApJ*, 346, 284
 Burkert A., 1995, *ApJ*, 447, L25
 Casanellas J., Lopes I., 2009, *ApJ*, 705, 135
 Casanellas J., Lopes I., 2010, preprint (arXiv e-prints)
 Christensen-Dalsgaard J., 2008, *Ap&SS*, 316, 113
 Christensen-Dalsgaard J., Houdek G., 2009, *Ap&SS*, 328, 264
 Couvidat S., Turck-Chièze S., Kosovichev A. G., 2003, *ApJ*, 599, 1434
 Cox J. P., 1980, *Theory of Stellar Pulsation*. Princeton Univ. Press, Princeton
 Cumberbatch D. T., Guzik J. A., Silk J., Watson L. S., West S. M., 2010, preprint (arXiv e-prints)
 Cunha M. S., Metcalfe T. S., 2007, *ApJ*, 666, 413
 Dappen W., Gilliland R. L., Christensen-Dalsgaard J., 1986, *Nat*, 321, 229
 de Blok W. J. G., 2010, *Advances Astron.*, Vol. 5
 de Lavalaz A., Fairbairn M., 2010, *Phys. Rev. D*, 81, 123521
 De Ridder J., Barban C., Carrier F., Mazumdar A., Eggenberger P., Aerts C., Deruyter S., Vanautgaerden J., 2006, *A&A*, 448, 689
 Dearborn D., Raffelt G., Salati P., Silk J., Bouquet A., 1990, *ApJ*, 354, 568
 Deheuvels S. et al., 2010, *A&A*, 515, A87
 Dekel A., Silk J., 1986, *ApJ*, 303, 39
 Diemand J., Kuhlen M., Madau P., 2007, *ApJ*, 667, 859
 Fairbairn M., Scott P., Edsjö J., 2008, *Phys. Rev. D*, 77, 47301
 Faulkner J., Gough D. O., Vahia M. N., 1986, *Nat*, 321, 226
 Frandsen M. T., Sarkar S., 2010, *Phys. Rev. Lett.*, 105, 11301
 Freese K., Bodenheimer P., Spolyar D., Gondolo P., 2008a, *ApJ*, 685, L101
 Freese K., Spolyar D., Aguirre A., 2008b, *J. Cosmol. Astropart. Phys.*, 11, 14
 Freese K., Ilie C., Spolyar D., Valluri M., Bodenheimer P., 2010, *ApJ*, 716, 1397
 García R. A. et al., 2009, *A&A*, 506, 41
 Gnedin O. Y., Kravtsov A. V., Klypin A. A., Nagai D., 2004, *ApJ*, 616, 16
 Gondolo P., Silk J., 1999, *Phys. Rev. Lett.*, 83, 1719
 Gondolo P., Edsjö J., Ullio P., Bergström L., Schelke M., Baltz E. A., 2004, *J. Cosmol. Astropart. Phys.*, 7, 8
 Gough D., 1985, *Nat*, 314, 14
 Gough D. O., 1990, in Osaki Y., Shibahashi H., eds, *Lect. Notes Phys.*, Vol. 367, *Progress of Seismology of the Sun and Stars*. Springer-Verlag, Berlin, p. 283
 Gould A., 1987, *ApJ*, 321, 571
 Iocco F., 2008, *ApJ*, 677, L1
 Iocco F., Bressan A., Ripamonti E., Schneider R., Ferrara A., Marigo P., 2008, *MNRAS*, 390, 1655
 Isern J., García-Berro E., Torres S., Catalán S., 2008, *ApJ*, 682, L109
 Isern J., García-Berro E., Althaus L. G., Córscico A. H., 2010, *A&A*, 512, A86
 Kervella P., Thévenin F., Morel P., Berthomieu G., Bordé P., Provost J., 2004, *A&A*, 413, 251
 Kormendy J., Freeman K. C., 2004, in Ryder S., Pisano D., Walker M., Freeman K., eds, *Proc. IAU Symp. 220, Dark Matter in Galaxies*. Astron. Soc. Pac., San Francisco, p. 377
 Kouvaris C., Tinyakov P., 2010, preprint (arXiv e-prints)
 Lopes I. P., Gough D., 2001, *MNRAS*, 322, 473
 Lopes I. P., Silk J., 2002, *Phys. Rev. Lett.*, 88, 151303
 Lopes I., Turck-Chièze S., 1994, *A&A*, 290, 845
 Lopes I., Turck-Chièze S., Michel E., Goupil M., 1997, *ApJ*, 480, 794
 Lopes I. P., Silk J., Hansen S. H., 2002a, *MNRAS*, 331, 361
 Lopes I. P., Bertone G., Silk J., 2002b, *MNRAS*, 337, 1179
 Merritt D., 2010, in Bertone G., ed., *Particle Dark Matter: Observations, Models and Searches*. Cambridge Univ. Press, Cambridge, p. 83
 Michel E. et al., 2008, *Sci*, 322, 558
 Monteiro M. J. P. F. G., Christensen-Dalsgaard J., Thompson M. J., 1994, *A&A*, 283, 247

- Morel P., 1997, *A&AS*, 124, 597
Moskalenko I. V., Wai L. L., 2007, *ApJ*, 659, L29
Natarajan A., Tan J. C., O'Shea B. W., 2009, *ApJ*, 692, 574
Perez-Garcia M. A., Silk J., Stone J. R., 2010, preprint (arXiv e-prints)
Press W. H., Spergel D. N., 1985, *ApJ*, 296, 679
Ripamonti E., Iocco F., Ferrara A., Schneider R., Bressan A., Marigo P., 2010, *MNRAS*, 406, 883
Roxburgh I. W., Vorontsov S. V., 2003, *A&A*, 411, 215
Salati P., Silk J., 1989, *ApJ*, 338, 24
Savage C., Gelmini G., Gondolo P., Freese K., 2009, *J. Cosmol. Astropart. Phys.*, 4, 10
Schleicher D. R. G., Banerjee R., Klessen R. S., 2009, *Phys. Rev. D*, 79, 43510
Scott P., Fairbairn M., Edsjö J., 2009, *MNRAS*, 394, 82
Silva Aguirre V., Ballot J., Serenelli A., Weiss A., 2010, preprint (arXiv e-prints)
Sivertsson S., Gondolo P., 2010
Spolyar D., Freese K., Gondolo P., 2008, *Phys. Rev. Lett.*, 100, 51101
Suárez J. C., Andrade L., Goupil M. J., Janot-Pacheco E., 2010, preprint (arXiv e-prints)
Taoso M., Bertone G., Meynet G., Ekström S., 2008, *Phys. Rev. D*, 78, 123510
Taoso M., Iocco F., Meynet G., Bertone G., Eggenberger P., 2010, preprint (arXiv e-prints)
Tassoul M., 1980, *ApJS*, 43, 469
Turck-Chièze S., Palacios A., Marques J. P., Nghiem P. A. P., 2010, *ApJ*, 715, 1539
Yoon S.-C., Iocco F., Akiyama S., 2008, *ApJ*, 688, L1
Zackrisson E. et al., 2010, *ApJ*, 717, 257

This paper has been typeset from a \TeX/L\TeX file prepared by the author.

A.3 Paper III

THE CAPTURE OF DARK MATTER PARTICLES THROUGH THE EVOLUTION OF LOW-MASS STARS

Lopes I., **Casanellas J.** & Eugénio D.
Physical Review D 83, 063521 (2011)
[arXiv:1102.2907](https://arxiv.org/abs/1102.2907)

The capture of dark matter particles through the evolution of low-mass stars

Ilídio Lopes*

*Departamento de Física, Universidade de Évora, Portugal and CENTRA, Instituto Superior Técnico, Lisboa, Portugal*Jordi Casanellas[†] and Daniel Eugénio[‡]*CENTRA, Instituto Superior Técnico, Lisboa, Portugal*
(Received 16 December 2010; published 22 March 2011)

We studied the rate at which stars capture dark matter (DM) particles, considering different assumptions regarding the DM characteristics and, in particular, investigating how the stellar physics influences the capture rate. Two scenarios were considered: first, we assumed the maximal values for the spin-dependent and spin-independent DM particle-nucleon scattering cross sections allowed by the limits from direct detection experiments. Second, we considered that both scattering cross sections are of the same order, with the aim of studying the dependencies of the capture rate on stellar elements other than hydrogen. We found that the characteristics of the capture rate are very different in the two scenarios. Furthermore, we quantified the uncertainties on the computed capture rate (C_χ) and on the ratio between the luminosities from DM annihilations and thermonuclear reactions (L_χ/L_{nuc}) derived from an imprecise knowledge of the stellar structure and DM parameters. For instance, while an uncertainty of 10% on the typical DM velocity leads to similar errors on the computed C_χ and L_χ/L_{nuc} , the same uncertainty on the stellar mass becomes more relevant and duplicates the errors. Our results may be used to evaluate the reliability of the computed capture rate for the hypothetical use of stars other than the Sun as DM probes.

DOI: 10.1103/PhysRevD.83.063521

PACS numbers: 95.35.+d, 97.10.-q

I. INTRODUCTION

The study of the rate at which stars capture dark matter (DM) particles is of vital importance to understand in which situations stars are able to accumulate enough DM to influence their evolution. The possibility of using the properties of stars within dense DM halos as an indirect method to investigate the nature of DM relies on the precision of the capture rate calculation. This quantity depends on both the DM characteristics and the details of the stellar structure [1,2].

In the case of the Sun, a precise calculation of the capture rate is very important to predict the neutrino flux from DM annihilations in the center of the star [3–6] and to calculate the changes in the solar neutrino flux induced by an isothermal core created by the energy transport due to DM particles conduction [7–10]. In this context, the systematic errors in the determination of the local DM density were recently studied [11–13], as well as the uncertainties coming from other astrophysical sources, as the shape of the velocity distribution of the DM particles or the motion of the Sun in respect to the DM halo [14,15]. These works have shown that the systematic errors introduced by such astrophysical parameters are considerably large if one wants to extract information about the type of DM particle only from current direct or indirect detection experiments.

On the other hand, the scope of our work is to characterize the capture rate for stars other than the Sun. Recent works have shown that, when embedded in dense halos of DM, stars may dramatically change their properties [16–26]. In these cases, the uncertainties in the knowledge of the typical parameters governing the capture rate are much larger. Generally, in the literature, when the capture rate of DM particles is calculated for stars other than the Sun, as for compact stars [27–30] or low-mass stars [31–33], the fiducial values for the local Keplerian velocity ($v_\star = 220 \text{ km s}^{-1}$) and DM velocity distribution (Maxwell-Boltzmann [MB] distribution with a velocity dispersion $\bar{v}_\chi = 270 \text{ km s}^{-1}$) are assumed. However, in the situations where these stars can exist, these parameters may have very different values. For instance, in a possible interesting place such as near the center of our Galaxy, the velocities of the stars range from 10 to 500 km s^{-1} [34] and the DM particles may have motions dominated by the gravitational potential of the hypothetical central black hole [35]. Simultaneously, the stellar velocity dispersions measured in nearby galaxies range from 10 to 400 km s^{-1} [36]. In the first part of this paper we explore how the stellar capture rate changes with the astrophysical parameters and DM characteristics in order to grasp the possible modifications in the effects that DM annihilation may have on stars other than the Sun.

In the second part of this paper we characterize how the capture rate changes during the life of a star (from the collapse of the protostar to the helium flash) considering stars with different masses ($0.5M_\odot$ to $7M_\odot$) and metallicities ($Z = 0.0004$ to $Z = 0.04$).

*ilidio.lopes@ist.utl.pt

†jordicasanellas@ist.utl.pt

‡dan.far.eugenio@gmail.com

We will consider two scenarios. First, a scenario where the capture is dominated by the spin-dependent (SD) collisions of hydrogen atoms with the DM particles, which corresponds to assuming the maximal DM particle-nucleon scattering cross sections allowed by the limits from direct detection experiments. Second, a scenario where the SD and spin-independent (SI) scattering cross sections are of the same order, a plausible possibility given that both interactions came from similar processes [37,38]. In fact, in many supersymmetric models the scalar interaction (SI) often dominates the elastic scattering [39,40]. Within this assumption, other stellar elements such as oxygen, helium, or iron arise as the more relevant ones in capturing DM particles. Thus, we also explore how different stellar and DM physics change the role of the dominant elements in the capture rate. Finally, in the last part of this paper we study how the uncertainties in the determination of these parameters influence the computed capture rate and the impact of the annihilation of DM particles inside stars.

II. STELLAR CAPTURE OF DM PARTICLES

To study the various dependencies of the capture rate some routines of the DARKSUSY code [41] were adapted in order to include them on a modified version of the stellar evolution code CESAM [42]. The latter code has a very refined stellar physics, tested against helioseismic data in the case of the Sun [43,44]. If not stated otherwise, we assume a stellar metallicity $Z = 0.019$, an helium mass fraction $Y = 0.273$, and abundances of the other elements as the solar ones [45].

The capture rate is computed in our code according to the expressions of Gould [46],

$$C_\chi(t) = \sum_i \int_0^{R_\star} 4\pi r^2 \int_0^\infty \frac{f_{v_\star}(u)}{u} w \Omega_{v,i}^-(w) du dr, \quad (1)$$

$$\Omega_{v,i}^-(w) = \frac{\sigma_{\chi,i} n_i(r)}{w} \left(v_e^2 - \frac{\mu_{\pm,i}^2}{\mu_i} u^2 \right) \theta \left(v_e^2 - \frac{\mu_{\pm,i}^2}{\mu_i} u^2 \right), \quad (2)$$

$$\mu_i \equiv \frac{m_\chi}{m_{n,i}}, \quad \mu_{\pm,i} \equiv \frac{\mu_i \pm 1}{2}, \quad (3)$$

where

$\Omega_{v,i}^-(w)$ is the rate of scattering of a DM particle with the nucleus of an element i , from an initial velocity w at the radius of the collision to a velocity lower than the escape velocity of the star $v_e(r)$ at that radius (kinetic factor);

$f_{v_\star}(u)$ is the velocity distribution of the DM particles seen by the star, which depends on the velocity of the star v_\star and on the velocity distribution of the DM particles in the halo $f_0(u)$;

m_χ is the mass of the DM particle;

$\sigma_{\chi,i}$ is its scattering cross section with an element i , which is $\sigma_{\chi,i} = \sigma_{\chi,SI} A_i^2 \left(\frac{m_\chi m_{n,i}}{m_\chi + m_{n,i}} \right)^2 \left(\frac{m_\chi + m_p}{m_\chi m_p} \right)^2$ for all stellar

elements except for hydrogen, which has also the contribution from the spin-dependent (SD) interactions $\sigma_{\chi,H} = \sigma_{\chi,SI} + \sigma_{\chi,SD}$;

$m_{n,i}$, A_i are the nuclear mass and the atomic number of the element i ;

$n_i(r)$ is the density of the element i at a radius r ; and

R_\star is the total radius of the star.

For stellar elements other than hydrogen a suppression form factor is considered, along the lines of Gould [46], to account for the influence of the size of the nucleus on the interactions. Thus, the scattering rate is

$$\begin{aligned} \Omega_{v,i}^-(w) = & \frac{\sigma_{\chi,i} n_i(r)}{w} \frac{2E_0}{m_\chi} \frac{\mu_{\pm,i}^2}{\mu_i} \\ & \times \left\{ \exp\left(-\frac{m_\chi u^2}{2E_0}\right) - \exp\left(-\frac{m_\chi u^2}{2E_0} \frac{\mu_i}{\mu_{\pm,i}^2}\right) \right. \\ & \left. \times \exp\left(-\frac{m_\chi v_e^2}{2E_0} \frac{\mu_i}{\mu_{\pm,i}^2} \left(1 - \frac{\mu_i}{\mu_{\pm,i}^2}\right)\right) \right\}, \quad (4) \end{aligned}$$

where $E_0 \approx 3\hbar/(2m_{n,i}(0.91m_{n,i}^{1/3} + 0.3)^2)$ is the characteristic coherence energy. The abundances of ^2H , ^4He , ^{12}C , ^{14}N , ^{16}O , and other isotopes which are produced or burned during the proton-proton (pp) chain, carbon-nitrogen-oxygen (CNO) cycle, or triple alpha nuclear reactions are followed by our code. For iron, neon, and silicon, among others, their proportion over the remaining mass is set as in the solar composition.

The new energy transport mechanism by conduction of the DM particles [47] and the new energy source by the annihilation of DM particles inside the star [48] are also included in this version of the code. However, these processes do not influence the total capture rate of the stars computed in this work.

III. CAPTURE RATE DEPENDENCE ON DM PROPERTIES

A. DM halo density and scattering cross sections

The total number of DM particles captured by a star is proportional to both the density of DM in the halo ρ_χ and the DM particle-nucleon scattering cross section σ_χ [see Fig. 1(a) and 1(b)]. Hence, all the capture rates that will be shown in this work may be simply rescaled if the reader wants to consider other values of ρ_χ or σ_χ . If not stated otherwise, a DM density $\rho_\chi = 0.3 \text{ GeV cm}^{-3}$ and DM-nucleon scattering cross sections $\sigma_{\chi,SD} = 10^{-38} \text{ cm}^2$ [49,50] and $\sigma_{\chi,SI} = 10^{-44} \text{ cm}^2$ [51] (the largest cross sections allowed by the limits from direct detection experiments) are assumed in our computations, as is generally done in the literature when the effects of DM particles on stars are studied [52,53]. Within this assumption, the capture rate is always dominated by the contribution of the SD collisions of the DM particles with hydrogen atoms.

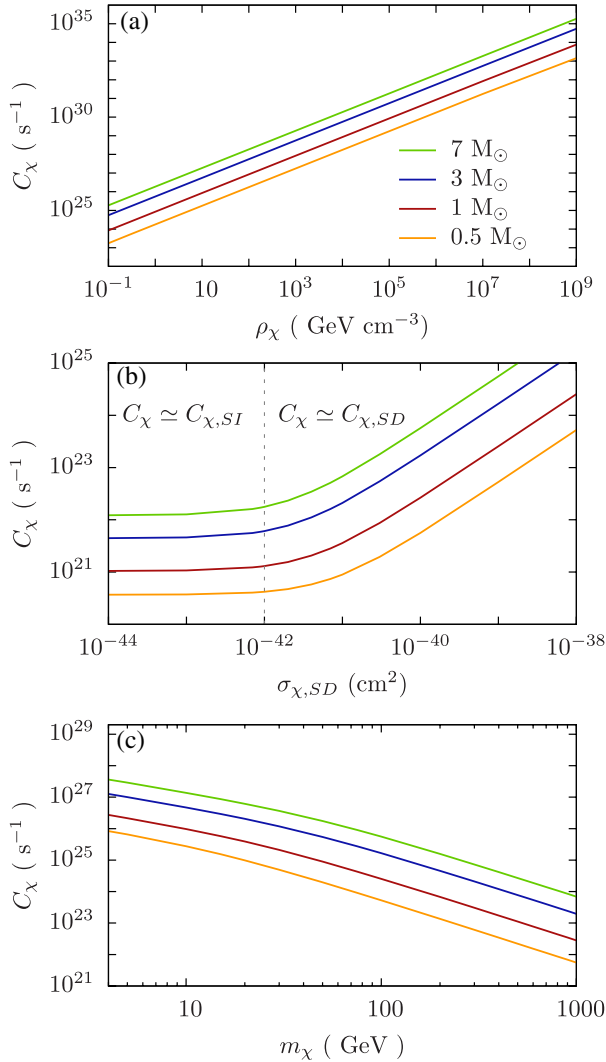


FIG. 1 (color online). Rate at which DM particles are captured for stars of different masses, considering different DM halo densities (a), different SD DM particle-nucleon scattering cross sections (b), and different masses of the DM particles (c). If not stated otherwise, a halo of DM particles with $\rho_\chi = 0.3 \text{ GeV cm}^{-3}$, $m_\chi = 100 \text{ GeV}$, and scattering cross sections $\sigma_{\chi,SD} = 10^{-38} \text{ cm}^2$ and $\sigma_{\chi,SI} = 10^{-44} \text{ cm}^2$ is assumed.

On the other hand, the dependencies of the capture rate change when values for the SD scattering cross section closer to the SI ones are considered. We found that for $\sigma_{\chi,SD}$ smaller than 10^{-42} cm^2 the SI interactions are responsible for most of the captures [see Fig. 1(b)]. More generally, for a SD scattering cross section smaller than a hundred times the SI one, the SI collisions dominate the total capture rate. In this scenario, other stellar elements, such as oxygen, iron, or helium, play an important role in the capture of DM particles. This situation is studied in depth in Sec. IV.

We note that, for stellar metallicities different from the solar one, the ratio $r \equiv \sigma_{\chi,SD}/\sigma_{\chi,SI}$ below which SI

interactions dominate changes: $r \simeq 70$ for $Z = 0.0004$ while $r \simeq 1000$ for $Z = 0.04$.

B. Mass of the DM particles

The capture rate is roughly inversely proportional to the mass of the DM particles m_χ , as it is proportional to the number density of DM particles in the halo $\frac{\rho_\chi}{m_\chi}$. In Fig. 1(c) are shown the big decreases found in C_χ when m_χ goes from 4 to 1000 GeV. We have chosen a range of masses above the limit from which evaporation can be considered negligible [2,54,55], which includes the light weakly interacting massive particles (WIMPs) recently invoked as the DM candidates that can reconcile the results from different direct detection experiments [56,57].

The drop in the capture rate due to a large m_χ has no consequences when considering the effects of DM annihilation inside stars. When m_χ is large, the star captures a small number of DM particles, but each of the few annihilations that take place releases more energy, compensating for the low capture. On the other hand, considering a different m_χ does influence the distribution of DM particles inside the star. This fact has consequences on the seismological signature of the isothermal core created in the center of the Sun by the transport of energy through DM conduction [58–62], and on the strong seismological signature of DM annihilation inside solarlike stars within very dense DM halos [63].

Alternatively, in the scenario where the capture rate is dominated by the SI interactions the drop in the capture rate when the DM mass increases is not so steep [see Fig. 2(a)]. This is a consequence of the capture due to the collisions of the DM particles with the heavier elements. These interact through SI scattering, while hydrogen, the lightest element, is the only one contributing to the SD capture. The capture rate of DM particles with different masses discriminated by the elements that are responsible for the collisions that lead to the capture, $C_{\chi,i}$, is shown in Fig. 2(b). While ^4He dominates the capture of lighter WIMPs, ^{16}O does the same for the heavier ones [64]. In Fig. 2(b) it can also be seen that each of the elements has a peak of its capture rate when the WIMP mass is roughly equal to its own mass [2,46]. Therefore, while the captures due to the hydrogen and helium are highly suppressed for larger DM masses, the capture for heavier elements decreases less steeply with m_χ .

The causes for the enhancement or suppression of the $C_{\chi,i}$ at different DM masses are found in three different factors, all of them functions of m_χ : the SI scattering cross section, the kinetic factor, and the form factor. Both of the first two factors introduce an A_i^2 dependence on $C_{\chi,i}$, thus enhancing the capture rate due to collisions with the heavier elements. On the other hand, the nuclear form factor slows down this effect suppressing the capture rate only for the isotopes with larger atomic numbers (see Ref. [46]).

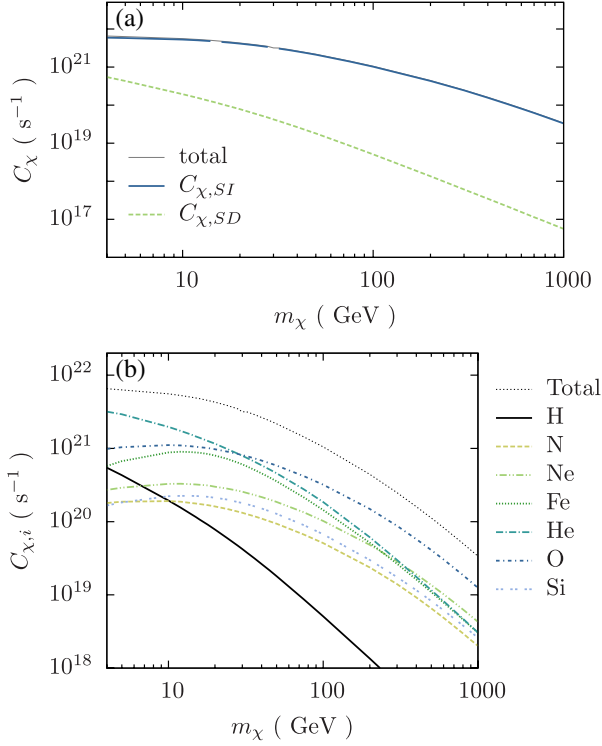


FIG. 2 (color online). (a) Rate at which DM particles are captured for a $1M_{\odot}$ MS star due to the SD interactions of the DM particles with hydrogen (green dashed line) and due to SI interactions with hydrogen, nitrogen, neon, iron, helium, oxygen, and silicon, among others (blue solid line). (b) Capture rate discriminated by the element responsible for the collision that led to the capture. We assumed a halo of DM particles with $\rho_{\chi} = 0.3 \text{ GeV cm}^{-3}$ and the DM-nucleon scattering dominated by the spin-independent (SI) component, $\sigma_{\chi,SI} = \sigma_{\chi,SD} = 10^{-44} \text{ cm}^2$.

C. Phase space of the DM particles

Generally, the literature assumes a Maxwell-Boltzmann distribution for the velocities of the DM particles $f_0(u)$, with a dispersion \bar{v}_{χ} , leading to a velocity distribution seen by the star of [46,65,66]

$$f_{v_{\star}}(u) = f_0(u) \exp\left(-\frac{3v_{\star}^2}{2\bar{v}_{\chi}^2}\right) \frac{\sinh(3uv_{\star}/\bar{v}_{\chi}^2)}{3uv_{\star}/\bar{v}_{\chi}^2} \quad (5)$$

$$f_0(u) = \frac{\rho_{\chi}}{m_{\chi}} \frac{4}{\sqrt{\pi}} \left(\frac{3}{2}\right)^{3/2} \frac{u^2}{\bar{v}_{\chi}^3} \exp\left(-\frac{3u^2}{2\bar{v}_{\chi}^2}\right). \quad (6)$$

Within this assumption, we explored how the capture rate changes for different values of v_{\star} and \bar{v}_{χ} . First, a MB distribution of the DM particles with a fixed $\bar{v}_{\chi} = 270 \text{ km s}^{-1}$ was considered and the stellar velocity v_{\star} was varied from 50 to 500 km s^{-1} [see Fig. 3(a)]. We found that at high stellar velocities the capture rate drops because the DM particles that the star encounters are more energetic and consequently are more difficult to capture. Second, a

fiducial value for $v_{\star} = 220 \text{ km s}^{-1}$ was considered and the dispersion velocity of the DM particles \bar{v}_{χ} was varied from 50 to 500 km s^{-1} . As expected, for higher dispersions of the DM velocity distribution the capture rate is lower, as more DM particles have high velocities and are not captured. We note that in this situation one may consider to truncate the velocity distribution at the galactic escape velocity. This was included in the capture rate computed by Ref. [65] in the case of main sequence (MS) stars at the Galactic center and by Ref. [14] in the case of the Sun. The latter authors found that the uncertainties in the knowledge of the local escape velocity lead to errors on the estimation of the solar capture rate of approximately 10%.

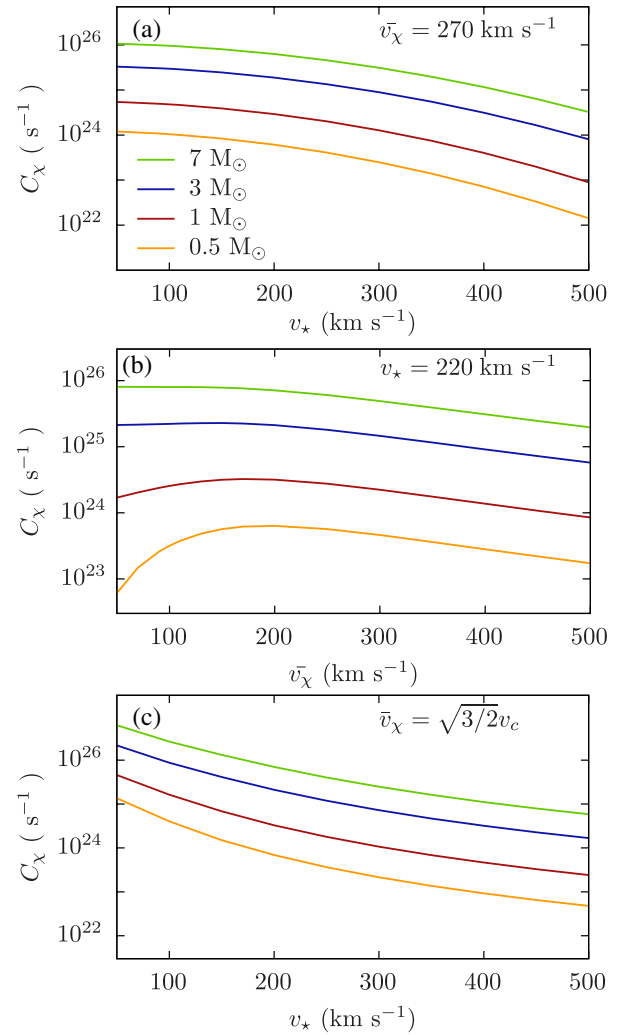


FIG. 3 (color online). Rate at which DM particles are captured for stars of different masses, considering different stellar velocities (a), different DM typical velocities (b), and varying both speeds relating them through $\bar{v}_{\chi} = \sqrt{3/2}v_c$ (c). We assumed a halo of DM particles with $\rho_{\chi} = 0.3 \text{ GeV cm}^{-3}$, $m_{\chi} = 100 \text{ GeV}$, and the DM-nucleon scattering dominated by the spin-dependent (SD) component, $\sigma_{\chi,SD} = 10^{-38} \text{ cm}^2$.

Assuming an isotropic, Gaussian velocity distribution of the DM particles, the velocity dispersion can be related to the circular speed (the velocity that a mass would have on a circular orbit in the galactic plane) using the Jeans equation [67], leading to $\bar{v}_\chi = \sqrt{3/2}v_c$. We considered the case of stars with $v_\star = v_c$ (an assumption that in the case of the Sun introduces an error of $\sim 10\%$ [14]) within DM halos with velocity dispersions $\bar{v}_\chi = \sqrt{3/2}v_\star$ and computed the capture rate for different stellar velocities. The results are shown in Fig. 3(c). As expected, the stars that encounter less energetic WIMPs (those traveling at small velocities) capture the DM particles more efficiently.

Other velocity distributions of the DM particles may be also considered. As a matter of fact, the MB distribution is not an accurate description of the velocity distribution in the Milky Way, as it corresponds to an isotropic isothermal sphere with a DM density profile $\rho_\chi \propto r^{-2}$, while both observations and simulations indicate other more plausible density profiles [68,69]. Better fits to the data are deviations from the Gaussian distribution (some examples can be found in Refs. [14,65]) or the Tsallis distribution [70]. Departures of the Maxwellian velocity distribution have been extensively studied to derive uncertainties for direct detection experiments [71–73], and will not be repeated here. These works found that more realistic descriptions for $f(v)$ may lead to deviations of $\sim 10\%$ in the signal expected on the detectors.

IV. STELLAR PHYSICS AND THE CAPTURE RATE

A. $\sigma_{\chi,SD} \gg \sigma_{\chi,SI}$ case

Throughout this section we assume as our fiducial values the maximum WIMP-nucleon scattering cross sections allowed by limits from direct detection experiments. In this scenario, the SD collisions of the DM particles with hydrogen are responsible for almost all the captured DM particles. In fact, the next element in importance for a star of $1M_\odot$ in the MS is oxygen, which is more than 10^4 times less efficient capturing DM particles than hydrogen.

1. Capture rate over stellar life

The evolution of the capture rate through the life of the star is studied in this section. Normally, a constant capture rate is assumed during the MS, and it is expected to vary rapidly during the pre- and post-MS phases due to the changes in the stellar structure. To address this question in detail, the capture rate was also computed during the gravitational collapse of the protostar and during the red giant branch (RGB) until the helium flash. The results are shown in Fig. 4(a) for stars with different masses.

As expected, we found that the capture rate increases continuously as the protostar collapses, remains constant during the MS, and finally drops suddenly in the RGB, when the star expands with hydrogen fusion undergoing only in a shell out of the contracting helium core. The

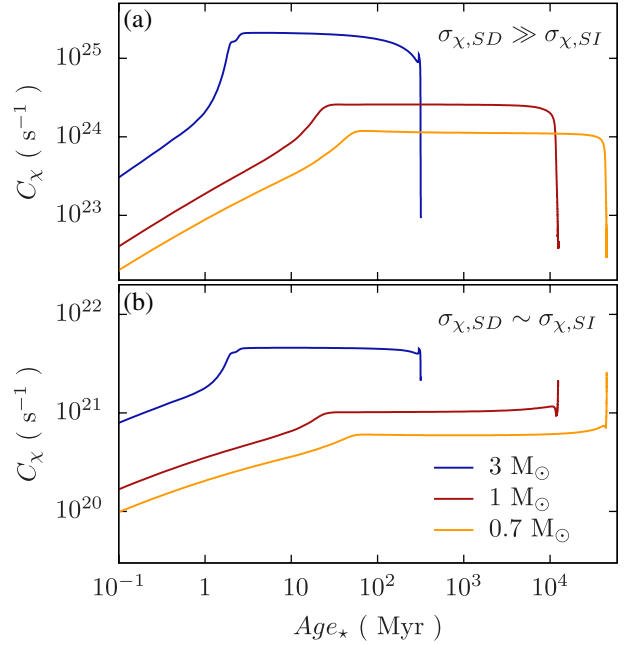


FIG. 4 (color online). Rate at which DM particles are captured during the life of stars with different masses. The capture rate increases during the pre-MS, is constant through the MS, and varies rapidly in the RGB. We assumed a halo of DM particles with $\rho_\chi = 0.3 \text{ GeV cm}^{-3}$, $m_\chi = 100 \text{ GeV}$, and the DM-nucleon scattering dominated (a) by the SD component, $\sigma_{\chi,SD} = 10^{-38} \text{ cm}^2$, and (b) by the SI one, $\sigma_{\chi,SI} = \sigma_{\chi,SD} = 10^{-44} \text{ cm}^2$.

changes in the capture rate mimic the changes in the global properties of the star, in particular, in the radius of the star and in the density of the various stellar elements $n_i(r)$, specially hydrogen.

However, as shown in Fig. 5(a), the predominance of hydrogen is reduced to just an order of magnitude in the RGB. At this stage the ^4He , produced in the center of the star through the proton-proton chain during the MS, now forms an inert helium core with a density that increases dramatically as the star evolves through the RGB. Therefore, the efficiency of this isotope in capturing DM particles increases, getting closer to hydrogen, much more abundant in the rest of the star and still responsible for most of the captures. Another isotope that gains importance during the RGB is ^{14}N , which is produced during the CNO cycle.

2. Capture and stellar metallicity

Stars with metallicities from $Z = 0.0004$ to $Z = 0.04$ (with their corresponding helium mass fractions from $Y = 0.2412$ to $Y = 0.340$, along the lines of Refs. [74,75]) were considered in order to study the dependence of the capture rate on the stellar metallicity. As expected, stars with a reduced hydrogen mass fraction (those richer in metals), capture DM particles less efficiently [see Fig. 6(a)].

However, regarding the importance of DM annihilation inside stars, this drop on the capture rate is too small and is balanced by the fact that metal-rich stars also produce energy through thermonuclear reactions at a lower rate [33].

B. $\sigma_{\chi,SD} \sim \sigma_{\chi,SI}$ case

A scenario in which the SD and SI scattering cross sections have similar values is also considered in this section. In fact, normally a larger SD cross section is assumed because the limits from detectors are less stringent, due to technological limitations. But, as the processes leading to these interactions are similar, both scattering cross sections are of the same order in most models if no resonances nor destructive interferences are invoked [40]. Thus, we choose $\sigma_{\chi,SD} = 10^{-44} \text{ cm}^2$ and $\sigma_{\chi,SI} = 10^{-44} \text{ cm}^2$ in order to explore in depth the role of the different stellar elements in the capture of DM particles.

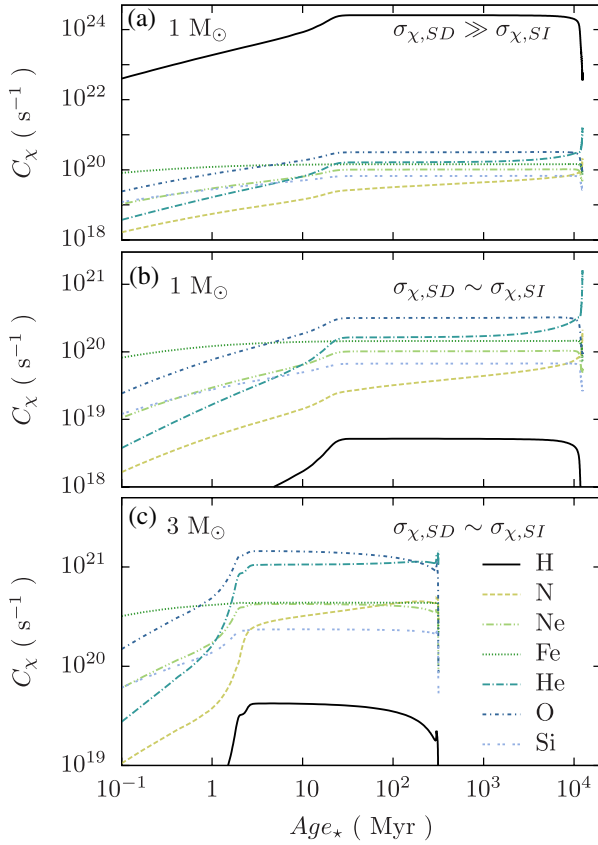


FIG. 5 (color online). Rate at which DM particles are captured, discriminated by the elements responsible for the collisions that led to the capture, during the life of stars with $1M_{\odot}$ and $3M_{\odot}$. We assumed a halo of DM particles with $\rho_{\chi} = 0.3 \text{ GeV cm}^{-3}$, $m_{\chi} = 100 \text{ GeV}$, and the DM-nucleon scattering dominated (a) by the spin-dependent (SD) component, $\sigma_{\chi,SD} = 10^{-38} \text{ cm}^2$, and (b) and (c) by the spin-independent (SI) component, $\sigma_{\chi,SI} = \sigma_{\chi,SD} = 10^{-44} \text{ cm}^2$.

In this case, and also even if we had chosen a $\sigma_{\chi,SD}$ up to 2 orders of magnitude greater than $\sigma_{\chi,SI}$ (for a star with $Z \sim Z_{\odot}$), the SI interactions are the dominant ones in capturing DM particles. The most important elements for the total capture rate, in a star of $1M_{\odot}$ during the MS, are oxygen, helium, iron, and neon. The heavier elements, such as iron, do not dominate the capture rate owing to the form-factor suppression.

Stars of different masses may have other elements contributing significantly to capturing DM particles. For instance, in a star of $7M_{\odot}$ in the MS, helium is the most important element, followed by oxygen and nitrogen [see Fig. 7(a)]. On the other hand, in a star of $0.5M_{\odot}$ oxygen arises as the element that captures DM particles more efficiently, followed by iron. These different contributions are explained by the abundances of the elements throughout the star (see Fig. 8). Some of the ^{16}O in a star of $7M_{\odot}$ is converted to ^{14}N through the CNO cycle, while the same does not happen for a star of $0.5M_{\odot}$ [76].

1. Capture rate over stellar life

The importance of helium and nitrogen on the capture rate increases at the final stages of evolution, in opposition to the cases of hydrogen and iron, whose contribution drops in the RGB [see Figs. 5 and 7]. As a consequence, when the SI interactions dominate, the capture rate does not drop so abruptly in the RGB. Moreover, we found

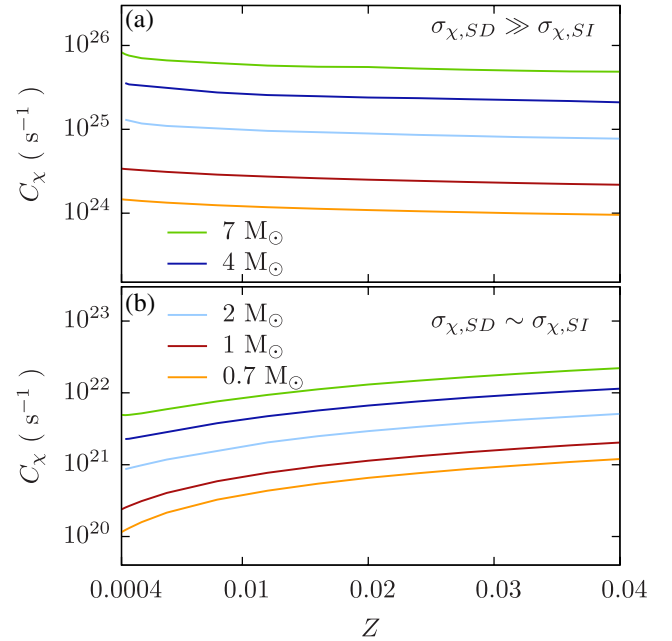


FIG. 6 (color online). Rate at which DM particles are captured during the MS for stars with different masses and metallicities. We assumed a halo of DM particles with $\rho_{\chi} = 0.3 \text{ GeV cm}^{-3}$, $m_{\chi} = 100 \text{ GeV}$, and the DM-nucleon scattering dominated (a) by the SD component, $\sigma_{\chi,SD} = 10^{-38} \text{ cm}^2$, and (b) by the SI one, $\sigma_{\chi,SI} = \sigma_{\chi,SD} = 10^{-44} \text{ cm}^2$.

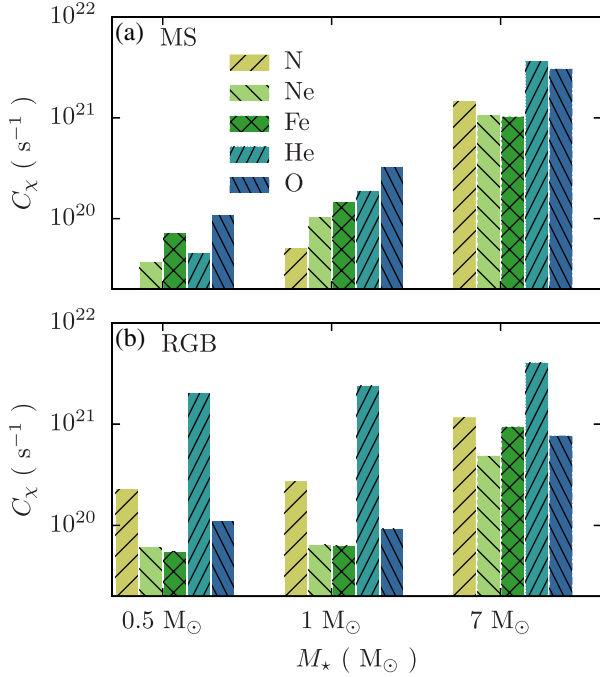


FIG. 7 (color online). Rate at which DM particles are captured discriminated by the elements responsible for the collisions that led to the capture, in the main sequence (a), and in the red giant branch (b) for stars with different masses. We assumed a halo of DM particles with $\rho_\chi = 0.3 \text{ GeV cm}^{-3}$, $m_\chi = 100 \text{ GeV}$, and the DM-nucleon scattering dominated by the spin-independent (SI) component, $\sigma_{\chi,\text{SI}} = \sigma_{\chi,\text{SD}} = 10^{-44} \text{ cm}^2$.

that for stars with masses smaller than $2M_\odot$ the total capture rate increases in the RGB instead of decreasing [see Fig. 4(b)]. Although the number of captured DM particles increases in the RGB, the influence of their self-annihilation on the stellar properties is not remarkable, as at the same time the energy from thermonuclear reactions also increases dramatically.

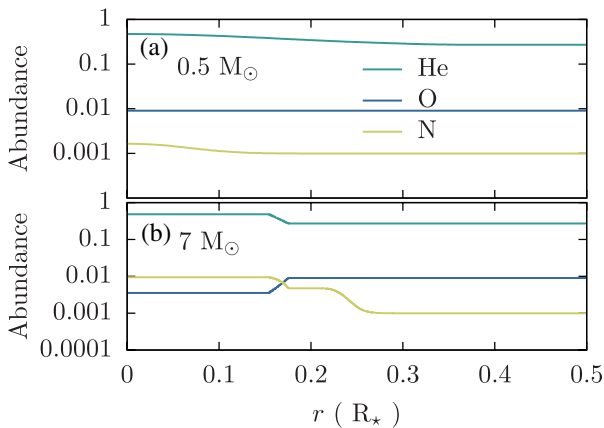


FIG. 8 (color online). Radial abundances of ^4He , ^{16}O , and ^{14}N for stars of $0.5M_\odot$ (a) and $7M_\odot$ (b) in the middle of the MS (when $X_c = 0.5$).

When the stars are in the RGB the elements responsible for most of the DM captures are different from those on the MS [Fig. 7]. In the RGB, helium is the most important element for all stars with masses in the range $0.5M_\odot - 7M_\odot$. The huge density reached by the helium core in the RGB ($\rho_{c,\text{RGB}} \sim 10^3 \rho_{c,\text{MS}}$) increases the efficiency of this element in capturing DM particles.

It is also remarkable that, in the pre-MS phase, the capture rate is not so small when compared with the one in the MS. In the scenario where the capture rate due to SD scattering dominates $C_{\chi,\text{PMS}} \sim 1/20 C_{\chi,\text{MS}}$ while, if both scattering cross sections are of the same order, then $C_{\chi,\text{PMS}} \sim 1/4 C_{\chi,\text{MS}}$ [see Fig. 4]. The explanation of this fact is found in the role of iron, which is the more efficient element in capturing DM particles in the pre-MS phase [see Fig. 5(b) and 5(c)]. For most of the stellar isotopes the capture process is ineffective due to the small escape velocity inside the protostar. However, the kinetic factor in the capture rate expression is not so strongly suppressed for those isotopes with heavy nuclear masses, and therefore the elements with a large A_i , as iron, are the more efficient ones capturing DM particles in the pre-MS phase.

2. Capture and stellar metallicity

In contrast to what is expected when the SD interactions dominate, in this scenario we found that stars with higher

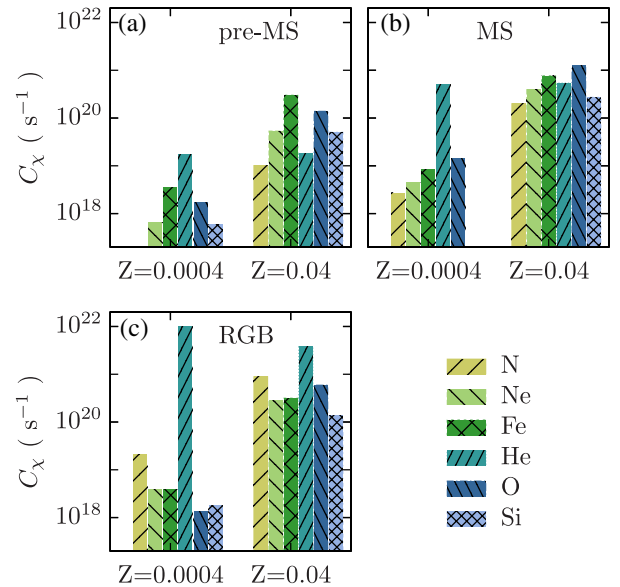


FIG. 9 (color online). Rate at which DM particles are captured discriminated by the elements responsible for the collisions that led to the capture, for $1M_\odot$ stars in different stages of evolution (pre-MS, MS, and RGB) and considering different stellar metallicities. We assumed a halo of DM particles with $\rho_\chi = 0.3 \text{ GeV cm}^{-3}$, $m_\chi = 50 \text{ GeV}$, and the DM-nucleon scattering dominated by the spin-independent (SI) component, $\sigma_{\chi,\text{SI}} = \sigma_{\chi,\text{SD}} = 10^{-44} \text{ cm}^2$.

metallicities capture DM particles more efficiently [see Fig. 6(b)], because these stars are richer in the isotopes that are responsible for most of the captures: ^{16}O , ^4He , ^{56}Fe , ^{20}Ne , and ^{14}N . Therefore, in this scenario, stars with higher metallicities are more affected by the capture and annihilation of DM particles in their interior. Moreover, as metal-rich stars have lower thermonuclear energy production rates, the energy from DM annihilation is even more important over the total energy of the star (the ratio L_χ/L_{nuc} for a $1M_\odot$ star with $Z = 0.04$ in the MS is more than 20 times greater than that for the same star with $Z = 0.0004$).

The contribution of the metals in the capture rate is of vital importance for stars with metallicity $Z = 0.04$, especially until the end of the MS, while for stars with $Z = 0.0004$ helium dominates the capture during all the stages [see Fig. 9]. On the other hand, on the RGB the role of the metals is less important because in this phase ^4He is the isotope that captures DM particles more efficiently due to its high density in the core.

V. DISCUSSION

We have characterized how the stellar capture of DM particles changes within different assumptions regarding the DM characteristics and the structure of the stars. These results are summarized in Table I, where we show the variations in the computed capture rate derived from an uncertainty of 10% in the knowledge of given parameters (such as the mass and velocities of the star and the DM particles, and the stellar metallicity). We found that the greater uncertainties in the capture rate occur due to the ignorance of the DM particle mass and especially when the stellar velocity (if very high) and the stellar mass are not well determined.

However, not all uncertainties in the computed capture rate contribute equally to the weight of the subsequent DM annihilations over the nuclear sources of energy of the star. To illustrate this fact the ratio L_χ/L_{nuc} is also shown in the third column of Table I. In this respect, the ignorance of the DM mass is much less important when compared with an imprecise determination of the velocities or the stellar mass. As an example, an overestimation of 10% in the mass of a star of $7M_\odot$ leads to a significant increment on the computed capture rate (+ 16%), while regarding the effects of DM annihilation on the same star, this overestimation is completely counterbalanced by the dependence of the thermonuclear energy sources on the stellar mass.

The errors on the estimation of the stellar metallicity are not significant for the computed capture rate, at least for the SD-dominated capture. In the scenario where the SI interactions dominate, the role of the metallicity is more important but still introduces errors on the capture rate below 10% (see Table II).

TABLE I. Variations in the total capture rate, C_χ , and in the ratio between the luminosities from DM annihilations and thermonuclear reactions, L_χ/L_{nuc} , when there is an uncertainty of 10% in the knowledge of one parameter of the DM characteristics or of the stellar structure. If not stated otherwise, we assumed a halo of DM particles with a mass $m_\chi = 100$ GeV, a velocity dispersion $\bar{v}_\chi = 270$ km s $^{-1}$, and a star of $1M_\odot$ in the middle of the MS, with a metallicity $Z = 0.019$ and a velocity $v_\star = 220$ km s $^{-1}$.

	C_χ		L_χ/L_{nuc}	
$m_\chi = 5$ GeV $\pm 10\%$	-10%	+12%	-1%	+1%
$m_\chi = 500$ GeV $\pm 10\%$	-18%	+23%	-9%	+11%
$\bar{v}_\chi = 100$ km s $^{-1}$ $\pm 10\%$	+6%	-7%	+6%	-7%
$\bar{v}_\chi = 500$ km s $^{-1}$ $\pm 10\%$	-20%	+26%	-20%	+26%
$v_\star = 100$ km s $^{-1}$ $\pm 10\%$	-3%	+3%	-3%	+3%
$v_\star = 500$ km s $^{-1}$ $\pm 10\%$	-58%	+120%	-58%	+120%
$M_\star = 0.5M_\odot$ $\pm 10\%$	+26%	-22%	-20%	+26%
$M_\star = 7M_\odot$ $\pm 10\%$	+16%	-13%	-16%	+26%
$Z = 0.0004 \pm 10\%$	-0.1%	+0.1%	+2%	-0.3%
$Z = 0.04 \pm 10\%$	-2%	+2%	-2%	+1%

TABLE II. Variations in the capture rate due to SD and SI interactions of the stellar elements with the DM particles ($C_{\chi,\text{SI}}$ and $C_{\chi,\text{SD}}$) when there is an uncertainty of 10% in the knowledge of the mass of the DM particles or on the stellar metallicity.

	$C_{\chi,\text{SD}}$		$C_{\chi,\text{SI}}$	
$m_\chi = 100$ GeV $\pm 10\%$	-16%	+22%	-10%	+13%
$Z = 0.019 \pm 10\%$	-2%	+2%	+8%	-8%

The relatively large variations on the computed capture rate due to a poor knowledge of the input physics stress the importance of combining different techniques to improve precision in the determination of the parameters. In the case of the stellar parameters, photometry, spectroscopy, and astroseismology should be combined when possible to reduce the uncertainties in the stellar mass and metallicity. Regarding the DM characteristics, only a combination of results from colliders, direct and indirect detection experiments will constrain sufficiently the free parameter space. In the cases where the detection of DM signatures seems more promising, such as the Galactic center and primordial stars, the uncertainty on the capture rate will be dominated by the ignorance on the exact value of the DM density.

Our results may be used to evaluate the reliability of the computed capture rate for stars observed in environments with high expected DM densities, and therefore to estimate if the effects predicted due to the self-annihilation of DM particles in the stellar interiors will allow us to extract information about the nature of DM.

ACKNOWLEDGMENTS

We acknowledge the authors of CESAM (P. Morel) and DARKSUSY (P. Gondolo, J. Edsjö, P. Ullio, L. Bergström, M. Schelke, and E. Baltz). Furthermore, we thank J. Edsjö for fruitful comments on the subject of the capture of dark

matter particles in the Sun. This work was supported by grants from “Fundação para a Ciência e Tecnologia” (SFRH/BD/44321/2008) and “Fundação Calouste Gulbenkian.”

-
- [1] W.H. Press and D.N. Spergel, *Astrophys. J.* **296**, 679 (1985).
- [2] K. Griest and D. Seckel, *Nucl. Phys.* **B283**, 681 (1987).
- [3] G. Wikström and J. Edsjö, *J. Cosmol. Astropart. Phys.* **4** (2009) 009.
- [4] J. Ellis, K. A. Olive, C. Savage, and V.C. Spanos, *Phys. Rev. D* **81**, 085004 (2010).
- [5] A. Esmaili and Y. Farzan, *Phys. Rev. D* **81**, 113010 (2010).
- [6] S. Demidov and O. Suvorova, *J. Cosmol. Astropart. Phys.* **6** (2010) 018.
- [7] I.P. Lopes and J. Silk, *Phys. Rev. Lett.* **88**, 151303 (2002).
- [8] M.T. Frandsen and S. Sarkar, *Phys. Rev. Lett.* **105**, 011301 (2010).
- [9] M. Taoso, F. Iocco, G. Meynet, G. Bertone, and P. Eggenberger, *Phys. Rev. D* **82**, 083509 (2010).
- [10] I. Lopes and J. Silk, *Science* **330**, 462 (2010).
- [11] R. Catena and P. Ullio, *J. Cosmol. Astropart. Phys.* **08** (2010) 004.
- [12] M. Weber and W. de Boer, *Astron. Astrophys.* **509**, A25 (2010).
- [13] M. Pato, O. Agertz, G. Bertone, B. Moore, and R. Teyssier, *Phys. Rev. D* **82**, 023531 (2010).
- [14] P.D. Serpico and G. Bertone, *Phys. Rev. D* **82**, 063505 (2010).
- [15] M. Kuhlen, N. Weiner, J. Diemand, P. Madau, B. Moore, D. Potter, J. Stadel, and M. Zemp, *J. Cosmol. Astropart. Phys.* **2** (2010) 030.
- [16] D. Spolyar, K. Freese, and P. Gondolo, *Phys. Rev. Lett.* **100**, 051101 (2008).
- [17] F. Iocco, *Astrophys. J.* **677**, L1 (2008).
- [18] G. Bertone and M. Fairbairn, *Phys. Rev. D* **77**, 043515 (2008).
- [19] K. Freese, P. Gondolo, and D. Spolyar, *AIP Conf. Proc.* **990**, 42 (2008).
- [20] F. Iocco, A. Bressan, E. Ripamonti, R. Schneider, A. Ferrara, and P. Marigo, *Mon. Not. R. Astron. Soc.* **390**, 1655 (2008).
- [21] D.R.G. Schleicher, R. Banerjee, and R.S. Klessen, *Phys. Rev. D* **79**, 043510 (2009).
- [22] D. Hooper, D. Spolyar, A. Vallinotto, and N. Y. Gnedin, *Phys. Rev. D* **81**, 103531 (2010).
- [23] E. Ripamonti, F. Iocco, A. Ferrara, R. Schneider, A. Bressan, and P. Marigo, *Mon. Not. R. Astron. Soc.* **406**, 2605 (2010).
- [24] P. Gondolo, J.-H. Huh, H. Do Kim, and S. Scopel, *J. Cosmol. Astropart. Phys.* **7** (2010) 026.
- [25] S. Sivertsson and P. Gondolo, *Astrophys. J.* **729**, 51 (2011).
- [26] E. Zackrisson *et al.*, *Astrophys. J.* **717**, 257 (2010).
- [27] C. Kouvaris, *Phys. Rev. D* **77**, 023006 (2008).
- [28] C. Kouvaris and P. Tinyakov, *Phys. Rev. D* **82**, 063531 (2010).
- [29] A. de Lavallaz and M. Fairbairn, *Phys. Rev. D* **81**, 123521 (2010).
- [30] I.V. Moskalenko and L.L. Wai, *Astrophys. J.* **659**, L29 (2007).
- [31] P. Scott, J. Edsjö, and M. Fairbairn, in *Proceedings of DARK2007*, edited by H.V. Klapdor-Kleingrothaus, I. Krivosheina, and G. Lewis (World Scientific, Singapore, 2008).
- [32] M. Fairbairn, P. Scott, and J. Edsjö, *Phys. Rev. D* **77**, 047301 (2008).
- [33] J. Casanellas and I. Lopes, *Astrophys. J.* **705**, 135 (2009).
- [34] J.R. Lu, A.M. Ghez, S.D. Hornstein, M.R. Morris, E.E. Becklin, and K. Matthews, *Astrophys. J.* **690**, 1463 (2009).
- [35] D. Merritt, in *Particle Dark Matter: Observations, Models, and Searches*, edited by G. Bertone (Cambridge University Press, Cambridge, England, 2010).
- [36] L.C. Ho, J.E. Greene, A.V. Filippenko, and W.L.W. Sargent, *Astrophys. J. Suppl. Ser.* **183**, 1 (2009).
- [37] M.W. Goodman and E. Witten, *Phys. Rev. D* **31**, 3059 (1985).
- [38] K. Griest, *Phys. Rev. D* **38**, 2357 (1988).
- [39] V.A. Bednyakov, H.V. Klapdor-Kleingrothaus, and S.G. Kovalenko, *Phys. Rev. D* **50**, 7128 (1994).
- [40] G. Jungman, M. Kamionkowski, and K. Griest, *Phys. Rep.* **267**, 195 (1996).
- [41] P. Gondolo, J. Edsjö, P. Ullio, L. Bergström, M. Schelke, and E.A. Baltz, *J. Cosmol. Astropart. Phys.* **7** (2004) 008.
- [42] P. Morel, *Astron. Astrophys. Suppl. Ser.* **124**, 597 (1997).
- [43] S. Couvidat, S. Turck-Chièze, and A.G. Kosovichev, *Astrophys. J.* **599**, 1434 (2003).
- [44] S. Turck-Chièze, A. Palacios, J.P. Marques, and P.A.P. Nghiem, *Astrophys. J.* **715**, 1539 (2010).
- [45] M. Asplund, N. Grevesse, and A.J. Sauval, in *Cosmic Abundances as Records of Stellar Evolution and Nucleosynthesis*, Astronomical Society of the Pacific Conference Series, Vol. 336, edited by T.G. Barnes and F.N. Bash (Astronomical Society of the Pacific, San Francisco, 2005), p. 25.
- [46] A. Gould, *Astrophys. J.* **321**, 571 (1987).
- [47] J. Faulkner and R.L. Gilliland, *Astrophys. J.* **299**, 994 (1985).
- [48] P. Salati and J. Silk, *Astrophys. J.* **338**, 24 (1989).
- [49] S. Archambault *et al.*, *Phys. Lett. B* **682**, 185 (2009).
- [50] E. Behnke *et al.*, *Phys. Rev. Lett.* **106**, 021303 (2011).
- [51] J. Angle *et al.*, *Phys. Rev. Lett.* **100**, 021303 (2008).

- [52] M. Taoso, G. Bertone, G. Meynet, and S. Ekström, *Phys. Rev. D* **78**, 123510 (2008).
- [53] S. C. Yoon, F. Iocco, and S. Akiyama, *Astrophys. J.* **688**, L1 (2008).
- [54] D. N. Spergel and W. H. Press, *Astrophys. J.* **294**, 663 (1985).
- [55] A. Gould, *Astrophys. J.* **321**, 560 (1987).
- [56] C. Savage, G. Gelmini, P. Gondolo, and K. Freese, *J. Cosmol. Astropart. Phys.* **4** (2009) 010.
- [57] A. L. Fitzpatrick, D. Hooper, and K. M. Zurek, *Phys. Rev. D* **81**, 115005 (2010).
- [58] I. P. Lopes, J. Silk, and S. H. Hansen, *Mon. Not. R. Astron. Soc.* **331**, 361 (2002).
- [59] I. P. Lopes, G. Bertone, and J. Silk, *Mon. Not. R. Astron. Soc.* **337**, 1179 (2002).
- [60] A. Bottino, G. Fiorentini, N. Fornengo, B. Ricci, S. Scopel, and F. L. Villante, *Phys. Rev. D* **66**, 053005 (2002).
- [61] D. T. Cumberbatch, J. Guzik, J. Silk, L. S. Watson, and S. M. West, *Phys. Rev. D* **82**, 103503 (2010).
- [62] I. Lopes and J. Silk, *Astrophys. J.* **722**, L95 (2010).
- [63] J. Casanellas and I. Lopes, *Mon. Not. R. Astron. Soc.* **410**, 535 (2011).
- [64] In the specific case of the present Sun, these results are confirmed by preliminary results presented by J. Edsjö at the workshop Dark Matter All Around, Paris, December 2010, for J. Edsjö, C. Savage, P. Scott, and A. Serenelli (work in progress).
- [65] P. Scott, M. Fairbairn, and J. Edsjö, *Mon. Not. R. Astron. Soc.* **394**, 82 (2009).
- [66] S. Sivertsson and J. Edsjö, *Phys. Rev. D* **81**, 063502 (2010).
- [67] J. Binney and S. Tremaine, edited by Binney, *Galactic Dynamics* (Princeton University, Princeton, NJ, 1987), p. 747.
- [68] J. F. Navarro, A. Ludlow, V. Springel, J. Wang, M. Vogelsberger, S. D. M. White, A. Jenkins, C. S. Frenk, and A. Helmi, *Mon. Not. R. Astron. Soc.* **402**, 21 (2010).
- [69] D. Merritt, A. W. Graham, B. Moore, J. Diemand, and B. Terzić, *Astron. J.* **132**, 2685 (2006).
- [70] S. H. Hansen, B. Moore, M. Zemp, and J. Stadel, *J. Cosmol. Astropart. Phys.* **1** (2006) 014.
- [71] M. Fairbairn and T. Schwetz, *J. Cosmol. Astropart. Phys.* **1** (2009) 037.
- [72] C. McCabe, *Phys. Rev. D* **82**, 023530 (2010).
- [73] A. M. Green, *J. Cosmol. Astropart. Phys.* **10** (2010) 034.
- [74] T. Lejeune and D. Schaerer, *Astron. Astrophys.* **366**, 538 (2001).
- [75] D. Schaerer, C. Charbonnel, G. Meynet, A. Maeder, and G. Schaller, *Astron. Astrophys. Suppl. Ser.* **102**, 339 (1993).
- [76] E. Boehm-Vitense, in *Stellar Structure and Evolution*, edited by E. Böhm-Vitense Introduction to Stellar Astrophysics Vol. 3 (Cambridge University Press, Cambridge, England, 1992), p. 300.

A.4 Paper IV

SIGNATURES OF DARK MATTER BURNING IN NUCLEAR STAR CLUSTERS

Casanellas J. & Lopes I.

The Astrophysical Journal Letters, 733:L51, 5pp (2011)

arXiv:1104.5465

SIGNATURES OF DARK MATTER BURNING IN NUCLEAR STAR CLUSTERS

JORDI CASANELLAS¹ AND ÍLÍDIO LOPES^{1,2}

¹ Centro Multidisciplinar de Astrofísica, Instituto Superior Técnico, Av. Rovisco Pais, 1049-001 Lisboa, Portugal; jordicasanelas@ist.utl.pt

² Departamento de Física, Universidade de Évora, Colégio Luis António Verney, 7002-554 Évora, Portugal; ilidio.lopes@ist.utl.pt

Received 2011 February 1; accepted 2011 April 27; published 2011 May 13

ABSTRACT

In order to characterize how dark matter (DM) annihilation inside stars changes the aspect of a stellar cluster, we computed the evolution until the ignition of the He burning of stars from $0.7 M_{\odot}$ to $3.5 M_{\odot}$ within halos of DM with different characteristics. We found that, when a cluster is surrounded by a dense DM halo, the positions of the cluster' stars in the H-R diagram have a brighter and hotter turnoff point than in the classical scenario without DM, therefore giving the cluster a younger appearance. The high DM densities required to produce these effects are expected only in very specific locations, such as near the center of our Galaxy. In particular, if DM is formed by the 8 GeV weakly interacting massive particles recently invoked to reconcile the results from direct detection experiments, then this signature is predicted for halos of DM with a density $\rho_{\chi} = 3 \times 10^5 \text{ GeV cm}^{-3}$. A DM density gradient inside the stellar cluster would result in a broader main sequence, turnoff, and red giant branch regions. Moreover, we found that for very high DM halo densities the bottom of the isochrones in the H-R diagram rises to higher luminosities, leading to a characteristic signature on the stellar cluster. We argue that this signature could be used to indirectly probe the presence of DM particles in the location of a cluster.

Key words: dark matter – Hertzsprung-Russell and C-M diagrams – galaxies: star clusters: general – Galaxy: center – stars: fundamental parameters

Online-only material: color figures, machine-readable table

1. INTRODUCTION

An unambiguous discovery of the particle nature of dark matter (DM) would have to come simultaneously from a variety of experiments and observations (Bertone 2010). Positive results from direct detection experiments (Cerdeño & Green 2010; Pato et al. 2011) and the hypothetical evidence of the existence of new particles from colliders (Bertone et al. 2010) must be complemented by indirect methods, such as the detection of DM annihilation products (Trotta et al. 2009; Scott et al. 2010; Bernal & Palomares-Ruiz 2010) or the observation of a peculiar signature in the solar neutrinos attributed to the effect of captured DM particles (Taoso et al. 2010; Lopes & Silk 2010a).

In recent years many works studied the effects of weakly interacting massive particle (WIMP) DM on stellar evolution (Spolyar et al. 2008; Bertone & Fairbairn 2008; Iocco 2008; Yoon et al. 2008; Taoso et al. 2008; Ripamonti et al. 2010; Gondolo et al. 2010; Sivertsson & Gondolo 2010; de Lavallaz & Fairbairn 2010; Zackrisson et al. 2010; Kouvaris & Tinyakov 2011; Yuan et al. 2011) as a promising complementary way to investigate the nature of DM. Remarkably, it has also been argued that the seismological analysis of the stellar oscillations could be used to detect the signature of captured DM particles in the Sun (Cumberbatch et al. 2010; Lopes & Silk 2010b) and in other Sun-like stars in environments with very high DM densities (Casanelas & Lopes 2011). All of these studies require DM particles to interact with a non-zero nuclear scattering cross section.

In this work we are interested in the global behavior of a large group of stars instead of being concerned with the influence of DM on a single star, whose observation would require a higher precision. We address the question of how a dense halo of DM particles changes the properties of an embedded cluster of stars. As we will show, the annihilation of captured DM particles inside the stars leaves strong signatures in the stellar cluster

when compared with a classical cluster without DM. The high DM densities required to produce measurable effects on the cluster restrict our study to the nuclear star clusters, present in the centers of galaxies, where the highest DM densities are expected. Our description of the cluster isochrones provides an indirect way to probe the presence of DM particles in the location of the cluster, as the signatures we describe here are difficult to attribute to other processes.

This Letter is organized as follows: the physics beyond the stellar models and the capture and annihilation of DM particles is briefly described in Section 2; the effects of DM on stellar evolution are characterized in Section 3; in Section 4, the properties of a cluster embedded in a dense DM halo are compared with those of a classical cluster; finally, we conclude in Section 5 with a brief discussion of our results.

2. STELLAR AND DARK MATTER PHYSICS

To compute our stellar models we used the stellar evolution code CESAM (Morel 1997). This code has an up-to-date and very refined microscopic physics tested against helioseismic data (Turck-Chieze & Lopes 1993; Turck-Chieze et al. 2010). Our stellar models were evolved from the zero-age main sequence (ZAMS; although some of them were also evolved from the pre-main sequence phase to check that both approaches led to similar results), at constant mass, with a metallicity $Z = 0.019$ and an initial helium mass fraction $Y = 0.273$ similar to the solar ones. The initial abundance of the other elements was set equal to the solar composition. The mixing-length parameter was set by calibrating a solar model with an accuracy of 10^{-5} on the solar radius and luminosity. The performance of our code in the range of masses ($0.7\text{--}3.5 M_{\odot}$) and evolutionary stages studied in this work was successfully tested by comparing our computed isochrones with those of Girardi et al. (2000).

The stars computed in this work are embedded in a dense halo of DM. To account for the impact of the DM particles on the stars, we considered that some of the DM particles that populate the halo are gravitationally captured by the stars and accumulate in their interior. The number of captured DM particles was computed using the integral expression of Gould (1987), as implemented in Gondolo et al. (2004). Note that, for the capture process to be efficient, the DM particles are assumed to have a non-negligible scattering cross section with baryons σ_χ , which we chose to be smaller than the present limits from direct detection experiments: $\sigma_{\chi,SI} = 10^{-44} \text{ cm}^2$ (Ahmed et al. 2010) and $\sigma_{\chi,SD} = 10^{-38} \text{ cm}^2$ (Behnke et al. 2011) for a WIMP with a mass of 100 GeV. For these values of σ_χ , the spin-dependent (SD) interactions with hydrogen atoms always dominate over the spin-independent (SI) ones with other stellar isotopes.

In the capture rate (C_χ) calculation we assumed a stellar velocity $v_\star = 220 \text{ km s}^{-1}$ and a Maxwellian DM velocity distribution with a dispersion $\bar{v}_\chi = 270 \text{ km s}^{-1}$. These values apply for the solar case, but are certainly inaccurate for a nuclear cluster. For instance, stars with velocities as high as 400 km s^{-1} are observed near the Galactic center (GC; Lu et al. 2009). In this case the capture rate would be reduced by a factor of six (for a more thorough analysis of how C_χ varies for different stellar and DM characteristics see Lopes et al. 2011). At the same time, it is complex to model the DM velocity distribution in the GC, as the motion of the DM particles is strongly influenced by the gravitational potential of the stars and the central black hole. Interestingly, Scott et al. (2009) tested other DM velocity distributions with the aim of grasping the possible variations on C_χ . When a non-Gaussian distribution (designed to fit an N -body simulation of a Milky Way size DM halo) was implemented, the capture rate was boosted by a factor of 3–5. On the other hand, the same authors found that the truncation of the isothermal distribution at the local escape velocity reduces C_χ by a factor of two. The same order of uncertainty on C_χ is expected in the cases presented in the present work.

After some scatterings, the DM particles sink to the core of the star and rapidly thermalize with stellar matter. The number of DM particles in the stellar core increases until their self-annihilation rate balances the capture rate. This equilibrium is reached in a timescale below 10^4 yr for all cases studied here. Thus, the annihilation of DM particles provides a new source of energy which contributes to the total luminosity of the star according to (Salati & Silk 1989)

$$L_\chi = f_\chi m_\chi C_\chi, \quad (1)$$

where m_χ is the mass of the DM particles and $f_\chi = 2/3$ to take into account that one-third of the energy may escape the star in the form of neutrinos (Iocco et al. 2008). This energy is injected to the stellar models following the thermal distribution of the DM particles, the characteristic radius of which is below 2% and 7% of the stellar radius for $m_\chi = 100 \text{ GeV}$ and 8 GeV , respectively. The total input of energy from DM annihilation, and thus also its impact on stellar evolution, will depend mainly on the product $\rho_\chi \sigma_\chi$.

3. STELLAR EVOLUTION WITHIN DENSE DM HALOS

The hydrostatic equilibrium (the balance between pressure and gravity) achieved by a star within a dense DM halo differs from the one reached in the classical picture due to the new source of energy added to the classical thermonuclear energy

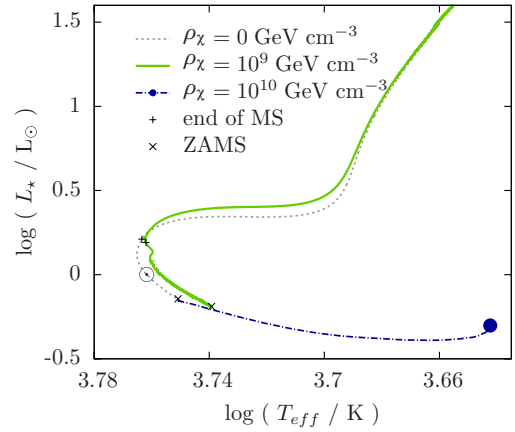


Figure 1. Tracks on the H-R diagram of stars of $1 M_\odot$ that evolved in halos with different DM densities. The blue point indicates a stationary state reached by a star only powered by DM burning. We considered DM particles with a mass $m_\chi = 100 \text{ GeV}$ and a spin-dependent scattering cross section with protons $\sigma_{\chi,SD} = 10^{-38} \text{ cm}^2$.

(A color version of this figure is available in the online journal.)

sources. This fact leads to three main consequences that will influence the characteristics of the whole cluster.

1. *Slowing of the evolutionary speed.* The central temperature of stars that evolve within dense DM halos is lower than that of classical stars due to their negative heat capacity. Another simple way to understand this is to imagine a forming star in the pre-main sequence. The cloud of gas that forms the proto-star shrinks, increasing its central temperature until the gravitational collapse is balanced by the thermonuclear reactions; if another source of energy helps to compensate gravity, the hydrostatic equilibrium is reached earlier, when the central temperature is lower. Therefore, stars within dense DM halos burn hydrogen at a lower rate, slowing down their evolution through later phases. For example, a star of $1 M_\odot$ will spend more than 20 Gyr in the main sequence (MS) if it evolves in a DM halo of density $\rho_\chi = 2 \times 10^9 \text{ GeV cm}^{-3}$ (assuming $\sigma_{\chi,SD} = 10^{-38} \text{ cm}^2$, although other values of ρ_χ and $\sigma_{\chi,SD}$ can be considered, leading to the same effects as long as the product $\rho_\chi \sigma_\chi$ is kept constant). This is a significant difference from the classical picture, in which a star as the Sun is expected to exhaust its hydrogen core in less than 10 Gyr. As shown in earlier works (Salati & Silk 1989), the more massive the star is, the less it is affected by WIMP annihilation. Considering the same DM halo of the previous example, a star of $3 M_\odot$ will not be affected.
2. *Different paths on the H-R diagram.* Since DM burning accounts for at least one-third of the total energy, the balance will be reached with a larger radius and a lower effective temperature than in the classical picture (Fairbairn et al. 2008). Therefore, stars that evolve in dense DM halos follow slightly different paths in the H-R diagram. We found that, in addition to the different paths followed during the MS, which was already reported in previous works (Casanelas & Lopes 2009), stars follow brighter tracks during the red giant branch (RGB). This feature is illustrated in Figure 1. Even if the difference in the paths is remarkable, its effect on the cluster is small compared with the slowing of the evolutionary speed.
3. *Stationary states.* For extremely high DM densities, stars are powered only by the energy from DM annihilation.

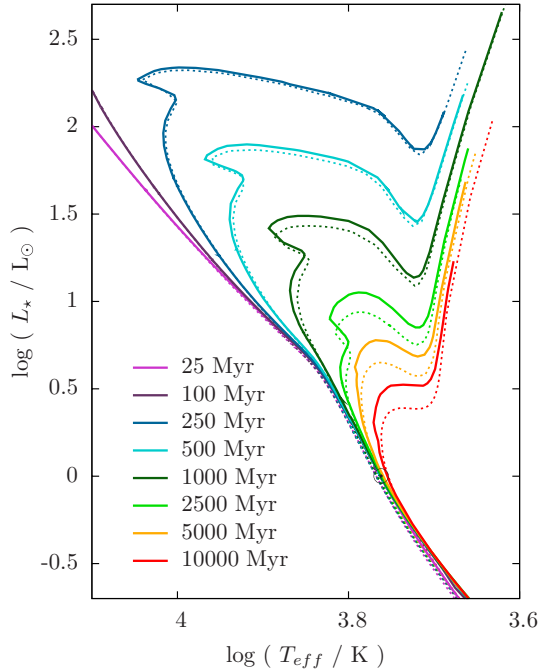


Figure 2. Isochrones for a cluster of stars with masses between $0.7 M_{\odot}$ and $3.5 M_{\odot}$ that evolved in a halo of DM with a density $\rho_{\chi} = 10^9 \text{ GeV cm}^{-3}$ (continuous lines) and for the same cluster in the classical scenario without DM (dashed lines). We considered DM particles with a mass $m_{\chi} = 100 \text{ GeV}$ and a spin-dependent scattering cross section with protons $\sigma_{\chi, \text{SD}} = 10^{-38} \text{ cm}^2$. (A color version of this figure is available in the online journal.)

Whether the star was formed in this environment or arrived there a posteriori, it will reach a state of equilibrium in the Hyashi track, far from the MS where most stars are found (Casanelas & Lopes 2009). In this case the star is fully convective and remains in the same position in the H-R diagram as long as there are DM particles to be captured in the halo (an illustrative example is shown in Figure 1).

4. GLOBAL STRUCTURE OF A STELLAR CLUSTER WITHIN A DENSE DM HALO

It is naturally expected then, that stellar clusters are affected by DM halos, since their basic constituents, namely stars, are themselves affected. The main reason is the fact that stars with lower masses evolve slower in dense DM halos. This effect is not noticeable for young clusters since in these clusters low-mass stars are still in the MS and the more massive ones, which are evolving through the RGB, are not affected by the presence of DM. However, in old clusters the RGB may be populated by stars that evolved slower, consequently making the cluster look younger than its real age. Moreover, the fact that low-mass stars within dense DM halos follow brighter paths in the RGB than classical stars contributes to amplify this effect.

In order to distinctly illustrate the younger appearance of a cluster when embedded in a dense DM halo, we computed the isochrones (the track drawn by the positions in the H-R diagram of all stars with different masses at a given age) of stellar clusters in different situations. Figure 2 shows the isochrones we obtained for a cluster evolving in a halo of DM with a density $\rho_{\chi} = 10^9 \text{ GeV cm}^{-3}$ (continuous lines) together with those obtained without the influence of DM (dashed lines). When the isochrones of $\geq 1000 \text{ Myr}$ in both situations are compared, we see that indeed the cluster within a dense DM halo looks

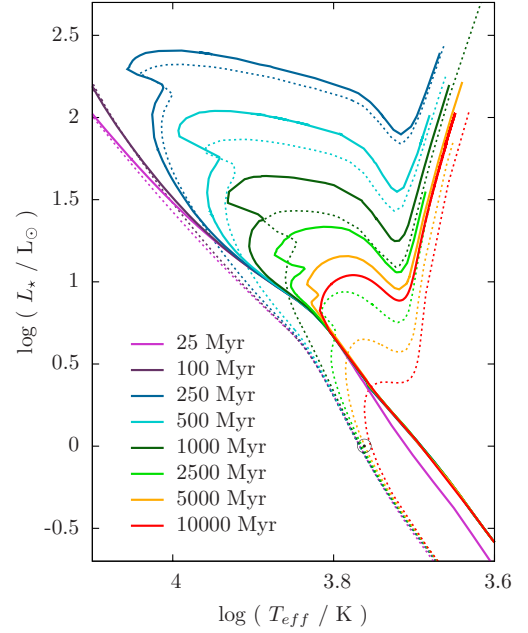


Figure 3. Isochrones for a cluster of stars with masses between $0.7 M_{\odot}$ and $3.5 M_{\odot}$ that evolved in a halo of DM with a density $\rho_{\chi} = 10^{10} \text{ GeV cm}^{-3}$ (continuous lines) and for the same cluster in the classical scenario without DM (dashed lines). The post-MS segment of the 10 Gyr isochrone is a conservative estimation (a lower limit on luminosity) of the true isochrone. We considered DM particles with a mass $m_{\chi} = 100 \text{ GeV}$ and a spin-dependent scattering cross section with protons $\sigma_{\chi, \text{SD}} = 10^{-38} \text{ cm}^2$.

(A color version of this figure is available in the online journal.)

younger, with a brighter and hotter turnoff point and a brighter RGB. In this case the turnoff and RGB are populated by more massive stars than in the classical scenario, because they took longer to burn out their hydrogen core and to leave the MS. It is almost impossible to distinguish both clusters at ages $\leq 500 \text{ Myr}$.

When even higher DM densities are considered (or, equivalently, larger WIMP-on-nucleon scattering cross sections), the characteristics of the cluster change dramatically. In addition to the previously described effect (which will now be visible for younger clusters, because at higher DM densities more massive stars will be affected), another strong signature of the presence of DM in the halo arises when looking at the position of stars with lower masses. These stars, which are mostly fueled by the energy from DM annihilation, go back in the Hyashi track and reach positions in the H-R diagram that were normally occupied only by forming stars in their way to the MS. Consequently, the bottom of the isochrones, corresponding to the lower mass stars, rises to higher luminosities, giving the cluster a very characteristic appearance. This peculiar signature is a strong indication of the presence of high concentrations of DM in a stellar cluster.

This strong signature is illustrated in Figure 3, where the isochrones of a stellar cluster surrounded by a halo of DM with a density $\rho_{\chi} = 10^{10} \text{ GeV cm}^{-3}$ are plotted. The main characteristic signature of the presence of DM is the fact that the bottom of all isochrones is more than three times brighter than the classical isochrones. In addition, the effect of a brighter and hotter turnoff point is now more pronounced and appreciable in clusters as young as 250 Myr.

We have also considered the hypothetical scenario in which DM is formed by the low-mass WIMPs invoked to reconcile the results of DAMA with the negative results of other direct detection experiments (Savage et al. 2009). As shown in

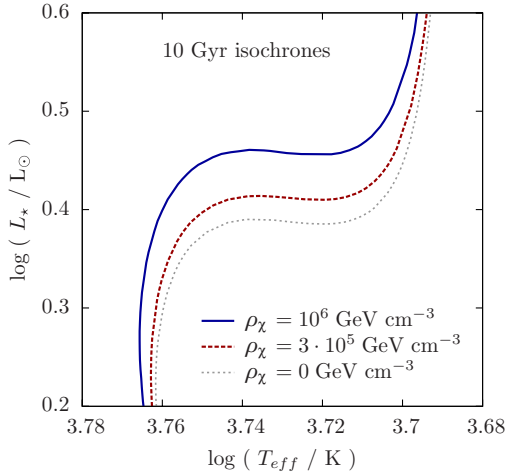


Figure 4. Isochrones of 10 Gyr for clusters of stars that evolved in halos of DM with different densities. We considered DM particles with the particular characteristics that fit DAMA observations and constraints from direct detection experiments: a mass $m_\chi = 8$ GeV and a spin-dependent scattering cross section with protons $\sigma_{\chi,SD} = 10^{-36}$ cm².

(A color version of this figure is available in the online journal.)

Figure 4, if such WIMPs form most of the DM then the DM density needed to have signatures on a stellar cluster would be as low as 3×10^5 GeV cm⁻³. Both the low mass of these WIMPs ($m_\chi = 8$ GeV) and especially their large SD scattering cross section with protons ($\sigma_{\chi,SD} = 10^{-36}$ cm²) contribute to producing effects on the stellar cluster at lower DM halo densities.

5. DISCUSSION AND CONCLUSIONS

We have shown that a cluster of stars that evolves in a dense halo of DM shows strong signatures in its appearance due to the self-annihilation of captured DM particles in the interior of stars. In comparison to the classical case, the cluster within a dense DM halo looks younger than its true age, due to the slower evolution of the stars when these are partially powered by DM annihilation. This is visible only for old clusters (e.g., for clusters older than 1 Gyr within a DM halo of density $\rho_\chi = 10^9$ GeV cm⁻³), because their RGB is populated by low-mass stars, which are the type of stars most affected by DM.

Our work focuses on environments with very high DM densities, which may be present only in specific locations, such as near the centers of galaxies (Gondolo & Silk 1999). In particular, considering an adiabatically contracted DM profile (Bertone & Merritt 2005), the DM densities discussed here may be found at the following distances from the GC: $\rho_\chi = 3 \times 10^5$ GeV cm⁻³ at $r_{GC} \approx 1$ pc and $\rho_\chi = 10^{10}$ GeV cm⁻³ at $r_{GC} \approx 0.01$ pc. The shape of the central profiles of galactic DM halos is still a topic of discussion (de Blok 2010): while simulations predict the existence of cusps, observations favor constant-density DM cores.

Our results indicate that the age of a cluster may be underestimated if embedded in a dense DM halo, which goes toward solving the “paradox of youth” in the center of the Milky Way, a possibility that was first suggested by Moskalenko & Wai (2007) in the context of compact stars. However, there are many astrophysical uncertainties, such as the velocities of stars and

Table 1
Isochrones of a Stellar Cluster Embedded in Halos of DM Particles with Different DM Densities

ρ_χ (GeV cm ⁻³)	Age (Myr)	$M(M_\odot)$	$\log(T_{\text{eff}} / \text{K})$	$\log(L_\star / L_\odot)$
0	25	0.75000	3.67148	-0.73140
			...	
10^9	25	0.75000	3.65940	-0.77514
			...	
10^{10}	25	0.80000	3.60171	-0.72426
			...	

Note. The DM particles are assumed to have a mass of 100 GeV and a spin-dependent scattering cross section with protons $\sigma_{\chi,SD} = 10^{-38}$ cm².

(This table is available in its entirety in a machine-readable form in the online journal. A portion is shown here for guidance regarding its form and content.)

DM particles, that may change the rate at which stars capture DM particles and therefore change the overall influence of DM on a cluster. Although our results do not explain the depletion of giants observed in the nuclear central cluster of the Milky Way (Do et al. 2009; Buchholz et al. 2009; Bartko et al. 2010), they show that the influence of DM on stellar evolution must be taken into account when studying nuclear clusters.

A DM halo density gradient inside the stellar cluster would result in a broader MS, turnoff, and RGB regions. This effect is usually attributed to photometric errors, variable reddening (Carraro et al. 2002), extended star formation (Twarog et al. 2011), and binaries (Zhao & Bailyn 2005). In the case of nuclear star clusters it could also be associated with the annihilation of DM particles inside the stars, given that within the typical size of nuclear clusters the DM density is expected to vary several orders of magnitude depending on the proximity of the galactic center.

For stellar clusters embedded in halos with extremely high DM densities we found an additional very strong signature: the bottom of the computed isochrones in the H-R diagram rises to higher luminosities because the low-mass stars, powered only with energy from DM annihilation, inflate and become fully convective. As this signature is hardly explained by other processes, we argue that this could be an indirect way to probe the presence of DM particles in the location of a cluster of stars.

We are grateful to the authors of DarkSUSY, from which some of the publicly available routines were adapted, and CESAM, as well as to the anonymous referee for a careful review. This work was supported by grants from FCT-MCTES (SFRH/BD/44321/2008) and Fundação Calouste Gulbenkian.

APPENDIX ISOCHRONE TABLES

Table 1 shows a summary of the data used in Figures 2 and 3, which corresponds to the isochrones of a classical stellar cluster and of stellar clusters embedded in halos of DM particles with densities $\rho_\chi = 10^9$ GeV cm⁻³ and $\rho_\chi = 10^{10}$ GeV cm⁻³. The mass of the stars ranges from 0.7 to 3.5 M_\odot and their metallicity is $Z = 0.019$. Our results do not rely on any specific initial mass function (IMF), i.e., any IMF could be used along with the table to obtain the relative number of stars in different sections of the isochrones.

REFERENCES

- Ahmed, Z., et al. (CDMS II Collaboration) 2010, *Science*, **327**, 1619
- Bartko, H., et al. 2010, *ApJ*, **708**, 834
- Behnke, E., et al. (COUPP Collaboration) 2011, *Phys. Rev. Lett.*, **106**, 021303
- Bernal, N., & Palomares-Ruiz, S. 2010, arXiv:1006.0477
- Bertone, G. 2010, *Nature*, **468**, 389
- Bertone, G., Cerdeno, D. G., Fornasa, M., de Austri, R. R., & Trotta, R. 2010, *Phys. Rev. D*, **82**, 055008
- Bertone, G., & Fairbairn, M. 2008, *Phys. Rev. D*, **77**, 043515
- Bertone, G., & Merritt, D. 2005, *Mod. Phys. Lett. A*, **20**, 1021
- Buchholz, R. M., Schödel, R., & Eckart, A. 2009, *A&A*, **499**, 483
- Carraro, G., Girardi, L., & Marigo, P. 2002, *MNRAS*, **332**, 705
- Casanelias, J., & Lopes, I. 2009, *ApJ*, **705**, 135
- Casanelias, J., & Lopes, I. 2011, *MNRAS*, **410**, 535
- Cerdeño, D. G., & Green, A. M. 2010, in *Particle Dark Matter: Observations, Models and Searches*, ed. G. Bertone (Cambridge: Cambridge Univ. Press), 347
- Cumberbatch, D. T., Guzik, J., Silk, J., Watson, L. S., & West, S. M. 2010, *Phys. Rev. D*, **82**, 103503
- de Blok, W. J. G. 2010, *Adv. Astron.*, **5**, 789293
- de Lavallaz, A., & Fairbairn, M. 2010, *Phys. Rev. D*, **81**, 123521
- Do, T., Ghez, A. M., Morris, M. R., Lu, J. R., Matthews, K., Yelda, S., & Larkin, J. 2009, *ApJ*, **703**, 1323
- Fairbairn, M., Scott, P., & Edsjö, J. 2008, *Phys. Rev. D*, **77**, 047301
- Girardi, L., Bressan, A., Bertelli, G., & Chiosi, C. 2000, *A&AS*, **141**, 371
- Gondolo, P., Edsjö, J., Ullio, P., Bergström, L., Schelke, M., & Baltz, E. A. 2004, *J. Cosmol. Astropart. Phys.*, JCAP07(2004)008
- Gondolo, P., Huh, J., Do Kim, H., & Scopel, S. 2010, *J. Cosmol. Astropart. Phys.*, JCAP07(2010)026
- Gondolo, P., & Silk, J. 1999, *Phys. Rev. Lett.*, **83**, 1719
- Gould, A. 1987, *ApJ*, **321**, 571
- Iocco, F. 2008, *ApJ*, **677**, L1
- Iocco, F., Bressan, A., Ripamonti, E., Schneider, R., Ferrara, A., & Marigo, P. 2008, *MNRAS*, **390**, 1655
- Kouvaris, C., & Tinyakov, P. 2011, *Phys. Rev. D*, **83**, 083512
- Lopes, I., Casanelias, J., & Eugénio, D. 2011, *Phys. Rev. D*, **83**, 063521
- Lopes, I., & Silk, J. 2010a, *Science*, **330**, 462
- Lopes, I., & Silk, J. 2010b, *ApJ*, **722**, L95
- Lu, J. R., Ghez, A. M., Hornstein, S. D., Morris, M. R., Becklin, E. E., & Matthews, K. 2009, *ApJ*, **690**, 1463
- Morel, P. 1997, *A&AS*, **124**, 597
- Moskalenko, I. V., & Wai, L. L. 2007, *ApJ*, **659**, L29
- Pato, M., Baudis, L., Bertone, G., Ruiz de Austri, R., Strigari, L. E., & Trotta, R. 2011, *Phys. Rev. D*, **83**, 083505
- Ripamonti, E., Iocco, F., Ferrara, A., Schneider, R., Bressan, A., & Marigo, P. 2010, *MNRAS*, **406**, 2605
- Salati, P., & Silk, J. 1989, *ApJ*, **338**, 24
- Savage, C., Gelmini, G., Gondolo, P., & Freese, K. 2009, *J. Cosmol. Astropart. Phys.*, JCAP04(2009)010
- Scott, P., Conrad, J., Edsjö, J., Bergström, L., Farnier, C., & Akrami, Y. 2010, *J. Cosmol. Astropart. Phys.*, JCAP01(2010)031
- Scott, P., Fairbairn, M., & Edsjö, J. 2009, *MNRAS*, **394**, 82
- Sivertsson, S., & Gondolo, P. 2010, *ApJ*, **729**, 51
- Spolyar, D., Freese, K., & Gondolo, P. 2008, *Phys. Rev. Lett.*, **100**, 051101
- Taoso, M., Bertone, G., Meynet, G., & Ekström, S. 2008, *Phys. Rev. D*, **78**, 123510
- Taoso, M., Iocco, F., Meynet, G., Bertone, G., & Eggenberger, P. 2010, *Phys. Rev. D*, **82**, 083509
- Trotta, R., Ruiz de Austri, R., & Pérez de los Heros, C. 2009, *J. Cosmol. Astropart. Phys.*, JCAP08(2009)034
- Turck-Chieze, S., & Lopes, I. 1993, *ApJ*, **408**, 347
- Turck-Chieze, S., Palacios, A., Marques, J. P., & Nghiem, P. A. P. 2010, *ApJ*, **715**, 1539
- Twarog, B. A., Carraro, G., & Anthony-Twarog, B. J. 2011, *ApJ*, **727**, L7
- Yoon, S. C., Iocco, F., & Akiyama, S. 2008, *ApJ*, **688**, L1
- Yuan, Q., Yue, B., Zhang, B., & Chen, X. 2011, *J. Cosmol. Astropart. Phys.*, JCAP04(2011)020
- Zackrisson, E., et al. 2010, *ApJ*, **717**, 257
- Zhao, B., & Bailyn, C. D. 2005, *AJ*, **129**, 1934

A.5 Paper V

FIRST ASTEROSEISMIC LIMITS ON THE NATURE OF DARK MATTER

Casanellas J. & Lopes I.
submitted for publication
[arXiv:1212.2985](https://arxiv.org/abs/1212.2985)

FIRST ASTEROSEISMIC LIMITS ON THE NATURE OF DARK MATTER

JORDI CASANELLAS^{1,3}, ILÍDIO LOPES^{1,2,3}

Draft version November 10, 2012

ABSTRACT

We report the first constraints on the properties of weakly interacting low-mass dark matter (DM) particles using asteroseismology. The additional energy transport mechanism due to accumulated asymmetric DM particles modifies the central temperature and density of low-mass stars and suppresses the convective core expected in 1.1-1.3 M_{\odot} stars even for an environmental DM density as low as the expected in the solar neighbourhood. An asteroseismic modelling of the stars KIC 8006161, HD 52265 and α Cen B revealed small frequency separations significantly deviated from the observations, leading to the exclusion of a region of the DM parameter space mass vs. spin-dependent DM-proton scattering cross section comparable with present experimental constraints.

Subject headings:

1. INTRODUCTION

The identification of the nature of the dark matter (DM) of the Universe is a major open problem in modern physics (Bertone 2010). Among the diverse strategies for DM searches, the study of the possible impact of DM in the properties of stars has been explored in recent years as a complementary approach to the DM problem (Spolyar et al. 2008; Iocco et al. 2008; Scott et al. 2009; Casanellas & Lopes 2009; Zackrisson et al. 2010; Sivertsson & Gondolo 2011; Casanellas & Lopes 2011a; Scott et al. 2011; Li et al. 2012; Ilie et al. 2012; Corsico et al. 2012). In particular, weakly interacting DM candidates with an intrinsic matter-antimatter asymmetry (Kaplan et al. 2009; Davoudiasl et al. 2011; Blennow et al. 2012) do not annihilate after gravitational capture by compact astrophysical objects and can therefore strongly influence their internal structure (Gelmini et al. 1987; Griest & Seckel 1987). Thus, both the observation or the lack of observation of the impact of asymmetric DM (ADM) on the properties of stars can be used to put constraints on the characteristics of these DM candidates.

The interior of the Sun, being known with a high accuracy thanks to solar neutrinos and helioseismic data, is an excellent laboratory to probe the existence and the properties of ADM particles. Such particles remove energy from the inner $\sim 4\%$ of the Sun, leading to a reduction of the central temperature and the creation of an isothermal core (Taoso et al. 2010; Frandsen & Sarkar 2010; Lopes & Silk 2012). In particular, ADM candidates with low-masses and large spin-dependent (SD) proton scattering cross sections may influence the internal solar structure so strongly that they would produce clear signatures in the low-degree frequency spacings and in the solar gravity modes (Lopes & Silk 2010; Cumberbatch et al. 2010; Turck-Chièze et al. 2012). Interestingly, low-mass WIMPs with similar characteristics provide an explanation for the signals in various direct detection experiments (Savage et al. 2009), strengthen-

ing the motivation for the search of indirect signatures of these particles.

It has also been shown that these low-mass ADM candidates may produce marked effects in very low-mass stars and brown dwarfs (Zentner & Hearin 2011). In environments with high ADM densities, solar-like stars may show significant deviations in their evolutionary tracks (Iocco et al. 2012). Also neutron stars, due to their compactness, capture DM very efficiently and may be strongly influenced by the accumulation of ADM (Bertone & Fairbairn 2008; Kouvaris & Tinyakov 2011; Leung et al. 2012). Here we will show that, even for a DM density as low as the expected in the solar neighbourhood, $\rho_{\chi} = 0.4 \text{ GeV cm}^{-3}$ (Garbari et al. 2012), main-sequence stars with masses similar to that of the Sun present distinct signatures of the captured ADM.

With the advent of asteroseismology, a precious insight into the stellar interiors is nowadays possible for the first time. The *CoRoT* (Michel et al. 2008) and *Kepler* (Gilliland et al. 2010) missions have already detected oscillations in about 500 stars (Chaplin et al. 2011). This fact has allowed to test theories of stellar evolution and to probe the stellar cores with an unprecedented precision (Garcia et al. 2010; Bonaca et al. 2012). The seismic analysis of stars other than the Sun is complementary to helioseismic DM searches because it allows the study of stars with lower masses, which are more strongly influenced by DM, and stars whose dominant energy transport mechanisms may change due to the DM influence. In this letter we will demonstrate, by studying the case of the stars KIC 8006161, HD 52265 and α Cen B, that present asteroseismic observations do constrain a significant region of the DM parameter space.

2. INTERACTION DARK MATTER-STARS

Nearby stars are embedded within the halo of DM particles that is presently believed to permeate our Galaxy. If these DM particles have a non-negligible scattering cross section off baryons (so they are WIMPs, for Weakly Interacting Massive Particles), then some of them may collide with the nucleons of the stellar plasma, losing kinetic energy. A fraction of these DM particles is gravitationally captured by the stars. To calculate the capture rate we follow the formalism that was early devel-

¹ CENTRA, Instituto Superior Técnico, Lisboa, Portugal

² Departamento de Física, Universidade de Évora, Portugal

³ E-mails: jordicasanellas@ist.utl.pt, ilidio.lopes@ist.utl.pt

TABLE 1
CONSTRAINTS ON THE STELLAR CHARACTERISTICS ADOPTED FOR THE MODELLING AND SELECTED RESULTS.

Star	M (M_{\odot})	R (R_{\odot})	L (L_{\odot})	T_{eff} (K)	$(Z/X)_s$	$\langle \Delta\nu_{n,0} \rangle^1$ (μHz)	$\langle \delta\nu_{02} \rangle^1$ (μHz)
KIC 8006161							
Observ. ²	0.92-1.10	0.90-0.97	0.61 ± 0.02	5340 ± 70	0.043 ± 0.007	148.94 ± 0.13	10.10 ± 0.16
Stand. mod./DM mod. ³	0.92	0.92	0.63	5379	0.039	149.03/149.08	10.12/9.13
HD 52265							
Observ. ²	1.18-1.25	1.19-1.30	2.09 ± 0.24	6100 ± 60	0.028 ± 0.003	98.07 ± 0.19	8.18 ± 0.28
Stand. mod./DM mod. ³	1.18	1.30	2.22	6170	0.028	97.92/98.05	8.16/7.65
α Cen B							
Observ. ²	0.934 ± 0.006	0.863 ± 0.005	0.50 ± 0.02	5260 ± 50	0.032 ± 0.002	161.85 ± 0.74	10.94 ± 0.84
Stand. mod./DM mod. ³	0.934	0.868	0.51	5245/5230	0.031	162.56/162.45	10.23/8.95

oped by Gould (1987), as implemented in Gondolo et al. (2004). We assume a Maxwell-Boltzmann distribution of the velocities of the DM particles, with a dispersion $\bar{v}_{\chi} = 270 \text{ km s}^{-1}$, and a stellar velocity of $v_{\star} = 220 \text{ km s}^{-1}$. The expected deviation from the mentioned fiducial values for the specific stars studied in this work may lead to a maximum error on the capture rate of approximately 10% (see Lopes et al. (2011) for details). The number of DM particles accumulated in the stellar core grows while more particles are being captured. The self-annihilation and evaporation processes can be neglected for the ADM candidates and stars considered in this work (we assumed an effective $\langle \sigma_a v \rangle = 10^{-40} \text{ cm}^3 \text{ s}^{-1}$ and $m_{\chi} \geq 4.5 \text{ GeV}$). While a low stellar mass tends to favour evaporation, this fact is compensated by the cooler stellar temperatures, $Evap \propto e^{-GMm_{\chi}/RT}$ (Griest & Seckel 1987), in agreement with the results of Zentner & Hearin (2011) for $\sim 0.1M_{\odot}$ stars.

The DM particles captured in the stellar core provide a new energy transport mechanism that removes energy from the centre of the star. The efficiency of this mechanism depends mainly on the ratio between the mean free path of the WIMPs inside the stellar plasma l_{χ} and the characteristic radius of the WIMPs distribution in the core of the star r_{χ} (Gilliland et al. 1986). For most of the WIMP-proton SD scattering cross sections $\sigma_{\chi,SD}$ considered here, $l_{\chi} > r_{\chi}$ and the energy transport by WIMPs is non-local. On the other hand, for large values of $\sigma_{\chi,SD}$, $l_{\chi} < r_{\chi}$ so the WIMPs are in local thermal equilibrium with the baryons and the energy transport can be assumed to proceed by conduction. The latter regime applies only to values of $\sigma_{\chi,SD}$ which are not considered in this work ($\sigma_{\chi,SD} \gtrsim 10^{-33} \text{ cm}^2$). However, we follow the prescription described in Gould & Raffelt (1990) that extends the formalism developed for the local thermal equilibrium to other regimes by the use of tabulated suppression factors.

The DM capture and energy transport mechanisms were implemented in CESAM (Morel 1997), a sophisticated stellar evolution code. In the case of the Sun, the results of our modified solar model (see *e.g.* Lopes & Silk (2012)) are in agreement with those of other codes in the literature (Taoso et al. 2010; Frandsen & Sarkar 2010).

¹ Averages for the intervals $2750 < \nu(\mu\text{Hz}) < 3900$ (KIC 8006161), $1600 < \nu(\mu\text{Hz}) < 2600$ (HD 52265), and $3300 < \nu(\mu\text{Hz}) < 5500$ (α Cen B).

² Data from Mathur et al. (2012); Bruntt et al. (2012) for KIC 8006161, from Ballot et al. (2011) for HD 52265, and from Kjeldsen et al. (2005) for α Cen B.

³ $m_{\chi} = 5 \text{ GeV}$, $\sigma_{\chi,SD} = 3 \cdot 10^{-36} \text{ cm}^2$, $\rho_{\chi} = 0.4 \text{ GeV cm}^{-3}$.

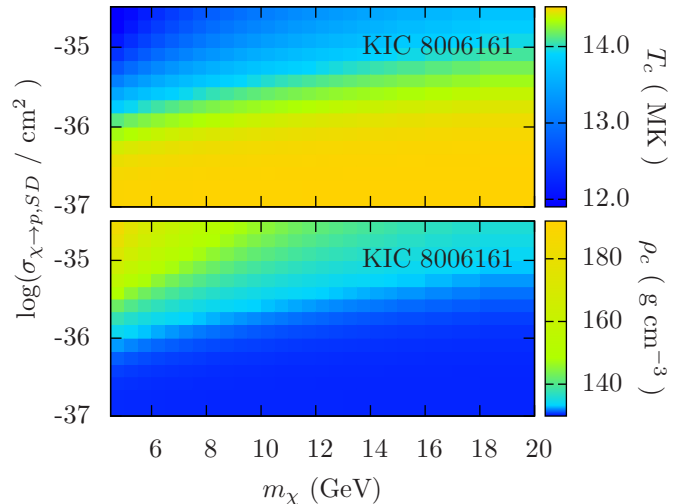


FIG. 1.— Central temperatures (top) and densities (bottom) of the DM-modified stellar models that reproduce the observed properties of the star KIC 8006161.

The observational constraints used for the modelling of the stars KIC 8006161, HD 52265, and α Cen B, as well as the results of some selected models with and without taking into account the DM effects, are summarized in Table 1.

3. IMPACT OF ADM ON THE PROPERTIES OF LOW-MASS STARS

3.1. Modifications of central temperature and density

The main signature of the additional DM cooling mechanism is a decrease in the central temperature and an increase in the central density. These variations are shown in Figure 1 for several DM-modified stellar models, calibrated to reproduce the observed properties of the star KIC 8006161, for a range of DM masses and SD scattering cross sections. Compared with the standard modelling, for $m_{\chi} = 5 \text{ GeV}$ and $\sigma_{\chi,SD} = 3 \cdot 10^{-36} \text{ cm}^2$ we found a $\sim 9\%$ decline in the central temperature. The variations on the internal properties are larger than those reported in the case of the Sun (Taoso et al. 2010) because the importance of the energy transported by the WIMPs ($\epsilon_{\chi,trans} \propto C_{\chi} \propto M_{\star}$) over the thermonuclear energy ($\epsilon_{nucl} \propto M_{\star}^{3.5}$) increases when the stellar mass decreases. In particular, in our computations we found the DM cooling to reduce the T_c of $0.7 M_{\odot}$ stars 9 times more efficiently than for $1.1 M_{\odot}$ stars. This fact reinforces the potential advantages of performing DM searches in stars other than the Sun.

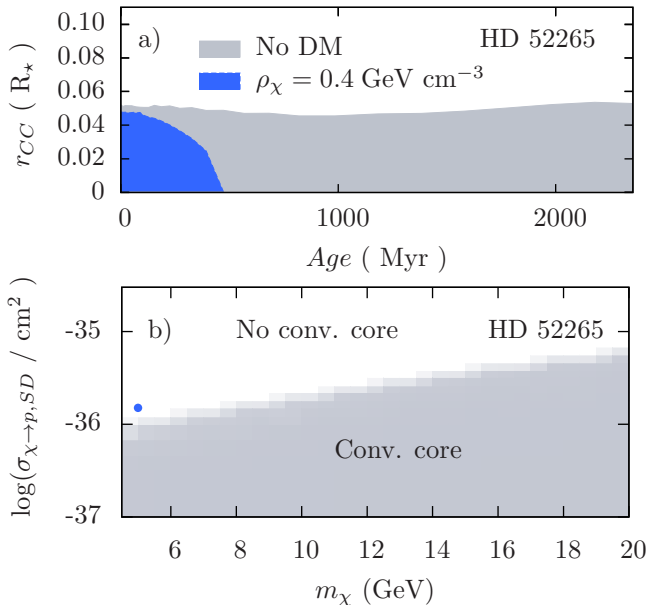


FIG. 2.— (a) Size and duration of the convective core in the modelling of the star HD 52265 in the classical picture (grey) and taking into account the energy transport due to the conduction of ADM particles with $m_\chi = 5$ GeV and $\sigma_{\chi,SD} = 1.5 \cdot 10^{-36}$ cm² (blue). (b) The presence of a convective core in HD 52265 depends on the mass and SD scattering cross section of the DM particles.

3.2. Suppression of convective core

In the standard picture of stellar evolution, stars with masses greater than $1.1 M_\odot$ are expected to keep a convective core during most of the main sequence, while stars with lower masses quickly lose their convective cores. Convection arises when the gradient of temperature in the core is so steep that a rising bubble of plasma does not cool enough with its adiabatic expansion, so that it continues to rise, leading to a convective instability. If the temperature gradient is reduced by an additional mechanism such as the energy transport by WIMPs, then the conditions for convection may no longer be achieved. This possibility was soon realised in Renzini (1987), where the suppression of convection in horizontal branch stars was predicted using analytical approximations. This scenario must not be confused with the creation of an unexpected convective core in $1 M_\odot$ stars due to the self-annihilation of DM particles captured in halos with very high DM densities (Casanellas & Lopes 2011b).

The reduction of the temperature gradient in the stellar interior due to the additional cooling by WIMPs was found to suppress the convective core expected in stars with masses slightly greater than that of the Sun. The standard modelling of the star HD 52265 predicted a convective core during all the main sequence, but this convective core rapidly disappeared when the energy transport by WIMPs was taken into account (see Figure 2.a). The range of DM masses and SD scattering cross sections for which the suppression of the HD 52265 convective core is expected is shown in Figure 2.b). Interestingly, hints of the signatures of a convective core in HD 52265 were reported in Ballot et al. (2011). However, no conclusive information can be extracted until there is no definitive diagnostic of its presence or its absence (see also Escobar et al. (2012)).

4. ASTEROSEISMIC DIAGNOSTIC OF THE PRESENCE OF DM

The characteristic signatures reported in the last section are potentially detectable with the analysis of the stellar oscillations. Asteroseismology is presently showing its power in determining with high precision not only the global properties of stars but also their internal structure. In particular, the small frequency separations of low angular degree ($l = 0$) and radial order n : $\delta\nu_{02} = \nu_{n,0} - \nu_{n-1,2}$ have been shown to provide useful information about the core of the stars (Gough 1986). Thus, we would expect the seismic parameter $\langle\delta\nu_{02}\rangle$ to be sensitive to the modifications introduced by the WIMPs on stars.

We have computed the oscillation frequencies and separations of the DM-modified stellar models of KIC 8006161, HD 52265 and α Cen B using the ADIPLS package (Christensen-Dalsgaard 2008). In order to disentangle the effects of DM from those arising from the variation of the stellar parameters, a very precise determination of the latter is of utmost importance. Although asteroseismology has already provided very accurate measurements of the mass and radius of KIC 8006161 (Mathur et al. 2012) and HD 52265 (Escobar et al. 2012), with uncertainties of the order of 1%, we preferred to focus here on the case of α Cen B, a star whose fundamental parameters are independently measured with high accuracy (see Table 1) because it belongs to a binary system.

All stellar models used to create Fig. 3 reproduce the measured M , L , R , T_{eff} , $(Z/X)_s$ and mean large frequency separation $\langle\Delta\nu_{n,l}\rangle$ of α Cen B within the observational error. However, while models without DM are also able to reproduce the observed $\langle\delta\nu_{02}\rangle$, we found that the stellar models with a strong influence of DM predict a $\langle\delta\nu_{02}\rangle$ significantly deviated from the observed value. The black lines in Figure 3, labelled 2σ and 5σ , show the DM characteristics corresponding to the calibrated models that predicted $\langle\delta\nu_{02}\rangle$ with a difference of 2 and 5 times the observational error, respectively, from the observed value. The dashed black lines around the 2σ line show the theoretical uncertainty in the modelling when the uncertainties in the stellar characteristics are taken into account. The errors around the 5σ line are not shown for clarity, but they would appear narrower because $\langle\delta\nu_{02}\rangle$ varies more abruptly in that region of the plot. This theoretical uncertainty corresponds to the standard deviation on $\langle\delta\nu_{02}\rangle$ when the stellar parameters vary within the observational errors, evaluated computing 1600 valid models of α Cen B. Therefore, we conclude that present asteroseismic measurements of α Cen B disfavour the existence of DM particles with parameters above the 2σ line with 95% confidence level.

Similarly, the presence of a convective core leads to strong asteroseismic signatures. The mixing of elements in convective regions introduce sharp structural variations in the border with radiative regions that produce a clear oscillatory signal in the frequency spectrum (Gough 1990). It has been shown that this feature may be used to detect and measure the size of a convective core through asteroseismic parameters such as r_{01} , r_{10} or dr_{0213} (Cunha & Brandão 2011; Silva Aguirre et al. 2011). If these asteroseismic diagnostic tools succeed in

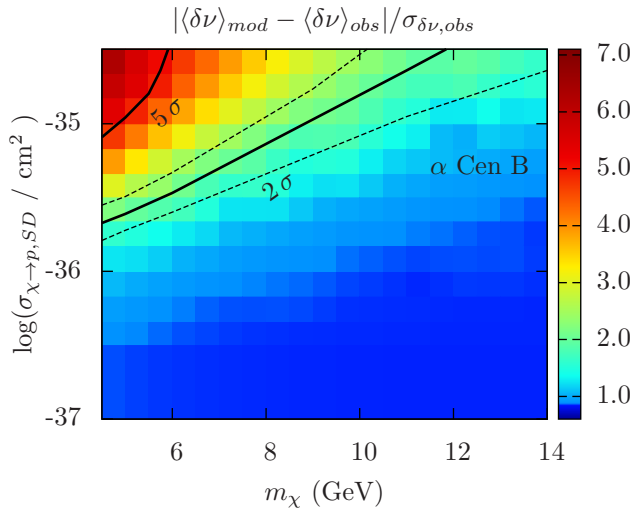


FIG. 3.— Deviation of the $\langle\delta\nu_{02}\rangle$ of the DM-modified stellar models from the true value measured in α Cen B. All the stellar models are calibrated to fit the M , R , L , T_{eff} , $(Z/X)_s$ and $\langle\Delta\nu_{n,l}\rangle$ of α Cen B within the observational error. The dashed black lines around the 2σ line show the theoretical uncertainty in the modelling arising from the uncertainties in the stellar characteristics.

the confirmation of the presence or the absence of a convective core in a star with 1.1-1.3 M_{\odot} , this hypothetical measurement may be used to place further constraints on the nature of the DM particles. The characteristic and localised effects of DM should allow the disentangling of its signatures from standard processes. Remarkably, several stars with the appropriate characteristics are presently being observed by the *CoRoT* and *Kepler* missions.

5. CONCLUSIONS AND DISCUSSION

We have shown the strong signatures that asymmetric DM particles with low masses and large SD scattering cross sections with baryons produce on low-mass stars. We have focused in the study of the stars KIC 8006161, HD 52265 and α Cen B, revealing large modifications in the central temperatures and densities of the models and the suppression of the convective core expected in 1.1-1.3 M_{\odot} stars.

In the case of α Cen B, we have shown that the asteroseismic parameter $\langle\delta\nu_{02}\rangle$ can be used to impose competitive constraints to the DM characteristics. In particular, we were able to exclude with 95% confidence

level asymmetric DM candidates with $m_{\chi} \simeq 5$ GeV and $\sigma_{\chi,SD} \geq 3 \cdot 10^{-36}$ cm². These new constraints are competitive with the present limits from direct detection experiments, because the sensitivity of the detectors drops at low WIMP masses.

Interestingly, low-mass WIMPs with similar characteristics have been advocated to explain the signals in the DAMA/LIBRA and CoGeNT detectors in terms of SD collisions. In ADM models the low mass of the WIMPs is strongly motivated because the relic density of DM is determined by the baryon asymmetry of the Universe, leading to $\Omega_{DM} \sim (m_{DM}/m_b)\Omega_b$. Our approach may provide a complementary test of these low-mass WIMP models, in the context of controversy over the incompatible results between different direct detection experiments.

Asteroseismology thus arises as a promising strategy for indirect DM searches. Compared to helioseismology, the asteroseismic searches of DM allow the study of stars with masses lower than that of the Sun, which are more strongly influenced by the additional cooling mechanism provided by the DM particles. In addition, the asteroseismic confirmation of the presence or the absence of convective cores in 1.1-1.3 M_{\odot} stars, such as HD 52265, may provide further constraints on the nature of DM.

The future perspectives of this approach are also exciting. If the small frequency spacings are identified in the oscillations of stars located in environments with high expected DM densities, such as globular clusters, then the sensitivity of the approach proposed in this work will reach much smaller WIMP-proton scattering cross sections and larger WIMP masses. Moreover, in the event of a successful identification of the properties of DM after hypothetical positive results in different experiments, asteroseismology may allow the determination of the density of DM at any specific location where a star is observed.

We are grateful to the authors of DarkSUSY, CESAM and ADIPLS for making their codes publicly available, and to the anonymous referees for constructive comments. JC thanks A. Serenelli and P. Tinyakov for helpful discussions. This work was supported by grants from FCT-MCTES (SFRH/BD/44321/2008) and Fundação Calouste Gulbenkian

REFERENCES

- Ballot, J., Gizon, L., Samadi, R., Vauclair, G., Benomar, O., et al. 2011, *Astron.Astrophys.*, 530, A97
- Bertone, G. 2010, *Nature*, 468, 389
- Bertone, G. & Fairbairn, M. 2008, *Phys.Rev.*, D77, 043515
- Blennow, M., Fernandez-Martinez, E., Mena, O., Redondo, J., & Serra, P. 2012
- Bonaca, A., Tanner, J. D., Basu, S., Chaplin, W. J., Metcalfe, T. S., et al. 2012
- Bruntt, H., Basu, S., Smalley, B., Chaplin, W., Verner, G., et al. 2012
- Casanellas, J. & Lopes, I. 2009, *Astrophys.J.*, 705, 135
- . 2011a, *Astrophys.J.*, 733, L51
- . 2011b, *Mon.Not.Roy.Astron.Soc.*, 410, 535
- Chaplin, W., Kjeldsen, H., Christensen-Dalsgaard, J., Basu, S., Miglio, A., et al. 2011, *Science*, 332, 213
- Christensen-Dalsgaard, J. 2008, *Astrophysics and Space Science*, 316, 113
- Corsico, A. H., Althaus, L. G., Bertolami, M. M. M., Romero, A. D., Garcia-Berro, E., et al. 2012
- Cumberbatch, D. T., Guzik, J., Silk, J., Watson, L. S., & West, S. M. 2010, *Phys.Rev.*, D82, 103503
- Cunha, M. S. & Brandão, I. M. 2011, *Astronomy and Astrophysics*, 529, A10
- Davoudiasl, H., Morrissey, D. E., Sigurdson, K., & Tulin, S. 2011, *Phys.Rev.*, D84, 096008
- Escobar, M., Vauclair, S. T. S., Ballot, J., Charpinet, S., Dolez, N., et al. 2012
- Frandsen, M. T. & Sarkar, S. 2010, *Physical Review Letters*, 105
- Garbari, S., Liu, C., Read, J. I., & Lake, G. 2012
- Garcia, R. A., Mathur, S., Salabert, D., Ballot, J., Regulo, C., et al. 2010, *Science*, 329, 1032
- Gelmini, G. B., Hall, L. J., & Lin, M. J. 1987, *Nuclear Physics B*, 281, 726
- Gilliland, R. L., Faulkner, J., Press, W. H., & Spergel, D. N. 1986, *ApJ*, 306, 703

- Gilliland, R. L. et al. 2010, *Publ.Astron.Soc.Pac.*, 122, 131
- Gondolo, P. et al. 2004, *JCAP*, 0407, 008
- Gough, D. O. 1986, in *Hydrodynamic and Magnetodynamic Problems in the Sun and Stars*, ed. Y. Osaki, 117
- Gough, D. O. 1990, in *Lecture Notes in Physics*, Berlin Springer Verlag, Vol. 367, *Progress of Seismology of the Sun and Stars*, ed. Y. Osaki & H. Shibahashi, 283
- Gould, A. 1987, *ApJ*, 321, 571
- Gould, A. & Raffelt, G. 1990, *Astrophys.J.*, 352, 669
- Griest, K. & Seckel, D. 1987, *Nuclear Physics B*, 283, 681
- Ilie, C., Freese, K., Valluri, M., Iliev, I. T., & Shapiro, P. R. 2012, *Mon.Not.Roy.Astron.Soc.*, 422, 2164
- Iocco, F., Bressan, A., Ripamonti, E., Schneider, R., Ferrara, A., et al. 2008, *Mon.Not.Roy.Astron.Soc.*, 390, 1655
- Iocco, F., Taoso, M., Leclercq, F., & Meynet, G. 2012, *Phys.Rev.Lett.*, 108, 061301
- Kaplan, D. E., Luty, M. A., & Zurek, K. M. 2009, *Phys.Rev.*, D79, 115016
- Kjeldsen, H., Bedding, T. R., Butler, R. P., Christensen-Dalsgaard, J., Kiss, L. L., et al. 2005, *Astrophys.J.*, 635, 1281
- Kouvaris, C. & Tinyakov, P. 2011, *Phys.Rev.Lett.*, 107, 091301
- Leung, S. C., Chu, M. C., & Lin, L. M. 2012
- Li, X., Wang, F., & Cheng, K. 2012, *JCAP*, 1210, 031
- Lopes, I., Casanellas, J., & Eugenio, D. 2011, *Phys.Rev.*, D83, 063521
- Lopes, I. & Silk, J. 2010, *Astrophys.J.*, 722, L95
- . 2012, *Astrophys.J.*, 757, 130
- Mathur, S., Metcalfe, T., Woitaszek, M., Bruntt, H., Verner, G., et al. 2012, *Astrophys.J.*, 749, 152
- Michel, E., Baglin, A., Auvergne, M., Catala, C., & Samadi, R. 2008, *Science*, 322, 558
- Morel, P. 1997, *Astronomy and Astrophysics Supplement series*, 124, 597
- Renzini, A. 1987, *A&A*, 171, 121
- Savage, C., Gelmini, G., Gondolo, P., & Freese, K. 2009, *JCAP*, 0904, 010
- Scott, P., Fairbairn, M., & Edsjo, J. 2009, *Mon.Not.Roy.Astron.Soc.*, 394, 82
- Scott, P., Venkatesan, A., Roebber, E., Gondolo, P., Pierpaoli, E., et al. 2011, *Astrophys.J.*, 742, 129
- Silva Aguirre, V., Ballot, J., Serenelli, A. M., & Weiss, A. 2011, *Astronomy and Astrophysics*, 529, A63
- Sivertsson, S. & Gondolo, P. 2011, *Astrophys.J.*, 729, 51
- Spolyar, D., Freese, K., & Gondolo, P. 2008, *Phys.Rev.Lett.*, 100, 051101
- Taoso, M., Iocco, F., Meynet, G., Bertone, G., & Eggenberger, P. 2010, *Phys.Rev.D*, 82
- Turck-Chièze, S., García, R. A., Lopes, I., Ballot, J., Couvidat, S., Mathur, S., Salabert, D., & Silk, J. 2012, *Astrophys. J.*, 746, L12
- Zackrisson, E., Scott, P., Rydberg, C.-E., Iocco, F., Edvardsson, B., et al. 2010, *Astrophys.J.*, 717, 257
- Zentner, A. R. & Hearin, A. P. 2011, *Phys.Rev.*, D84, 101302

A.6 Paper VI

TESTING ALTERNATIVE THEORIES OF GRAVITY USING THE SUN

Casanellas J., Pani P., Lopes I. & Cardoso V.
The Astrophysical Journal, 745:15, 6pp, (2012)
[arXiv:1109.0249](https://arxiv.org/abs/1109.0249)

TESTING ALTERNATIVE THEORIES OF GRAVITY USING THE SUN

JORDI CASANELLAS¹, PAOLO PANI¹, ILÍDIO LOPES^{1,2}, AND VITOR CARDOSO^{1,3}

¹ CENTRA, Departamento de Física, Instituto Superior Técnico, Universidade Técnica de Lisboa-UTL, Av. Rovisco Pais 1, 1049 Lisboa, Portugal;
jordicasanelas@ist.utl.pt, paolo.pani@ist.utl.pt, ilidio.lopes@ist.utl.pt, vitor.cardoso@ist.utl.pt

² Departamento de Física, Universidade de Évora, Colégio Luis António Verney, 7002-554 Évora, Portugal

³ Department of Physics and Astronomy, The University of Mississippi, MS 38677, USA

Received 2011 August 12; accepted 2011 October 17; published 2011 December 27

ABSTRACT

We propose a new approach to test possible corrections to Newtonian gravity using solar physics. The high accuracy of current solar models and new precise observations allow us to constrain corrections to standard gravity at unprecedented levels. Our case study is Eddington-inspired gravity, an attractive modified theory of gravity which results in non-singular cosmology and collapse. The theory is equivalent to standard gravity in vacuum, but it sensibly differs from it within matter. For instance, it affects the evolution and the equilibrium structure of the Sun, giving different core temperature profiles, and deviations in the observed acoustic modes and in solar neutrino fluxes. Comparing the predictions from a modified solar model with observations, we constrain the coupling parameter of the theory, $|\kappa_g| \lesssim 3 \times 10^5 \text{ m}^5 \text{ s}^{-2} \text{ kg}^{-1}$. Our results show that the Sun *can* be used to efficiently constrain alternative theories of gravity.

Key words: gravitation – neutrinos – Sun: general – Sun: helioseismology – Sun: oscillations

Online-only material: color figures

1. INTRODUCTION

In the last century general relativity passed several stringent tests and it is now accepted as the standard theory of gravity and one of mankind's greatest achievements (Will 2005). In the weak-field regime, general relativity reduces to Newtonian gravity, which is encoded in the famous Poisson equation for the gravitational field

$$\nabla^2 \Phi = 4\pi G \rho, \quad (1)$$

where G is the gravitational constant and ρ is the matter density. In vacuum, the gravitational field of a spherically symmetric mass M simply reads

$$\Phi(r) = -GM/r. \quad (2)$$

The validity region of the equation above has been tested and confirmed from submillimeter (Hoyle et al. 2001) to solar system experiments (Will 2005). However, much less is known about Poisson's Equation (1) inside matter. In fact, the coupling to matter is one of the most delicate points in Einstein's theory. Several alternative theories have been proposed, which introduce modifications in the coupling between matter and gravity (see, e.g., Damour & Esposito-Farese 1993). The investigation of possible alternatives to the general relativity paradigm are important. Extrapolating Einstein's theory to regimes in which it is not well tested may lead to bias, potentially affecting astrophysical observations and our understanding of the universe.

At the relativistic level, corrections in gravity-matter coupling would affect the interior of neutron stars and the cosmological evolution of the universe (Clifton et al. 2011). However, the uncertainty on the correct equation of state (EOS) describing the interior of a neutron star makes it difficult to disentangle the effects of an alternative theory from those due to a different EOS.

On the other hand, deviations from standard gravity have been proposed even at the Newtonian level (Milgrom 1983; Banados & Ferreira 2010) in a way that is compatible with current

experimental bounds. Theories such as these are consistent with all observations and at the same time are able to avoid long-standing problems of standard gravity. Thus, modified theories should be taken seriously and as important alternatives to explain our universe; it is of utmost importance to develop methods to test and constrain them against standard gravity.

In this work we propose a new approach, which is not affected by the degeneracy problems in neutron star physics and is complementary to cosmological tests. We shall investigate how deviations in Equation (1) would affect the evolution and the equilibrium structure of the Sun and other stars, leaving potentially observable effects. The high accuracy obtained with current standard solar models and precise observations of the acoustic modes and neutrino fluxes allow us to perform stringent tests of the physics governing stellar evolution and interior (Turck-Chièze & Couvidat 2011). In the past, stellar evolution has been used to constrain a possible time dependence of Newton's constant G (Teller 1948). More recently, similar ideas have been used to put constraints on the value of G (Lopes & Silk 2003), on the properties of dark matter particles (Lopes et al. 2002; Lopes & Silk 2010; Casanelas & Lopes 2011), and on the couplings of other particles (Gondolo & Raffelt 2009). Finally, possible modifications to the stellar structure in some alternative scenarios were studied by Bertolami & Paramos (2005, 2008) using polytropic models. Given the high (and increasing) accuracy of present realistic solar models and related observations, using the Sun as a *theoretical laboratory* where alternative theories of gravity can be challenged is a very promising tool to constrain deviations from Newtonian gravity.

2. PARAMETERIZED POST POISSONIAN APPROACH FOR MODIFIED GRAVITY

The parameterized post-Newtonian approach proved to be extremely efficient in constraining weak-field deviations from general relativity *in orbital motion* (Will 2005). The approach is based on a very general parameterization of the metric functions, and does not require any knowledge of the underlying

alternative (metric) theory. Following a similar approach, here we parameterize viable couplings between matter and gravity in the non-relativistic limit, i.e., within Newtonian theory. We require a modified Poisson equation which reduces to the usual one in vacuum, but which can accommodate extra terms in the coupling with matter. Assuming this theory is the non-relativistic limit of some covariant relativistic theory, we also require spatial covariance. Finally, we assume the theory contains at most second-order derivatives in the fields, although this condition can be easily relaxed. A general modified Poisson equation, up to second order in Φ , ρ , and derivatives, that satisfies these requirements reads

$$\begin{aligned} \nabla^2\Phi = & 4\pi G\rho + \frac{\kappa_g}{4}\nabla^2\rho + \alpha_g\epsilon^{ij}\nabla_i\Phi\nabla_j\rho \\ & + \eta\rho^2 + \gamma\nabla\rho\cdot\nabla\rho + \epsilon_1\nabla\Phi\cdot\nabla\rho \\ & + \epsilon_2\Phi\nabla^2\rho + \epsilon_3\rho\nabla^2\Phi + \dots \end{aligned} \quad (3)$$

The first term on the right-hand side of the equation above is the standard Poisson term. The second one, proportional to κ_g , arises from the Eddington-inspired gravitational theory recently proposed by Banados & Ferreira (2010). The other terms are higher order corrections and ϵ^{ij} is the Levi-Civita symbol. All the parameterized corrections vanish in vacuum, so that the theory above is consistent with the inverse square law behavior (2), but most of the extra terms in Equation (3) violate the equivalence principle and are therefore already strongly constrained by experiments (Will 2005). Two notable exceptions are the terms proportional to κ_g and, for spherically symmetric configurations, the term proportional to α_g . These two terms are consistent with the equivalence principle, and mostly unconstrained presently.

2.1. A Case Study

For concreteness, here we focus on a particular case, setting $\gamma = \eta_i = \epsilon_i = 0$ in Equation (3). The modified Poisson equation reduces to

$$\nabla^2\Phi = 4\pi G\rho + \frac{\kappa_g}{4}\nabla^2\rho + \alpha_g\epsilon^{ij}\nabla_i\Phi\nabla_j\rho, \quad (4)$$

where $[[\kappa_g]] = \text{cm}^5/(\text{g s}^2) = [[G]][[R^2]]$. Requiring spherical symmetry, the hydrostatic equilibrium equation follows

$$\frac{dP}{dr} = -\frac{Gm(r)\rho}{r^2} - \frac{\kappa_g}{4}\rho\rho', \quad (5)$$

where no terms proportional to α_g arise due to spherical symmetry. The choice $\gamma = \eta_i = \epsilon_i = 0$ is motivated by several reasons. First of all, the terms we are neglecting would introduce violations to the equivalence principle, which is experimentally confirmed with great precision (Will 2005). Second, the equation above represents the most general modified Poisson equation which is first order in Φ , ρ and satisfies the requirements previously discussed. The extra terms would only introduce higher order corrections. Furthermore, this theory is the non-relativistic limit of a well-motivated theory of gravity, which prevents the formation of singularities in cosmology and in the stellar collapse of compact objects (Banados & Ferreira 2010; Pani et al. 2011). Here, we investigate how this theory would modify the interior and the evolution of the Sun.

3. THE EVOLUTION OF THE SUN

The high accuracy of current solar models and precise observations allow us to test standard gravity against alternative

theories at unprecedented levels. Alternative theories would affect the evolution and the equilibrium structure of the Sun, giving different core temperature profiles and deviations in the observed acoustic modes and in solar neutrino fluxes. Comparing the predictions from a modified solar model with observations, we can constrain the coupling parameter of the theory.

Modeling the solar interior not only requires us to describe the present solar structure, but also to explain the evolution of the Sun from the ignition of hydrogen nuclear fusion to the present day (see, e.g., Turck-Chièze & Lopes 1993 for a review). The solar models are constructed on the basis of plausible assumptions, which translate to a set of four ordinary differential equations. The star is considered in hydrostatic equilibrium, which means that the hydrostatic pressure resulting from the thermonuclear fusion of hydrogen to helium must be exactly balanced by gravity. The nuclear reactions are produced in the pp chain and in the CNO cycle, the former affecting more strongly the temperature profile in the solar core. Furthermore, the star is assumed to be in thermal equilibrium, i.e., the energy produced by nuclear reactions balances the total energy loss via radiative energy flux and via the energy carried away by neutrinos.

Within $\sim 70\%$ of the solar radius, the most efficient transport mechanism of energy from the solar center outward to the stellar surface is due to electromagnetic radiation, while in the outer region, the so-called convective zone, the energy is mainly transported by convection. The radiative energy transport (and, in turn, the temperature profile) is governed by the Rosseland mean opacity, which takes into account that photons interact with electrons and ions in the dense plasma in the solar interior, while they mostly interact with atoms and molecules at the solar surface, where radiative transport is again significant.

One of the basic assumptions of any solar model, namely, the hydrostatic equilibrium, ultimately depends on how strong and efficient the gravitational self-interaction is inside the Sun, i.e., on Poisson's Equation (3). Any corrections would affect the thermal balance and, in turn, the temperature profile inside the star, leaving potentially observable signatures.

Finally, effects due to rotation (Pinsonneault et al. 1989) and magnetic fields (Passos & Lopes 2008) are usually neglected in standard solar models. These processes take place on a much shorter timescale than the evolutionary timescale of the Sun and their inclusion results in minor structure changes in the solar interior (see, e.g., Turck-Chièze et al. 2010).

3.1. Equations Governing Stellar Equilibrium and Evolution

Under the previous assumptions, the internal structure of the Sun is governed by the following ordinary differential equations for (r, P, L, T) , the radius, pressure, luminosity, and temperature, respectively,

$$\frac{dr}{dq} = \frac{M_\odot}{4\pi r^2 \rho}, \quad (6)$$

$$\frac{dP}{dq} = -\frac{GM_\odot^2 q}{4\pi r^4} - \frac{\kappa_g}{4}\rho \frac{d\rho}{dq}, \quad (7)$$

$$\frac{dL}{dq} = M_\odot \left(\epsilon - r \frac{dS}{dt} \right), \quad (8)$$

where $q = m/M_\odot$ is a convenient choice of the independent variable, since mass loss is neglected (Clayton 1968). The first

and third equations above are the standard continuity equation and conservation of thermal energy, respectively, while the second equation describes the hydrostatic equilibrium (note that Equation (7) is equivalent to Equation (5) when expressed in terms of the independent variable q). Finally, the equations above must be supplied by an appropriate transport energy equation for the convective zone and for the radiative zone (Morel 1997). Due to the modified Poisson Equation (7), the standard equation for the convective energy transport is indirectly modified as follows:

$$\frac{dT}{dq} \equiv \frac{dP}{dq} \frac{dT}{dP} = - \left[\frac{GM_{\odot}^2 q}{4\pi r^4} + \frac{\kappa_g}{4} \rho \frac{d\rho}{dq} \right] \frac{T}{P} \nabla, \quad (9)$$

where $\nabla \equiv d \log T / d \log P$ is the temperature gradient. For adiabatic changes, the temperature gradient can be simply related to one of the adiabatic exponents, $\nabla_{\text{ad}} = (\Gamma_2 - 1) / \Gamma_2$ (Weiss et al. 2004). In the radiative zone, the transport energy equation is unaffected by κ_g and it simply reads

$$\frac{dT}{dq} = - \frac{3 M_{\odot} \kappa}{16 \sigma T^3} \frac{L}{16 \pi^2 r^4}, \quad (10)$$

where κ is the Rosseland mean opacity and σ is the Boltzmann constant.

3.2. Numerical Procedure

The modified equations above have been included, together with all the relevant physical processes, in CESAM (Morel 1997), a self-consistent numerical code for stellar structure and evolution. The main physical inputs of the solar models are the following: the nuclear reaction rates are taken from Adelberger et al. (1998), with the Mitler (1977) intermediate screening; the opacities are taken from the OPAL95 tables (Iglesias & Rogers 1996) for temperatures above 5600 K and from Alexander & Ferguson (1994) for lower temperatures; we used the tabulated OPAL EOS (Rogers et al. 1996); microscopic diffusion is included following the prescription of Michaud & Proffitt (1993); and finally, the solar abundances are taken from Asplund et al. (2005). For comparison, all the models were also computed with the older, low-metallicity solar abundances (Grevesse & Sauval 1998), leading to nearly identical results. This test stresses the robustness of our approach and shows that our analysis is virtually independent of the current uncertainties of solar modeling.

In order to constrain the values of the coupling parameter κ_g which are compatible with present observations of the Sun, we constructed calibrated solar models for different values of κ_g . The models are calibrated to fit the solar properties with an accuracy of 10^{-5} . The calibration is performed by varying the parameters X_0 (the initial abundance of hydrogen in the young Sun) and α (which parameterizes the efficiency of convection as a mechanism of energy transport), and by fixing the solar surface heavy-element content $(Z/X)_{\odot} = 0.0165$, age $t_{\odot} = 4.57$ Gyr, radius $R_{\odot} = 6.9599 \times 10^{10}$ cm, mass $M_{\odot} = 1.9891 \times 10^{33}$ g, and luminosity $L_{\odot} = 3.846 \times 10^{33}$ erg s $^{-1}$.

It was possible to construct calibrated solar models for $-0.032 G R_{\odot}^2 \lesssim \kappa_g \lesssim 0.02 G R_{\odot}^2$. For $\kappa_g \lesssim -0.032 G R_{\odot}^2$, no equilibrium stars can be constructed, in agreement to what is shown in Pani et al. (2011) for simple polytropic models. On the other hand, for $\kappa_g \gtrsim 0.02 G R_{\odot}^2$, equilibrium stellar configurations can be constructed, but their internal structure is so strongly modified that the observed solar properties (namely,

Table 1
Characteristics of Some Solar Models for Different Values of κ_g

κ_g ($G R_{\odot}^2$)	X_0	α	T_c (10^7 K)	ρ_c (g cm^{-3})	P_c (dyn cm^{-2})
-0.032	0.78	2.77	15.54	161.5	2.56×10^{17}
-0.01	0.76	2.07	15.25	150.1	2.36×10^{17}
0	0.74	1.84	15.18	146.7	2.29×10^{17}
0.01	0.73	1.65	15.12	144.8	2.25×10^{17}
0.02	0.72	1.48	15.09	143.6	2.22×10^{17}

Note. All stellar models have $M = M_{\odot}$, $L = L_{\odot}$, and $R = R_{\odot}$ at the solar age $t_{\odot} = 4.57$ Gyr.

Z/X , t_{\odot} , R_{\odot} , M_{\odot} , and L_{\odot}) cannot be matched simultaneously. In Table 1, we show the values of X_0 and α required to calibrate the solar models, together with the central temperature, density, and pressure of the models.

Solar models with $\kappa_g > 0$ have a lower central density and a lower core temperature, whereas models with $\kappa_g < 0$ work in the opposite direction. These results can be qualitatively understood as follows. Equation (5) can be written in a more evocative form as

$$\frac{dP}{dr} = -G_{\text{eff}}(r) \frac{m(r)\rho(r)}{r^2}, \quad (11)$$

where we have defined an ‘‘effective’’ Newton’s constant

$$G_{\text{eff}}(r) \equiv G + \frac{\kappa_g r^2 \rho'(r)}{4 m(r)}. \quad (12)$$

Since $\rho'(r) < 0$ inside the Sun, $G_{\text{eff}} < G$ ($G_{\text{eff}} > G$) when $\kappa_g > 0$ ($\kappa_g < 0$). When $\kappa_g < 0$, we expect a stronger effective gravitational force which, for main-sequence stars in hydrostatic equilibrium, leads to an increase in the central temperature and, consequently, in the rate of thermonuclear reactions. The solar models constructed with $\kappa_g < 0$ also require a higher initial abundance of hydrogen to match the solar observables. This fact can be explained by homology scaling (see, e.g., Kippenhahn & Weigert 1990): the luminosity of a star scales as a high power of G and the mean molecular weight, and therefore an effective increase in the gravitational force must be compensated by a decrease in the mean molecular weight (and consequently an increase in the hydrogen abundance) to achieve the same luminosity. This qualitative picture is in agreement with results obtained for different (constant) values of G (cf. Table 1 in Lopes & Silk 2003).

4. RESULTS

The Eddington-inspired theory of gravity leads to strong modifications in the solar structure. In a wide region of the parameter space of the theory, the modified solar models show important variations in the central temperature and in the density profile (see Figure 1). These two signatures can be tested against solar observables. In particular, we shall show that solar neutrino measurements (which are sensible to T_c) and helioseismic acoustic data (sensible to sound speed and density profiles) strongly constrain the values of the parameter κ_g that are compatible with present observations.

4.1. Solar Neutrinos

Solar neutrinos provide a unique window to the solar interior due to the high sensitivity of thermonuclear reactions to the temperature at which they take place. In particular, the ^8B flux,

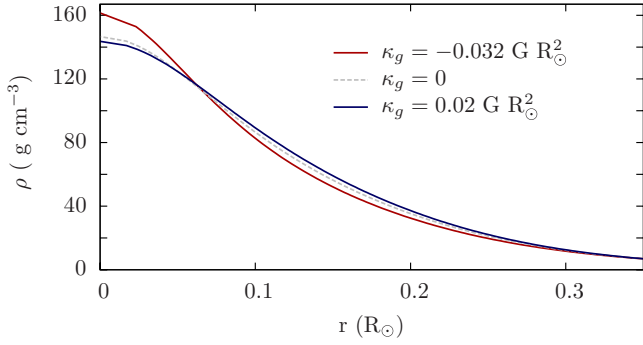


Figure 1. Density profiles of the modified solar models computed with different values of κ_g .

(A color version of this figure is available in the online journal.)

produced in the inner 10% (in radius) through the pp chain, is very sensitive to the central temperature of the Sun: $\phi_{^8\text{B}} \propto T_c^{18}$ (Turck-Chièze & Couvidat 2011). The predicted neutrino flux is expected to depend strongly on κ_g since different couplings lead to different central temperatures (modified solar models may lead to variations of up to 3% in T_c). The observed ^8B neutrino flux is currently measured with high precision by neutrino telescopes: $(5.046 \pm 0.16) \times 10^6 \text{ cm}^{-2} \text{ s}^{-1}$ (Aharmim et al. 2010; Bellini et al. 2010). Thus, the theory can be constrained on the basis of incompatibility with observations.

Our results for the solar neutrino fluxes are shown in Figure 2. As expected, the dependence on the coupling parameter κ_g can be understood in terms of effective gravitational constant. Positive values of κ_g lead to a smaller G_{eff} , contributing to a lower central temperature and, in turn, to a lower expected neutrino flux. Negative values of κ_g work in the opposite direction.

The theoretical uncertainty of standard solar modeling have to be consistently taken into account when comparing the predictions of our models with the observations. Previous works have shown that the largest source of uncertainty in the calculation of the solar neutrino fluxes comes from the uncertainty in the values of the surface heavy element abundances of the Sun (Bahcall et al. 2006; Gonzalez-Garcia et al. 2010; Noreña et al. 2011). Bahcall & Serenelli (2005) determined, using Monte Carlo simulations for 10,000 solar models, that the total 1σ theoretical uncertainty in the predicted ^8B neutrino flux is below 17%, in the most conservative scenario. In addition, we also take into account the deviation of 20% in the predicted ^8B flux when different estimations of the solar abundances are implemented (see, e.g., Serenelli et al. 2009). Considering both the theoretical and experimental uncertainties, we estimated that models that predict a ^8B flux which deviates more than 30% from our standard solar model can be conservatively ruled out, in agreement with the threshold considered by other authors (Taoso et al. 2010). Following this analysis, we conclude that values of $\kappa_g \lesssim -0.024 G R_\odot^2$ are excluded by the observation of ^8B solar neutrinos (see Figure 2).

On the other hand, we found that the ^7Be neutrino flux only provides less stringent constraints on κ_g , as ^7Be neutrinos are produced in a wider region in the center of the Sun and, consequently, are less sensitive to its central temperature ($\phi_{^7\text{Be}} \propto T_c^8$; Turck-Chièze & Couvidat 2011).

4.2. Helioseismology

The solar acoustic modes are nowadays measured with exquisite precision by helioseismic missions on board

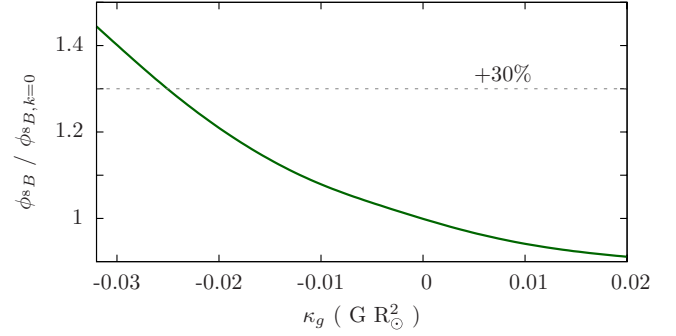


Figure 2. ^8B neutrino flux predicted by our modified solar models normalized to the flux predicted by our standard solar model.

(A color version of this figure is available in the online journal.)

spacecrafts, such as GOLF/SOHO (Turck-Chièze et al. 1997), MDI/SOHO (Scherrer et al. 1995), and HMI/SDO (Zhao et al. 2011), and by ground networks such as BiSON (Broomhall et al. 2009) and GONG (Harvey et al. 1996). The analysis of helioseismic data has provided a valuable tool to probe the solar interior, revealing the sound-speed and density profiles down to 10% of the solar radius (Christensen-Dalsgaard et al. 1985; Gough et al. 1996).

Different helioseismic parameters have been used to investigate various aspects of solar physics (Thompson et al. 1996; Gizon et al. 2010). In particular, the small separation between the frequencies of modes with different degrees l and radial orders n , $\delta\nu_{n,l} = \nu_{n,l} - \nu_{n-1,l+2}$ is a helioseismic quantity that is very sensitive to the temperature gradient in the deep interior of the Sun (Oti Floranes et al. 2005). In addition, the modes with degree $l = 0$ correspond to acoustic waves that traveled through the entire stellar radius and carry information about the density profile of the Sun (Lopes & Turck-Chièze 1994; Roxburgh & Vorontsov 2000). Therefore, $\delta\nu_{n,l=0}$, also known as fine spacing or d_{02} , is a very suitable parameter to detect the signatures that alternative theories of gravity leave on the solar interior.

The small separations in modified solar models are compared with solar data in Figure 3(a). As expected, for $\kappa_g = 0$ the fine spacings exhibit a moderate disagreement with the observations. This discrepancy, which disappears when the older, low- Z solar abundances are considered, has been discussed in detail by Basu et al. (2007). On the other hand, for large values of κ_g the deviations from helioseismic data are much larger, providing a clear way to discriminate viable models.

As discussed for solar neutrinos, when the helioseismic quantities are used to constrain solar models in modified theories of gravity, the uncertainties of solar modeling have also to be taken into account. Compared to solar neutrinos, the theoretical uncertainties on the mean small separation ($\langle \delta\nu_{n,l=0} \rangle$) are much smaller. The variation on $\langle \delta\nu_{n,l=0} \rangle$ resulting from different solar models is of the order of 2%–3% (Basu et al. 2007). Considering this uncertainty, we can rule out those models that lead to deviations in $\langle \delta\nu_{n,l=0} \rangle$ greater than 4%. This diagnostic establishes strong constraints on κ_g , ruling out the regions $\kappa_g \gtrsim 0.016 G R_\odot^2$ and $\kappa_g \lesssim -0.01 G R_\odot^2$ (see Figure 3(b)).

4.2.1. Other Helioseismic Constraints

Another constraint on deviations from Newtonian gravity comes from the comparison of the solar and model sound speed profiles, the former being obtained with high precision from helioseismic observations. Remarkably, the standard solar

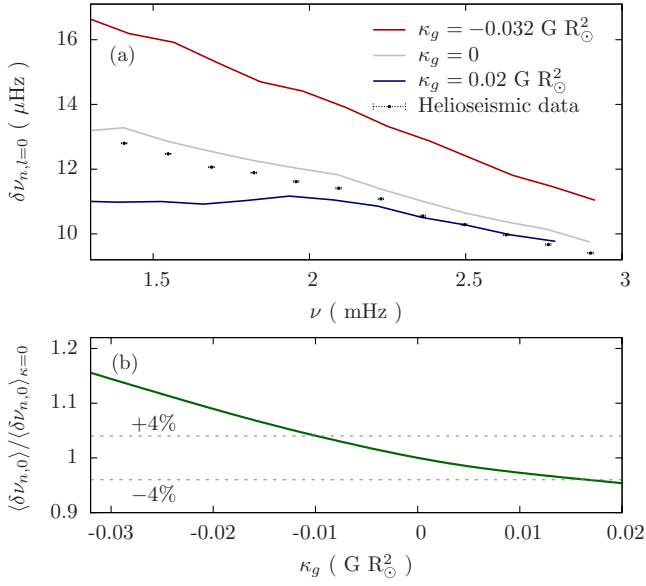


Figure 3. (a) Small separations for $l = 0$ calculated in our models compared with helioseismic data (Broomhall et al. 2009). (b) Mean small separation for $l = 0$ and $\nu > 2000 \mu\text{Hz}$ for our modified solar models, normalized to the prediction for $\kappa_g = 0$.

(A color version of this figure is available in the online journal.)

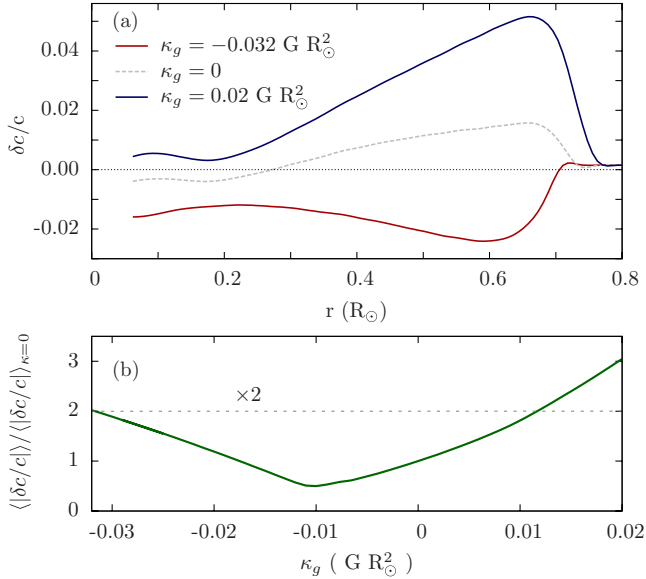


Figure 4. (a) Relative differences between the sound speed profiles of our modified solar models and the solar sound speed from helioseismic data (Broomhall et al. 2009). (b) Mean deviation between the solar and model sound speed profiles, normalized to our standard solar model.

(A color version of this figure is available in the online journal.)

model reproduces the sound speed profile of the Sun with an accuracy better than 1% in most of its interior. However, right below the convective envelope the deviations from the observed sound speed are larger (this discrepancy is common in models adopting the latest, high-Z solar abundances; Montalbán et al. 2004; Delahaye & Pinsonneault 2006; Serenelli et al. 2009). Figure 4(a) shows the relative differences between the helioseismically inverted and the sound speed profiles of some of the modified solar models, $\delta c/c = (c_\odot - c_{\text{model}})/c_{\text{model}}$. The mean difference $\langle |\delta c/c| \rangle$ is a measure of how accurately a solar model reproduces the sound speed profile of the Sun, and

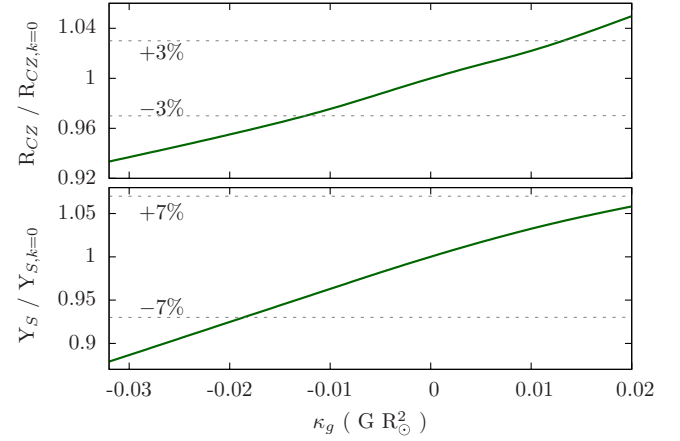


Figure 5. (a) Depth of the convective envelope R_{CZ} and (b) helium surface abundance Y_S of the modified solar models normalized to our standard solar model.

(A color version of this figure is available in the online journal.)

Table 2
Summary of the Range of the Parameter κ_g Ruled Out using Different Solar Characteristics

Observed Quantity	Range of κ_g Excluded
ϕ_8^B	$\kappa_g < -0.024 G R_\odot^2$
$\langle \delta\nu_{n,l=0} \rangle$	$\kappa_g < -0.01 G R_\odot^2$ and $\kappa_g > 0.016 G R_\odot^2$
$\langle \delta c/c \rangle$	$\kappa_g > 0.012 G R_\odot^2$
R_{CZ}	$\kappa_g < -0.013 G R_\odot^2$ and $\kappa_g > 0.013 G R_\odot^2$
Y_S	$\kappa_g < -0.018 G R_\odot^2$

therefore it can be used to put constraints to modified theories of gravity. Those models leading to a relative deviation $\langle |\delta c/c| \rangle$ more than two times larger than the $\langle |\delta c/c| \rangle$ obtained for $\kappa_g = 0$ can be conservatively ruled out. As shown in Figure 4(b), the constraints from the sound speed profile rule out models with $\kappa_g \gtrsim 0.012 G R_\odot^2$.

Helioseismology also provides accurate measurements of the depth of the convective envelope, $R_{CZ} = 0.713 \pm 0.001$ (Basu & Antia 1997) and the helium surface abundance $Y_S = 0.2485 \pm 0.0035$ (Basu & Antia 2004). Monte Carlo simulations have shown that the theoretical uncertainty from solar modeling is below 2% for R_{CZ} and 5% for Y_S (Bahcall et al. 2006). Consequently, we can conservatively rule out models that predict deviations of these quantities larger than 3% and 7%, respectively. As shown in Figure 5, this allows us to put the following constraints on the parameter κ_g : $-0.016 G R_\odot^2 < \kappa_g < 0.013 G R_\odot^2$ and $\kappa_g > -0.018 G R_\odot^2$, respectively, from the observations of R_{CZ} and of Y_S .

5. DISCUSSION AND CONCLUDING REMARKS

Our results show that the Sun is a very good testing ground for constraining generic modified theories of gravity, for instance theories such as the ones described in Equation (3) and even more exotic or yet to be proposed corrections. For the particular case of Eddington-like theories, Table 2 summarizes the constraints on the coupling parameter κ_g of the theory. Our results show that, in order to obtain a viable solar model, a theory as general as Equation (4) is strongly constrained. Combining all the experimental bounds, the coupling constant κ_g must lie in the interval $-0.01 < \kappa_g / (G R_\odot^2) < 0.012$, i.e., approximately $|\kappa_g| \lesssim 3 \times 10^5 \text{ m}^5 \text{ s}^{-2} \text{ kg}^{-1}$.

It is important to stress that this result does not rule out Eddington-inspired theory as a promising alternative to Einstein's theory. Previous studies showed that most of the appealing features of the theory would persist even for an (positive) arbitrarily small coupling parameter (Banados & Ferreira 2010; Pani et al. 2011), which is perfectly consistent with current observations of solar neutrinos and helioseismology.

Modified gravity is also relevant as an alternative approach to the solar abundance problem. The particular theory we considered only offers a partial solution to this problem. Indeed, models with $\kappa_g < 0$ predict the base of the convective envelope at a smaller radius than the standard solar model, reconciling the prediction with the helioseismically inferred value. However, the predicted helium surface abundance for the same models with $\kappa_g < 0$ is then even more underestimated than for standard solar models. Similar partial solutions were discussed in different contexts (Castro et al. 2007; Christensen-Dalsgaard et al. 2009; Guzik & Mussack 2010; Serenelli et al. 2011). Although Eddington-inspired gravity suffers from the same limitations, other gravitational corrections could affect the solar interior in a different way and they should be investigated more carefully. We leave this interesting topic for future work.

We are grateful to the authors of CESAM (Morel 1997) and ADIPLS (Christensen-Dalsgaard 2008) for making their codes publicly available and to Clifford Will for comments and suggestions. This work was supported by the *DyBHo-256667* ERC Starting Grant, by FCT-Portugal through PTDC projects FIS/098025/2008, FIS/098032/2008, CTE-AST/098034/2008 and the grant SFRH/BD/44321/2008 and by allocations at cesaraugusta through project AECT-2011-2-0006 and MareNostrum through project AECT-2011-2-0015 at the Barcelona Supercomputing Center (BSC).

REFERENCES

- Adelberger, E. G., Austin, S. M., Bahcall, J. N., et al. 1998, *Rev. Mod. Phys.*, **70**, 1265
- Aharmim, B., Ahmed, S. N., Anthony, A. E., et al. 2010, *Phys. Rev. C*, **81**, 055504
- Alexander, D. R., & Ferguson, J. W. 1994, *ApJ*, **437**, 879
- Asplund, M., Grevesse, N., & Sauval, A. J. 2005, in ASP Conf. Ser. 336, *Cosmic Abundances as Records of Stellar Evolution and Nucleosynthesis*, ed. T. G. Barnes, III. & F. N. Bash (San Francisco, CA: ASP), 25
- Bahcall, J. N., & Serenelli, A. M. 2005, *ApJ*, **626**, 530
- Bahcall, J. N., Serenelli, A. M., & Basu, S. 2006, *ApJS*, **165**, 400
- Banados, M., & Ferreira, P. G. 2010, *Phys. Rev. Lett.*, **105**, 011101
- Basu, S., & Antia, H. M. 1997, *MNRAS*, **287**, 189
- Basu, S., & Antia, H. M. 2004, *ApJ*, **606**, L85
- Basu, S., Chaplin, W. J., Elsworth, Y., et al. 2007, *ApJ*, **655**, 660
- Bellini, G., Benziger, J., Bonetti, S., et al. 2010, *Phys. Rev. D*, **82**, 033006
- Bertolami, O., & Paramos, J. 2005, *Phys. Rev. D*, **71**, 023521
- Bertolami, O., & Paramos, J. 2008, *Phys. Rev. D*, **77**, 084018
- Broomhall, A.-M., Chaplin, W. J., Davies, G. R., et al. 2009, *MNRAS*, **396**, L100
- Casanellas, J., & Lopes, I. 2011, *MNRAS*, **410**, 535
- Castro, M., Vauclair, S., & Richard, O. 2007, *A&A*, **463**, 755
- Christensen-Dalsgaard, J. 2008, *Astrophys. Space Sci.*, **316**, 113
- Christensen-Dalsgaard, J., di Mauro, M. P., Houdek, G., & Pijpers, F. 2009, *A&A*, **494**, 205
- Christensen-Dalsgaard, J., Duvall, T. L., Jr., Gough, D. O., Harvey, J. W., & Rhodes, E. J., Jr. 1985, *Nature*, **315**, 378
- Clayton, D. D. (ed.) 1968, *Principles of Stellar Evolution and Nucleosynthesis* (Chicago, IL: Univ. Chicago Press)
- Clifton, T., Ferreira, P. G., Padilla, A., & Skordis, C. 2011, arXiv:1106.2476
- Damour, T., & Esposito-Farese, G. 1993, *Phys. Rev. Lett.*, **70**, 2220
- Delahaye, F., & Pinsonneault, M. 2006, *ApJ*, **649**, 529
- Gizon, L., Birch, A. C., & Spruit, H. C. 2010, *ARA&A*, **48**, 289
- Gondolo, P., & Raffelt, G. 2009, *Phys. Rev. D*, **79**, 107301
- Gonzalez-Garcia, M. C., Maltoni, M., & Salvado, J. 2010, *J. High Energy Phys.*, **JHEP052010072**
- Gough, D. O., Kosovichev, A. G., Toomre, J., et al. 1996, *Science*, **272**, 1296
- Grevesse, N., & Sauval, A. J. 1998, *Space Sci. Rev.*, **85**, 161
- Guzik, J. A., & Mussack, K. 2010, *ApJ*, **713**, 1108
- Harvey, J. W., Hill, F., Hubbard, R. P., et al. 1996, *Science*, **272**, 1284
- Hoyle, C., Schmidt, U., Heckel, B. R., et al. 2001, *Phys. Rev. Lett.*, **86**, 1418
- Iglesias, C. A., & Rogers, F. J. 1996, *ApJ*, **464**, 943
- Kippenhahn, R., & Weigert, A. (ed.) 1990, *Stellar Structure and Evolution* (Berlin: Springer)
- Lopes, I., & Silk, J. 2010, *Science*, **330**, 462
- Lopes, I., & Turck-Chièze, S. 1994, *A&A*, **290**, 845
- Lopes, I. P., Bertone, G., & Silk, J. 2002, *MNRAS*, **337**, 1179
- Lopes, I. P., & Silk, J. 2003, *MNRAS*, **341**, 721
- Michaud, G., & Proffitt, C. R. 1993, in ASP Conf. Ser. 40, *IAU Colloq. 137: Inside the Stars*, ed. W. W. Weiss & A. Baglin (San Francisco, CA: ASP), 246
- Milgrom, M. 1983, *ApJ*, **270**, 365
- Mitler, H. E. 1977, *ApJ*, **212**, 513
- Montalbán, J., Miglio, A., Noels, A., Grevesse, N., & di Mauro, M. P. 2004, in *SOHO 14 Helio- and Asteroseismology: Towards a Golden Future*, ed. D. Danesy (ESA Special Publication, Vol. 559; Noordwijk: ESA), 574
- Morel, P. 1997, *A&AS*, **124**, 597
- Noreña, J., Verde, L., Jimenez, R., Peña Garay, C., & Gomez, C. 2011, *MNRAS*, **1681**
- Oti Floranes, H., Christensen-Dalsgaard, J., & Thompson, M. J. 2005, *MNRAS*, **356**, 671
- Pani, P., Cardoso, V., & Delsate, T. 2011, *Phys. Rev. Lett.*, **107**, 031101
- Passos, D., & Lopes, I. 2008, *ApJ*, **686**, 1420
- Pinsonneault, M. H., Kawaler, S. D., Sofia, S., & Demarque, P. 1989, *ApJ*, **338**, 424
- Rogers, F. J., Swenson, F. J., & Iglesias, C. A. 1996, *ApJ*, **456**, 902
- Roxburgh, I. W., & Vorontsov, S. V. 2000, *MNRAS*, **317**, 141
- Scherrer, P. H., Bogart, R. S., Bush, R. I., et al. 1995, *Sol. Phys.*, **162**, 129
- Serenelli, A., Basu, S., Ferguson, J. W., & Asplund, M. 2009, *ApJ*, **705**, L123
- Serenelli, A. M., Haxton, W. C., & Pena-Garay, C. 2011, *ApJ*, **743**, 24
- Taoso, M., Iocco, F., Meynet, G., Bertone, G., & Eggenberger, P. 2010, *Phys. Rev. D*, **82**, 083509
- Teller, E. 1948, *Phys. Rev.*, **73**, 801
- Thompson, M. J., Toomre, J., Anderson, E. R., et al. 1996, *Science*, **272**, 1300
- Turck-Chièze, S., Basu, S., Brun, A. S., et al. 1997, *Sol. Phys.*, **175**, 247
- Turck-Chièze, S., & Couvidat, S. 2011, *Rep. Prog. Phys.*, **74**, 086901
- Turck-Chièze, S., & Lopes, I. 1993, *ApJ*, **408**, 347
- Turck-Chièze, S., Palacios, A., Marques, J. P., & Nghiem, P. A. P. 2010, *ApJ*, **715**, 1539
- Weiss, A., Hillebrandt, W., Thomas, H.-C., & Ritter, H. (ed.) 2004, *Cox and Giuli's Principles of Stellar Structure* (Cambridge: Cambridge Scientific Publishers)
- Will, C. M. 2005, *Living Rev. Rel.*, **9**, 3 (update of the Living Review article originally published in 2001)
- Zhao, J., Couvidat, S., Bogart, R. S., et al. 2011, *Sol. Phys.*, **163**, 1

Bibliography

- [1] J. C. Kapteyn. First Attempt at a Theory of the Arrangement and Motion of the Sidereal System. *Astrophys. J.*, 55:302, May 1922.
- [2] J. H. Jeans. The motions of stars in a Kapteyn universe. *Mon. Not. Roy. Astron. Soc.*, 82:122–132, January 1922.
- [3] B. Lindblad. *Upsala Meddelanden*, 11:30, 1926.
- [4] J. H. Oort. The force exerted by the stellar system in the direction perpendicular to the galactic plane and some related problems. *Bulletin of the Astronomical Institutes of the Netherlands*, 6:249, August 1932.
- [5] F. Zwicky. Die Rotverschiebung von extragalaktischen Nebeln. *Helvetica Physica Acta*, 6:110–127, 1933.
- [6] Wolfgang Voges, Bernd Aschenbach, Thomas Boller, Heinrich Brauninger, Ulrich Briel, et al. The ROSAT all - sky survey bright source catalogue. *Astron. Astrophys.*, 349:389, 1999.
- [7] Thomas H. Reiprich and Hans Boehringer. The Mass function of an X-ray flux-limited sample of galaxy clusters. *Astrophys.J.*, 567:716–740, 2002.
- [8] V. C. Rubin and W. K. Ford, Jr. Rotation of the Andromeda Nebula from a Spectroscopic Survey of Emission Regions. *Astrophys.J.*, 159:379, February 1970.
- [9] K. G. Begeman, A. H. Broeils, and R. H. Sanders. Extended rotation curves of spiral galaxies - Dark haloes and modified dynamics. *Mon. Not. Roy. Astron. Soc.*, 249:523–537, April 1991.
- [10] Richard Massey, Jason Rhodes, Richard Ellis, Nick Scoville, Alexie Leauthaud, et al. Dark matter maps reveal cosmic scaffolding. *Nature*, 445:286, 2007.

-
- [11] M. Milgrom. A Modification of the Newtonian dynamics as a possible alternative to the hidden mass hypothesis. *Astrophys.J.*, 270:365–370, 1983.
- [12] Jacob D. Bekenstein. Relativistic gravitation theory for the MOND paradigm. *Phys.Rev.*, D70:083509, 2004.
- [13] Maxim Markevitch. Chandra observation of the most interesting cluster in the universe. 2005.
- [14] Douglas Clowe, Marusa Bradac, Anthony H. Gonzalez, Maxim Markevitch, Scott W. Randall, et al. A direct empirical proof of the existence of dark matter. *Astrophys.J.*, 648:L109–L113, 2006.
- [15] Chandra x-ray observatory acis image. <http://chandra.harvard.edu/photo/2006/1e0657/>, 2006.
- [16] M. Mateo. Dark Matter in Dwarf Spheroidal Galaxies: Observational Constraints. In G. Meylan and P. Prugniel, editors, *European Southern Observatory Conference and Workshop Proceedings*, volume 49 of *European Southern Observatory Conference and Workshop Proceedings*, page 309, January 1994.
- [17] Volker Springel, Carlos S. Frenk, and Simon D.M. White. The large-scale structure of the Universe. *Nature*, 440:1137, 2006.
- [18] W.L. Freedman et al. Final results from the Hubble Space Telescope key project to measure the Hubble constant. *Astrophys.J.*, 553:47–72, 2001.
- [19] Edward L. Wright. <http://www.astro.ucla.edu/~wright/BBNS.html>.
- [20] E. Komatsu et al. Seven-Year Wilkinson Microwave Anisotropy Probe (WMAP) Observations: Cosmological Interpretation. *Astrophys.J.Suppl.*, 192:18, 2011.
- [21] N. Jarosik, C.L. Bennett, J. Dunkley, B. Gold, M.R. Greason, et al. Seven-Year Wilkinson Microwave Anisotropy Probe (WMAP) Observations: Sky Maps, Systematic Errors, and Basic Results. *Astrophys.J.Suppl.*, 192:14, 2011.
- [22] D. Larson, J. Dunkley, G. Hinshaw, E. Komatsu, M.R. Nolta, et al. Seven-Year Wilkinson Microwave Anisotropy Probe (WMAP) Observations: Power Spectra and WMAP-Derived Parameters. *Astrophys.J.Suppl.*, 192:16, 2011.
- [23] M. Kowalski et al. Improved Cosmological Constraints from New, Old and Combined Supernova Datasets. *Astrophys.J.*, 686:749–778, 2008.

- [24] G. Steigman and M. S. Turner. Cosmological constraints on the properties of weakly interacting massive particles. *Nuclear Physics B*, 253:375–386, 1985.
- [25] J. Ellis, J. S. Hagelin, D. V. Nanopoulos, K. Olive, and M. Srednicki. Supersymmetric relics from the big bang. *Nuclear Physics B*, 238:453–476, June 1984.
- [26] Hsin-Chia Cheng, Jonathan L. Feng, and Konstantin T. Matchev. Kaluza-Klein dark matter. *Phys.Rev.Lett.*, 89:211301, 2002.
- [27] John F. Gunion, Dan Hooper, and Bob McElrath. Light neutralino dark matter in the NMSSM. *Phys.Rev.*, D73:015011, 2006.
- [28] Geraldine Servant and Timothy M.P. Tait. Is the lightest Kaluza-Klein particle a viable dark matter candidate? *Nucl.Phys.*, B650:391–419, 2003.
- [29] M. E. Peskin and D. V. Schroeder. *An Introduction to Quantum Field Theory*. Westview Press, 1995.
- [30] David E. Kaplan, Markus A. Luty, and Kathryn M. Zurek. Asymmetric Dark Matter. *Phys.Rev.*, D79:115016, 2009.
- [31] C. Savage, G. Gelmini, P. Gondolo, and K. Freese. Compatibility of DAMA/LIBRA dark matter detection with other searches. *JCAP*, 0904:010, 2009.
- [32] Jihn E. Kim and Gianpaolo Carosi. Axions and the Strong CP Problem. *Rev.Mod.Phys.*, 82:557–602, 2010.
- [33] John R. Ellis, Keith A. Olive, Yudi Santoso, and Vassilis C. Spanos. Gravitino dark matter in the CMSSM. *Phys.Lett.*, B588:7–16, 2004.
- [34] Alexander Kusenko. Sterile neutrinos: The Dark side of the light fermions. *Phys.Rept.*, 481:1–28, 2009.
- [35] Matteo Viel, Julien Lesgourgues, Martin G. Haehnelt, Sabino Matarrese, and Antonio Riotto. Constraining warm dark matter candidates including sterile neutrinos and light gravitinos with WMAP and the Lyman-alpha forest. *Phys.Rev.*, D71:063534, 2005.
- [36] C. Stenge, G. Bertone, D.G. Cerdeno, M. Fornasa, R. Ruiz de Austri, et al. Updated global fits of the cMSSM including the latest LHC SUSY and Higgs searches and XENON100 data. *JCAP*, 1203:030, 2012.
- [37] E. Aprile et al. Dark Matter Results from 100 Live Days of XENON100 Data. *Phys.Rev.Lett.*, 107:131302, 2011.

-
- [38] M. Felizardo, T.A. Girard, T. Morlat, A.C. Fernandes, A.R. Ramos, et al. Final Analysis and Results of the Phase II SIMPLE Dark Matter Search. *Phys.Rev.Lett.*, 108:201302, 2012.
- [39] Z. Ahmed et al. Dark Matter Search Results from the CDMS II Experiment. *Science*, 327:1619–1621, 2010.
- [40] S. Archambault, F. Aubin, M. Auger, E. Behnke, B. Beltran, et al. Dark Matter Spin-Dependent Limits for WIMP Interactions on F-19 by PICASSO. *Phys.Lett.*, B682:185–192, 2009.
- [41] E. Behnke, J. Behnke, S.J. Brice, D. Broemmelsiek, J.I. Collar, et al. Improved Limits on Spin-Dependent WIMP-Proton Interactions from a Two Liter CF₃I Bubble Chamber. *Phys.Rev.Lett.*, 106:021303, 2011.
- [42] R. Bernabei, P. Belli, R. Cerulli, F. Montecchia, M. Amato, G. Ignesti, A. Incicchitti, D. Prosperi, C. J. Dai, H. L. He, H. H. Kuang, and J. M. Ma. Search for WIMP annual modulation signature: results from DAMA/NaI-3 and DAMA/NaI-4 and the global combined analysis. *Physics Letters B*, 480:23–31, May 2000.
- [43] C.E. Aalseth, P.S. Barbeau, J. Colaresi, J.I. Collar, J. Diaz Leon, et al. Search for an Annual Modulation in a P-type Point Contact Germanium Dark Matter Detector. *Phys.Rev.Lett.*, 107:141301, 2011.
- [44] G. Angloher, M. Bauer, I. Bavykina, A. Bento, C. Bucci, et al. Results from 730 kg days of the CRESST-II Dark Matter Search. *Eur.Phys.J.*, C72:1971, 2012.
- [45] A. Bottino, F. Donato, N. Fornengo, and S. Scopel. Interpreting the recent results on direct search for dark matter particles in terms of relic neutralino. *Phys.Rev.*, D78:083520, 2008.
- [46] J. Cherwinka, R. Co, D. F. Cowen, D. Grant, F. Halzen, K. M. Heeger, L. Hsu, A. Karle, V. A. Kudryavtsev, R. Maruyama, W. Pettus, M. Robinson, and N. J. C. Spooner. A search for the dark matter annual modulation in South Pole ice. *Astroparticle Physics*, 35:749–754, June 2012.
- [47] Alex Geringer-Sameth and Savvas M. Koushiappas. Exclusion of canonical WIMPs by the joint analysis of Milky Way dwarfs with Fermi. *Phys.Rev.Lett.*, 107:241303, 2011.
- [48] S. Desai et al. Search for dark matter WIMPs using upward through-going muons in Super-Kamiokande. *Phys.Rev.*, D70:083523, 2004.

- [49] R. Abbasi et al. Limits on a muon flux from neutralino annihilations in the Sun with the IceCube 22-string detector. *Phys.Rev.Lett.*, 102:201302, 2009.
- [50] Oscar Adriani et al. An anomalous positron abundance in cosmic rays with energies 1.5-100 GeV. *Nature*, 458:607–609, 2009.
- [51] Aous A. Abdo et al. Measurement of the Cosmic Ray e^+ plus e^- spectrum from 20 GeV to 1 TeV with the Fermi Large Area Telescope. *Phys.Rev.Lett.*, 102:181101, 2009.
- [52] Christoph Weniger. A Tentative Gamma-Ray Line from Dark Matter Annihilation at the Fermi Large Area Telescope. *JCAP*, 1208:007, 2012.
- [53] Elmo Tempel, Andi Hektor, and Martti Raidal. Fermi 130 GeV gamma-ray excess and dark matter annihilation in sub-haloes and in the Galactic centre. *JCAP*, 1209:032, 2012.
- [54] G. G. Raffelt. *Stars as laboratories for fundamental physics : the astrophysics of neutrinos, axions, and other weakly interacting particles*. 1996.
- [55] S. Chandrasekhar. *An introduction to the study of stellar structure*. 1939.
- [56] M. Schwarzschild. *Structure and evolution of the stars*. 1958.
- [57] S. Turck-Chieze and I. Lopes. Toward a unified classical model of the sun - On the sensitivity of neutrinos and helioseismology to the microscopic physics. *Astrophys. J.*, 408:347–367, May 1993.
- [58] Douglas Gough. What have we learned from helioseismology, what have we really learned, and what do we aspire to learn? *Solar Physics*, pages 1–33. 10.1007/s11207-012-0099-1.
- [59] J. P. Cox and R. T. Giuli. *Principles of stellar structure*. 1968.
- [60] D. D. Clayton. *Principles of stellar evolution and nucleosynthesis*. 1968.
- [61] E. Boehm-Vitense. *Introduction to stellar astrophysics. Vol. 3 - Stellar structure and evolution*. 1992.
- [62] Martin Asplund, Nicolas Grevesse, A. Jacques Sauval, and Pat Scott. The chemical composition of the Sun. *Ann. Rev. Astron. Astrophys.*, 47:481–522, 2009.
- [63] Aldo Serenelli, Sarbani Basu, Jason W. Ferguson, and Martin Asplund. New Solar Composition: The Problem With Solar Models Revisited. *Astrophys.J.*, 705:L123–L127, 2009.

-
- [64] S. Turck-Chièze and S. Couvidat. Solar neutrinos, helioseismology and the solar internal dynamics. *Reports on Progress in Physics*, 74(8):086901, August 2011.
- [65] B. Aharmim et al. Low Energy Threshold Analysis of the Phase I and Phase II Data Sets of the Sudbury Neutrino Observatory. *Phys. Rev.*, C81:055504, 2010.
- [66] G. Bellini et al. Measurement of the solar 8B neutrino rate with a liquid scintillator target and 3 MeV energy threshold in the Borexino detector. *Phys.Rev.*, D82:033006, 2010.
- [67] C. Arpesella et al. Direct Measurement of the Be-7 Solar Neutrino Flux with 192 Days of Borexino Data. *Phys.Rev.Lett.*, 101:091302, 2008.
- [68] J. L. Kohl, G. Noci, E. Antonucci, G. Tondello, M. C. E. Huber, L. D. Gardner, P. Nicolosi, L. Strachan, S. Fineschi, J. C. Raymond, M. Romoli, D. Spadaro, A. Panasyuk, O. H. W. Siegmund, C. Benna, A. Ciaravella, S. R. Cranmer, S. Giordano, M. Karovska, R. Martin, J. Michels, A. Modigliani, G. Naletto, C. Pernechele, G. Poletto, and P. L. Smith. First Results from the SOHO Ultraviolet Coronagraph Spectrometer. *Solar Phys.*, 175:613–644, October 1997.
- [69] S. Basu, W. J. Chaplin, Y. Elsworth, R. New, and A. M. Serenelli. Fresh Insights on the Structure of the Solar Core. *Astrophys. J.*, 699:1403–1417, July 2009.
- [70] J. Christensen-Dalsgaard, T. L. Duvall, Jr., D. O. Gough, J. W. Harvey, and E. J. Rhodes, Jr. Speed of sound in the solar interior. *Nature*, 315:378–382, May 1985.
- [71] Jeremy J. Drake and Paola Testa. The Solar model problem solved by the abundance of neon in stars of the local cosmos. *Nature*, 436:525–528, 2005.
- [72] Aldo M. Serenelli, W.C. Haxton, and Carlos Pena-Garay. Solar models with accretion. I. Application to the solar abundance problem. *Astrophys.J.*, 743:24, 2011.
- [73] W.J. Chaplin, H. Kjeldsen, J. Christensen-Dalsgaard, S. Basu, A. Miglio, et al. Ensemble Asteroseismology of Solar-Type Stars with the NASA Kepler Mission. *Science*, 332:213, 2011.
- [74] D. Huber, M.J. Ireland, T.R. Bedding, I.M. Brandao, L. Piau, et al. Fundamental Properties of Stars using Asteroseismology from Kepler and CoRoT and Interferometry from the CHARA Array. 2012.
- [75] D. O. Gough. In Y. Osaki & H. Shibahashi, editor, *Progress of Seismology of the Sun and Stars*, volume 367 of *Lecture Notes in Physics*, Berlin Springer Verlag, page 283, 1990.

- [76] J. Christensen-Dalsgaard and G. Houdek. Prospects for asteroseismology. *Astrophys.Space Sci.*, 328:51–66, 2010.
- [77] G. Steigman, C. L. Sarazin, H. Quintana, and J. Faulkner. Dynamical interactions and astrophysical effects of stable heavy neutrinos. *Astronom. J.*, 83:1050–1061, September 1978.
- [78] D. N. Spergel and W. H. Press. Effect of hypothetical, weakly interacting, massive particles on energy transport in the solar interior. *Astrophys. J.*, 294:663–673, July 1985.
- [79] W. H. Press and D. N. Spergel. Capture by the sun of a galactic population of weakly interacting, massive particles. *Astrophys. J.*, 296:679–684, September 1985.
- [80] L. M. Krauss, K. Freese, D. N. Spergel, and W. H. Press. Cold dark matter candidates and the solar neutrino problem. *Astrophys. J.*, 299:1001–1006, December 1985.
- [81] R. L. Gilliland, J. Faulkner, W. H. Press, and D. N. Spergel. Solar models with energy transport by weakly interacting particles. *Astrophys. J.*, 306:703–709, July 1986.
- [82] S. Raby and G. B. West. A simple solution to the solar neutrino and missing mass problems. *Nuclear Physics B*, 292:793–812, 1987.
- [83] D. Dearborn, K. Griest, and G. Raffelt. Window for the dark matter solution to the solar neutrino problem. *Astrophys. J.*, 368:626–632, February 1991.
- [84] J. Faulkner, D. O. Gough, and M. N. Vahia. Weakly interacting massive particles and solar oscillations. *Nature*, 321:226–229, May 1986.
- [85] W. Dappen, R. L. Gilliland, and J. Christensen-Dalsgaard. Weakly interacting massive particles, solar neutrinos, and solar oscillations. *Nature*, 321:229–231, May 1986.
- [86] A. Renzini. Effects of cosmions in the sun and in globular cluster stars. *Astron. Astrophys.*, 171:121, January 1987.
- [87] D. N. Spergel and J. Faulkner. Weakly interacting, massive particles in horizontal-branch stars. *Astrophys. J. Lett.*, 331:L21–L24, August 1988.
- [88] P. Salati and J. Silk. A stellar probe of dark matter annihilation in galactic nuclei. *Astrophys. J.*, 338:24–31, March 1989.
- [89] A. Bouquet and P. Salati. Life and death of cosmions in stars. *Astron. Astrophys.*, 217:270–282, June 1989.

-
- [90] D. Dearborn, G. Raffelt, P. Salati, J. Silk, and A. Bouquet. Dark matter and thermal pulses in horizontal-branch stars. *Astrophys. J.*, 354:568–582, May 1990.
- [91] K. S. Hirata, T. Kajita, M. Koshiba, M. Nakahata, S. Ohara, Y. Oyama, N. Sato, A. Suzuki, M. Takita, Y. Totsuka, T. Kifune, T. Suda, K. Nakamura, K. Takahashi, T. Tanimori, K. Miyano, M. Yamada, E. W. Beier, L. R. Feldscher, E. D. Frank, W. Frati, S. B. Kim, A. K. Mann, F. M. Newcomer, R. van Berg, W. Zhang, and B. G. Cortez. Experimental study of the atmospheric neutrino flux. *Physics Letters B*, 205:416–420, April 1988.
- [92] Q.R. Ahmad et al. Measurement of the rate of interactions produced by B-8 solar neutrinos at the Sudbury Neutrino Observatory. *Phys.Rev.Lett.*, 87:071301, 2001.
- [93] A. Gould. Resonant enhancements in weakly interacting massive particle capture by the earth. *ApJ*, 321:571–585, October 1987.
- [94] D. Dearborn, G. Raffelt, P. Salati, J. Silk, and A. Bouquet. Dark matter and thermal pulses in horizontal-branch stars. *Astrophys. J.*, 354:568–582, May 1990.
- [95] D. Dearborn, K. Griest, and G. Raffelt. Window for the dark matter solution to the solar neutrino problem. *Astrophys. J.*, 368:626–632, February 1991.
- [96] J. Kaplan, F. Martin de Volnay, C. Tao, and S. Turck-Chieze. A critical look at cosmions. *Astrophys. J.*, 378:315–325, September 1991.
- [97] A. Gould and G. Raffelt. Thermal conduction by massive particles. *Astrophys. J.*, 352:654–668, April 1990.
- [98] A. Gould. Weakly interacting massive particle distribution in and evaporation from the sun.
apj, 321:560–570, October 1987.
- [99] Ilidio Lopes and Joseph Silk. Solar neutrinos: Probing the quasiisothermal solar core produced by SUSY dark matter particles. *Phys.Rev.Lett.*, 88:151303, 2002.
- [100] P. Morel. CESAM: A code for stellar evolution calculations. *Astron. Astrophys. Suppl.*, 124:597–614, September 1997.
- [101] Eric G. Adelberger, Sam M. Austin, John N. Bahcall, A.B. Balantekin, Gilles Bogaert, et al. Solar fusion cross-sections. *Rev.Mod.Phys.*, 70:1265–1292, 1998.
- [102] H. E. Mitler. Thermonuclear ion-electron screening at all densities. I - Static solution. *Astrophys. J.*, 212:513–532, March 1977.

- [103] C. A. Iglesias and F. J. Rogers. Updated Opal Opacities. *Astrophys. J.*, 464:943–+, June 1996.
- [104] D. R. Alexander and J. W. Ferguson. Low-temperature Rosseland opacities. *Astrophys. J.*, 437:879–891, December 1994.
- [105] F. J. Rogers, F. J. Swenson, and C. A. Iglesias. OPAL Equation-of-State Tables for Astrophysical Applications. *Astrophys. J.*, 456:902–+, January 1996.
- [106] G. Michaud and C. R. Proffitt. Particle transport processes. In W. W. Weiss & A. Baglin, editor, *IAU Colloq. 137: Inside the Stars*, volume 40 of *Astronomical Society of the Pacific Conference Series*, pages 246–259, January 1993.
- [107] M. Asplund, N. Grevesse, and A. J. Sauval. The Solar Chemical Composition. In T. G. Barnes III & F. N. Bash, editor, *Cosmic Abundances as Records of Stellar Evolution and Nucleosynthesis*, volume 336 of *Astronomical Society of the Pacific Conference Series*, pages 25–+, September 2005.
- [108] Jordi Casanellas and Ilidio Lopes. Low-mass stars within dense dark matter halos. *AIP Conf.Proc. 1241 (2010)*, 2010.
- [109] P. Gondolo, J. Edsjo, P. Ullio, L. Bergstrom, Mia Schelke, et al. DarkSUSY: Computing supersymmetric dark matter properties numerically. *JCAP*, 0407:008, 2004.
- [110] P. Morel and Y. Lebreton. CESAM: a free code for stellar evolution calculations. *Astrophys. Spa. Sci.*, 316:61–73, August 2008.
- [111] J. Christensen-Dalsgaard. ADIPLS – the Aarhus adiabatic oscillation package. *Astrophys. Space Sci.*, 316:113–120, 2008.
- [112] Ilidio P. Lopes, Gianfranco Bertone, and Joseph Silk. Solar seismic model as a new constraint on supersymmetric dark matter. *Mon.Not.Roy.Astron.Soc.*, 337:1179–1184, 2002.
- [113] I. P. Lopes, J. Silk, and S. H. Hansen. Helioseismology as a new constraint on supersymmetric dark matter. *MNRAS*, 331:361–368, March 2002.
- [114] A. Bottino, G. Fiorentini, N. Fornengo, B. Ricci, S. Scopel, et al. Does solar physics provide constraints to weakly interacting massive particles? *Phys.Rev.*, D66:053005, 2002.
- [115] M. T. Frandsen and S. Sarkar. Asymmetric Dark Matter and the Sun. *Physical Review Letters*, 105(1), July 2010.

-
- [116] M. Taoso, F. Iocco, G. Meynet, G. Bertone, and P. Eggenberger. Effect of low mass dark matter particles on the Sun. *Phys.Rev.D*, 82(8), October 2010.
- [117] D. T. Cumberbatch, J. A. Guzik, J. Silk, L. S. Watson, and S. M. West. Light WIMPs in the Sun: Constraints from helioseismology. *Phys.Rev.D*, 82(10):103503, November 2010.
- [118] Ilidio Lopes and Joseph Silk. Probing the Existence of a Dark Matter Isothermal Core Using Gravity Modes. *Astrophys.J.*, 722:L95, 2010.
- [119] S. Turck-Chièze, R. A. García, I. Lopes, J. Ballot, S. Couvidat, S. Mathur, D. Salabert, and J. Silk. First Study of Dark Matter Properties with Detected Solar Gravity Modes and Neutrinos. *Astrophys. J.*, 746:L12, 2012.
- [120] Sylvaine Turck-Chieze, S. Couvidat, L. Piau, J. Ferguson, P. Lambert, et al. Surprising sun. *Phys.Rev.Lett.*, 93:211102, 2004.
- [121] I. Lopes and J. Silk. Solar Neutrino Physics: Sensitivity to Light Dark Matter Particles. *Astrophys. J.*, 752:129, June 2012.
- [122] I. Lopes and J. Silk. Neutrino Spectroscopy Can Probe the Dark Matter Content in the Sun. *Science*, 330:462–, October 2010.
- [123] I. V. Moskalenko and L. L. Wai. Dark Matter Burners. *Astrophys. J. Lett.*, 659:L29–L32, April 2007.
- [124] Chris Kouvaris. WIMP Annihilation and Cooling of Neutron Stars. *Phys.Rev.*, D77:023006, 2008.
- [125] Chris Kouvaris and Peter Tinyakov. Can Neutron stars constrain Dark Matter? *Phys.Rev.*, D82:063531, 2010.
- [126] J. Isern, E. García-Berro, S. Torres, and S. Catalán. Axions and the Cooling of White Dwarf Stars. *Astrophys. J. Lett.*, 682:L109–L112, August 2008.
- [127] J. Isern, E. García-Berro, L. G. Althaus, and A. H. Córscico. Axions and the pulsation periods of variable white dwarfs revisited. *Astron. Astrophys.*, 512:A86, March 2010.
- [128] A. H. Córscico, L. G. Althaus, M. M. Miller Bertolami, A. D. Romero, E. García-Berro, J. Isern, and S. O. Kepler. The rate of cooling of the pulsating white dwarf star G117-B15A: a new asteroseismological inference of the axion mass. *Mon. Not. Roy. Astron. Soc.*, 424:2792–2799, August 2012.

- [129] Gianfranco Bertone and Malcolm Fairbairn. Compact Stars as Dark Matter Probes. *Phys.Rev.*, D77:043515, 2008. 9 pages, 5 figures, revtex.
- [130] Arnaud de Lavallaz and Malcolm Fairbairn. Neutron Stars as Dark Matter Probes. *Phys.Rev.*, D81:123521, 2010.
- [131] Chris Kouvaris and Peter Tinyakov. Constraining Asymmetric Dark Matter through observations of compact stars. *Phys.Rev.*, D83:083512, 2011.
- [132] M. Angeles Perez-Garcia, Joseph Silk, and Jirina R. Stone. Dark matter, neutron stars and strange quark matter. *Phys.Rev.Lett.*, 105:141101, 2010.
- [133] Paolo Ciarcelluti and Fredrik Sandin. Have neutron stars a dark matter core? *Phys.Lett.*, B695:19–21, 2011.
- [134] Chris Kouvaris and Peter Tinyakov. Excluding Light Asymmetric Bosonic Dark Matter. *Phys.Rev.Lett.*, 107:091301, 2011.
- [135] S. C. Leung, M. C. Chu, and L. M. Lin. Equilibrium Structure and Radial Oscillations of Dark Matter Admixed Neutron Stars. 2012. 11 pages, 18 figures. Accepted for publication by Phys. Rev. D.
- [136] D. Spolyar, K. Freese, and P. Gondolo. Dark Matter and the First Stars: A New Phase of Stellar Evolution. *Physical Review Letters*, 100(5):051101–+, February 2008.
- [137] F. Iocco. Dark Matter Capture and Annihilation on the First Stars: Preliminary Estimates. *Astrophys. J. Lett.*, 677:L1–L4, April 2008.
- [138] M. Taoso, G. Bertone, G. Meynet, and S. Ekström. Dark matter annihilations in Population III stars. *Phys. Rev. D*, 78(12):123510–+, December 2008.
- [139] K. Freese, D. Spolyar, and A. Aguirre. Dark matter capture in the first stars: a power source and limit on stellar mass. *Journal of Cosmology and Astro-Particle Physics*, 11:14–+, November 2008.
- [140] Katherine Freese, Paolo Gondolo, and Douglas Spolyar. The Effect of Dark Matter on the First Stars: A New Phase of Stellar Evolution. *AIP Conf. Proc.*, 990:42–44, mar 2008.
- [141] K. Freese, P. Bodenheimer, D. Spolyar, and P. Gondolo. Stellar Structure of Dark Stars: A First Phase of Stellar Evolution Resulting from Dark Matter Annihilation. *Astrophys. J. Lett.*, 685:L101–L104, October 2008.

-
- [142] S.-C. Yoon, F. Iocco, and S. Akiyama. Evolution of the First Stars with Dark Matter Burning. *Astrophys. J. Lett.*, 688:L1–L4, November 2008.
- [143] A. Natarajan, J. C. Tan, and B. W. O’Shea. Dark Matter Annihilation and Primordial Star Formation. *ApJ*, 692:574–583, February 2009.
- [144] E. Ripamonti, F. Iocco, A. Ferrara, R. Schneider, A. Bressan, and P. Marigo. First star formation with dark matter annihilation. *MNRAS*, pages 883–+, June 2010.
- [145] Rowan J. Smith, Fabio Iocco, Simon C.O. Glover, Dominik R.G. Schleicher, Ralf S. Klessen, et al. WIMP DM and first stars: suppression of fragmentation in primordial star formation. 2012.
- [146] K. Freese. Review of Observational Evidence for Dark Matter in the Universe and in upcoming searches for Dark Stars. In *EAS Publications Series*, volume 36 of *EAS Publications Series*, pages 113–126, 2009.
- [147] F. Iocco, A. Bressan, E. Ripamonti, R. Schneider, A. Ferrara, and P. Marigo. Dark matter annihilation effects on the first stars. *Mon. Not. Roy. Astron. Soc.*, 390:1655–1669, November 2008.
- [148] D. R. G. Schleicher, R. Banerjee, and R. S. Klessen. Dark stars: Implications and constraints from cosmic reionization and extragalactic background radiation. *Phys. Rev. D*, 79(4):043510–+, February 2009.
- [149] F. Iocco. An idea for detecting capture dominated Dark Stars. *ArXiv e-prints*, June 2009.
- [150] Pat Scott, Aparna Venkatesan, Elinore Roebber, Paolo Gondolo, Elena Pierpaoli, et al. Impacts of Dark Stars on Reionization and Signatures in the Cosmic Microwave Background. *Astrophys.J.*, 742:129, 2011.
- [151] K. Freese, C. Ilie, D. Spolyar, M. Valluri, and P. Bodenheimer. Supermassive Dark Stars: Detectable in JWST. *ApJ*, 716:1397–1407, June 2010.
- [152] E. Zackrisson et al. Finding High-redshift Dark Stars with the James Webb Space Telescope. *ApJ*, 717:257–267, July 2010.
- [153] Erik Zackrisson, Pat Scott, Claes-Erik Rydberg, Fabio Iocco, Bengt Edvardsson, et al. Finding high-redshift dark stars with the James Webb Space Telescope. *Astrophys.J.*, 717:257–267, 2010.

- [154] P. C. Scott, J. Edsjö, and M. Fairbairn. Low Mass Stellar Evolution with WIMP Capture and Annihilation. In H. V. Klapdor-Kleingrothaus and G. F. Lewis, editors, *Dark Matter in Astroparticle and Particle Physics*, pages 387–392, April 2008.
- [155] M. Fairbairn, P. Scott, and J. Edsjö. The zero age main sequence of WIMP burners. *Phys. Rev. D*, 77(4):047301–+, February 2008.
- [156] P. Scott, M. Fairbairn, and J. Edsjö. Dark stars at the Galactic Centre - the main sequence. *Mon. Not. Roy. Astron. Soc.*, 394:82–104, March 2009.
- [157] P. Scott, J. Edsjö, and M. Fairbairn. The Darkstars Code: a Publicly Available Dark Stellar Evolution Package. In H. V. Klapdor-Kleingrothaus and I. V. Krivosheina, editors, *Dark Matter in Astrophysics and Particle Physics, Dark 2009*, pages 320–327, December 2010.
- [158] G. Bertone and D. Merritt. Dark Matter Dynamics and Indirect Detection. *Modern Physics Letters A*, 20:1021–1036, 2005.
- [159] A.M. Ghez, G. Duchene, K. Matthews, Seth D. Hornstein, A. Tanner, et al. The first measurement of spectral lines in a short - period star bound to the galaxy’s central black hole: A paradox of youth. *Astrophys.J.*, 586:L127–L131, 2003.
- [160] R. Genzel, F. Eisenhauer, and S. Gillessen. The Galactic Center massive black hole and nuclear star cluster. *Reviews of Modern Physics*, 82:3121–3195, October 2010.
- [161] R. M. Buchholz, R. Schödel, and A. Eckart. Composition of the galactic center star cluster. Population analysis from adaptive optics narrow band spectral energy distributions. *Astron. Astrophys.*, 499:483–501, May 2009.
- [162] T. Do, A. M. Ghez, M. R. Morris, J. R. Lu, K. Matthews, S. Yelda, and J. Larkin. High Angular Resolution Integral-Field Spectroscopy of the Galaxy’s Nuclear Cluster: A Missing Stellar Cusp? *Astrophys. J.*, 703:1323–1337, October 2009.
- [163] H. Bartko, F. Martins, S. Trippe, T. K. Fritz, R. Genzel, T. Ott, F. Eisenhauer, S. Gillessen, T. Paumard, T. Alexander, K. Dodds-Eden, O. Gerhard, Y. Levin, L. Mascetti, S. Nayakshin, H. B. Perets, G. Perrin, O. Pfuhl, M. J. Reid, D. Rouan, M. Zilka, and A. Sternberg. An Extremely Top-Heavy Initial Mass Function in the Galactic Center Stellar Disks. *Astrophys. J.*, 708:834–840, January 2010.
- [164] Maximo Banados and Pedro G. Ferreira. Eddington’s theory of gravity and its progeny. *Phys.Rev.Lett.*, 105:011101, 2010.

- [165] A-M. Broomhall et al. Definitive Sun-as-a-star p-mode frequencies: 23 years of BiSON observations. 2009.